MECHANISMS OF TUMOUR CELL DISSEMINATION IN LUNG CANCER – A STUDY OF CIRCULATING TUMOUR CELLS

A thesis submitted to The University of Manchester for the degree of PhD in the Faculty of Medical and Human Sciences

2016

ROBERT L METCALF

SCHOOL OF MEDICINE

LIST OF CONTENTS

Final word count 61,431

LIST OF TABLES

LIST OF FIGURES

LIST OF ABBREVIATIONS

AJCC	American Joint Committee on Cancer
AKT	Ak-thymoma
ALK	Anaplastic lymphoma kinase
BCA	Bicinchoninic acid
BCL-2	B cell chronic lymphocytic leukaemia/lymphoma 2
BSA	Bovine serum albumin
BSC	Best supportive care
CD	Cluster of differentiation
CDH1	Cadherin 1 (epithelial cadherin)
CDH2	Cadherin 2 (neuronal cadherin)
CDH5	Cadherin 5 (vascular endothelial cadherin)
CDX	Circulating tumour cell derived explant
CEC	Circulating endothelial cell
CR	Complete response
CT	Computerised tomography
CTC	Circulating tumour cell
CXCR4	Chemokine receptor 4
Cy5	Cyanine 5
DAPI	4',6-diamidino-2-phenylindole
DCE-MRI	Dynamic contrast enhanced magnetic resonance imaging
DNA	Deoxyribonucleic acid
DTC	Disseminated tumour cell
EDTA	Ethylenediaminetetraacetic acid
EGFR	Epidermal growth factor receptor
EML4	Echinoderm microtubule associated protein like 4
EMT	Epithelial to mesenchymal transition
EpCAM	Epithelial cell adhesion molecule
EPHA2	Ephrin receptor type A2
ERK	Extracellular-signal regulated kinase
ESM1	Endothelial cell specific molecule 1
FAK	Focal adhesion kinase

FDA	Food and drugs administration
FITC	Fluorescein isothiocyanate
GAPDH	Glyceraldehyde-3-Phosphate Dehydrogenase
GFP	Green fluorescent protein
GRHL2	Grainyhead-Like 2
HD-CTC	High definition circulating tumour cell
HIF1α	Hypoxia inducible factor 1, alpha subunit
HRP	Horseradish peroxidase
HU	Hounsfield units
HUVEC	Human umbilical vein endothelial cells
HVB	Health volunteer blood
ICP-MS	Inductively coupled plasma mass spectrometry
ISET	Isolation by size of epithelial tumour cells
KRT19	Keratin 19
LAMC2	Laminin subunit gamma 2 gene
LED	Light emitting diode
LOX	Lysyl oxidase
MAPK	Mitogen activated protein kinase
MET	Mesenchymal to epithelial transition
NA	Not applicable
NR	Not reached
NSCLC	Non-small cell lung cancer
NSG	Non-obese diabetic (NOD) severe combined immune deficient (SCID Cg-*Prkdc*^{scid}*)* interleukin 2 receptor gamma chain null (*l2rg*^{tm1Wjl}/SzJ)
PACS	Picture archiving and communication system
PAS	Periodic acid Schiff
PBMC	Peripheral blood mononuclear cell
PBS	Phosphate buffered saline
PBS-T	Phosphate buffered saline and 0.02% Tween-20
PD	Progressive disease
PDPN	Podoplanin
PDX	Patient derived xenograft
PECAM1	Platelet endothelial cell adhesion molecule 1

PET	Positron emission tomography
PFS	Progression free survival
pH	$-\log^{10}(H^+)$
PLAU	Plasminogen activator, urokinase
ppb	Parts per billion
ppm	Parts per million
PS	Performance status
RAC1	Rat sarcoma viral oncogene homolog (RAS) related C3 botulinum toxin substrate 1
RNA	Ribonucleic acid
RNAi	Ribonucleic acid interference
ROC	Receiver operating characteristic
RPMI	Roswell Park Memorial Institute
RR	Response Rate
SCLC	Small cell lung cancer
SD	Stable disease
SDS-PAGE	Sodium dodecyl sulphate-polyacrylamide gel electrophoresis
SEER	Surveillance epidemiology and end results
SEM	Standard error of the mean
shRNA	Short hairpin ribonucleic acid
SNAI2	Snail family zinc finger 2
SWOG	Southwest oncology group
TIE1	Tyrosine kinase with immunoglobulin-like and EGF-like domains 1
TKI	Tyrosine kinase inhibitor
TRACERx	Tracking cancer evolution through treatment
TRITC	Tetramethylrhodamine
UK	United Kingdom
US	United States
VEGFA	Vascular endothelial growth factor A
VIM	Vimentin
VM	Vasculogenic mimicry
WHO	World Health Organisation
ZEB1	Zinc finger E box binding homeobox 1
ZEB2	Zinc finger E box binding homeobox 2

ABSTRACT

Mechanisms of tumour cell dissemination in lung cancer – a study of circulating tumour cells. A Thesis submitted to The University of Manchester for the Degree of PhD by Robert Lewin Metcalf, March 2016.

Background: Circulating tumour cell (CTC) number is a prognostic biomarker in non-small cell lung cancer (NSCLC) and small cell lung cancer (SCLC). However, it is recognised that CTCs are heterogeneous and a better appreciation of CTC biology is required to reveal avenues of therapeutic intervention in metastatic lung cancer. CTC immunofluorescent assays were developed to evaluate two proposed mechanisms of tumour cell dissemination: epithelial to mesenchymal transition (EMT) and vasculogenic mimicry (VM). **Methods:** An immunofluorescent assay was developed to profile ISET filtered CTCs for the expression of epithelial and mesenchymal markers (cytokeratins and vimentin). This assay was evaluated in a pilot cohort of NSCLC and SCLC patient blood samples. In an index NSCLC patient, a CTC derived explant (CDX) tumour was generated from the same blood draw allowing comparison between CTCs in the donor blood sample and the tumour arising from tumorigenic CTCs. As VM had not been reported in SCLC, SCLC patient biopsies were evaluated from 41 limited stage patients to demonstrate VM vessels (Periodic Acid Schiff $(PAS)^{+}/CD31^{-}$) and correlate with clinical outcomes. A second assay was developed to profile SCLC CTCs for co-expression of cytokeratins and VE-cadherin (a biomarker of VM) and applied to blood samples from 38 SCLC patients (8 limited stage, 30 extensive stage). *In vitro* and *in vivo* studies were performed using VE-cadherin positive and negative SCLC cell lines (H446 and H446 shRNA VE-cadherin knock down) to determine if VE-cadherin played a functional role in the formation of VM networks. **Results:** Sub-populations of CTCs which were epithelial ($cytokeratins^{+}/vimentin^{-}$), mesenchymal ($cytokeratins^{-}/vimentin^{+}$) and mixed epithelial/mesenchymal ($cytokeratins^{+}/vimentin^{+}$) were identified in all NSCLC and SCLC samples studied. In the index NSCLC patient from whom CTCs generated a CDX, the $cytokeratins^{+}/vimentin^{+}$ expression profile was consistent between CTCs and CDX tumour. In 41 limited stage SCLC patients, VM was identified for the first time and was associated with shorter patient survival, consistent with the adverse prognosis reported in association with VM in other cancer types. A second immunofluorescent assay identified sub-populations of CTCs with a putative 'VM phenotype' ($cytokeratins^{+}/VE\text{-}cadherin^{+}$) in 37/38 SCLC patients. In pre-clinical studies, VE-cadherin was shown to be necessary for formation of VM networks in Matrigel and for the formation of $PAS^{+}/CD31^{-}$ VM structures *in vivo* in xenografts. VM vessels were also observed across a panel of CDX tumours that were a superior model to study VM compared to the typically small, necrotic primary tumour biopsies. **Conclusion**: Sub-populations of lung cancer CTCs were detected and classified based upon their markers of EMT (cytokeratins and vimentin) and VM (VE-cadherin), two putative mechanisms leading to tumour cell dissemination in lung cancer. A better understanding of mechanisms of EMT and VM in lung cancer, via study of CTCs, has the potential to reveal novel therapeutic avenues. CTCs could provide a minimally invasive predictive biomarker.

DECLARATION

No portion of the work referred to within this thesis has been submitted in support of an application of another degree or qualification of this or any other university or other institute of learning.

COPYRIGHT STATEMENT

i. The author of this thesis (including any appendices and/or schedules to this thesis) owns certain copyright or related rights in it (the "Copyright") and he has given The University of Manchester certain rights to use such Copyright, including for administrative purposes.

ii. Copies of this thesis, either in full or in extracts and whether hard or electronic copy, may be made **only** in accordance with the Copyright, Designs and Patents Act 1988 (as amended) and regulations issued under it or, where appropriate, in accordance with licensing agreements which the University has from time to time. This page must form part of any such copies made.

iii. The ownership of certain Copyright, patents, designs, trade marks and other intellectual property (the "Intellectual Property") and any reproductions of copyright works in the thesis, for example graphs and tables ("Reproductions"), which may be described in this thesis, may not be made available for use without the prior written permission of the owner(s) of the relevant Intellectual Property and/or Reproductions.

iv. Further information on the conditions under which disclosure, publication and commercialisation of this thesis, the Copyright and Intellectual Property and/or Reproductions described in it may take place is available in the University IP Policy (see http://documents.manchester.ac.uk/DocuInfo.aspx?DocID=487), in any relevant Thesis restriction declarations deposited in the University Library, The University Library's regulations (see http://www.manchester.ac.uk/library/aboutus/regulations) and in The University's policy on Presentation of Theses.

ACKNOWLEDGEMENTS

I am very grateful to my supervisors Prof Caroline Dive (Group Leader in Clinical and Experimental Pharmacology, and Deputy Director, CRUK Manchester Institute), Dr Fiona Blackhall (Senior Lecturer and Consultant in Medical Oncology, The University of Manchester and The Christie NHS Foundation Trust) and Prof Andrew Hughes (Global Vice President, Early Clinical Development, Astra-Zeneca Pharmaceuticals) for their supervision and guidance throughout this project. I am also grateful to Dr Ged Brady (Deputy Group Leader, Clinical and Experimental Pharmacology) for his guidance with planning and conducting laboratory research. I thank both Cancer Research UK and AstraZeneca Pharmaceuticals for their joint funding of this project.

The research described within this thesis was conducted by the author as part of the broader research of the CEP lab. As such, there are numerous people within the CRUK Manchester Institute I would like to thank for their advice and training in the methods employed. I am indebted to Dr Kathryn Simpson for her support throughout this research, reviewing data from the vasculogenic mimicry work and her helpful advice on scientific writing and specifically for the creation of a VE-cadherin knock down small cell lung cancer cell line (H446) which was used as part of this work. Thanks also go to Dr Chris Morrow and Cassandra Hodgkinson and the CTC pre-clinical lab for their advice on planning pre-clinical experiments and the conduct of the *in-vivo* experiments which are reported in this thesis. I am grateful for the training and support provided by Dr Francesca Trapani in undertaking immunohistochemistry of CDX and xenograft tumours. Finally, thanks go to Dr Karen Morris and the CTC GCP lab for their training and support in CTC analysis including ISET and CellSearch.

I thank Prof Mary J Hendrix and Dr R Seftor and Dr E Seftor (Ann and Robert Lurie Children's Hospital of Chicago) for their generous donation of the C8161 cell line, their comments on the vasculogenic mimicry data and their advice on the conduct of *in vitro* assays of vasculogenic mimicry.

I thank the core facilities at the CRUK Manchester Institute, specifically Steve Bagley and the Imaging Facility for their advice on fluorescent microscopy, Gary Ashton and the Histology Facility for their support in processing tumour samples for IHC. I thank the nurses and phlebotomists at the Christie NHS Foundation Trust for their contribution to patient blood sample collection and am grateful to the patients who donated their blood samples and clinical data.

Dedication

I dedicate this research to my wife, Kelly, and daughter, Theodora Metcalf, the large rocks in my life, and to my parents Carol and John Metcalf who provided me with the support and opportunities to be in this position.

The Author

I graduated in Medicine from the University of Manchester (U.K.) in 2004 with a First Class Intercalated BSc. in Law and Medical Ethics. Having undertaken postgraduate general medical training in Greater Manchester (Salford Royal Hospitals NHS FT and Central Manchester University Hospitals NHS FT) and achieving Membership of the Royal Colleges of Physicians (U.K.) in 2008, I completed Medical Oncology Specialty Certification in 2015. I was appointed to a three year clinical research fellowship in 2012 based at the CRUK Manchester Institute, University of Manchester. The research conducted during this time is the subject of this thesis.

1 GENERAL INTRODUCTION

1.1 Introduction to lung cancer

Lung cancer is the most common cancer globally, and the leading cause of cancer related death.[1] Lung cancer is classified based upon its histological appearances and immunophenotype into small cell lung cancer (SCLC) and non-small cell lung cancer (NSCLC). SCLC accounts for between 9 and 22% of all cases of lung cancer, the remainder being NSCLC.[2] There are clear epidemiological data identifying an association between tobacco smoking and lung cancer.[3,4] There is a thirty-fold increased risk of developing lung cancer in people who smoke tobacco.[5] However, 10 to 15% of lung cancer deaths in developed countries are not smoking related. Other risk factors for the development of lung cancer include exposure to radon gas, diesel fumes, radiation, particulate air matter, asbestos, silica and arsenic.[2]

Lung cancer is characterised by early metastatic dissemination. Survival data (Table 1.1) show that 92% of SCLC cases and 76% of NSCLC cases have spread beyond the primary site when diagnosed. The implication of distant metastatic spread at diagnosis is that the disease is no longer curable and as a consequence, the 5 year survival of all patients with lung cancer is between 6 and 18% globally.[2]

Patients with localised or regional SCLC which is confined so that it may be encompassed within a radiotherapy field are defined as having limited stage disease. The remaining patients have extensive stage disease. For all patients with extensive stage disease and the majority of patients with limited stage

disease, SCLC is not curable. Surgery has minimal role to play in the management of SCLC and the mainstay of therapy remains chemotherapy, with or without the addition of radiotherapy.

Extent of Disease	% cases	5 year Relative Survival (%)	Staging SCLC	Staging NSCLC
SCLC				
All cases	100	6.3		
Localised	5	22.9	Limited	-
Regional	21	14.0	Limited or Extensive*	-
Distant	71	2.8	Extensive	-
Unstaged	4	8.5	Unstaged	-
NSCLC				
All Cases	100	17.5		
Localised	17	53.6	-	I, II
Regional	22	26.7	-	III
Distant	54	3.8	-	IV
Unstaged	7	7.9	-	Unstaged

Table 1.1 Five year relative survival of lung cancer patients by stage of disease
Adapted from US National Cancer Institute Surveillance Epidemiology and End Results (SEER) data, based on November 2011 SEER data submission, http://seer.cancer.gov/csr/1975_2009_pops09/ posted April 2012. Five year relative survival is defined as the percentage of patients alive 5 years following diagnosis divided by the percentage of the general population patched by age and sex alive at 5 years following diagnosis (2002- 2008). * SCLC with regional spread is either limited or extensive stage depending on the extent of regional spread and whether the area is able to be encompassed within a radiotherapy field.

1.2 Chemotherapy resistance in lung cancer

A major clinical problem limiting survival in both SCLC and NSCLC is that of chemotherapy resistance. The clinical pattern of disease response to treatment differs between these diseases. SCLC is characterised by initial chemotherapy sensitivity, with high response rates to treatment, followed by chemotherapy

resistance upon disease relapse. Clinical trials of first line platinum based chemotherapy (containing cisplatin or carboplatin) and etoposide show radiological response rates of up to 75%[6-9] and second line chemotherapy, in the setting of recurrent disease, produces response rates of less than 25%.[10-13]

NSCLC is typically chemotherapy resistant from the outset with only 20 – 30% of patients having a radiological response to first-line platinum-based chemotherapy and improvements in survival measuring only a small number of months.[14,15] The response rates to second line chemotherapy with docetaxel or pemetrexed are less than 10%.[16,17]

Although the developments in personalised medicine have improved patient outcomes in NSCLC (discussed in section 1.3 below), in the context of chemotherapy use for advanced lung cancer (SCLC or NSCLC), intrinsic or acquired resistance is almost universal.

Research into platinum resistance attracts significant interest, as overcoming this phenomenon offers the hope of increasing patient benefit from existing therapies. Varied molecular mechanisms of resistance have been reviewed elsewhere.[18] One such mechanism which shows promise to translate into therapeutic gain in lung cancer is an excess of resistance factors or defects in apoptosis such as would occur with increased activity of the anti-apoptotic protein BCL-2.[19] BCL-2 is relevant to lung cancer chemotherapy resistance as it is over-expressed in 65 -75% of cases of SCLC[20,21] and ongoing studies are looking to exploit these advances, for example through the development of novel inhibitors of the BCL-2 family member BCL-xl.[22] In addition to this, other molecular mechanism of resistance are proposed including the acquisition of

drug efflux pumps[23] or the activity of DNA repair pathways.[24] The DNA repair protein ERCC1 is being evaluated as a biomarker or response/resistance to platinum chemotherapy.[24]

In addition to molecular mechanisms of resistance, it is also hypothesised that chemotherapy resistance arises due to the association between the tumour cells and the tumour vessels, whereby cells at increased distance from tumour vessels show increasing resistance to chemotherapy. Three reasons are proposed to explain the relationship between tumour vasculature and chemotherapy resistance.[25] First, tumour cells at increased distance from the vessel show decreased proliferation[26] and may therefore be spared by chemotherapy which is selective for cells undergoing division. Second, areas of the tumour at increased distance from the vessels show increased hypoxia or reduced pH[27] which may impair the activity of chemotherapy agents.[28] Third, areas of the tumour at increased distance from the vessels may have lower chemotherapy delivery.[29] Indeed, it is postulated that reduction in tumour blood flow and subsequent reduction in chemotherapy delivery to the tumour is a potential explanation for the lack of clinical benefit seen with anti-angiogenic agents, which disrupt the tumour vasculature, when given with cytotoxic chemotherapy.[30]

An understanding of chemotherapy resistance, either through insights into molecular mechanisms of resistance or through an understanding of the dynamic role of the tumour vasculature in determining tumour growth and response to systemic therapies, is required to optimise the development of new treatment approaches and to improve survival for lung cancer patients.

1.3 Personalised therapy for lung cancer

Whereas chemotherapy for SCLC remains unchanged for thirty years,[6] there have been significant advances in the treatment of NSCLC. The identification of molecular drivers has led to the development of 'targeted therapies' prescribed to patients who may be expected to benefit due to the presence of an objectively measureable characteristic which predicts response to therapy (a predictive biomarker). The epidermal growth factor receptor (EGFR) tyrosine kinase inhibitors (TKIs) gefitinib, erlotinib and afatinib, and the anaplastic lymphoma kinase (ALK) TKI crizotinib have progressed into clinical practice. For each of these classes of therapy, a predictive biomarker has been identified. In the case of EGFR TKI therapy this is an activating mutation in the tyrosine kinase domain of the EGFR gene[31,32] and in the case of ALK TKI therapy this is the presence of a fusion gene between echinoderm microtubule-associated protein like-4 (EML4) and ALK.[33] Targeted therapies in selected patients have response rates up to 74% and median survival is significantly improved compared with cytotoxic chemotherapy (Table 1.2). These clinical studies show that meaningful advances are being made in lung cancer through an improved understanding of the molecular changes arising in this disease.

Treatment	Patients	RR (%)	PFS (mo)	Ref
ALK fusion positive NSCLC				
Crizotinib	82	57	NR	[33]
EGFR mutation positive NSCLC				
Gefitinib	132	71.2*	NR	[34]
Carbo/Taxol	129	47.3	NR	
Gefitinib	114	73.7*	10.8*	[35]
Carbo/Taxol	114	30.7	5.4	
Erlotinib	83	NR	13.1*	[36]
Carbo/Gem	82	NR	4.6	
Erlotinib	86	NR	9.7*	[37]
Plat/Doc or Gem	87	NR	5.2	
Afatinib	230	56.0*	11.1*	[38]
Cis/Pem	115	23.0	6.9	

Table 1.2 Results of clinical trials of ALK and EGFR targeted therapies in ALK rearranged and EGFR mutated NSCLC. Statistically significant difference indicated by *. Abbreviations: Carbo/Taxol carboplatin with paclitaxel; Carbo/Gem carboplatin with gemcitabine; Plat/Doc or Gem carboplatin or cisplatin in combination with docetaxel or gemcitabine; NSCLC non-small cell lung cancer; RR response rate; PFS progression free survival, BSC best supportive care; Carbo/Taxol carboplatin and paclitaxel; NR not reported.

1.4 Biomarkers in clinical trial design

The clinical trials reported in Table 1.2 above demonstrate that the inclusion of predictive biomarkers into clinical trials can streamline clinical trial design by enriching the population being studied for those patients likely to benefit. A larger difference should be seen between treatment arms and fewer patients would be required, making clinical trials more affordable and producing results more quickly. Fewer studies should fail in the late stage of drug development. However, a limitation of the sub-division of lung cancer into many small sub-

types of lung cancer is that each trial is only able to recruit a small proportion of all patients as candidate genetic mutations are typically present in less than 5 to 10% of all lung cancer patients.[39] To overcome this hurdle, the United Kingdom National Lung Matrix trial commenced in 2015 and is a genetic biomarker led non-randomised phase II study in which NSCLC patients will undergo molecular pre-screening and be allocated to one of 18 molecular cohorts.[40] Allocation to study drug will be determined by the results of screening the tumour biopsy for a panel of predictive biomarkers. This study aims to determine whether there is sufficient signal of activity for the drug-biomarker combination to warrant further investigation, marking a step change in the way clinical trials are conducted.

Drug development has also improved through the use of pharmacodynamic (PD) biomarkers (objectively measurable variables which provide information on a pharmacological response to a therapeutic intervention). In an era of molecularly targeted therapy, PD biomarkers can be incorporated into early phase clinical trials to identify evidence of drug-target interaction and the molecular effect of the drug 'downstream' of the target.[41] PD biomarkers may be studied as part of a 'window trial' which involves the assessment of tumour tissue before and after the administration of an investigational drug.

The clinical implementation of personalised medicine and predictive and pharmacodynamic biomarker development requires ready access to tumour material, often at multiple time points. In patients with lung cancer, the tumour is rarely resectable and often inaccessible deep within the thorax. Even if accessible, the risk of a biopsy due to co-morbidity may be judged too high to proceed. In the United Kingdom in 2008, only 73% of the patients diagnosed

with lung cancer had a successful biopsy, and in some regions this figure was as low as 25%.[42]

It has long been recognised that tumour cells circulate within the blood stream in patients with epithelial tumours (circulating tumour cells – CTCs).[43] If CTCs are shown to be representative of the heterogeneous disease burden as a whole, tumour material derived from blood samples (a 'liquid biopsy') may replace the need for multiple invasive biopsies.

1.5 Circulating tumour cells (CTCs)

Tumour cells were first identified within the blood stream by Ashworth in 1869.[43] Since the 1950s, and although akin to searching for needles in the haystack, the study of CTCs has been gradually increasing. Even in the absence of overt metastases, tumour cells have been identified within the bone marrow of patients with cancer (disseminated tumour cells - DTCs), and these cells are dormant and have the capacity to reactivate and proliferate and may be the precursors to metastases.[44] DTCs are present in localised NSCLC (85/159 cases studied) and their presence predicts the risk of subsequent relapse.[45] This prognostic effect of DTCs in 'localised' NSCLC emphasises the clinical importance of micro-metastatic disease which spreads via the circulation early in the natural history of the disease.

1.6 Platforms for the enrichment of CTCs from patients

Diverse CTC enrichment and isolation platforms are under development[46-53] and have been comprehensively reviewed elsewhere.[54] The approaches to isolation of CTCs from blood samples can be divided into marker dependent and marker independent methods.

1.6.1 Marker dependent enrichment

Marker dependent methods enrich the sample by selecting for cells expressing tumour cell markers. This process is semi-automated with the CellSearch platform. CellSearch uses epithelial cell adhesion molecule (EpCAM) ferrofluid enrichment followed by automated immunofluorescent staining for the nuclear stain DAPI, cytokeratins 8, 18 and 19 (CK) and CD45 (the common leukocyte antigen).[55] The cells are imaged with an automated scanner which presents a gallery for review to confirm the identity of CTCs as cytokeratin^{+} and CD45^{-} cells. CellSearch therefore identifies the EpCAM^{+}/cytokeratin^{+} sub-population of tumour cells within the circulation. CellSearch has been used extensively in multiple cancer types (reviewed in[54]) and is considered the gold standard for CTC enumeration. Our lab has previously shown that CellSearch detects EpCAM^{+}/cytokeratin^{+} CTCs in 21% of patients with stage IIIA to IV NSCLC (median 1, range 0 to 146 CTCs/7.5 ml)[56] and in 85% of patients with SCLC (median 24, range 0 to 44,896 CTCs/7.5ml).[57] In these studies, CTCs are associated with shorter patient survival (when present >5/7.5ml in NSCLC[56] and >50/7.5ml in SCLC[57]) and CTC enumeration is FDA approved for the prognostic information it contributes in colorectal, breast and prostate cancers. The utility of CTCs for clinical prognostication is discussed in section 1.7.1 below.

Other marker dependant methods which have demonstrated utility for lung cancer CTC detection are the 'CTC-chip'[46] and the herringbone chip (HB-chip)[47] which are anti-EpCAM antibody coated microfluidic devices. The blood sample is passed through the device and EpCAM^{+} cells are captured for immunofluorescent analysis with cytokeratin and CD45 staining. Cytokeratin^{+}/CD45^{-} cells retained on the EpCAM micro-posts are defined as

CTCs and therefore this approach also identifies the EpCAM^{+}/cytokeratin^{+} CTC subpopulation within the circulation. In a study of 55 samples analysed with the 'CTC chip' from patients with advanced NSCLC, EpCAM^{+}/cytokeratin^{+} CTCs were isolated from all patients, (mean 155 cells/ml, range 5 to 1,281/ml).[46] Although direct comparison between the results of these studies of CellSearch and the CTC chip is not possible due to the inclusion of different NSCLC patient populations, the differences in the number of EpCAM^{+}/cytokeratin^{+} NSCLC CTCs detected using each of these approaches provides evidence to suggest that CellSearch significantly underestimates the true CTC burden in NSCLC.

A limitation of both the CellSearch and CTC-chip platforms is their reliance on tumour cell expression of specific markers for capture and identification. CTCs which do not express the capture antigen (EpCAM) or cytokeratins will remain undetected. However, to complement these approaches, there are antigen independent enrichment platforms which are an alternative approach to CTC detection which have been studied in lung cancer.

1.6.2 Marker independent enrichment

ISET (isolation by size of epithelial tumour cells) microfiltration uses an 8 µm polycarbonate microfilter through which a blood sample is processed following red cell lysis. This enriches for CTCs based upon their large size relative to other circulating blood cells, the majority of the leukocytes passing through the filter.[49] The cells on the filter can then be analysed by immunocytochemistry or immunofluorescence and are confirmed as CTCs based upon cytomorphology (malignant features including irregular nuclear membrane, irregular nuclear shape, a high nuclear to cytoplasmic ratio and the presence of three

dimensional sheets[58]) and immunophenotype (expression of tumour specific markers and/or absence of haematogenous markers).

The performance of CellSearch and ISET has been directly compared in patients with stage IIIA to IV NSCLC by our lab. In this study, CTCs (defined as CD45 negative cells by immunocytochemistry with large, hyperchromatic, irregular shaped nuclei) were seen in 80% by ISET and 23% by CellSearch.[59] A subpopulation of CTCs captured by ISET did not express epithelial markers which may explain in part the decreased CTC numbers identified by CellSearch, which relies on the expression of epithelial markers for cell capture and identification. ISET also detects CTCs (defined as circulating non-haematological cells with malignant cytopathological features) in 36% of patients with localised NSCLC.[58] A separate study using CellSearch in localised NSCLC found CTCs in only 16% of patients.[60]

A more recently described enrichment free method of isolation utilised to detect lung cancer CTCs is that of performing a blood plate and immunofluorescent staining of the cells for cytokeratin and CD45 without an enrichment step (the HD-CTC assay).[61] In 78 patients with stage I to IV NSCLC, cytokeratin^{+} CTCs were identified in 73% using this method (median 4.4, range 0 – 516 CTCs/1 ml) confirming its sensitivity for CTC detection. Again this method shows how many CTCs are likely going undetected by CellSearch.

1.6.3 Enrichment of viable CTCs

The only approach which has been demonstrated to enrich for viable patient CTCs which are able to form tumours in immune-compromised mice is the RosetteSep CTC enrichment kit (Stemcell technologies). This comprises a

cocktail of tetrameric antibody complexes recognizing leukocyte antigens CD2, CD16, CD19, CD36, CD38, CD45, CD66b and the erythrocyte antigen glycophorin. The antibody cocktail is incubated with the blood sample followed by a ficoll spin which depletes the leukocyte and erythrocyte populations enriching for the CTC fraction.[62]

To test the sensitivity of this method for CTC detection, studies of $EpCAM^{+}$ breast cancer cell lines (CAMA) spiked into whole blood found the purity of enrichment is 91% (+-4%) with RosetteSep and density gradient centrifugation compared with 4% (+-2%) with density gradient centrifugation alone.[63] Although it has not undergone extensive clinical validation, when applied to patients with breast and prostate cancer, RosetteSep enrichment detects CTCs in 25% of patients.[64] Although this would be predicted to have greater sensitivity than marker dependent enrichment, it has not been tested head to head against any other approaches to date.

One clear benefit of RosetteSep enrichment is the CTCs are unlabeled and therefore it reduces the effect of the sample processing on the integrity of the CTCs and makes them more amenable to subsequent functional studies. Moreover, as it is marker independent, it does not enrich for any sub-populations of tumour cells therefore would be expected to better capture the heterogeneity between CTCs. A seminal paper in breast cancer[65] and our own work in SCLC[66] have confirmed that tumour initiating sub-populations of RosetteSep enriched CTCs exist. In the breast cancer study,[65] the enriched CTC fraction was administered into the femoral medullary cavity of profoundly immune-compromised NSG (NOD.Cg-*Prkdc*^{scid}*Il2rg*^{tm1Wjl}/SzJ) mice. The merits of different strains of immune-suppressed mice for tumour xenograft growth are

discussed later within this General Introduction (Section 1.8.4), however, NSG mice are profoundly immune-suppressed providing a permissive environment for the growth of xenograft tumours from CTCs. Metastases arose in the mice following administration of samples taken from 3 of 109 patients, all of whom had >1000 $EpCAM^{+}$/$cytokeratin^{+}$ CTCs/7.5 ml in paired samples enumerated by CellSearch.

In the study of tumour initiating properties of SCLC CTCs performed by our lab,[66] the enriched fraction was administered sub-cutaneously in NSG mice and tumours arose from 4 of 6 SCLC patients, all of whom had >400 $EpCAM^{+}$/$cytokeratin^{+}$ CTCs/7.5ml in paired samples. Two SCLC CTC derived explant (CDX) tumours arose from patients with chemotherapy sensitive disease and two from patients with chemotherapy resistant disease. The animals were treated with cisplatin and etoposide chemotherapy and the patient responses to treatment were mirrored in the CDX tumours showing that this model reflects the disease in patients. These findings are significant for two reasons. Firstly, they prove that at least a sub-population of CTCs are able to initiate tumour growth, confirming that CTCs are not merely dead or dying tumour cells shed into the circulation and that they warrant ongoing study. Secondly, this approach provides a new *in vivo* model system of SCLC capable of generating abundant tissue which recapitulates the treatment response in patients for analysis, addressing the challenge that is limited access to patient tumour tissue acting as a barrier to clinical and translational research.

1.7 Clinical utility of CTC analysis

In addition to the genesis of novel model systems to address translational research questions, CTCs may have clinical application through their enumeration or molecular characterisation. CTC number has been evaluated as a prognostic biomarker (an objectively measurable characteristic that provides information on patient survival) and as a surrogate end point biomarker (an objectively measureable characteristic which is a surrogate for a clinical end point such as overall survival) and a predictive biomarker in lung cancer (described in sections 1.7.1 to 1.7.3 below). In addition, CTCs are beginning to be utilised to address questions of tumour biology which in turn provides a foundation for development of novel therapeutic approaches. It was this application of CTCs to interrogate lung cancer biology that was the main goal of this thesis.

1.7.1 CTC enumeration as a prognostic biomarker

CTC number measured with CellSearch at baseline (before any therapy) is FDA approved as a prognostic biomarker in breast,[67,68] colorectal[69,70] and prostate[71,72] cancers. The presence of CTCs has now been incorporated into the American Joint Committee on Cancer (AJCC) staging system for patients with breast cancer who have CTCs present (or DTCs in the bone marrow) but no overt metastases staged as cM0(i+). This amendment to the AJCC staging recognises the association with shorter patient survival and demonstrates the application of CTC analysis to clinical practice.

Our group has previously shown that elevated CTC number is associated with worse survival in NSCLC (with a prognostic cut off 5 CTCs/7.5 ml).[73] However, this test has insufficient sensitivity to be applied to patient treatment decisions,

with a sensitivity of 26% and specificity 100% (using a cut off of 5 CTCs) with respect to survival at 6 months from ROC curve analysis. Although two subsequent studies in Japanese populations found that CellSearch CTCs are associated with shorter patient survival in stage 4 NSCLC[74,75] these studies were underpowered to resolve this debate, including only 33 and 24 patients in each.

In patients with SCLC, three reports were published in 2012 offering different prognostic cut-off levels ranging from 2 to 50 CTCs/7.5 ml (summarised in Table 1.3).[57,76-78] These studies included heterogeneous patient populations. In the UK study by our lab (Hou *et al.*[57]) there were a greater proportion of patients with extensive stage disease, more metastatic sites and a greater frequency of liver and bone metastases than the Japanese study by Naito *et al*..[76] The proportion of patients with performance score of 2-4 was highest in the UK study. In addition, other than the bias between patient characteristics, there may also be biological differences between a mainly male Japanese population and a mixed (male/female) European population in the other two studies. Furthermore, the largest sample size reported in the study by Hou *et al*. is more likely to give an accurate prognostic cut-off. More recently, this area was added to by a study by Normanno *et al.* reporting the prognostic impact of CTC number in 60 patients with extensive stage SCLC.[78] This Italian study reported a prognostic cut off of 282 CTCs/7.5 ml. This dramatic difference may be due in part to the inclusion of exclusively extensive stage patients in this study.

Although meta-analyses have been performed of the studies of the prognostic utility of CellSearch CTCs in both NSCLC[79] and SCLC,[80] more accurate interpretation of these data may be obtained by pooled analyses of CTC and

clinical data. This approach however may be limited by variation in the protocols for clinical data collection and sample collection between studies.

	Hou[57]	Naito[76]	Hiltermann[77]	Normanno[78]
Prognostic cut off in CTC number/ 7.5 ml	≥50	≥8	≥2	≥282
Number of patients	97	51	59	60
Population studied	UK	Japan	Netherlands	Italy
Gender (%)				
Male	44	86	59	80
Female	56	14	41	20
PS (%)				
0	12	41	46	22
1	47	41	37	52
2	32	18	7	26
3/4	8	0	10	0
Stage (%)				
Limited	32	53	36	0
Extensive	68	47	64	100

Table 1.3 Clinical characteristics of SCLC patients included in studies evaluating the prognostic significance of CTCs detected by CellSearch prior to chemotherapy
Abbreviations: PS performance status; UK United Kingdom

Beyond enumeration of CTCs as a prognostic biomarker, the identification of CTC sub-populations based upon either genetic alterations or protein expression may also have the potential to act as a prognostic biomarker. Such CTC sub-populations predicting clinical outcomes are yet to be defined, however, future studies should consider whether relative sub-populations of CTCs rather than total CTC populations may have utility as a prognostic biomarker.

1.7.2 CTC enumeration as a surrogate end-point biomarker

CTCs also have potential clinical application as a surrogate end point biomarker. CTC enumeration is advantageous compared with radiological assessment as a change in number after one cycle of chemotherapy is an earlier assessment compared with the timing of radiological assessment which is typically after 3 months of therapy, allowing for a more timely change in treatment in the absence of clinical benefit.

In a study of 41 patients with NSCLC receiving erlotinib and pertuzumab, CTCs isolated by CellSearch were evaluated alongside radiological assessment with computerised tomography (CT) and positron emission tomography (PET). A decrease in CTC number with treatment correlated with a radiological response to treatment and was associated with longer progression free survival.[81] Although the scarcity of CTCs in NSCLC patients by CellSearch limits their use as a surrogate end-point (in the study by our lab, only 21% of advanced NSCLC patients have CTCs detected at baseline[73]), the greater sensitivity of other methods of CTC isolation,[46,47,61] as discussed above, may allow CTC enumeration to be used as a surrogate end-point biomarker in NSCLC in the future, and further studies are warranted to define the role of CTCs as a surrogate end point biomarker in NSCLC.

The potential to use CTCs as a surrogate end point would be greater in patients with SCLC, where up to 85-90% of patients with extensive stage disease would be expected to have CTCs present by CellSearch.[78,82] This has been the subject of three studies[76,78,83] showing a decrease in CTC number after one cycle of chemotherapy was the strongest predictor of overall survival and superior to radiological assessment.

This role of CTCs as a surrogate end point is a promising finding which challenges the current use of radiological assessment for the same purpose in lung cancer. In breast cancer, this has been addressed in a clinical trial. The SWOG S0500 study assessed the potential for CTC directed clinical decision making, evaluating the utility of a change in CTC number following therapy in directing clinical practice. This prospective study randomized patients with metastatic breast cancer who had a persistently elevated CTC count (≥5/7.5 ml blood) after commencing chemotherapy to either maintain current therapy or switch to an alternative chemotherapy regimen.[84] This study did not detect a significant improvement in patient survival following early switching of therapy in patients without a CTC response. One reason for the absence of benefit in this study may be due to the failure to offer an effective intervention. A patient whose cancer progresses through one line of chemotherapy rarely responds well to a second line of chemotherapy even if it is a different class of drug.

By selecting the patients with the worst outcomes using persistent CTC elevation, but not offering any intervention other than earlier than planned change from one ineffective chemotherapy regimen to another which was likely to be also ineffective, the SWOG S0500 study failed to show that the CTC directed change in clinical practice brought any patient benefit. For future studies of CTC directed patient management such as this to show benefit, they will have to incorporate the identification of early progression with an effective second line therapy.

1.7.3 CTC characterisation as a predictive biomarker

Molecular characterisation of enriched populations of CTCs to identify molecular drivers of the disease is beginning to be explored with the potential to have a

significant impact on clinical practice if this approach can be utilised as a 'liquid biopsy'. As described above, in NSCLC, predictive biomarkers in clinical practice using primary tumour biopsies include the EML4-ALK gene rearrangement[33] and the activating and treatment resistance mutations in the EGFR gene.[34] ALK gene rearrangement was reported in ISET enriched CTCs by *fluorescent in situ hybridization* and this correlated with ALK status in the patients' tumour samples,[85] demonstrating the potential to be used as a predictive biomarker to select patients who are likely to benefit from ALK inhibition therapy with crizotinib. In addition, EGFR activating mutations and T790M resistance mutations were identified in enriched populations of $EpCAM^+$ NSCLC CTCs isolated using the HB-CHIP[86] and CellSearch.[87] Although these approaches to CTC profiling are not yet validated for clinical decision making, these results show the potential clinical applications of these platforms. Future clinical studies characterising CTCs as a predictive biomarker will have to address the issue of whether to profile single cells or pools of cells.

In parallel with the development of CTC enrichment platforms, there have been advances in genome and transcriptome profiling of single CTCs which may be superior to profiling enriched populations. Firstly, the sensitivity and specificity of the analysis of single CTCs may be superior due to the complete separation of CTCs from contaminating leukocytes. Secondly, analysis of single cells will permit identification and interrogation of specific sub-populations of CTCs rather than entire populations. Since the first study reporting genetic mutational profiling of single tumour cells isolated from the bone marrow,[88] this approach has been applied to single CTCs from patients with melanoma[89] and colorectal cancer,[90,91] identifying tumour specific mutations within CTCs which are absent

from the leukocytes and showing heterogeneity between the primary tumour and metastases and between individual CTCs. Gene expression profiling has also been performed on single CTCs from prostate cancer,[92,93] breast cancer[94] and melanoma[95] demonstrating the technical feasibility of RNA profiling from patient CTCs. Future studies will be required, however, to identify clinically relevant changes in gene expression which have utility in patient management.

1.7.4 CTC characterisation to interrogate tumour biology

In addition to the characterisation of CTCs to aid their implementation as a biomarker for the personalisation of cancer treatment, characterisation of CTCs may be used alongside biopsies of primary tumors and metastatic sites to interrogate tumour biology.

Profiling of CTCs provides two clear benefits over the use of tumour biopsies in the characterisation of tumour biology. Firstly, as CTC sampling is safer than performing a tumour biopsy, repeat sampling is feasible and this facilitates analysis at multiple time-points throughout the course of the disease process (longitudinal analysis). This longitudinal analysis is required to evaluate tumour evolution in response to treatment and upon disease relapse and progression through therapy. Understanding the cellular and molecular events driving tumour progression through therapy will enable the development of novel approaches to overcoming resistance to therapy.

Secondly, as a single tumour biopsy is unlikely to reflect the complete tumour heterogeneity, CTCs may better reflect this heterogeneity, although this is yet to be confirmed.[96] Understanding the degree to which CTCs can be utilised to understand tumour evolution and tumour heterogeneity in lung cancer is one of

the objectives of the recently launched TRACERx (tracking non-small cell lung cancer evolution through therapy) study.[97] In one element of this study, CTCs from patients with lung cancer will be collected and analysed from diagnosis to relapse and before and after surgery and chemotherapy treatment (see Figure 1.1) and these findings may shed further light on clonal evolution and tumour heterogeneity in lung cancer.

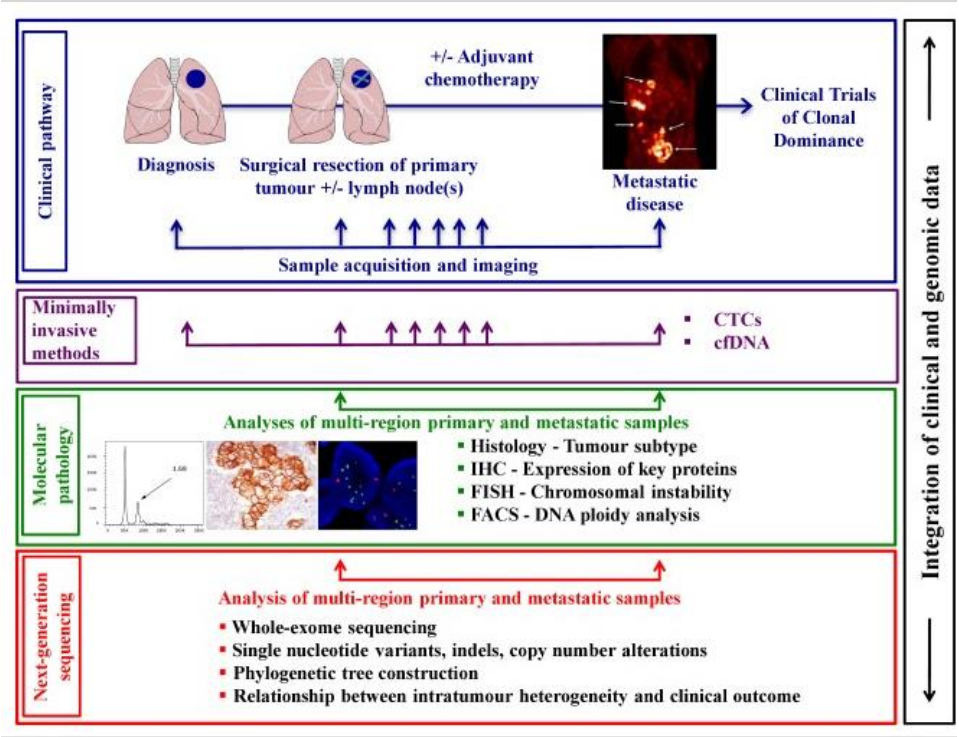

Figure 1.1 Schematic for the TRACERx consortium protocol incorporating CTCs to the investigation of tumour heterogeneity and clinical outcomes
Figure adapted from Jamal-Hanjani 2014.[97]

Within this thesis, I have sought to evaluate the utility of CTCs to interrogate two areas of tumour biology which are currently the subject of much academic debate and which have been proposed as putative mechanisms of tumour progression and resistance to chemotherapy: Epithelial to mesenchymal

transition (EMT) and vasculogenic mimicry (VM). Both of these biological processes have been described in association with cancer stem cells. The remainder of this introduction will cover these three concepts within tumour biology, an improved understanding of which will facilitate exploitation of these areas for therapeutic gain.

1.8 Epithelial to mesenchymal transition

Epithelial to mesenchymal transition (EMT) was initially described in embryogenesis.[98] In order for this process to occur, cells undergo a complete cellular reprogramming which changes their structure and function. During gastrulation within the developing embryo, ectodermal cells lose their apical-basal polarization and cell-cell contacts allowing them to detach from the adjacent cells and migrate to produce the mesoderm (type 1 EMT). This permits their motility through the embryo as spindle-shaped mesenchymal cells with a motile cytoskeleton.

This same cellular re-programming reported in gastrulation is also reported to play an important role in wound healing and fibrosis (type II EMT).[99] The concept has been extended to cancer metastatic progression (type III EMT), where it is proposed that epithelial tumour cells (reviewed in Thiery 2002[100]) are also able to adopt the same characteristics as those described during EMT in the developing embryo in order to break away from the tumour mass, invade the adjacent tissues and enter the circulation in order to metastasise to distant sites. This is summarised in the schematic below (Fig 1.2 (adapted from[100]).

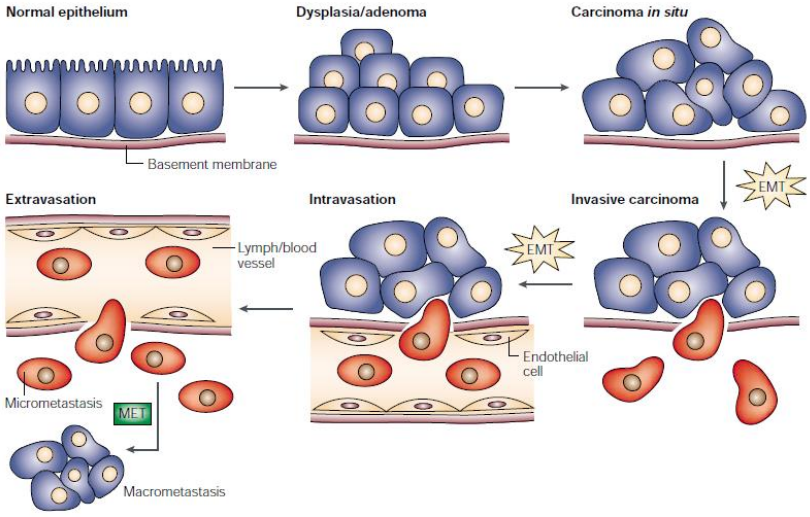

Figure 1.2 Schematic of epithelial to mesenchymal transition in cancer metastatic progression
Epithelial tumour cells are shown in blue forming the primary tumour and the macroscopic metastases. Mesenchymal tumour cells are shown in red invading the circulation, travelling as CTCs and exiting the vasculature (extravasating) at distant sites. In this paradigm, EMT is proposed to occur within the developing tumour to enable invasion through tissue and distant metastasis. To enable colonisation and epithelial tumour outgrowth at distant sites, the reverse process or mesenchymal to epithelial transition (MET) is proposed to occur. Figure adapted from Thiery 2002.[100]

1.8.1 Approaches to tumour classification as epithelial or mesenchymal

1.8.1.1 Analysis of tissue architecture

Taking an anatomical approach, epithelial tumours (or carcinomas) arise from epithelial structures lining the viscera and mesenchymal tumours (or sarcomas) arise from mesenchymal structures such as muscle, bone and cartilage. Mesenchymal tumours are described as having a distinct histological appearance including loss of intercellular adhesions, spindle shape and invasion of adjacent tissue.[100] These appearances contrast with those of epithelial tumours which retain cells organised with some degree of differentiation (eg glandular or squamous) consistent with the original tissue. However, some epithelial tumours have mesenchymal appearances such as the

spindle cell carcinoma and sarcomatoid carcinoma and these counterparts of epithelial tumours are characterised by aggressive clinical behaviour.[101]

1.8.1.2 Analysis of protein expression

In addition to having a mesenchymal histological appearance, protein expression by tumours has been used to aid their classification as epithelial or mesenchymal. Panels of markers are typically used to classify regions of tumours or individual tumour cells, but there is no defined panel of epithelial and mesenchymal markers. Although when analysing tumour biopsies, multiple markers can be analysed as long as sufficient tumour tissue is available in the sample, when using immunohistochemistry or immunofluorescence to analyse CTCs, most studies are limited to a small panel of epithelial and mesenchymal markers.[102-105]

Using this approach to analyse biopsy specimens, replacement of the epithelial intermediate filaments cytokeratins with the mesenchymal intermediate filament vimentin or loss of the epithelial calcium dependent cell adhesion protein E-Cadherin and gain of its mesenchymal counterpart N-cadherin are amongst the most commonly described alterations associated with EMT.[106,107]

The significance of mesenchymal markers is highlighted by correlative studies showing their presence is associated with worse clinical outcomes in many cancer types[108-111] including NSCLC.[112-115] However, these studies involving clinical samples have been descriptive, and correlative studies are not able to provide direct evidence that EMT occurs. Indeed, the presence of mesenchymal markers in clinical specimens has yet to be definitively linked to the process of

EMT. This remains a hindrance to the acceptance of the EMT hypothesis. This debate surrounding EMT and the potential application of CTCs to its resolution are discussed in section 1.8.3 below.

1.8.1.3 Analysis of gene expression

Use of gene expression signatures allows larger panels of epithelial and mesenchymal markers to be evaluated compared with analysis of protein expression as described above.[106,116-122] The most comprehensive of these which has been applied to lung cancer patients was recently reported by the Lab of Prof Thiery.[106] It comprises a 315 gene EMT signature incorporating three of the earlier published signatures[116,121,122] which has been cross validated using cell lines and clinical samples and applied to patients with lung cancer. Within this signature the authors highlight 11 genes encoding previously published EMT transcripts[123-126] which were consistently selected in the lung cancer specific EMT signature and generic EMT signatures. Table 1.4 summarises these 11 genes within the EMT signature which include the epithelial intermediate filaments cytokeratin and mesenchymal intermediate filament vimentin among the most highly weighted genes within the epithelial and mesenchymal signatures respectively. These two markers were selected to be taken forwards within this thesis for CTC profiling.

Gene	Gene name	Function
Epithelial		
KRT19	Cytokeratin 19, Keratin, type 1 cytoskeletal 19	Intermediate filament, structural constituent of cytoskeleton
RAB25	Ras related protein Rab-25	Small GTPase, membrane trafficking
CDH1	E-cadherin, Cadherin 1, type 1,	Cell adhesion protein, calcium ion binding, G-protein coupled receptor activity
EPCAM	Epithelial cell adhesion molecule	Calcium independent cell adhesion molecule, receptor activity
GRHL2	Grainyhead-like protein 2 homolog	Transcription factor activity
Mesenchymal		
VIM	Vimentin	Intermediate filament, structural constituent of cytoskeleton
ZEB1	Zinc finger E-box binding homeobox 1	Transcription factor activity
ZEB2	Zinc finger E-box binding homeobox 2	Transcription factor activity
CDH2	N-cadherin, Cadherin-2, type 1	Cell adhesion protein, calcium ion binding, G-protein coupled receptor activity
TWIST1	Twist-related protein 1	Transcription factor activity
SNAI2	Zing finger protein SNAI2	Transcription factor activity

Table 1.4 The epithelial and mesenchymal genes consistently selected within the generic EMT gene expression signature reported by Tan 2014.
Adapted from Tan *et al.* 2014.[106]

1.8.2 Studies of the mesenchymal cytoskeletal protein vimentin and the epithelial cytoskeletal protein cytokeratin in EMT

The family of cytokeratin proteins were first described as the intermediate filaments characterising epithelial cells in 1982,[127] and shortly after, vimentin was described as the intermediate filament characterising mesenchymal cells.[128] Intermediate filaments make up the cytoskeleton, connecting the nuclear envelope to the plasma membrane and connecting with intermediate filaments of adjacent cells via desmosomes or to the extracellular matrix via hemi-desmosomes. As such, they define the cell shape and its relationship with its surroundings, and additionally they organise proteins involved in attachment, migration and cell signalling.

Although the expression of vimentin in patient tumours is known to associate with poor clinical outcomes,[110,129-131] there are few mechanistic studies on cytoskeletal proteins in EMT. Cell motility and invasion are key traits attributed to EMT which are consistent with the histological description of mesenchymal tumour described above as being composed of sheets of spindle cells which lose cell-cell contacts and invade adjacent tissue. The properties of motility and invasion have been evaluated in pre-clinical studies with respect to vimentin expression as a surrogate for EMT. In a study of prostate cancer cell lines, vimentin was shown to be highly up-regulated in CL1, an aggressive sub-line derived from continuous passaging of LNCaP in hormone depleted medium. Using an *in vitro* invasion assay, transfection of CL1 with vimentin antisense was shown to reduce vimentin expression and reduce invasiveness. However, forced over-expression of vimentin in LNCaP cells had no effect on invasiveness, suggesting that in this context although

vimentin expression may contribute to invasive potential of these cell lines, it was not sufficient alone to confer this property in this setting.[132] In a more recent study in melanoma cell lines, vimentin over-expression was sufficient to promote cell motility and invasion.[133]

Co-expression of cytokeratins and vimentin has also been shown to promote invasive cell behaviour *in vitro*. Forced co-expression of vimentin and cytokeratins in breast cancer cell lines increased cell motility and invasion and this effect was abrogated by vimentin anti-sense oligonucleotide.[134,135]

More recently the function of vimentin in cell motility was evaluated in lung cancer cell lines[136] by using a phosphoproteomics screen to identify cell motility proteins that show changes in phosphorylation following depletion of vimentin. The greatest loss of phosphorylation was seen in VAV2 (which regulates cell motility and adhesion through its role as a guanine nucleotide exchange factor for the small Rho GTPase RAC1).[137] VAV2 normally complexes with vimentin and focal adhesion kinase (FAK) at focal adhesion complexes. In addition to loss of phosphorylation of VAV2, FAK phosphorylation was also reduced following vimentin depletion, suggesting that vimentin promotes stabilisation of FAK via VAV2 mediated RAC1 activation.[136]

These few studies assessing the functional role of cytokeratins and vimentin in motility and invasion (these attributes being described as characteristics of EMT) provide some preliminary experimental evidence to support that notion that switching intermediate filaments from cytokeratins to vimentin may have

a functional role in driving EMT. In addition, as cytokeratins and vimentin are well described as the intermediate filaments defining epithelial and mesenchymal cells respectively[127,128,138] and they were identified as epithelial and mesenchymal markers in the gene expression signature described above[106] they were selected for inclusion in the CTC profiling assay developed during this research.

1.8.3 Criticism of the EMT model of cancer progression

A high profile criticism of EMT in cancer progression was posited by Tarin in 2005.[139] Tarin attributes the histological features of type III EMT (described in 1.8.1.1 above) to degrees of cellular disorder extending to pleomorphism and anaplasia which are characteristic of carcinomas and not as evidence for the existence of a fundamental switch from epithelial to mesenchymal lineage *per se*. However, gene expression profiling of mesenchymal tumours and comparison with epithelial tumours shows more widespread changes consistent with published EMT gene expression panels suggesting a more complete cellular reprogramming.[140,141]

The challenge to the EMT hypothesis that CTC profiling has the greatest potential to contribute to arises from clinical observations that metastatic deposits often resemble the mainly epithelial primary tumour, rather than being mesenchymal in appearance,[142] and this issue is discussed below.

1.8.3.1 Epithelial and mesenchymal plasticity in metastasis

To explain this similarity between epithelial primary tumours and metastatic sites, it has been proposed[100] that tumour cells transition from epithelial to

mesenchymal states, reverting back to an epithelial state at distant sites by the reverse process, mesenchymal-to-epithelial transition (MET) as described in embryological organ development[143] (Figure 1.2). Direct evidence of this plasticity between epithelial and mesenchymal states remains elusive. However, CTC analysis provides a unique opportunity to contribute to this debate. If applied alongside analysis of primary tumour biopsies and metastatic sites, a validated CTC profiling assay will be able to characterise CTCs in the process of metastasis for evidence of EMT as cells transit the circulation prior to the reverse MET process.

1.8.3.2 Epithelial and mesenchymal cell co-operation in metastasis

Two recent studies developed the EMT paradigm further by proposing evidence for epithelial-mesenchymal cell co-operation in metastasis as an alternative model to EMT and MET as a fluid process. This was first demonstrated using a model of epithelial and mesenchymal cancer cells derived from hamster oral keratinocytes.[144] Pure populations of either epithelial or mesenchymal cells formed tumours at the sub-cutaneous injection site in mice. Only mesenchymal cells entered the blood but neither cell type alone led to formation of lung metastases. When administered intravenously, only the epithelial cells formed lung metastases. The sub-cutaneous administration of mixed epithelial and mesenchymal cells led both cell types to enter the circulation and lung metastases formed from the epithelial population. These observations suggest that cellular co-operation may be required (mesenchymal cells invading and allowing 'passenger' epithelial cells to follow) for tumour cells to complete the metastatic cascade

(Figure 1.3). If this hypothesis is correct, it provides an explanation for the observation that the primary sites and metastatic sites both have a similar epithelial appearance even though EMT has occurred to enable metastasis.

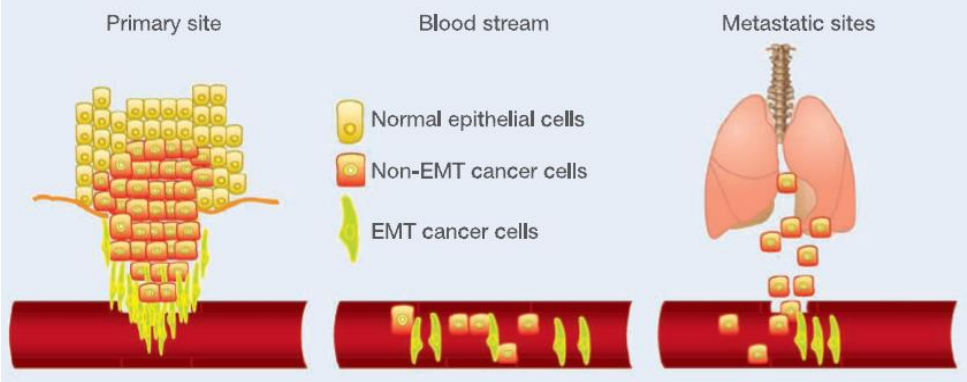

Figure 1.3 Schematic of epithelial and mesenchymal cell cooperativity in cancer metastatic progression
Mesenchymal cells are shown in green invading the circulation allowing both epithelial and mesenchymal tumour cells to metastasise as CTCs. Epithelial tumour cells alone form metastatic colonies at distant sites. (Adapted from Tsuji *et al.* 2009).[145]

A second mouse model of small cell lung cancer classified tumour cells as neuroendocrine or mesenchymal and supports the co-operation hypothesis.[146] When either neuroendocrine or mesenchymal cell type was administered separately by sub-cutaneous injection into immune-compromised mice, local tumours formed without liver metastases whereas both cell types administered together led to development of liver metastases. These studies together suggest that both epithelial and mesenchymal cells may be required to co-operate in the production of metastasis, although the exact mechanisms underpinning this cellular co-operation remain unclear. This area remains an intriguing hypothesis to be tested and the development of a validated CTC EMT profiling assay may contribute to this debate,

providing a unique opportunity to characterise tumour cells in the process of metastasis.

1.8.4 Association between EMT and cancer stem cells

1.8.4.1 The cancer stem cell hypothesis

There has been recent interest in defining the relationship between EMT and cancer stem cells. However, the concept of cancer stem cells in non-haematological malignancies such as lung cancer remains controversial and will be introduced first before expanding on the association between EMT and cancer stem cells. The cancer stem cell hypothesis posits that cells within a tumour are hierarchically organised akin to normal tissues. Cancer stem cells are proposed to be a small sub-population of cancer cells which are able to self-renew (producing other cancer stem cells) and maintain the tumour by differentiating into the multiple cell lineages (other sub-populations of cancer cells which are not cancer stem cells) which make up the tumour.[147,148]

The existence or otherwise of cancer stem cells within a hierarchically organised tumour is significant as it is postulated that these rare cells within the tumour are responsible for maintaining tumour growth, driving chemotherapy resistance and fomenting relapse following standard therapy,[148] and the identification and targeting of these sub-populations may therefore result in cures for metastatic disease where this is not presently achievable.[149] This contrasts with the traditional approach of treating the cancer by eliminating as many cells as possible, on the assumption that most cells are capable of recapitulating the tumour. However, definitive proof that

cells within the tumour are organised in this hierarchical way is difficult to produce.

1.8.4.2 Transplantation assay to detect tumour initiating cells

The gold standard experimental approach to identify and define cancer stem cells as having the properties of self-renewal and multi-potent differentiation has been through transplantation assays. A schematic of the transplantation assay is set out in Figure 1.4 (adapted from Shackleton 2009).[150] Solid tumours are dissociated into their cellular constituents, and dead cells and non-cancer cells (stromal cells including leukocytes, endothelial cells and fibroblasts) are excluded. Cells are then sorted into sub-populations based upon their expression of cell surface markers (hypothetical markers shown here as red and blue) before being transplanted into immune-compromised mice to evaluate for tumour growth. The stem cell population (shown as red cells in this schematic) are able to initiate tumour growth and must then be confirmed to produce tumours with serial transplantation (confirming self-renewal) and give rise to the non-tumourigenic cancer cells (confirming multi-potent differentiation). Non-tumourigenic cells should be shown to be alive and also to have genetic or epigenetic variation from tumourigenic cells.

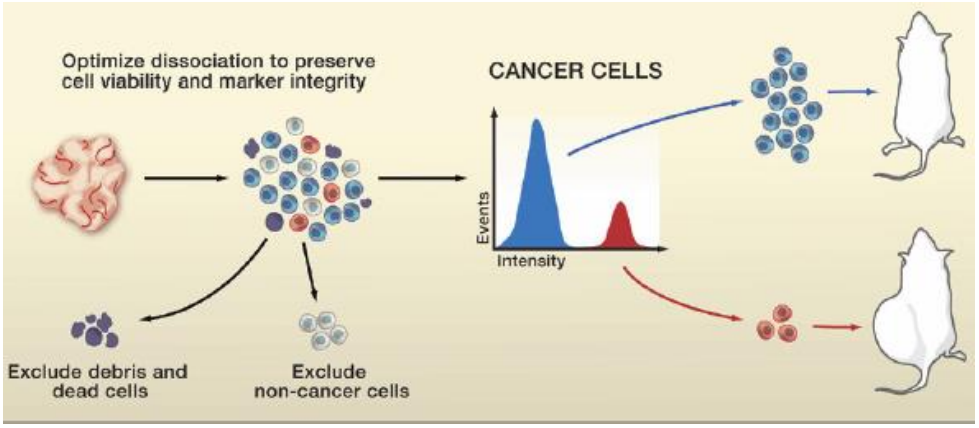

Figure 1.4 Schematic of the transplantation assay used as the gold standard experimental approach to define and characterise cancer stem cells
Adapted from Shackleton 2009.[150]

Early studies used the immunodeficient non obese diabetic/ severe combined immune-deficiency (NOD/SCID) mice. In these mice the SCID mutation is transferred on a NOD background. Homozygous SCID mutation impairs B and T lymphocyte development and the NOD background impairs NK cell function.[151] The use of such immune-compromised mice permits xenotransplantation to take place circumventing the immune surveillance which would ordinarily prevent tumour growth. The mice are evaluated for tumour growth at the site of injection confirming tumour initiating ability. Cells are immunophenotyped before implantation and then passaged to identify 'tumour-initiating' sub-populations which are able to demonstrate self-replication and produce differentiated progeny. Using this approach, small sub-populations of cells with these properties (self-renewal and differentiation) have been identified in multiple cancer types including breast cancer,[152] glioblastoma,[153] colon cancer,[154] melanoma,[155,156] ovarian cancer,[157,158] prostate cancer[159] and pancreatic cancer.[160] Based on their

tumour initiating properties in this assay, these cells are often referred to as 'tumour initiating cells'.

1.8.4.3 Limitations of the transplantation assay

These data showing small tumour cell sub-populations capable of self-renewal and differentiation are the best evidence to date that stem-cells exist within solid tumours. However, there are limitations to this approach. These early studies have shown that only small sub-populations of tumour cells have these properties, typically 0.001% to 0.01%.[150] This is consistent with the cancer stem cell hypothesis which predicts that stem cells would be rare.[161] However, more recent reports suggest that tumour initiating cells are not as rare as previously thought. The NOD/SCID mouse model has been further immune-depleted, generating an interleukin-2 receptor gamma chain null (NOD/SCID IL2rg$^{-/-}$ or NSG) strain resulting in a more profound depletion of mature B and T lymphocytes and NK cells.[162] In direct comparison between NOD/SCID and NOD/SCID IL2rg$^{-/-}$ mice using lung cancer cell lines (A549 and EBC1), tumour growth was more successful in the NOD/SCID IL2rg$^{-/-}$ mice following sub-cutaneous administration of tumour cells.[163] In this study, using a limiting dilution analysis, when 10^4 EBC1 were administered, tumours formed in 5/5 NOD/SCID IL2rg$^{-/-}$ mice and 2/5 NOD/SCID mice. When 10^3 EBC1 cells were administered, again tumours formed in 5/5 NOD/SCID IL2rg$^{-/-}$ mice and 0/5 NOD/SCID mice. These data using cell lines confirmed that this model increased the likelihood of tumour cells being classified as tumorigenic. More recently, female NOD/SCID IL2rg$^{-/-}$ mice

have been demonstrated to be more efficient at engraftment than male mice.[164]

This NOD/SCID IL2rg$^{-/-}$ model has improved the success of xenotransplantation assays in producing tumour growth. In a study on human melanoma xenografts in this model by Quintana *et al*.[165] using single cell transplants, 27% (69/254 transplants) of single melanoma cells formed tumours when administered with Matrigel sub-cutaneously. Tumorigenic cells were common in tumour from primary and metastatic melanoma and from patient samples and xenografts. This contrasts with 1/827,000 tumour cells forming tumours in NOD/SCID mice.[156,165] This rarity of tumour initiating cells identified using NOD/SCID mice was consistent with previous reports in other cancer types.[152,154,166-168] These findings suggest that the low frequency of tumour initiating cells described in the early studies may be a reflection on the experimental model rather than due to properties of the tumour cells studied.[169]

In subsequent studies in other cancer types including NSCLC, pancreatic cancer and head and neck cancer, although the NOD/SCID IL2rg$^{-/-}$ model increased the frequency of cells which were tumour initiating, compared with NOD/SCID model, tumour initiating cells remained rare (fewer than 1 in 2500 cells).[170] The finding that tumour initiating cells are not as rare a population as previously thought brings into question the hierarchical organisation of tumour tissue in melanoma which is a pre-requisite of the stem cell hypothesis. If this finding in melanoma cells is consistent among other solid tumours, and the transplantation assay is able to identify tumour stem cells,

then it does not follow that we will be able to more effectively treat cancer by targeting small minority sub-populations. However, it may be the case that melanoma does not closely follow the stem cell paradigm whereas other cancers such as lung cancer do.

A further limitation of the transplantation assay is that it fails to account for the influence of the immune system on the behaviour of the tumour cell populations being studied. The frequency of tumorigenic cells within a tumour may be significantly overestimated due to the removal of immune surveillance which would operate to remove cancer cells. Conversely, tumourigenic sub-populations may be underestimated due to the incompatibility between human receptors on the transplanted tumour cells and mouse ligands for growth factors or adhesion molecules.

Although it remains uncertain whether cells identified using transplantation assays truly are cancer stem cells, with the hierarchical implications this infers for the cells ability to initiate tumour growth and drive resistance to therapy, these studies using transplantation assays have shown quite clearly is that there is intra-tumour heterogeneity defined as multiple sub-populations within a tumour of a single patient with different tumour initiating ability and displaying different capacity to survive treatment with chemotherapy. However this intra-tumour heterogeneity with respect to tumourigenic ability is consistent with both the tumour stem cell paradigm or with this variation having arisen through clonal evolution.

1.8.4.4 Explaining the heterogeneity: Tumour stem cells or clonal evolution

Much or even all of the variation seen within tumours may be due to clonal variation produced during tumour evolution[171,172] which does not require a strict hierarchical organisation of the tumour. The clonal evolution paradigm first proposed in the 1970s suggests that cancers typically arise from a single cell of origin and as a consequence of variation during cell replication, genetic or epigenetic changes are accumulated over time giving rise to intra-tumour genetic heterogeneity.[173] This results in functional differences arising between populations of cells within a tumour with some sub-clones gaining a survival advantage. Within the clonal evolution paradigm, tumourigenic cells would be predicted to be frequent within the transplantation assays, as limitless replicative potential is described as a hallmark of cancer.[174] This contrasts to the stem cell model which predicts that tumour initiating cells would be rare.[150]

This debate over the existence or otherwise of the cancer stem cell has significant implications for future clinical practice in treating cancer. If cancers followed the stem cell paradigm then it may be possible to cure the cancer by eradicating the stem cell population. In contrast, if cancers followed the clonal evolution paradigm then one would have to target most or all cells within the cancer, as is the goal of cancer treatment currently. However, to further complicate the interpretation of studies in this field, these two paradigms may co-exist, in that cancer stem cells may themselves be expected to evolve by clonal evolution.[150] Accepting the limitations of our understanding of cancer stem cells outlined above, EMT has been described

in association with cancer stem cells in pre-clinical models[175] and these studies defining the association between EMT and cancer stem cells are introduced below.

1.8.4.5 The relationship between EMT and cancer stem cells

EMT has been described as arising due to the effect of signals from the tumour micro-environment on the tumour cells, both through direct signalling from extracellular matrix and the release of signalling molecules such as TGF-β[176] and Wnt which ultimately induce the expression of EMT associated transcription factors (eg SNAIL and TWIST). TGF-β induces cellular changes of EMT as described above, interacting with other pathways including ERK, p38 MAP kinase, Wnt-β catenin, and PI3 kinase.

EMT has been associated with the acquisition of stem-cell properties.[175,177] In the seminal study linking EMT with cancer stem cells,[175] immortalised breast epithelial cell lines were induced to undergo EMT by ectopic expression of the transcription factors snail or twist. These cells developed a mesenchymal gene expression profile consistent with EMT and were able to form mammospheres in culture*. In vitro* mammosphere formation is a property previously demonstrated in breast cancer cells with stem cell properties (multi-lineage differentiation, self-renewal and gene expression profiles consistent with stem cell phenotypes e.g. up regulation of genes such as stem cell growth factor).[178]

Moreover, following EMT these immortalised breast epithelial cells expressed $CD44^{high}/CD24^{low}$ phenotype consistent with previously reported breast cancer tumour initiating cell profiles originally derived from

transplantation assays[152] and they were more tumorigenic when injected into immune-compromised mice and these cells are capable of multi-lineage differentiation.[177] These observations provide the best evidence linking EMT with cancer stem cells. This suggests that EMT may be an intermediate step in the generation of cancer stem cells and, accepting the limitations in our understanding of the cancer stem cell hypothesis described above; therapeutic inhibition of EMT may have a role in the prevention of cancer stem cell generation.

1.8.4.6 EMT and chemotherapy resistance

Acquisition of EMT is associated with resistance to chemotherapy.[149,179] Breast cancer cell line HMLER with E-cadherin shRNA knockdown demonstrated mesenchymal features in vitro; spindle shaped cells with loss of cell-cell contacts. The proportion of cells with a $CD44^{high}/CD24^{low}$ phenotype (previously used to characterise breast cancer stem cells in transplantations assays[152]) increased 10 fold following E-cadherin knock down. When the sensitivity of these cell lines to breast cancer chemotherapy agents (doxorubicin and paclitaxel) were tested *in vitro*, the E-cadherin knock down cell line demonstrated increased resistance to both these agents. This model of breast cancer therefore suggests that induction of EMT enables cells to acquire resistance to cytotoxic chemotherapy and is associated with the acquisition of stem-cell like characteristics.[149]

To conclude on EMT and lung cancer stem cells, our understanding of cancer stem cells in lung cancer remains limited. No study has identified a caner stem cell population, consistent with the definition above, using the

transplantation assay in lung cancer. The best data we have is from analysis of NSCLC patient derived explant (PDX) models, finding cells with the phenotype $CD133^{+}/CXCR4^{+}/EpCAM^{-}$ were enriched within metastases[180] and transcriptional profiling found significant overlap between differentially expressed genes in the $CD133^{+}/CXCR4^{+}/EpCAM^{-}$ population and known EMT and tumour initiating cell profiles.[181] In addition to analysis of patient tumour material, analysis of CTCs provides a unique opportunity to understand the role of EMT in the metastatic cascade in lung cancer. The second area of tumour biology which is explored in this thesis is that of vasculogenic mimicry and this is introduced below.

1.9 Vasculogenic mimicry (VM)

Vasculogenic mimicry is a process whereby tumour cells hijack the normal biological process of vasculogenesis to produce their own primitive vascular networks. To understand the production of VM networks by tumour cells, first consider the biological processes involved in the production of blood vessels in the developing embryo and in normal physiology.[182] Vasculogenesis is a mechanism which gives rise to the primitive vascular network within a developing embryo from mesodermal precursors (haemangioblasts). During angiogenesis, this primitive vascular network is remodelled by endothelial sprouting or intussusceptive microvascular growth to form mature vascular networks.[183]

Tumours have been reported to produce their own primitive vascular networks lined by tumour cells that provide micro-circulation independently of non-cancer cells/stroma. It is hypothesised that they achieve this by hijacking

the embryonic mechanisms utilised by mesenchymal haemangioblasts during vasculogenesis. This process by tumour cells has therefore been termed vasculogenic mimicry (VM).[184,185]

In the seminal studies of VM in uveal melanoma,[186,187] it was observed that human uveal melanomas lacked necrosis and contained patterned loops of interconnected extracellular matrix. These loops were shown to contain erythrocytes and conduct fluorescent dye consistent with their identity as vascular channels. Electron microscopy confirmed these channels were lined by melanoma cells rather than endothelial cells. This was the first description of VM vessels in patient samples. Subsequent studies explored VM in melanoma further using a melanoma cell line (C8161) which was classified as aggressive due to its *in vitro* and *in vivo* invasive properties compared with the non-aggressive counterpart cell line (C81-61). Only C8161 was able to form fluid conducting channels in three-dimensional cultures *in vitro*.[186,187] Doppler studies of C8161 xenografts in nude mice before and after injection of micro-bubbles confirmed that the tumour cell lined vascular channels conducted blood within the tumour.[187]

In common with angiogenesis,[184] VM can be driven by a hypoxic tumour microenvironment providing an alternative to angiogenesis for the delivery to tumour of oxygen and nutrients and a potential escape mechanism for tumours treated with anti-angiogenic therapies.[188] The role of hypoxia in driving VM was first studied using *in vivo* studies of the VM competent melanoma cell line C8161 and the non-aggressive melanoma cell line C81-61. These cell lines were both injected into an experimentally induced

ischemic hind limb of nude mice. Only the C8161 cell line developed tumours and there was evidence of tumour cell lined vessels within them[189] demonstrating once again that C8161 was more tumourigenic and suggesting that it was better adapted to this hypoxic environment. This study did not however demonstrate that hypoxia drives VM. However, subsequent studies have addressed this further in glioblastoma, a disease in which VM has been described in patients.[190,191] Using glioblastoma xenografts, VM networks (described in this study as tumour derived endothelial cells) arose from tumour cells rather than stromal cells and an *in vitro* differentiation assay identified tumour hypoxia as a driver of the trans-differentiation of tumour cells into endothelial cells.[192] The significance of hypoxia signalling was further emphasised by a study using fibrosarcoma HT1080 cells showing that the hypoxia induced transcription factor HIF-1a is functional in VM. In this study, when the cells were primed with hypoxic conditions, they went on to produce VM structures *in vitro* and *in vivo* which was shown to be due to HIF-1a mediated up-regulation of neuropilin-1.[193]

The translational relevance of this research into VM formation in response to hypoxia is reinforced by the study of VM in glioblastoma, in which treatment of glioblastoma xenografts with a VEGF receptor inhibitor led to an increased frequency of the VM networks[192] suggesting that tumour cell VM may be an avenue for resistance to anti-angiogenic therapy.

1.9.1 VM vessels in patient tumours as a prognostic biomarker

Several studies, summarised below, have used immunohistochemistry analysis of patient tumours to evaluate for the presence of VM and correlated

this with clinical outcome. In the seminal study of VM in uveal melanoma, VM vessels were differentiated from endothelial vessels in tumour specimens by Periodic Acid Schiff (PAS) and CD31 (PECAM1, platelet endothelial cell adhesion molecule) immunohistochemistry.[186] PAS stains carbohydrate-rich macromolecules and therefore identifies basement membrane structures (in addition to collagen and intracellular glycogen) which envelop the tumour vessels. CD31 is an endothelial cell marker, staining both immature and mature endothelial cells.[194] This staining therefore permits the definition of $PAS^{+}/CD31^{-}$ structures as VM vessels, and endothelial vessels as $PAS^{+}/CD31^{+}$.

It is likely that the vasculature of a tumour comprises a dynamic mix of $PAS^{+}/CD31^{-}$ VM vessels and $PAS^{+}/CD31^{+}$ endothelial vessels and the term 'mosaic tumour vessels' has been proposed to this scenario.[195,196] In studies of colon carcinoma xenografts, vessels lacked expression of the endothelial markers CD31 or CD105 and tumour cells labelled with GFP contacted the vessel lumen. The tumour-lined vessels comprised 4% of the total vascular area in these studies.

Since the first report of VM vessels, CD31/PAS staining method has since been used to describe VM in multiple tumour types. A systematic review and meta-analysis including 1088 patients with multiple cancer types including NSCLC demonstrated that the presence of VM within the tumour is associated with poor 5 year survival (relative risk of death 1.36, 95% CI 1.218 – 1.517, p=<0.001).[197] To date there have been no reports of VM in

SCLC, although VM has been reported in patients with Merkel cell carcinoma, which, like SCLC is of neuroendocrine origin.[198]

The observation that VM networks are associated with worse patient survival has been proposed to be related to stem-like behaviour of tumour cells which enables their trans-endothelial differentiation. Acknowledging the caveats regarding cancer stem cells outlined in section 1.8.3 above, this hypothesis is supported by the expression of a stem cell gene signature in C8161 VM competent cells.[199]

However, when considering the impact of VM on clinical outcomes, it is possible that VM may have context dependent effects. For example, as outlined in Section 1.2 above, through enhancing the tumour vasculature VM may improve chemotherapy penetration[29] and therefore chemotherapy efficacy. Additionally, by enhancing the vasculature, VM networks may act to increase cell proliferation,[26] reduce hypoxia,[28] or normalise pH,[27] all of which may augment the activity of chemotherapy agents delivered to the tumour. It is likely that the effect of VM on an individual patient exhibits context dependency, determined by the chemotherapy sensitivity of the tumour which in itself varies between cancer types and typically reduces following exposure to chemotherapy. However, in the setting of chemotherapy naive small cell lung cancer, as this is usually a chemotherapy sensitive disease, if VM plays a significant role in SCLC biology, targeting the VM may have a detrimental effect on clinical outcomes unless it takes place after treatment with chemotherapy.

1.9.2 VM gene expression signature

Through the analysis of VM competent cell line C8161, in addition to identifying a stem cell gene expression profile, this study also identified the up-regulation of genes involved in angiogenesis and vasculogenesis.[199] The genes reported with the greatest fold-change in expression level are shown in Table 1.5. The gene encoding the cell-adhesion protein vascular endothelial (VE)-cadherin (CDH5) is amongst those most highly up-regulated (>100 fold up-regulation). VE-cadherin is a trans-membrane calcium dependent cell adhesion glycoprotein involved in homophilic adhesion, normally functioning to maintain endothelial cell polarity and a vascular lumen.[200,201] This protein was the first to be reported as having functional significance in VM,[202] described below. The role of other signalling pathways which have been reported to be functional in VM including laminin 5 ɣ2,[203] VEGFA,[204] notch[205] and nodal[206] and HIF1α[207] are reviewed elsewhere[208].

1.9.3 The role of VE-cadherin in VM

The seminal study reporting a functional role for VE-cadherin in VM in melanoma[202] demonstrated that VM competent C8161 melanoma cells expressed VE-cadherin. C81-61 cells which were not VM competent did not express VE-cadherin. Silencing of VE-cadherin in the C8161 cells prevented the formation of VM networks *in vitro*. Subsequent studies found that VE-cadherin modulates the activity and cellular location of EPHA2 (an epithelial cell associated kinase involved in angiogenesis) and down-regulation of EPHA2 also inhibits tumour cell VM.[209,210] Furthermore, focal adhesion kinase[211] (FAK) and phosphoinositide-3 kinase[212] (PI3K) are phosphorylated downstream of VE-cadherin and EPHA2 in melanoma VM which represent

potential avenues for therapeutic intervention. Subsequent to this work in VE-cadherin in melanoma, VE-cadherin has been shown to have a role in VM in other cancer types including oesophageal cancer,[213] glioblastoma[214] and osteosarcoma,[215] however, the role of VE-cadherin, if any, in lung cancer remains to be determined. Given that VE-cadherin was amongst the genes most highly up-regulated in the VM signature[199] and that it was the first to be shown to have a functional role in VM and subsequently the most extensively studied in VM, this protein was taken forwards as a putative biomarker of VM to be included in the CTC profiling carried out within this thesis.

Gene	Name	Function
CDH5	Vascular endothelial (VE)-cadherin	Cell-cell adhesion molecule
LAMC2	Laminin 5 ɣ2	Extracellular matrix protein
ESM1	Endothelial cell specific molecule 1	Endothelium specific signalling molecule
TIE1	Tyrosine kinase receptor 1	Endothelial tyrosine kinase
LOX	Lysyl oxidase	ECM remodelling
PLAU	Plasminogen activator, urokinase	ECM remodelling
PDPN	Podoplanin	Elongates endothelial extensions

Table 1.5 Angiogenesis and vasculogenesis related genes with the greatest fold-change increase in expression level in the 'VM signature' reported by Bittner 2000.
Gene expression of melanoma cells capable of forming VM networks *in vitro* (C8161) and those not capable of forming VM networks (C81-61) were compared and genes with the greatest reported increase in expression (>100 fold) in VM competent cells are shown. Table adapted from Seftor 2012[208] and Bittner *et al*.[199]

1.9.4 Association between VM and cancer stem cells

In addition to the cellular plasticity described with respect to EMT and the association with cancer stem cells, the same assessment has been made between VM and stem like plasticity. That is, there is evidence that tumour cells are able to give rise to endothelial cells, which are able to in turn give rise to tumours. Two key papers addressed this issue. Ricci-Vitiani *et al.*[216] showed that neural stem cells are able to differentiate into functional endothelial cell and that this association is critical in glioblastoma. They demonstrated that glioblastoma stem cells release VEGF and stroma derived factor 1. Cells lining the vasculature in tumour endothelium were demonstrated to carry tumour specific mutations demonstrating the neoplastic origin of the tumour vasculature, and a subset of these cells was able to generate anaplastic tumours which contained VM networks.

Additionally, Wang *et al.*[217] also demonstrated that a sub-population of endothelial cells within glioblastoma tumour vasculature contain tumour specific mutations consistent with them having tumour origin. Moreover, a subpopulation of CD133+ glioblastoma stem-like cells expressed VE-cadherin. A sub-population of these CD133+ glioblastoma cells were capable of maturation along both tumour and endothelial lineages. These studies together provide evidence of a tumour-endothelial cellular plasticity which may be a mechanism through which VM vessels arise.

1.9.5 Rationale for studying VM in SCLC

Given the observations that SCLC is known to have a hypoxic tumour micro-environment[218] and VM is driven by hypoxia,[189] this research sought to test the hypothesis that VM is a mechanism of SCLC dissemination. Further support is given to this hypothesis as SCLC yields the highest number of CTCs of all cancer types studied with CellSearch,[57] and the presence of VM may in part contribute to this by removing the endothelial cell barrier which would ordinarily need to be transgressed for tumour cells to enter the circulation. Thirdly, support is also given to this hypothesis as SCLC is a highly metastatic disease and VM has been described as a characteristic of aggressive tumour cells due to the association with stem-like plasticity.[199] Finally, there remains a real unmet clinical need in SCLC with platinum based chemotherapy being unchanged as the standard of care for the past 30 years.[6]

1.10 Conclusions

Lung cancer, which is characterised by early metastatic spread and chemotherapy resistance, is the commonest cause of cancer death. Improvements in survival through biomarker led personalised medicine and through understanding tumour biology requires access to tumour tissue which is difficult to obtain from patients with lung cancer. CTCs provide an alternative to tumour biopsy which is less invasive and readily repeatable. However, a better understanding of the biology of CTCs is needed for their potential to be fully exploited. The clinically relevant sub-populations of CTCs which are able to survive passage through the circulation to initiate

metastasis at distant sites, or are able to survive exposure to chemotherapy remain to be defined.

1.10.1 Overall hypothesis

The overall hypothesis tested within this thesis was that novel CTC sub-populations could be characterised in lung cancer patients permitting the evaluation of their clinical and biological significance.

1.10.2 Overall aim

The overall aim within this work was to identify novel sub-populations of lung cancer CTCs based upon their expression of markers of epithelial to mesenchymal transition and vasculogenic mimicry. Specifically, this research aimed to classify CTCs based upon their expression of the epithelial intermediate filament cytokeratin and its mesenchymal counterpart vimentin, or by the expression of VE-cadherin which has a well described functional role in vasculogenic mimicry and to explore the clinical and biological significance of these novel CTC sub-populations.

These areas of tumour biology were selected for two main reasons. Firstly, both EMT and VM have been proposed as mechanisms of resistance to anti-cancer therapy and therefore a better understanding of their role in lung cancer will facilitate the development of more effective treatments for this disease. Secondly, as both EMT and VM are implicated in metastatic dissemination, studying CTCs alongside tumour biopsies provides a unique opportunity as a window on the metastatic cascade to contribute to the existing debate, the clinical literature around which has to date been dominated by studies involving tumour biopsies.

2 GENERAL METHODS

Within this section are described the methods used for tissue culture and extraction of protein lysates for Western blotting. In addition, the procedures for CTC enrichment using ISET, CellSearch and RosetteSep and CTC processing to generate CTC derived explant models, and to analyse ISET filtered CTCs which were used within this thesis are described here. General statistical considerations are also reported here. The details of other methods used which are specific to each of the results chapters are described in the relevant chapters.

All research reported within the results of this Thesis was conducted by the author with the exception of the generation of VE-cadherin knock down H446 cell line (which was generated by Dr Kathryn Simpson, Clinical and Experimental Pharmacology lab) and the animal handling for in vivo experiments which was performed by the pre-clinical team (Clinical and Experimental Pharmacology lab, led by Dr Chris Morrow).

2.1 Culture of cell lines

The SCLC cell lines NCI-H526, NCI-H1048, NCI-H69, NCI-H187, NCI-H524, NCI-H345, NCI-H1694, NCI-H446, NCI-H146, DMS79, DMS114, CorL103 (American Type Culture Collection) and the C8161 cell line (a kind gift from Prof Mary J Hendrix) were authenticated (ampflstr, Applied Biosystems) and cultured in RPMI media (Life Technologies) and 10% foetal bovine serum (Biowest) at 37 degrees Celsius and 5% carbon dioxide. Once cells were grown to confluence, they were washed in PBS and adherent cell lines (DMS114, NCI-H1048, NCI-H1694, NCI-H446 and C8161) detached using 2

ml 0.25% Trypsin-EDTA (Sigma, Dorset, UK) for use in experimental procedures or to be passaged back into culture. Suspension cell lines were centrifuged at 400 x g for 5 minutes and washed again in PBS for use in experimental procedures or to be passaged back into culture.

2.2 Generation of protein lysates from cell lines

Cells were extracted from culture as described and mixed in 8 ml RPMI and centrifuged at 400 x g for 5 minutes and washed in PBS. Protein was extracted from the cell pellet using Cytobuster Protein Extraction Reagent (Novagen, Darmstadt, Germany). The volume of Cytobuster Protein Extraction Reagent as recommended in the manufacturer's instruction was added to the cell pellet and incubated with 1:100 dilution of protease inhibitor cocktail (Calbiochem, Ca, USA) at 4 degrees Celsius for 5 minutes. The extract was transferred to a micro-tube and centrifuged at 16,000 x g for 5 minutes at 4 degrees Celsius. The supernatant was transferred to new tube for measurement of protein concentration.

2.3 Determination of protein concentration within protein lysates

Protein concentrations were measured using BCA Protein Assay Kit (Pierce, IL, USA). 30µg of each protein lysate was denatured by mixing 1:1 with 2x laemlli buffer and heated to 100 degrees Celsius for 5 minutes. A series of albumin (BSA) standards were diluted as per manufacturer's instructions producing a series of standard concentrations ranging from 0 to 2000 µg/ml. BCA working reagent was prepared combining reagents A and B. 25 µl of each standard and each sample replicate were added to a 96 well plate and 200 µl of working reagent added to the well. The plate was incubated at 21

degrees Celsius for 2 hours then the absorbance measured at 562 nm on a plate reader. A standard curve was prepared by plotting the average Blank minus corrected 562 nm measurement for each BSA standard against its concentration in µg/ml. The standard curve was then used to determine the protein concentration of each sample.

2.4 Western blotting

Proteins were separated using SDS-PAGE (8 to 12% resolving gels) at 100 volts (Invitrogen, Paisley, UK) and protein size measured with Rainbow molecular weight marker (Amersham, Sweden). Proteins were transferred to nitrocellulose membrane (Bio-Rad, Herts, UK) at 100 volts for 90 minutes. Membranes were blocked for 1 hour with 5% milk in 0.1% PBS-T (Sigma, Dorset, UK) and incubated with primary antibody overnight at 4 degrees Celsius. Antibodies were used against cytokeratins (1:500, Clone C11, mouse, Sigma, F3418), vimentin (1:500, clone V9 mouse, Santa-Cruz sc6260), CD45 (1:500, Polyclonal, rabbit, Abcam, ab10559), VE-cadherin (1:500, Clone 16B1, eBioscience, mouse, 14-1449), GAPDH (1:2500, polyclonal, rabbit, Abcam ab9485) and tubulin (1:2500, polyclonal, rabbit, Abcam, ab15246) were diluted in 1% milk in 0.1% PBS-T. Membranes were washed and incubated for 1 hour at 21 degrees Celsius with HRP linked secondary goat anti-mouse or goat anti-rabbit (Dako, CA USA) diluted 1:2500 in 1% milk in 0.1% PBS-T then washed and visualised with chemiluminescence (ECL+ system, Amersham).

2.5 CTC enrichment from blood samples using RosetteSep

Peripheral venous blood was collected into 10 ml tubes containing EDTA (Becton Dickinson, NJ, USA, 368589) and stored at 21 degrees Celsius prior to processing within 30 minutes. The RosetteSep CTC enrichment cocktail containing tetrameric antibodies recognising leukocyte markers CD3, CD14, CD16, CD19, CD38, CD45, CD61, CD66b and glycophorin A on red blood cells was added whole blood at a concentration of 50 µl/ml and mixed by inversion. The sample was incubated at 21 degrees Celsius for 20 minutes. The sample was then diluted in an equal volume of PBS + 2% FBS and mixed gently by inversion. The sample was then layered gently on a density gradient medium, taking care to minimise any mixing of the density gradient medium and the sample. The volume of density gradient medium was used as advised in the manufacturer's instructions. The sample was centrifuged at 1200 x g for 20 minutes with the brake off at room temperature. The plasma layer was discarded then the enriched cells were removed from the interface between the plasma and the density gradient medium. The enriched cells were washed in PBS + 2% FBS ready for further use.

2.6 CTC derived explant (CDX) tumour growth

The author was part of the team performing the RosetteSep cell preparation step for CTC enrichment prior to CDX implantation and the design of experiments and analysis of results. The animal handling was carried out by the pre-clinical team within the Clinical and Experimental Pharmacology Lab with the support of the Cancer Research UK Manchester Institute Core Facility. Following RosetteSep enrichment, the CTCs were mixed with 100 µl

HITES (Life Technologies) and 100 µl Matrigel (BD Biosciences) and injected sub-cutaneously into the flank of NOD.Cg-*Prkdc*^{scid}*Il2rg*^{tm1Wjl}/SzJ (NSG) mice (Jackson Laboratories). Procedures were carried out in accordance with Home Office Regulations (UK) and the UK Coordinating Committee on Cancer Research guidelines and by locally approved protocols (Home Office Project license no. 40-3306 and Cancer Research UK Manchester Institute Animal Welfare and Ethical Review Advisory Board). In some instances, CDX were passaged following disaggregation using a human tumour dissociation kit (Miltenyi Biotech) following manufacturer's instructions. Murine cells were removed by mixing 20 µl anti-mouse IgG2a+b microbeads, 10 µl anti-mouse MHC Class I antibody (eBioscience) and 500 µl binding buffer, incubating at 4 degrees Celsius for 30 minutes, mixing with disaggregated tumour cells and incubating at room temperature for 15 minutes. Cell bead mixture was then applied to an LS column (Miltenyi Biotech) in a MidiMACS separator (Miltenyi Biotech) and flow through collected, the column washed with 4 x 3 ml binding buffer and the flow through and wash containing the human cells combined. Disaggregated cells were collected by centrifugation, resuspended in 10% DMSO in FBS and stored at -80 degrees Celsius or liquid nitrogen prior to re-implantation. Animals were monitored for tumour growth and tumours harvested when they reached 800 to 1000 mm^3.

2.7 CTC enrichment from blood samples using CellSearch

Peripheral blood was collected into CellSave preservative tubes (7900005, Veridex, Raritan NJ) and stored at room temperature prior to processing

within 96 hours. Once the sample arrived in the lab and was logged, the tube was mixed 5 times by inversion. 7.5 ml of blood was transferred from the CellSave preservative tube to a 15 ml CellSearch conical centrifuge tube. 6.5 ml of dilution buffer was added to the tube (containing PBS, 0.5% BSA, 0.6% other animal protein, and 0.1% sodium azide) and the tube was capped and mixed by inversion 5 times. The sample was centrifuged at 800 x g for 5 minutes with the brake off at room temperature. The tube was removed and visually inspected for the separation of plasma and red blood cells. The sample was then transferred to the CellTracks Autoprep (9541, Veridex, Raritan NJ) for processing within 1 hour. The Autoprep performs fully automated immunomagnetic cell separation and cell staining. The steps were aspiration of the plasma, addition of EpCAM ferrofluid (containing a suspension of 0.022% magnetic particles conjugated to a mouse monoclonal anti-EpCAM in 0.03% BSA buffer and 0.05% ProClin 300 preservative) and dilution buffer containing 0.1% sodium azide. Following incubation, a magnet was used to attract the ferrobeads and hold the EpCAM positive cells in position and unlabelled cells were aspirated. The magnet was removed and EpCAM positive cells re-suspended in buffer. Cells were then labelled following permeabilisation (using 0.011% proprietary permeabilisation reagent with 0.1% sodium azide with buffer) with anti-cytokeratin-PE (0.0006% mouse monoclonal antibody labelling cytokeratins 8, 18 and 19) and anti CD45-APC (0.0012% mouse monoclonal antibody against CD45) to identify leukocytes. Antibody buffer contained 0.5% BSA and 0.1% sodium azide. Nuclei were stained with DAPI (0.005% in 0.5% ProClin 300). The stained cells were processed into a magnest cartridge holder which was

placed on the CellTracks analyser. The analyser presented a gallery of cells for review and CTCs were identified by the operator as DAPI positive, cytokeratin positive and CD45 negative.

2.8 CTC enrichment from blood samples using *ISET*

Blood samples were collected in 10ml EDTA tubes (Becton Dickinson, NJ, USA, 368589) and stored at 4 degrees Celsius prior to ISET microfiltration (RareCells Diagnostics, Paris, France) within 4 hours of collection as described previously.[49] The sample was divided into 1ml aliquots and diluted 1:10 in proprietary ISET buffer including 0.8% formaldehyde. The other components of the buffer are not disclosed by the manufacturer, however based upon the first publication on this method,[49] the components of ISET buffer at that time were 0.175% saponin, 0.0372% EDTA and 0.1% BSA. The sample was incubated for 10 minutes at room temperature. Samples were then filtered at a regulated negative pressure through a polycarbonate membrane containing 8µm pores. The majority of leukocytes pass through the pores enriching for larger cells including tumour cells. ISET membranes were washed once with PBS, air dried overnight and stored at -20ºC prior to immunofluorescent staining.

2.9 Microscopy of ISET microfilters following immunofluorescent staining

During the development of the method of ISET staining and the pilot implementation in clinical samples, ISET filters were mounted on a glass slide and imaged using the Olympus BX51 fluorescent microscope with fluorescent filters used for analysis of the ISET filter to detect emission in the

range of DAPI, FITC, TRITC and Cy5. Samples were screened at x20 magnification and representative images were taken at x40 and x100 magnification and saved as TIF files.

2.10 Digital image capture of ISET microfilters following immunofluorescent staining

Once immunofluorescent staining was demonstrated to be capable of reliably detecting CTCs on patient ISET filters and distinguishing them from blood cells, a systematic approach was developed to scanning and viewing ISET filters permitting standardisation of analysis and allowing archiving of all the data from entire filters from clinical samples.

Stained ISET membrane spots were mounted on a glass slide and examined using a Mirax automated slide scanner (3DHistech, Budapest, Hungry). Slides were cleaned with 70% alcohol and the boundary of the area of interest (around the ISET membrane spot) was defined on each slide in permanent black marker. Digitization of the samples was achieved by employing a Panoramic Scan system (3DHistech, Budapest, Hungary). The samples were illuminated with a Sola white light LED (Lumencor, Beaverton, Oregon) and ultra violet filter blocks (Semrock, Rochester, New York) to control the illumination and detection range (DAPI-1160B, GFP-3035C, TRITC-B and Cy5-4040B). The data was scanned with an x 40 objective lens (Carl Zeiss, Jenna, Germany) at a resolution of 0.1613 microns per pixel and the camera, an AxioCam MRm (Carl Zeiss), captured each field of view at a size of 1388 x 1040. Panoramic View (3DHistech) version 6.4 software was

used to control the devices, standardise equipment response and collect data.

To set up the equipment, a range of slides were considered to set an independent manual exposure setting for each detection channel. For healthy volunteer blood (HVB) samples spiked with tissue cultured cells compared to clinical samples different exposures were required because of the differing levels of protein expression and hence fluorophore concentrations. Slides were scanned by setting a focus range to account for any irregularities across the filter by scanning every fifth field of view in the FITC fluorophore channel to produce a height map to describe the overall data. Rather than routinely scanning the whole slide, detection was limited to the filter only by identifying the area drawn by hand and all areas within the marker boundary were scanned sequentially with all defined illumination channels. Application of the generated height map for each slide whilst scanning ensured the maintenance of focus. As the equipment generated data, fields of view are automatically stitched together (typically 4300) by XY stage location rather than feature to form an image that is typically 7700x7700 pixels (2.7 x 2.7 m) in size. Images were visually accessed using the freeware version of the 3DHistech panoramic viewing software (version 1.15.1.10). All analysts were trained on the classification of CTCs and all CTCs identified were tagged for review by the author.

2.11 General statistical considerations

Statistical analysis was performed using SPSS version 20 (SPSS Inc., Chicago, USA) and GraphPad Prism version 5.02 for Windows, (GraphPad

Software, San Diego, USA). A p-value of <0.05 was considered statistically significant throughout.

Correlation matrices were generated to evaluate for associations between clinical and biomarker variables. When both co-variates were continuous, a correlation co-efficient was calculated using Spearman's rank (if parametric) and Pearson's rank (if non-parametric distribution). To compare continuous and with categorical data, the mean was compared with a student's T test. To compare categorical co-variates, Fisher's exact test was used to evaluate for associations. Where multiple analyses were performed to identify trends or associations, this was considered an exploratory or hypothesis generating analysis and no Bonferroni correction was applied.

Univariate survival analysis was performed using Kaplan-Meier analysis, and difference between survival distributions was evaluated with the Log Rank test. Survival times were calculated as the time between date of biopsy and date of death or last follow up. Patients alive at last follow up were censored.

In order to determine a cut off in CTC sub-populations associated with survival, receiver operating characteristic (ROC) curves were analysed to calculate the area under the ROC curve and to determine the sensitivity and specificity of assays to predict a clinical end point for prediction of survival at 3 years (for data sets including patients with limited stage SCLC) and at 9 months (for data sets including patients with extensive stage SCLC). These differing end points were purposefully selected as the most clinically relevant in each circumstance. In limited stage disease, with treatment with curative intent, long term (3 year) survival is considered the successful outcome

following treatment. Current treatment in extensive stage disease is associated with few survivors at 3 years, however studies report a median survival of up to 9 months and this figure was therefore selected as an appropriate end-point. The sensitivity and specificity of multiple thresholds around the median of each score were calculated to select the optimum cut-point.

3 CHARACTERISATION OF CTCs DERIVED FROM PATIENTS WITH LUNG CANCER FOR A PANEL OF MARKERS IMPLICATED IN EPITHELIAL TO MESENCHYMAL TRANSITION

3.1 Introduction

As outlined in the General Introduction (Section 1.1) early metastatic dissemination and chemotherapy resistance are common in lung cancer. A consequence of early metastatic spread is that the disease is infrequently operable at diagnosis and the 5 year survival of all patients following a diagnosis of lung cancer is between 6 and 18% globally.[2] In this situation, treatment is given with palliative intent and there are very few long term survivors. Chemotherapy resistance occurs in virtually all patients and this failure of existing treatments to provide long term clinical benefit is a major obstacle to the effective treatment of lung cancer patients.

As detailed in the General Introduction (Section 1.8), epithelial to mesenchymal transition (EMT)[100] or epithelial and mesenchymal cell co-operation[144,146] have been proposed as mechanisms of cancer dissemination. Moreover, EMT may have direct clinical relevance as it has been proposed as driving chemotherapy resistance which may arise through EMT producing tumour cells with the properties of stem cells.[175,179] However, there remains unresolved active academic debate in both the fields of EMT[121,139] and cancer stem cells[171] (detailed in the General Introduction,

Section 1.8). Different tumour types may utilise different mechanisms of dissemination to different degrees. A significant controversy in the EMT debate arises from the observation that metastatic deposits frequently resemble the primary tumour in their epithelial appearances.[142] To account for this observation, two explanations are proposed. The first is that tumour cells adopt a mesenchymal phenotype in order to invade and disseminate (EMT) then revert to an epithelial phenotype in order to successfully colonise at distant sites (MET).[100,143] This is consistent with tumour plasticity between epithelial and mesenchymal cell states, i.e. it is a dynamic process.

The second explanation proposed is that mesenchymal tumour cells arising from EMT cooperate with epithelial tumour cells to enable them to invade tissue, enter the circulation and colonise at distant sites.[144,146] Sub-classifying CTCs using their expression of markers of EMT (the epithelial intermediate filament cytokeratin and the mesenchymal intermediate filament vimentin) may enable their use to understand EMT in lung cancer. Accepting that any analysis of tumour cells in patients (either from the primary/metastatic tumour or from CTCs) will not be able to overcome the dynamics of the process of EMT in tumour progression in patients, the analysis of CTCs will however complement data generated from tumour biopsy analysis and this can be performed at multiple time points. However, analysis of patient samples will remain observational and will not be able to distinguish between E and M co-operation and EMT in metastasis. In addition to the question of tumour biology, analysis of the EMT profile of CTC at multiple time points may address the clinical question of drug resistance and its association with the

emergence of a dominant mesenchymal phenotype upon tumour progression through chemotherapy.

In addition to CTCs being studied as a 'liquid biopsy', they are being increasingly used for clinical decision making which is exemplified by their incorporation in the breast cancer staging. As detailed in the General Introduction (Section 1.6), CellSearch remains the most extensively studied CTC enrichment platform, validated for the prognostic information that it provides in breast,[67,68] colorectal[69,219] and prostate[71,220] cancers. We have previously reported on the prognostic utility of CTCs in NSCLC[73] and SCLC.[57] However, in NSCLC patients, CTCs isolated by CellSearch ($EpCAM^+$/$cytokeratin^+$ CTCs) are scarce in comparison to SCLC patients (NSCLC median 1/7.5 ml range 0 – 146; SCLC median 24/7.5 ml, range 0 – 44,896). The degree to which CellSearch underestimates the total CTC burden in NSCLC, and the significance of the CTCs that are overlooked by this approach, can be further understood by identifying and characterising mesenchymal sub-populations of CTCs with other enrichment approaches. We have previously reported that ISET size based enrichment has a greater sensitivity for detection of NSCLC patient CTCs than CellSearch.[59] More recently, a novel enrichment platform showing promise for detection of EpCAM negative tumour cells which are not detected by CellSearch is the size based Parsotix microfluidic device which is currently being evaluated by our lab for clinical application.[221]

Clinical studies have started to evaluate the EMT marker expression by CTCs[105,222]. Table 3.1 summarises these studies. One of the first studies

from our lab used single and dual marker IHC on cells isolated using ISET in patients with SCLC and NSCLC.[222] CTCs had heterogeneous expression of markers of EMT. This was in keeping with previous reports that describe EMT occurring to degrees within cells rather than a binary epithelial or mesenchymal state.[107] These observations were supported by further studies published during the first year of my PhD showing EMT marker heterogeneity using immunofluorescent analysis of CTCs in NSCLC,[102] breast,[104,105] prostate[104] and head and neck[103] cancers. In the breast cancer study by Kallergi *et al*.,[105] CTCs expressing mesenchymal markers were identified more frequently in patients with advanced than with localised disease suggesting an association between EMT and disease progression. More recently, Yu *et al*.[223] reported on EMT profile of breast cancer CTCs using RNA in situ hybridisation for a panel of epithelial and mesenchymal gene transcripts. In this study, emergence of a mesenchymal CTC phenotype was seen at times of disease progression and suppressed at times of response to therapy, further implicating mesenchymal CTCs in metastatic progression.

Cancer site (n)	Enrichment	Staining	Epithelial markers	Mesenchymal markers	Other markers	Ref
Immunocytochemistry						
NSCLC (3) SCLC (3)	ISET microfiltration	Single/dual marker IHC	Cytokeratins E-cadherin	Vimentin N-cadherin	NA	222
NSCLC (6)	ISET microfiltration	Dual marker IHC	Cytokeratins	Vimentin	NA	102
Immunofluorescence						
Breast (50)	Immunomagnetic CD45 depletion	Triple marker IF	Cytokeratins	Vimentin TWIST	CD45	105
Breast (10) Prostate (41)	Immunomagnetic EpCAM enrichment	Triple marker IF	Cytokeratins E-cadherin EpCAM	Vimentin N-cadherin O-cadherin	CD45 CD133	104
SCC head/neck (10)	Immunomagnetic CD45 depletion	Triple marker IF	EGFR	Vimentin N-cadherin	CD44	103
RNA in situ hybridisation						
Breast (11)	Microfluidic EpCAM, EGFR and HER2 capture	RNAish	E-Cadherin Cytokeratins EpCAM	N-cadherin Fibronectin Serpine 1	NA	223

Table 3.1 Summary of clinical studies evaluating markers of epithelial to mesenchymal transition in CTCs

Abbreviations: ISET isolation by size of epithelial tumour cells, IHC immunohistochemistry, NA not applicable, RNAish ribonucleic acid in situ hybridisation.

Of note, all studies of EMT profiling of CTCs have included the evaluation of the epithelial intermediate filament cytokeratin and/or the mesenchymal intermediate filament vimentin. Although it is evident from work done to date that CTC sub-populations exist with heterogeneous expression of their markers of EMT, these studies have limitations. The studies by Yu *et al*.[223] and Armstrong *et al*.[104] both utilise epithelial marker dependent CTC enrichment platforms. As the mesenchymal CTC population of interest is the one which is hypothesised to have gone through the process of EMT and therefore down-regulated some or all of its epithelial markers, purely mesenchymal tumour cells would not be reliably captured by this method, limiting the applicability of this approach to CTC EMT profiling. In contrast, the remaining studies apply CTC marker independent enrichment platforms using negative selection (CD45 depletion)[103,105] or size based enrichment (ISET microfiltration).[102,222] However, none of these studies included the leukocyte marker CD45 in their classification of enriched cells as CTCs. This is relevant as the accepted criteria for a CTC by the gold standard approach (CellSearch) is based upon the expression profile cytokeratins^{+}/CD45^{-}. Objects classified as cytokeratins $^{+}$/CD45^{+} were identified in 37% of NSCLC patients by CellSearch pre-chemotherapy (mean 2.6 cytokeratins $^{+}$/CD45^{+} events per 7.5ml, SEM 1.1) and although they were not associated with shorter survival, their significance is not known.[224] Moreover, leukocytes are mesenchymal and express the mesenchymal marker vimentin and lack epithelial cytokeratins,[225] reinforcing the need to include a marker to exclude leukocytes within an EMT assay to prevent their misclassification as mesenchymal tumour cells.

A further criticism of the existing studies is that none of the studies account for the presence of circulating endothelial cells (CECs). CECs, which are also vimentin positive[194] (therefore risking their misclassification as mesenchymal CTCs), are present in the blood of healthy volunteers[226,227] and patients with multiple cancer types[226,228-234] including NSCLC[227,235-240] and SCLC.[227] A study quantifying CECs in lung cancer[227] using CellSearch CEC detection kit which identifies CECs using CD146 immunomagnetic capture and CD105 positive staining (therefore defining CECs as $CD146^{+}/CD105^{+}$) was published during the course of this PhD. This study found that using this platform, CECs were present in early stage NSCLC patients in significantly higher numbers (n=74, median 114/ml range 22 – 661/ml) than detected in SCLC patients (n=20, median 46/ml, range 26 – 94/ml) which was in turn higher than detected in healthy volunteers (n=60, median 3/ml range 1 – 14/ml). In order to characterise CTCs for markers of EMT using the markers cytokeratin and vimentin with the greatest confidence, an EMT assay should therefore include markers to exclude leukocytes and CECs alongside epithelial and mesenchymal markers such as cytokeratin and vimentin.

Hypothesis

Sub-populations of lung cancer CTCs exist which can be characterised by their expression of epithelial and mesenchymal markers and distinguished from leucocytes and CECs based upon their marker expression.

Aims

- The first aim, completed prior to the 2014 publication by Ilie *et al*.,[227] was to determine the frequency of CECs in SCLC and thus the risk of misclassification as mesenchymal CTCs.

Further aims were:

- To develop and validate an immunofluorescent assay for staining ISET filtered CTCs for a panel of markers implicated in EMT in addition to markers of leukocytes and circulating endothelial cells.

- To perform pilot studies to profile CTCs with the newly developed EMT assay in small cohorts of SCLC and NSCLC patients.

3.2 Methods

3.2.1 Patient recruitment and blood sampling

14 patients with histological or cytological confirmation of SCLC and 3 patients with NSCLC attending the Christie NHS Foundation Trust were recruited to our broader spectrum of lung cancer research (European Union CHEMORES FP6 contract number LSHC-CT-2007-037665) according to ethically approved protocols (NHS North West 9 Research Ethics Committee).

10 ml blood was drawn into CellSave preservative tubes (7900005, Veridex, Raritan NJ) and processed within 96 hours from 5 SCLC patients for CTC enumeration by CellSearch and a paired 10 ml CellSave sample was taken from each patient at the same blood draw for CEC enumeration using CellSearch (described below).

A further 9 SCLC patients had 10ml blood drawn into EDTA tubes (BD Vacutainer, 368589) to enrich for circulating tumour cells (CTCs) by ISET microfiltration as previously described[49] and a paired sample for CellSearch CTC enumeration. The method for ISET microfiltration is described in detail in the General Methods chapter (Section 2.8) and outlined in Section 3.2.2.3 below.

Three NSCLC patients had 10ml blood drawn into EDTA tubes to enrich for circulating tumour cells (CTCs) by ISET microfiltration and a paired 10 ml CellSave sample for CellSearch CTC enumeration. One of the NSCLC patients had all blood samples drawn at two time points (time point 1 (TP1)

prior to any treatment and time point 2 (TP2) following chemotherapy and cranial radiotherapy treatment). In addition, these 3 NSCLC patients had 10 ml blood drawn into EDTA for RosetteSep CTC enrichment. Cells remaining after depletion of leukocytes were implanted sub-cutaneously into immune-compromised mice to evaluate for the generation of CTC derived explant (CDX) tumours[66] as described in the General Methods (Section 2.7) and outlined below (Section 3.2.2.4).

3.2.2 Sample processing

3.2.2.1 CEC enumeration by CellSearch

Peripheral blood was collected into CellSave preservative tubes (7900005, Veridex, Raritan NJ) and stored at room temperature prior to processing within 96 hours. The tube was mixed 5 times by inversion and 7.5 ml of blood was transferred from the CellSave preservative tube to a 15 ml CellSearch conical centrifuge tube. 6.5 ml of dilution buffer was added to the tube (containing PBS, 0.5% BSA, 0.6% other animal protein, and 0.1% sodium azide) and the tube was capped and mixed by inversion 5 times. The sample was centrifuged at 800 x g for 5 minutes with the brake off at room temperature. The tube was removed and visually inspected for the separation of plasma and red blood cells. The sample was then transferred to the CellTracks Autoprep (9541, Veridex, Raritan NJ) for processing within 1 hour, aspirating of the plasma, adding CD146 ferrofluid (containing a suspension of 0.012% magnetic particles conjugated to a mouse monoclonal antibody against CD146 in 0.3% BSA and 0.05% ProClin 300 preservative) and dilution buffer containing 0.1% sodium azide. Following incubation, a

magnet was used to attract the ferrobeads and hold the CD146 positive cells, aspirating the other cells. The magnet was removed and CD146 positive cells re-suspended in buffer. Cells were then labelled following permeabilisation (using 0.011% proprietary permeabilisation reagent with 0.1% sodium azide with buffer) with anti-CD105 (<0.0006% mouse monoclonal antibody conjugated to PE) and anti CD45 (<0.0013% mouse monoclonal antibody conjugated to APC) to identify leukocytes. Antibody buffer contained 0.5% BSA and 0.1% sodium azide. Nuclei were stained with DAPI (0.005% in 0.5% ProClin 300). The stained cells were processed into a magnest cartridge holder which was placed on the CellTracks analyser. The analyser presented a gallery of cells for review and CECs were identified by the operator as DAPI positive, CD105 positive and CD45 negative.

3.2.2.2 CTC enumeration by CellSearch

CTC enrichment by CellSearch is described in detail in the General Methods chapter (Section 2.7). Briefly, the prepared blood sample was placed on the CellTracks Autoprep (9541, Veridex, Raritan NJ) which performs automated EpCAM immunomagnetic enrichment and immunofluorescent cell labelling of the EpCAM captured cells with antibodies against cytokeratins and CD45 and with the nuclear stain DAPI. The stained cells were then processed into a magnest cartridge holder which was placed on the CellTracks analyser which presented a gallery of cells for review. CTCs were identified by the operator as DAPI positive, cytokeratin positive and CD45 negative.

3.2.2.3 CTC enrichment by ISET

CTC enrichment by ISET is described in detail in the General Methods chapter (Section 2.8) and briefly outlined here. The prepared blood sample underwent red cell lysis and fixation with formaldehyde (0.8%) and was processed on the ISET device using regulated negative pressure to draw the sample through an 8 µm polycarbonate microfilter. The majority of the leucocytes (typically measuring <8 µm) pass though the filter retaining the larger tumour cells on the filter for subsequent analysis. SCLC cells typically have a diameter two times that of leukocytes with a mean diameter (+/-SD) of 9.2µm (+/-2.1).[241] The majority of NSCLC cells measure >8 µm.[242]

3.2.2.4 CTC enrichment by RosetteSep and CDX tumour growth

CTC enrichment by RosetteSep and CDX tumour growth is described in detail in the General Methods (Section 2.5 and 2.6) and is briefly outlined here. The prepared blood sample was incubated with an antibody tetramer cocktail (against CD3, CD14, CD16, CD19, CD38, CD45, CD61, CD66b and glycophorin A) which recognises leukocytes and erythrocytes, binding them together into rafts. Through density gradient centrifugation, these were separated from the CTC fraction and the leukocyte/erythrocyte depleted fraction was collected and implanted sub-cutaneously into immune compromised mice which were monitored for subsequent tumour growth.

3.2.3 Culture of cell lines and Western blotting

The culture or cell lines, the generation of protein lysates, the determination of protein concentration and Western blotting are described in detail in the General Methods chapter (Section 2.1 – 2.4).

3.2.4 Immunofluorescence of ISET filtered CTCs

This chapter describes the development of an immunofluorescent assay for staining ISET filtered CTCs from lung cancer patients. The final method for EMT CTC profiling of both clinical samples and cell lines spiked into volunteer blood was as follows. CTCs were stained using antibodies against the leukocyte marker CD45, the epithelial tumour cell marker cytokeratins (4, 5, 6, 8, 10, 13 and 18), the mesenchymal tumour cell marker vimentin, and the endothelial cell marker VE-cadherin (CD144). The ISET module has 10 wells allowing 10ml blood per patient to be filtered to produce 10 discrete 6 mm diameter filter 'spots' on which cells contained within a 1 ml aliquot of blood are deposited. Individual filter 'spots' were excised and rehydrated for 1 minute in PBS-T (PBS + 0.02% Tween-20). The filters were placed in 0.2% Triton X-100 for 10 minutes in a humidity chamber (used for all subsequent incubations at room temperature) to permeabilise deposited cells for antibody entry and washed for 1 minute in PBS-T. Filter spots were incubated with 10% goat serum block (Dako X0907) for 30min, then incubated in a cocktail (80µl) of two primary antibodies, unconjugated anti-CD45, (1:400 of 0.4mg/ml, Rabbit, Abcam AB10559) and unconjugated anti-VE-cadherin, (1:200 of 0.5mg/ml, Mouse, eBioscience 14-1449-82), for 1 hour. The filters were washed twice in PBS-T, then incubated with a cocktail (80µl) of two fluorescent secondary antibodies: goat anti-mouse AF555 (1:500 of 2mg/ml Invitrogen A21422) and goat anti-rabbit DY549 (1:500 of 1mg/ml Thermo Scientific 35558) for 1 hour. The filters were washed twice in PBS-T, then incubated with a cocktail (80µl) of two conjugated primary antibodies, anti-vimentin 647 (1:50 of 0.05mg/ml Santa Cruz sc-6260) and

anti-cytokeratin FITC (1:100 of 3mg/ml, Sigma F3418, clone C11 against CKs 4, 5, 6, 8, 10, 13 and 18), for 1 hour. The filters were washed twice in PBS-T, and then incubated with 80 µl DAPI (1:10,000 of 5mg/ml, Invitrogen D3571) for 5 minutes. Filters were washed twice in PBST and twice in double distilled water before mounting and coverslipping (1.5 grade) on a glass slide with ProLong Gold anti-fade (Invitrogen P36934). Slides were left overnight at 21 degrees Celsius to dry before analysis.

3.2.5 Classification of cells following immunofluorescent staining

Tumour cells were defined as being negative for CD45 and or VE-cadherin expression as these are the markers used to exclude leukocytes and endothelial cells respectively (both antibodies labelled with fluorophores with the same spectral emission). CTCs were then sub classified as epithelial (E) if they had the profile cytokeratin^{+}/vimentin^{-}, mesenchymal (M) if they had the profile cytokeratin^{-}/vimentin^{+} and mixed epithelial and mesenchymal (E/M) if they had the profile cytokeratin^{+}/vimentin^{+}.

3.2.6 Analysis of ISET filters following immunofluorescent staining

Following immunofluorescent staining, ISET filters of cell lines spiked into healthy volunteer blood and the first 5 SCLC patients included in the method development and pilot implementation were analysed using fluorescent microscopy (Olympus BX51) as described in the General Methods (Section 2.9). ISET filters of the subsequent 4 SCLC patients and the 3 NSCLC patients had the whole filter scanned using the Mirax slide scanner and the digital image files were viewed in Panoramic viewing software as described in the General Methods (Section 2.10). This latter approach permitted

systematic evaluation of all the cells retained on the ISET filter. As such, all the data was captured and stored for subsequent analysis. This permitted the entire image of the filter to be assessed without duplication or omission of areas of the filter. A CTC profile was generated plotting the percentage of the total CTC count with each of these expression profiles.

3.2.7 Immunohistochemistry of patient biopsy and CDX samples

Formalin fixed and paraffin embedded sections from the patient biopsy and CDX tumours were stained on an automated stainer (i6000, BioGenex) by immunohistochemistry using antibodies against cytokeratins (pan-cytokeratin antibody to cytokeratins 1–8, 10, 13–16 and 19, mouse AE1/AE3, M3515, 1:60, Dako), TTF-1 (mouse 8FTG3/1, 1:200, Dako), CK7 (mouse OV-TL 12/30, 1:1000, Dako) and vimentin (mouse, V9, CC1, Roche). Sections were prepared by de-waxing in xylene for 10 minutes three times and rehydrating in alcohol. Antigen retrieval was performed in pH 6.0 citrate target retrieval solution (from 10x stock, DAKO S2369, in distilled water) at 120 degrees Celsius for 5 minutes. Antibody incubations took place at room temperature for 60 minutes using antibody diluent (DAKO S0809). Sections were blocked with 3% endogenous peroxidase block (from hydrogen peroxide 10x stock (Sigma Aldrich 95321) and the avidin and biotin blocking kit (Vector Elite SP-2001) as per manufacturer's instructions. The biotinylated secondary antibody with chromogen (vector elite avidin and biotinylated horseradish peroxidase macromolecular complex (ABC) kit (Rabbit IgG) (Vector PK-6101) and DAB + Substrate chromogen kit (DAKO K3468)) was applied as per manufacturer's instructions.

3.3 Results

3.3.1 Risk of misclassification of CECs as mesenchymal CTCs

As described in the introduction to this chapter, circulating endothelial cells (CECs) are present in the blood of healthy volunteers and cancer patients.[227] They are mesenchymal in origin and express vimentin and lack expression of cytokeratins.[194] Although studies have been performed by other groups to characterise CTCs for markers of EMT (detailed in Table 3.1) none of these assays have accounted for the presence of CECs. At the start of this PhD, there were no published data on the prevalence of CECs in SCLC. Therefore in order to determine the risk of misclassification of CECs as mesenchymal CTCs, the relative numbers of CECs in SCLC (using the CellSearch CEC kit, which selects for $CD146^+/CD105^+$ cells) and CTCs (using the CellSearch CTC kit, which selects for $EpCAM^+/CK^+$ cells) were characterised in a pilot study of 5 SCLC patients.

Figure 3.1 shows that CECs were detected in all patients (median 53/7.5 ml, range 19-120). The number of CECs was lower than the range subsequently reported for a cohort of 20 SCLC patients (median 345/7.5 ml) but was in turn higher than detected in 60 healthy volunteers in this same study (median 22/7.5 ml)[227]. The lower CEC numbers detected in the current study may be due to the small number of patients included in the current analysis allowing for the confounding effect of other clinical characteristics. The CEC number exceeded CTC number in 4 out of 5 patients studied. CTC prevalence in these patients was consistent with our previous data for a cohort of 98 SCLC patients (median 24, range 0 to 44,896 CTCs/7.5ml).[57] The presence of

CECs in addition to CTCs in these samples indicated that a specific CEC marker is required in any multi-colour immunofluorescence assay to distinguish mesenchymal tumour cells (vimentin^{+}/cytokeratin^{-}) and CECs. VE-cadherin was therefore selected as a marker of CECs as it is expressed on mature endothelial cells,[194] to be included alongside CD45 (the latter used as a marker of leukocytes).[243]

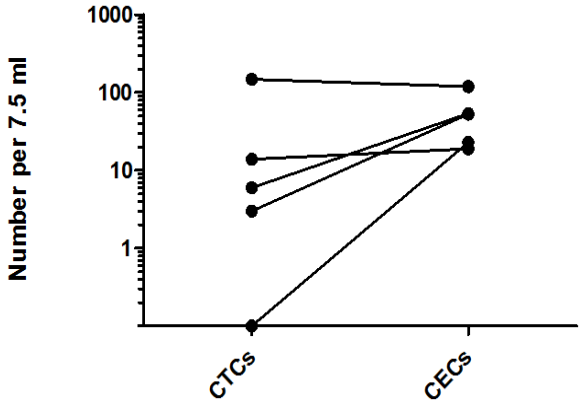

Figure 3.1 Comparison of circulating tumour cell and circulating endothelial cell numbers in SCLC patients
Paired blood samples were collected at a single time point from SCLC patients (n=5) and CTCs and CECs enumerated using the CellSearch CTC and CEC kits. Results of paired CTC and CEC samples from individual patients are shown connected by a black line.

3.3.2 Antibody specificity and multi-parameter immunofluorescent assay validation for EMT profiling of CTCs

In order to establish a method which could reliably discriminate CTCs from CECs and leukocytes, SCLC cell lines were screened for expression of cytokeratins and vimentin (Figure 3.2) and then used as positive and negative antibody controls in a series of cultured cell 'spikes' into healthy volunteer blood (HVB) filtered by ISET (Figure 3.3). Figure 3.2A shows that DMS114 express vimentin and not cytokeratins and H526 express cytokeratins and not vimentin, therefore these two cell lines were chosen to

assess the specificity of antibody staining for these proteins. These findings are consistent with published data on mRNA levels for cytokeratins and vimentin in the Cancer Cell Line Encyclopaedia.[244] Human umbilical vein endothelial cells (HUVECs, expressing VE-cadherin and vimentin) and peripheral blood mononuclear cells (PBMCs, expressing CD45 and vimentin) were used as control cells for VE-cadherin and CD45 antibody staining respectively.

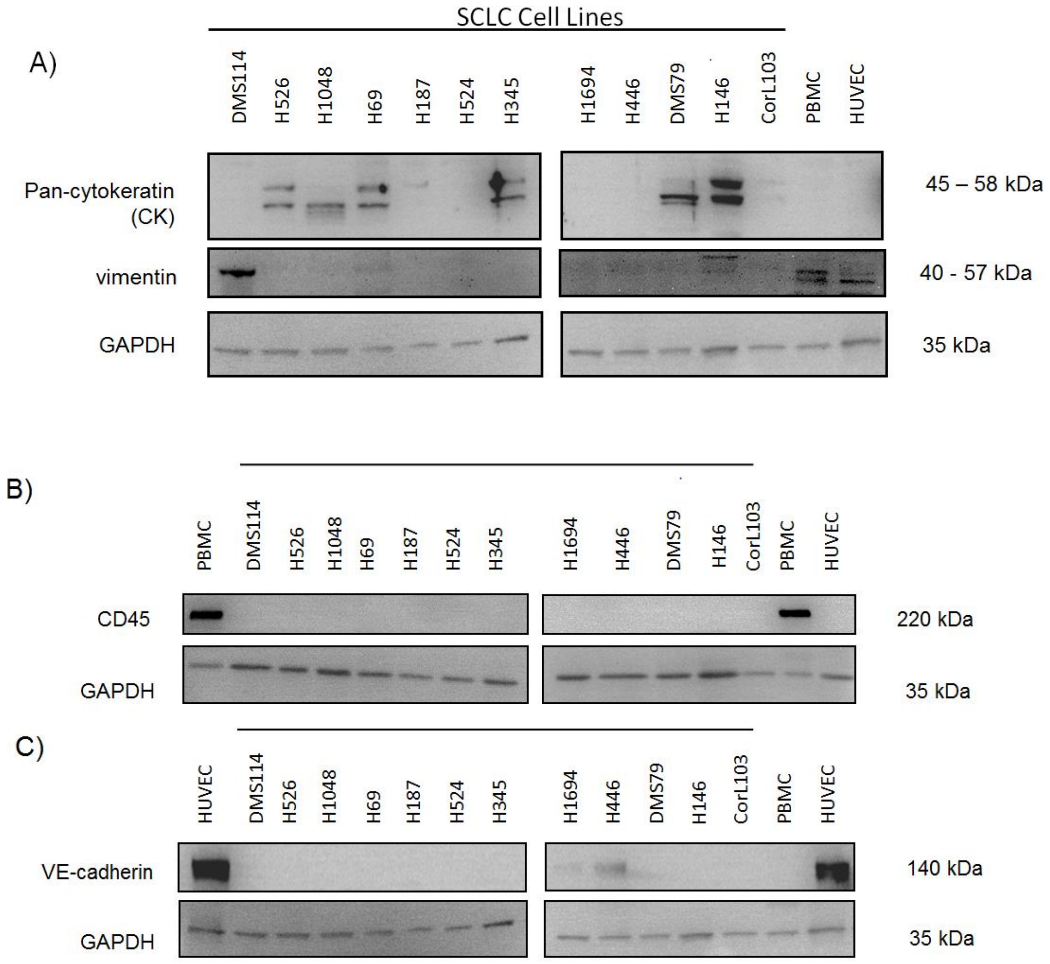

Figure 3.2 Western blotting for cytokeratins, vimentin, CD45, VE-cadherin, and GAPDH (loading control) in a panel of SCLC cell lines, peripheral blood mononuclear cells (PBMCs) and human umbilical vein endothelial cells (HUVEC)

Panel A shows Western blotting for cytokeratin and vimentin. Dual bands are present on the blot for CKs which indicates the different molecular weights of the CK isoforms. The multiple bands seen on the vimentin blot may represent protein degradation or splice variation. Panel B shows Western blotting for CD45. Peripheral blood mononuclear cells are the positive control. Panel C shows Western blotting for VE-cadherin. Human umbilical vein endothelial cells are the positive control for VE-cadherin. Representative blots from >3 replicates are shown.

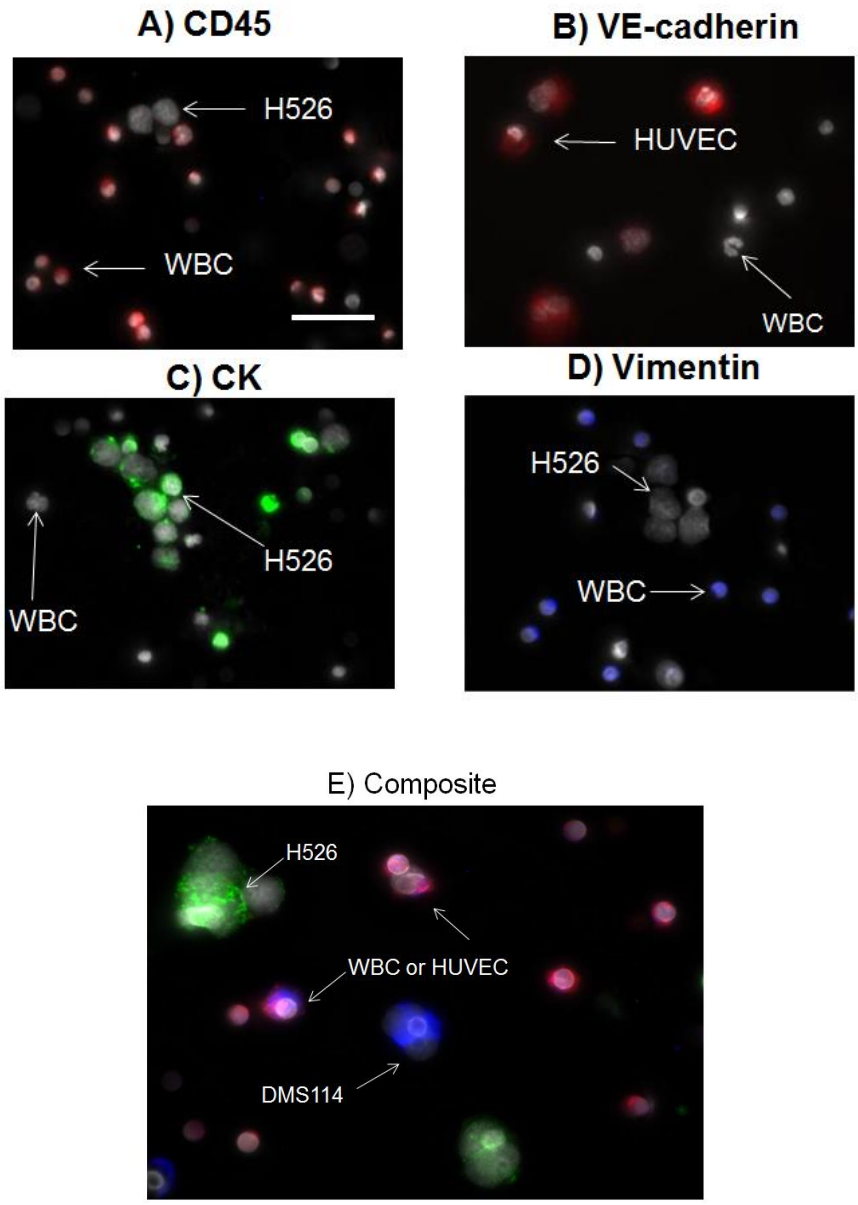

Figure 3.3 Fluorescence microscopy images of control cell lines spiked into healthy volunteer blood samples and processed by ISET filtration

Cells are shown stained for CD45 (shown in red, A) and or VE-cadherin (CD144) (shown in red, B), cytokeratins (CK) (shown in green, C) and vimentin (shown in blue, D). All antibodies combined are shown in composite image (E). Nuclei are shown stained for DAPI (white) in all images. Scale bar 50 um. Abbreviations: WBC, white blood cells; HUVEC, human umbilical vein endothelial cells.

Following selection of appropriate cell lines, it was necessary to demonstrate that the immunofluorescent staining protocol was specific and sensitive for the chosen antibodies (cytokeratins, vimentin, VE-cadherin and CD45). Cell line(s) were 'spiked' into healthy normal volunteer blood, filtered using ISET, stained and imaged (Figure 3.3). Firstly, each antibody was tested alone on positive and negative cell lines (Figure 3.3A-D), then evaluating all combinations of antibodies together, before combining all four antibodies to form the EMT assay (Figure 3.3E). Figure 3.3 shows that for cell lines spiked into healthy volunteer blood the individual antibodies were sufficiently sensitive and specific to distinguish between the different cell populations. This confirms the specificity of staining in a heterogeneous population within an ISET filtered blood sample giving confidence that leukocytes and CECs will be distinguished from CTCs in clinical samples using this approach.

3.3.3 Pilot study to characterise an EMT profile of SCLC CTCs

Following validation of the EMT assay using spiked SCLC cell lines described above, a further 5 SCLC patients had paired blood samples drawn for CellSearch and ISET analyses in order to test the ability of this assay to detect CTCs and characterise their EMT profile. Clinical details of these patients are summarised in Table 3.2. CellSearch was performed confirming up to 1236 CTCs/ 7.5 ml were present using the gold standard approach (range 1 – 1236/7.5 ml). As outlined above, ISET microfiltration should retain the majority of CTCs in the sample given the mean SCLC tumour cell diameter of 9.2µm (+/-2.1)[241] and the microfilter pore size of 8 µm.

During this part of the study, filters were imaged using fluorescent microscopy (Olympus BX51 microscope) which demonstrated CTCs were detectable in all 5 patients. However, an accurate systematic and complete evaluation of all cells on the filters, which would be reproducible, was not possible with this approach as the amount of time taken to analyse all events captured on a single ISET filter was too great to permit this. It was therefore not possible to perform a formal comparison between CellSearch and ISET CTC numbers using the Olympus BX51 fluorescent microscope. This was one of the reasons why subsequent imaging of the ISET filters was performed using the Mirax automated slide scanner permitting systematic manual evaluation on a desk-top computer using Panoramic image analysis software. This allowed the sections of the slide that had been reviewed to be marked and events of interest tagged and labelled. Results of CTC profiling from Section 3.3.4 onwards used this approach. It was also in an effort to make the analysis more reproducible that this research also evaluated the Definiens tissue studio automated digital image analysis software (reported in Chapter 5).

Patient ID	Sex	Age	Smoking History (pack years)	PS (WHO)	Sites of metastases	CellSearch CTC Number /7.5 ml	Survival (months)
1	Female	71	41	2	Liver, LN	1236	7
2	Male	57	36	2	Liver	72	6.3
3	Male	79	30	1	LN, adrenal	523	10.5
4	Male	57	52	2	LN, lung, adrenal	113	6.1
5	Female	67	60	3	LN, pleura, pericardium	1	3.5

Table 3.2 Clinical characteristics of SCLC patients who were included in the pilot study to characterise CTCs using the multi-parameter EMT assay
Abbreviations: PS, performance status; LN, lymph nodes.

In addition to the cells which meet the established definition of CTCs (cytokeratin^{+}/CD45^{-}), Figure 3.4 shows representative images of additional sub-populations identified on the patient filters. Figure 3.4A shows two CD45 and/or VE-cadherin negative cells (within the boxed area, Figure 3.4A(v)) thus defined as CTCs; one of these cells (the upper cell) co-expresses cytokeratins (CK) and vimentin (green and blue) and the other (the lower cell) expresses only vimentin (blue). They are surrounded by four cells which are either leukocytes or CECs (vimentin positive and CD45 or VE-cadherin positive). Figure 3.4B shows an enlarged image of the two CTCs within the boxed area in Figure 3.4A(v) to view cellular staining of cytokeratins and vimentin. These cell phenotypes were observed in all patients studied in addition to cytokeratin^{+}/CD45^{-}/vimentin^{-} CTCs.

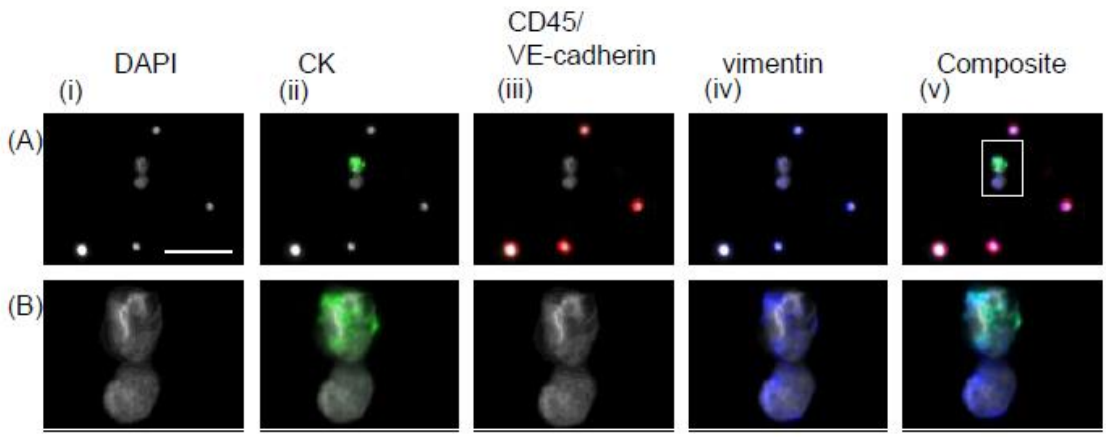

Figure 3.4 Fluorescence microscopy images of CTCs enriched from SCLC patients' blood samples by ISET filtration

Filters are shown stained for DAPI (vertical panel, i, white) cytokeratins (ii, green), CD45 and VE-cadherin (iii, red) and vimentin (iv, blue). Scale bar 50 um. Magnification x40. The two CTCs within the box in the composite image (Av) are shown at x100 magnification in row Bi to Bv. These cells are cytokeratin^{+}/vimentin^{+} and cytokeratin^{+}/vimentin^{-}.

3.3.4 Approach to systematic classification of SCLC CTCs on ISET filters to generate a CTC EMT profile

Having demonstrated that this assay is able to identify CTCs in SCLC patients and categorise them by their expression of an epithelial marker (cytokeratins), a mesenchymal marker (vimentin) or both, I next sought to identify the relative size of CTC sub-populations (epithelial, mesenchymal or mixed epithelial/mesenchymal) within and between SCLC patients, by generating a CTC EMT profile per patient. As discussed above, for the analysis reported so far, ISET filters were imaged manually at a fluorescent microscope (Olympus BX51). However, to allow systematic analysis and annotation of the cells on the ISET filter, imaging of subsequent filters stained was performed on the Mirax slide scanner creating an image file of the whole ISET spot at x40 magnification for analysis within imaging software (Panoramic Viewer).

Upon systematic analysis and enumeration of the first patients' ISET filters following digital slide scanning there were over 600 CTCs retained on each ISET filter spot (one spot from 1ml of filtered blood). Distinguishing CTCs following EMT assay staining from CECs and leukocytes, and then classifying all CTCs into epithelial (cytokeratin^{+}/vimentin^{-}, E), mesenchymal (cytokeratin^{-}/vimentin^{+}, M) or mixed (cytokeratin^{+}/vimentin^{+}, E/M) subpopulations was very time consuming taking up to 8 hours for this single filter spot (from 1 ml of blood). If this analysis was to be applied to a larger number of patient samples in the future, it was therefore necessary to determine how many CTCs from this patient required profiling in order to be representative of the total CTC population on the filter. 600 cells from a single ISET spot underwent manual classification to identify the size of E, M and E/M populations. Figure 3.5 shows the relative % error from the results of the total CTC populations when different numbers of cells ranging from 50 to 500 from the same single filter spot were used to quantify the subpopulations (mean and SEM are shown from 9 technical replicates). When compared with classification of all 600 CTCs, sub-population size varied by a mean of 5.3% if 100 CTCs are scored and 2.9% if over 200 are scored and this dropped to 2.2% when scoring 500 CTCs. Based upon these findings, in order to generate an EMT profile of ISET filtered CTCs, it was determined that over 200 CTCs were to be profiled per patient if the total CTC population was in excess of this figure.

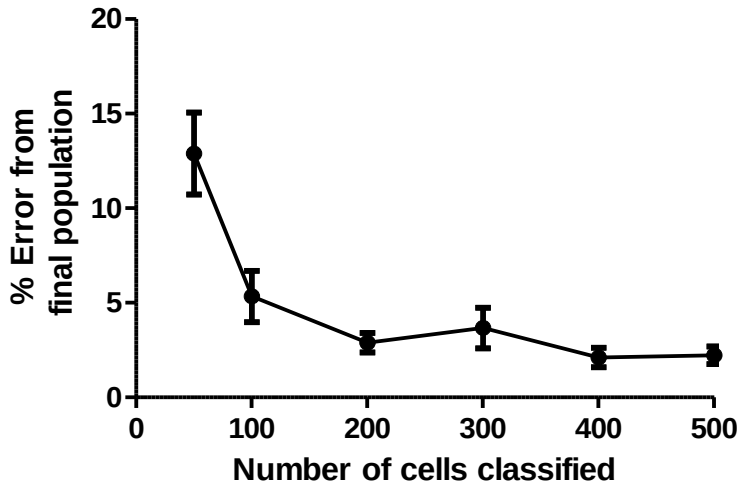

Figure 3.5 Analysis to determine the number of cells which require to be classified to accurately measure the size of CTC sub-populations on and ISET filter from a total CTC population of over 500 cells
600 CTCs from a single ISET spot were classified into 3 sub-populations (E, E/M and M) following staining with the EMT assay. The size of each sub-population as a percentage of all CTCs was measured. This was then repeated classifying a range of 50 to 500 cells from the same ISET filter and the absolute difference between the results recorded as the error. Mean and SEM are shown from 9 technical replicates.

CTCs in blood samples from four SCLC patients were phenotyped using the EMT assay to characterise the CTC sub-populations. Table 3.3 shows the clinical details of these patients. Figure 3.6 shows the EMT profiles of CTCs from these four patients. Epithelial CTCs made up 51 - 72% of all CTCs, mesenchymal CTCs 3 - 32% and mixed epithelial/mesenchymal 16 - 41%. This pilot study demonstrated that the developed workflow for staining, automated scanning and manual CTC classification can be applied to the profiling of SCLC patient CTCs. However, the manual identification and classification of CTCs on the ISET filter is very time consuming and the small patient numbers so far preclude any clinical correlative analysis. This assay is now ready to be utilised within a larger cohort in SCLC in order to

determine any associations with clinical characteristics. This study next aimed to demonstrate that application of this assay to NSCLC patient CTCs where EpCAM CellSearch enumeration is known to significantly underestimate the number of CTCs identified[59].

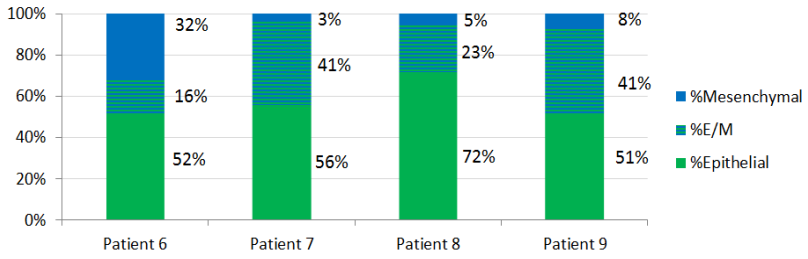

Figure 3.6 EMT profile of CTCs in a pilot study of SCLC patients
CTCs were profiled for 4 SCLC patients. The percentage of all CTCs classified as mesenchymal (cytokeratin$^-$/vimentin$^+$) are shown in blue, epithelial (cytokeratin$^+$/vimentin$^-$) are shown in green and mixed epithelial/mesenchymal (cytokeratin$^+$/vimentin$^+$) are shown in blue and green.

Patient ID	Sex	Age	Smoking History (pack years)	PS (WHO)	Sites of metastases	CellSearch CTC Number /7.5 ml	Survival (months)
6	Male	56	40	3	Bone, lung, LN	458	7.3
7	Female	63	84	2	Bone, brain, meningeal	1625	3.6
8	Male	70	58	3	LN	507	8.4
9	Female	78	27	2	Liver, lung, LN	1376	0.9

Table 3.3 Clinical characteristics of SCLC patients underwent EMT profiling of CTCs

Abbreviations: PS, performance score; LN, lymph nodes.

3.3.5 Pilot study to characterise an EMT profile of NSCLC CTCs

It has previously been shown that ISET has greater sensitivity for NSCLC CTC detection than CellSearch following IHC staining of ISET filters[59]. To extend this comparison from the previous study, which used ISET cytopathology, to the current study using EMT immunofluorescent staining, I recruited three patients (patients 10 to 12, clinical details summarised in Table 3.4) with stage 4 NSCLC and took blood samples for CellSearch enumeration and ISET EMT profiling.

Clinical details of patient 10 will be described in detail as this patient's sample subsequently gave rise to a NSCLC CDX tumour. Patient 10 was a 48 year old male. Diagnostic computer tomography identified a T1aN2M1b tumour (TNM 7th edition[245]) with a 2 cm right lung primary and metastases to brain, bone, kidney and lymph nodes. His diagnostic biopsy from a para-aortic lymph node contained sheets of polygonal poorly differentiated adenocarcinoma cells that were positive for lung markers, thyroid transcription factor 1 (TTF1) and cytokeratin 7 and negative for p40 (squamous marker), CD56, chromogranin A, synaptophysin (neuroendocrine markers) and CK20 (gastrointestinal marker). Molecular testing demonstrated wild type EGFR and was negative for ALK gene rearrangement. The patient commenced on chemotherapy with cisplatin and pemetrexed but discontinued after one cycle with deterioration in his general condition due to brain metastases. Despite administration of whole brain radiotherapy (20Gy in 5 fractions), he continued to deteriorate with progressive neurological symptoms and died 2 months following initial

diagnosis. Blood samples were drawn from patient 10 at two time points: pre-chemotherapy (time point 1, TP1) and at progression of disease post chemotherapy and cranial radiotherapy (time point 2, TP2). The other patients (Patients 11 and 12) had blood taken at progression of disease post chemotherapy only.

Consistent with previous data obtained from NSCLC patients,[73] NSCLC CTCs ($EpCAM^+$/$cytokeratin^+$) were rarely isolated by CellSearch, whereas ISET CTCs (CK^+ and/or $vimentin^+$) enriched by marker independent ISET microfiltration were detectable at levels of >150/ml in all samples (Figure 3.7).

Patient ID	Histology Sub-type	Age	Smoking History (pack years)	Site of metastases
10	Adenocarcinoma	48	0	Brian, Bone, LN, kidney
11	Adenocarcinoma	73	30	Bone, peritoneum
12	Squamous	60	30	Lung, LN

Table 3.4 Clinical characteristics of NSCLC patients who underwent EMT profiling of CTCs

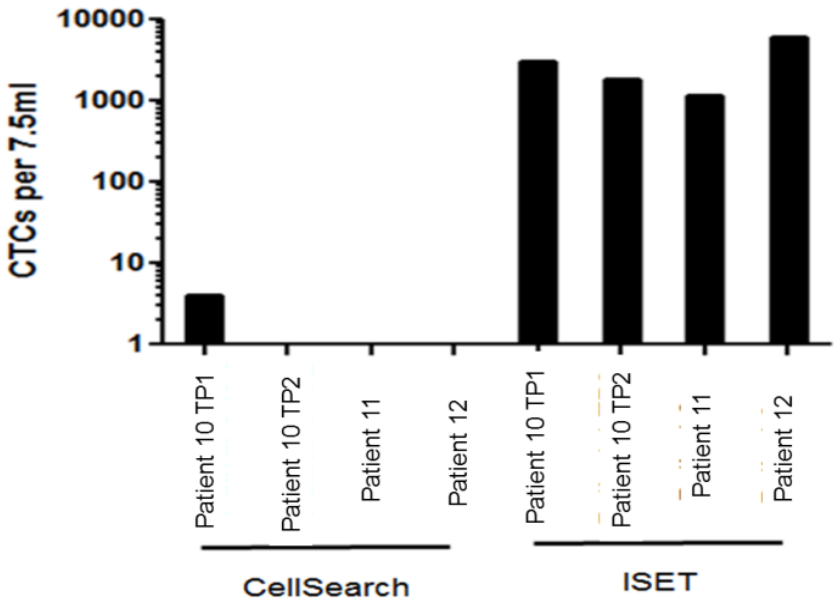

Figure 3.7 Comparison between the number of CTCs detected by CellSearch and ISET microfiltration followed by immunofluorescent staining in NSCLC patients
Paired blood samples were drawn from 3 NSCLC patients (patients 10 to 12) and CTCs enumerated by CellSearch ($EpCAM^+/CK^+$) and by ISET ($cytokeratin^+$, $vimentin^+$ or $cytokeratin^+/vimentin^+$). Patient 10 had two samples drawn for analysis. Time point 1 (TP1) was prior to any treatment and time point 2 (TP2) was following chemotherapy and radiotherapy. All ISET CTCs were counted from 4ml blood then final values extrapolated to 7.5 ml for comparison with CellSearch values.

3.3.6 Development of a novel NSCLC CDX model

EMT has been proposed to be associated with cancer stem cell behaviour, leading to aggressive disease and treatment failure[175] as detailed in the General Introduction (Section 1.8.3). One indicator of 'stem-ness' is the ability to form tumours in immune-compromised mice. Although tumourigenicity alone is not sufficient to classify cancer cells as cancer stem cells, in order to test the *in vivo* tumourigenicity of these NSCLC patient CTCs, a parallel blood sample was taken from each of the patients described above (Table 3.4) at the specified time-points and CTCs were enriched using RosetteSep enrichment (CTC marker independent; leukocyte and

erythrocyte depletion) and administered sub-cutaneously in immunocompromised mice as previously described in SCLC[66] (and detailed in Section 2.6 and 2.6). Mice were monitored for CTC derived explant (CDX) tumour growth.

The CDX project was an integrated team project within the Clinical and Experimental Pharmacology (CEP) Lab in both NSCLC and SCLC patients, the results of the latter published in Nature Medicine[66] during the course of this PhD. My role within this team was in the identification of patients and patient recruitment, sample collection and CTC enrichment by RosetteSep. Sample processing was also performed by other members of the pre-clinical team, led by Dr Chris Morrow and Ms Cassandra Hodgkinson. The enriched CTC samples were passaged *in vivo* and subsequent *in vivo* work was carried out by the CEP pre-clinical team. Analysis of the CDX tissue by IHC was performed by the author and Dr Francesca Trapani. Analysis of patient biopsy samples was performed by Dr Daisuke Nonaka as part of their clinical care. Clinical data collection, interpretation and analysis were performed by the author.

From patient 10, no CDX tumour growth was detected at baseline (TP1). However, the post-chemotherapy and radiotherapy sample (TP2) gave rise to a CDX at 95 days post implant. The tumour was passaged (measuring 53mm^3) into three mice at 116 days and CDX fragments gave rise to palpable tumours ~30 days later. Passage 2 tumour growth curves are shown in Figure 3.8(A). No CDX tumours grew from the other patient samples after follow up of 99 days (patient 11) and 72 days (patient 12). The

CDX resembled a poorly differentiated lung adenocarcinoma, comprising diffuse sheets of large polygonal cells with abundant eosinophilic cytoplasm, vesicular chromatin and enlarged nucleoli. The expression of the NSCLC markers are shown in the biopsy (Figure 3.8B(i)) and the CDX (Figure 3.8B(ii)). Both the biopsy and the CDX expressed TTF1. CK7 was expressed in approximately 10% of cells in the CDX sample and 100% of cells in the patient biopsy suggesting a less epithelial CDX phenotype. However, pan-cytokeratin staining (cytokeratins 1–8, 10, 13–16 and 19) showed retention of other cytokeratin expression in the CDX although this same antibody was not used in the patient sample. There was insufficient diagnostic material remaining to stain the patient biopsy for pan-cytokeratin or vimentin expression highlighting the need for new models such as the CDX to study lung cancer biology.

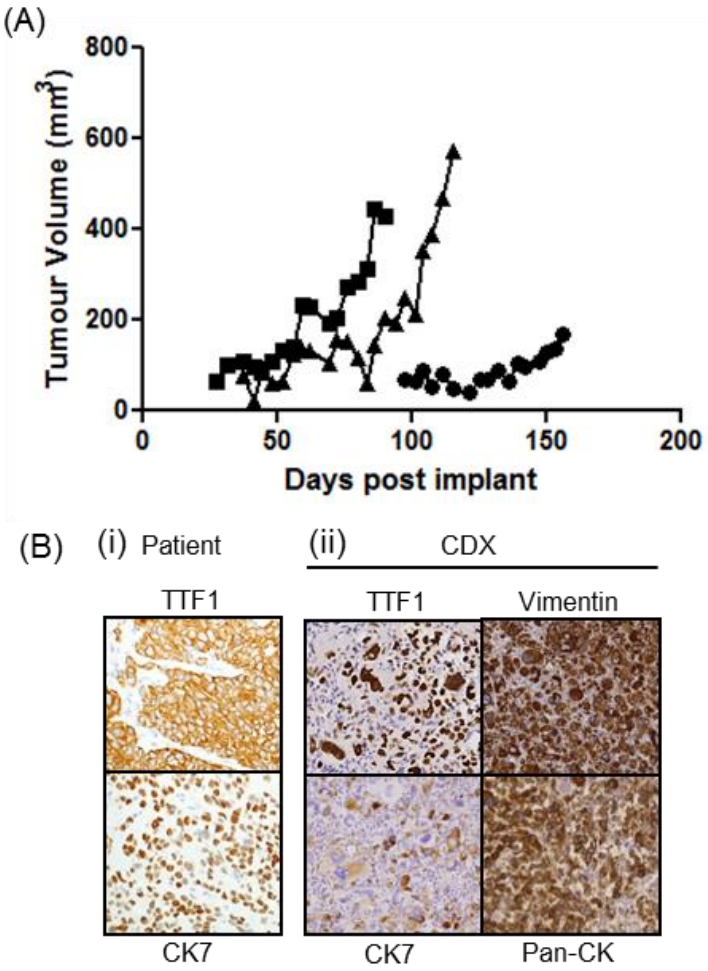

Figure 3.8 NSCLC CTC derived explant (CDX) tumour growth in NSG mice from the blood sample drawn from patient 10 post-chemotherapy

Tumour growth curves are shown (A) for passage 2 as the passage 1 tumour was harvested and passaged into three NSG mice at 53mm^3 due to animal ill health. Diagnostic patient lymph node specimen from patient 10 (B(i)) and the paired CDX (B(ii)) are shown stained for the NSCLC markers thyroid transcription factor 1 (TTF1) and cytokeratin 7 (CK7). The CDX tumour was also stained for pan-cytokeratin and vimentin expression.

In order to characterise the CTC EMT profile between these patients who have shown tumorigenic and non-tumorigenic CTC capability, and to begin to evaluate whether there are any associations between tumorigenic CTCs and markers of EMT, the ISET enriched CTCs from patients 10 – 12 were stained with the EMT assay and classified as epithelial (cytokeratin$^+$/vimentin$^-$), mesenchymal (cytokeratin$^-$/vimentin$^+$) or mixed (cytokeratin$^+$/vimentin$^+$).

Figure 3.9A shows representative ISET enriched CTCs (i – iii) from patient 10 TP2, shown staining positive for cytokeratins alone (A(i), green) vimentin alone (A(iii), blue) or cytokeratins and vimentin (A(ii), green and blue). A leukocyte or circulating endothelial cell is shown in Figure 3.9A(ii) (staining for CD45 or VE-cadherin shown in red). The proportion of CTCs expressing cytokeratins or vimentin or both is shown for each time point (Figure 3.9B, cytokeratin$^-$/vimentin$^+$ as blue block, cytokeratin$^+$/vimentin$^-$ as green block, mixed as blue and green). This demonstrates that the CTCs of patient 10 were mainly vimentin$^+$ in contrast to the CTCs of patients 11 and 12. Interestingly, this positive vimentin staining seen in the majority of CTCs from patient 10 mirrors that seen in the paired CDX tumour suggesting there is no evidence of MET having taken place during the development of a CDX tumour in this patient.

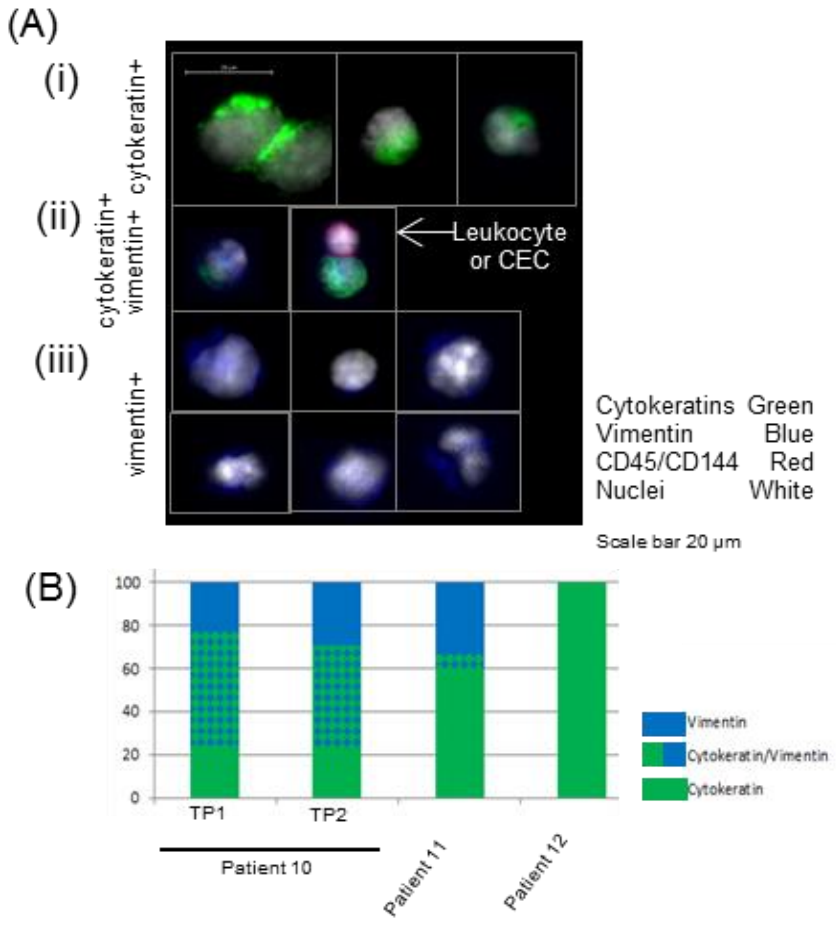

Figure 3.9 EMT profile of CTCs in in a pilot study of NSCLC patients
ISET filtered CTCs stained with the EMT assay are shown staining positive for cytokeratins (green, i and ii), and vimentin (blue, ii and iii). A leukocyte or CEC is excluded based upon its staining for CD45 or VE-cadherin (red, ii). A CTC profile was plotted for each patient (B) showing the sub-populations of CTCs which are cytokeratin$^+$ (green), vimentin$^+$ (blue) and mixed cytokeratin$^+$/vimentin$^+$ (green and blue). Raw data is included as a gallery in Appendix 1.

Following completion of my PhD lab work, further research was performed by the pre-clinical team and nucleic acid biomarker team within CEP to validate the NSCLC CDX model. This combined research has been accepted for publication in Annals of Oncology (*Tumourigenic non-small cell lung cancer circulating tumour cells – a clinical case study; Morrow, Trapani, Metcalf (joint first authors) et al., in press 2016* Appendix 2). These additional studies

included cisplatin/pemetrexed treatment of the CDX to evaluate for response to chemotherapy; single cell laser capture micro-dissection and Sanger sequencing of the ISET filtered CTCs to identify common mutations between the primary tumour, CTCs and CDX; and whole exome sequencing and RNAseq of the CDX tumour to evaluate for epithelial or mesenchymal gene expression profiles. The results of these follow on studies are included at the start of the Discussion below.

3.4 Discussion

3.4.1 Summary and ongoing research

CellSearch detects only a proportion of the entire CTC population within individual patients.[59] One explanation for this is that CTCs which have down regulated their expression of EpCAM and cytokeratins, consistent with epithelial to mesenchymal transition, would remain undetected by this approach. This chapter describes the validation of a multicolour immunofluorescent assay to characterise the expression of epithelial and mesenchymal markers (cytokeratins and vimentin respectively) by ISET enriched CTCs from patients with lung cancer. This assay improves upon previous studies in this field (summarised in Table 3.1) as it incorporated both CD45 as a marker to exclude leukocytes and VE-cadherin to exclude circulating endothelial cells (CECs). The significance of CECs in the interpretation of an EMT profiling assay is discussed in section 3.4.2 below. In two small pilot studies, this EMT profiling assay was applied to 4 SCLC samples and 4 NSCLC samples identifying sub-populations of epithelial (cytokeratin$^+$/vimentin$^-$), mesenchymal (cytokeratin$^-$/vimentin$^+$) and mixed E/M (cytokeratin$^+$/vimentin$^+$) CTCs.

This work then reports, for the first time NSCLC CTCs with tumour initiating potential and CDX generation. Analysis of the CTCs from the NSCLC CDX donor's blood revealed the absence of EpCAM$^+$/cytokeratin$^+$ CTCs using the CellSearch EpCAM dependant platform, whereas the size based ISET

enrichment revealed abundant heterogeneous CTCs of which approximately 80% were mesenchymal marker vimentin positive. The ongoing research to validate these findings was continued by the group once I had completed my PhD studies and is briefly reported here.

3.4.1.1 Confirmation of CTC tumour origin by comparison of somatic mutations in CTCs, CDX and primary tumour

In order to confirm the tumour origin of CTCs, somatic mutations in CTCs, CDX tumour and the primary tumour were compared. CDX whole exome sequencing revealed somatic mutations in 247 genes, including TP53 and KEAP1, both commonly mutated in NSCLC. To confirm tumour origin of the filtered CTCs, we sought a common mutation in tumour biopsy, CDX and ISET CTCs which were not present in leukocytes/endothelial cells. CTCs were retrieved by laser capture micro-dissection and underwent genomic DNA extraction and amplification. Confirmation of CTC tumour origin by Sanger sequencing was demonstrated by the absence of G340A mutation in PACRG in germline DNA which was present in the primary tumour, CDX and single epithelial, mesenchymal and mixed E/M phenotype CTCs (Figure 3.10).

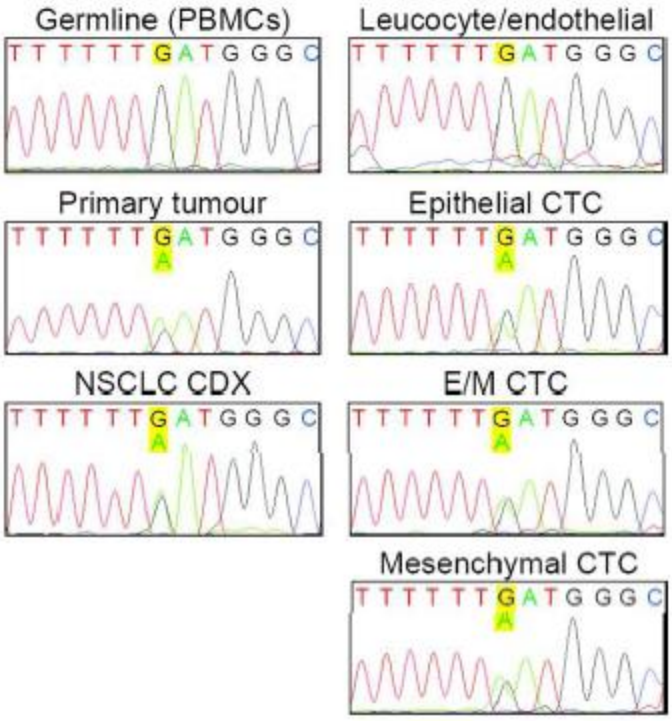

Figure 3.10 Sanger sequencing of ISET CTCs, CDX, patient tumour and germline DNA
Single cells from the ISET filter classed as a leukocyte/endothelial cell (labelled PBMC, peripheral blood mononuclear cell), epithelial CTC, mixed E/M CTC, or a mesenchymal CTC underwent laser capture identification. The PACRG locus, shown by WES to be mutated in the CDX, was Sanger sequenced in DNA extracted from the captured CTCs and leukocytes/endothelial cells, from the patients peripheral blood mononuclear cells (PBMCs, germline sample), from their primary tumour biopsy and from the passage 2 CDX. Adapted from Morrow, Trapani, Metcalf et al., in press 2016.

3.4.1.2 Evaluation of expression of epithelial and mesenchymal transcripts in the NSCLC CDX tumour

Expression of genes associated with epithelial or mesenchymal phenotypes[123,175] was evaluated after RNAseq of 3 second passage NSCLC CDX. Consistent with a mesenchymal phenotype, the NSCLC CDX expressed low levels of epithelial genes EPCAM and KRT8, high levels of mesenchymal genes vimentin and S100A4[123] and a high ratio of CD44:CD24 (Figure 3.11). These RNA profiles contrasted with a SCLC CDX from a donor

patient with 458 EpCAM^{+}/cytokeratin^{+} CTCs/7.5 ml which displayed a strong epithelial phenotype.

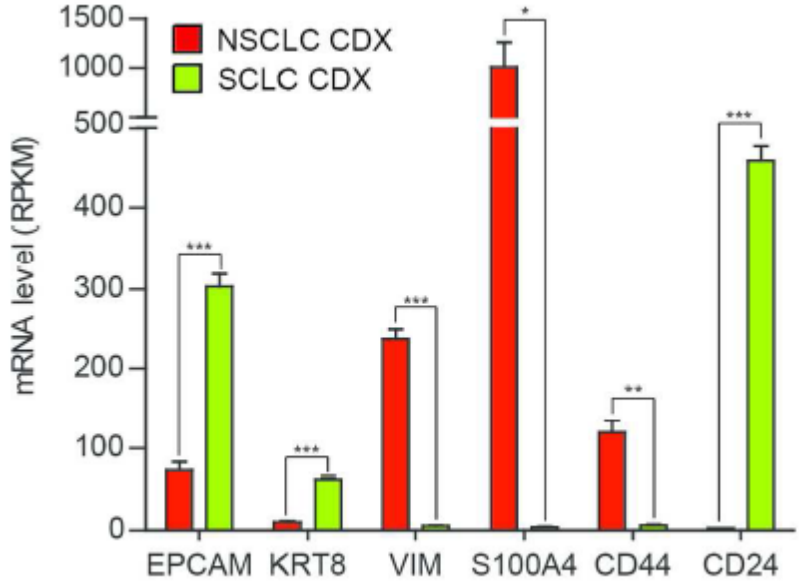

Figure 3.11 RNAseq of epithelial and mesenchymal transcripts from CDX models (comparing NSCLC and SCLC) RNAseq was performed on passage 2 NSCLC CDX tumours and passage 3 SCLC CDX from 2 SCLC CDX models. Expression of EPCAM, KRT8, VIM, S100A4, CD44 and CD24 are shown as RPKM (reads per kilobase million) values. Data represent a mean of 3 independent tumours +/- SEM. *p<0.05. ***p<0.001 according to two tailed unpaired t-test. Adapted from Morrow , Trapani, Metcalf et al., In press 2016.

3.4.2 Incorporation of markers of CECs in EMT phenotyping assay

The current study has shown that CECs (CD146^{+}/CD105^{+} detected by CellSearch) were present in excess of CellSearch CTC number (EpCAM^{+}/CK^{+}) in 4/5 SCLC patients studies (median CEC count 53/7.5 ml, range 19-120). This finding was used to justify the inclusion of a marker of CECs (VE-cadherin) the EMT profiling assay to prevent the misclassification

of CECs (which are vimentin positive)[194] as mesenchymal tumour cells (Fig 3.1). A study on CECs in 20 SCLC patients was published during the conduct of this research finding higher numbers of CECs (median 345/7.5 ml) in this larger cohort. The reason for this difference is unclear and may be due in part to the small sample size in the current study. The clinical characteristics of the 20 SCLC were not included in the report by Ilie *et al*.,[227] making comparison between these studies difficult. The same study also enumerated CECs in NSCLC patients finding significantly higher numbers (median 855/7.5 ml) in this setting, reinforcing the need to exclude CECs when incorporating vimentin^{+}/cytokeratin^{-} cells as CTCs in lung cancer.

3.4.3 Application of EMT profiling to SCLC CTCs

This assay was used to distinguish between CTCs and CECs/leukocytes in and initial pilot study in SCLC. A benefit of CTC analysis in SCLC is the predicted greater CTC abundance compared with NSCLC which would permit an evaluation of a larger number of cells per patient profiled. This high expectation of CTCs being present is a significant advantage when analysing SCLC patient samples.

However, there are limitations to processing SCLC patient samples by ISET. Firstly, SCLC CTCs are, as the name suggests, small cells. The mean diameter of SCLC cells (+/-SD) is 9.2µm (+/-2.1)[241] and the pores on the ISET microfilter are 8 µm. SCLC tends to be a spectrum of disease histologically, with a large cell component which may predominate to varying degrees[246]. However, it is not known what role the smallest SCLC CTCs (<8 µm) have in EMT, and these cells would not be reliably captured with the

ISET approach. Decreasing the pore size on the micro-filter may be expected to increase the capture rate of SCLC cells, at the expense of increased leukocyte contamination. Another group has evaluated the capture efficiency and contamination of micro-filters ranging from 5 to 8µm pore size[247] demonstrating that reducing the pore diameter results in significantly increased leukocyte contamination. Experience with manual evaluation of the 8 µm ISET platform confirms that any increased leukocyte contamination would be prohibitively time consuming in the analysis. This is the chief limitation of this approach. However, this could be overcome with the successful development of automated analysis of the micro-filters following immunofluorescent staining. The data generated using enrichment free blood plating and immunofluorescent staining with automated analysis published by the lab of Prof Kuhn[248] proves that this approach is feasible. An evaluation of an automated analysis platform for the ISET filtered CTCs is the subject of Chapter 5. Validating this approach would permit the use of smaller pore size or even enrichment free analysis which would capture the SCLC CTCs at the smaller end of the spectrum.

Additionally, given the high prevalence of $EpCAM^{+}$/$cytokeratin^{+}$ CellSearch CTCs in SCLC[57], there may be expected to be a predominant population of epithelial CTCs compared with NSCLC. However, there is pre-clinical evidence to support of pursuit of the EMT hypothesis in SCLC provided by the mouse model of SCLC from the lab of Prof. Berns.[146] In this study, detailed in the General Introduction (Section 1.8.2.3), tumour cells were classified as neuroendocrine or mesenchymal. When either neuroendocrine

or mesenchymal SCLC cell type was administered separately by sub-cutaneous injection into immune-compromised mice, local tumours formed without liver metastases whereas both cell types administered together led to the development of liver metastases. This study suggests that co-operation between mesenchymal and non-mesenchymal cells (be they neuroendocrine or epithelial) may have a role to play in SCLC metastatic progression and thus justifies the interrogation of EMT in this setting.

EMT profiling of SCLC CTCs has the potential to contribute to this debate. The pilot data reported in this thesis has confirmed that a population of SCLC CTCs exist which are mesenchymal (vimentin^{+}). The next step would be to confirm this finding in a larger patient cohort. However, during the processing step for ISET microfiltration, cells are fixed and therefore not amenable to further functional studies. In order to test the hypothesis that co-operation is required for metastatic progression further using patient samples, a combined approach using CTC profiling prior to cell implantation and attempted CDX generation. For example, patients could have an ISET sample taken for CTC profiling to confirm the presence of mesenchymal CTC populations. Subsequently, blood samples could be split three ways prior to CTC enrichment and implantation. This could be achieved, for example, by modification of the RosetteSep antibody cocktail to include antibodies against epithelial or mesenchymal antigens. One sample would have epithelial cells removed, one sample having mesenchymal cells removed and one having both populations together. The greatest challenge with conducting this experiment using clinical samples would be that additional

processing steps may decrease the likelihood of successful CDX generation and reduce the overall number of CTCs available for implantation. However, the data published by our lab on CDX generation was achieved using a 10ml blood sample. The current Ethics approval allows the collection of up to 50ml blood at a single time point and by increasing the volume of blood obtained for this purpose and larger blood volumes could be analysed in future studies.

3.4.4 Application of EMT profiling to NSCLC CTCs

A key finding from the NSCLC results reported in this chapter is to highlight the potential for generation of CDX models from metastatic cancers with low prevalence of CellSearch CTCs. This reinforces the importance of utilising marker independent technologies for CTC enrichment such is ISET alongside marker dependent CTC enrichment. Secondly, this research also identified a significant population of NSCLC CTCs that co-expressed cytokeratins and vimentin. Thirdly, whilst this research is not able to unpick the interplay between epithelial and mesenchymal cells in metastatic dissemination, this assay is now ready to be applied to test the functional importance of mesenchymal tumour cells in tumour dissemination and the need for treatment strategies that target them. These areas will be addressed in the remainder of this discussion.

3.4.5 Increased sensitivity of the immunofluorescent assay for CTC detection compared with ISET immunocytochemistry

This study has shown that CTCs are more abundant by ISET than CellSearch (Fig 3.7). The data presented also suggests that this fluorescence-based method for detection of CTCs on ISET filters has increased sensitivity for the detection of CTCs compared with IHC analysis of ISET filters. Using immunofluorescent staining of ISET filters for CTC enumeration in NSCLC patients, the current study detected >1000 CTCs/7.5 ml in all patients (mean 3026/7.5ml, range 1150 to 6091). In contrast, when 23 stage IV NSCLC patients had IHC analysis of ISET filters,[59] mean CTC number (classified as CD45 negative with malignant cytomorphology) was 98/7.5 ml (range 0 – 1045). One possible reason for this observation is that a significant difference between the published method for IHC and the current method for immunofluorescent staining is the absence of an antigen retrieval step in the immunofluorescent assay. During assay development with spike in cell lines no difference was seen in fluorescent staining with and without this step and therefore it was omitted. It is possible, however, that cells are lost from the filter membrane during this step. Although this is an interesting observation, no direct comparison can be made between the studies and this will require confirmation in an adequately powered study comparing the two approaches.

3.4.6 Mixed epithelial-mesenchymal CTCs in metastasis

The identification of tumour cells in the circulation which express both cytokeratins and vimentin in SCLC and NSCLC patients (which was most marked in NSCLC patient 10, from whom the NSCLC CDX was developed) is consistent with the findings of co-expression of epithelial and mesenchymal markers by CTCs in our previous study in NSCLC.[102] Over 30 years ago, it was observed in patients with multiple cancer types associated with malignant effusions and ascites that cytokeratin^{+}/vimentin^{+} metastatic tumour cells were seen within pleural effusions and ascites more frequently than in primary tumours or metastatic sites.[249] Subsequently, seminal *in vitro* studies showed that co-expression of cytokeratins and vimentin correlated with invasive and metastatic potential.[134,135,250] In these studies, forced co-expression of vimentin and cytokeratins in cytokeratin positive breast cancer cell lines increased cell motility and invasion and this effect was abrogated by vimentin anti-sense. In another study using vimentin positive melanoma cell lines, forced expression of cytokeratins 8 and 18 increased invasive and migratory behaviour *in vitro*. The mechanism which was postulated for this migratory behaviour was increased cytoskeletal interactions at extracellular matrix focal contacts.[250] It has been reported that vimentin may contribute to cell motility and invasiveness following activation by AKT signalling[251] resulting in stabilisation of focal adhesions through RAC1 activation.[136] These cytokeratin^{+}/vimentin^{+} tumour cells identified in the current study represent a population with a putative intermediate EMT phenotype,[252] consistent with the hypothesis that this intermediate state may be associated with characteristics associated with stem cells.[253-255] It is interesting to note

that of the three NSCLC patients studied, the patient from whom a CDX tumour was generated had the greatest proportion of CTCs expressing both cytokeratins and vimentin. This association between intermediate EMT phenotype of CTCs and tumour initiating ability can now be the subject of further study.

It is important to consider a limitation of this research with respect to the applicability of the immunofluorescent assay described in this Results Chapter to test hypotheses concerning tumour cell EMT. Classification of cells based upon cytokeratin and vimentin expression is useful to identify sub-sets of CTCs, however, it is insufficient to claim that a cell has undergone a whole-scale complex and co-ordinated set of molecular changes which fundamentally alter cell behaviour, sufficient to describe that cell as having undergone a true transition from epithelial to mesenchymal cell state. In order to address this, it would be preferable to perform gene expression profiling of epithelial and mesenchymal CTCs. However, there is no method to apply gene expression profiling to ISET filtered cells due to the requirement for sample fixation, filtration, immunofluorescent staining, mounting and imaging in order to identify CTCs. Our lab has, however, developed a single-cell RNA amplification protocol which can be applied to RNA extracted from single CTCs for example enriched by CellSearch.[181] If this protocol can be applied to gene expression profiling of sub-populations of patient CTCs which are characterised as epithelial, mesenchymal or mixed, it will permit a more comprehensive analysis of cell phenotype to be determined.

3.4.7 EMT is not always necessary for metastasis

Subsequent to the completion of the research within this thesis, two publications have demonstrated that EMT is not always necessary for metastasis,[256,257] suggesting that any requirement for EMT in metastatic cascade is context dependent. In the first of these studies by Fischer *et al*.,[256] the authors used a mesenchymal specific cre-mediated fluorescent marker to demonstrate that in an epithelial tumour, a small proportion of cells undergo EMT. However, inhibiting EMT using mir200 over-expression does not impact on the development of metastasis, although it does contribute to chemotherapy resistance.

In the second study by Zheng *et al*.,[257] using mouse models of pancreatic ductal adenocarcinoma, EMT was suppressed by deletion of SNAIL or TWIST. Suppressing EMT with this approach did not impact on the development of invasive cancer or metastasis. However, consistent with the findings of Fischer *et al.,* suppression of EMT contributed to increased chemotherapy sensitivity.

However, although these studies demonstrate that EMT may not always be required for metastasis, highlighting the likely context dependency of EMT in metastatic progression, it does not decrease the relevance of this work, as the clinical utility of drugging EMT (if this is indeed possible) is expected to be delivered through overcoming chemotherapy resistance rather than through preventing metastatic spread as the latter is likely an early event in cancer progression.

3.4.8 Potential applications of EMT profiling in drug development for NSCLC patients

As detailed in the General Introduction (Section 1.8.3), EMT may play a role in the invasion-metastasis process[100] or exist as a potential cause for resistance to chemotherapy.[117,258-260] It remains unlikely that inhibition of metastasis will lead to the clinical implementation of metastasis inhibitors. This is because tumour cell dissemination is frequently an early event in cancer progression[261] and the majority of lung cancer patients will have at least microscopic metastatic spread at diagnosis.[262]

However, there is potential for clinical utility for targeting EMT as an approach to overcoming intrinsic or acquired resistance to chemotherapy, as chemotherapy resistance is a near universal phenomenon in advanced lung cancer. Two candidate pathways implicated in EMT which may be the subject of therapeutic targeting are discussed below.

3.4.8.1 Inhibition of Axl kinase as a treatment for NSCLC

Axl kinase is a receptor tyrosine kinase which is over-expressed in solid tumours including lung cancer.[263] Binding by its ligand, Gas6[264] activates oncogenic signalling via PI3K-AKT-S6[265,266] and ERK-MAPK pathways.[267] A seminal study in EGFR mutation positive NSCLC identified Axl kinase activation as a mechanism of acquired resistance to EGFR TKI therapy[268]. In this study, using xenograft models of erlotinib resistant NSCLC, inhibition of Axl either with RNAi or by treating with an Axl inhibitor re-sensitised the tumours to erlotinib, providing a rationale for the development of Axl kinase inhibitors in NSCLC.

Subsequent studies used a 76-gene EMT signature to classify lung cancer cell lines as epithelial or mesenchymal, and the mesenchymal cells expressed higher levels of Axl and showed sensitivity to pharmacological Axl kinase inhibition (with SGI-7079).[117] Using a xenograft model of NSCLC, erlotinib resistance was overcome by treating with erlotinib and SGI-7079 suggesting this may have therapeutic application to overcoming EMT associated treatment resistance in NSCLC. A broader study including 643 cancer cell lines found that elevated Axl was most strongly associated with mesenchymal phenotype in NSCLC and that inhibition of Axl kinase sensitised mesenchymal cancer cells to docetaxel chemotherapy.[269] The same synergy was not present in epithelial cancer cells reinforcing the potential therapeutic role for Axl inhibition in targeting EMT. These studies show Axl kinase as a promising novel treatment target in NSCLC and clinical trials of Axl inhibitors in NSCLC are currently recruiting (e.g. NCT00697632).

3.4.8.2 Inhibition of TGFβ-Zeb1 signalling pathway

Transforming growth factor- β (TGF-β) is a growth factor secreted by tumour cells and surrounding stroma which has been demonstrated as having a crucial role in EMT in development[176] and more recently is described in EMT in cancer progression, driving EMT through down-regulation of mir-200, stabilising zinc finger E-box-binding homeobox 1 (Zeb1) expression.[270] Zeb1 is a zinc finger transcription factor, and Zeb1 depletion in mesenchymal like cells was demonstrated to produce a partial epithelial metaplasia which suggests this caused a reversal of EMT (mesenchymal to epithelial transition) in these cells[271] which increased chemotherapy sensitivity.[272]

Therefore it is proposed that inhibition of the TGFβ-Zeb1 pathway has a role in prevention of EMT related chemotherapy resistance and cancer progression.[273]

In vivo studies have shown that delivery of therapeutic micro-RNAs is feasible and shows anti-tumour effect[274] which may represent an approach to targeting this pathway by delivery of mir200. Another approach to targeting this pathway, by inhibition of tank-binding kinase-1 (TBK1) has been evaluated in lung cancer cell lines.[275] TBK1 has been identified as a downstream effector of the mir-200 pathway and inhibition of TBK1 was shown to cause repression of Zeb1 resulting in the attenuation of EMT changes in A549 lung cancer cells following treatment with radiotherapy.[275]

3.4.8.3 Potential application of CTC EMT profiling as a biomarker in studies of 'EMT inhibitors'

A potential utility for the EMT CTC profiling assay is to be applied as a biomarker in clinical trials of agents inhibiting AXL kinase or TGFβ signalling, based on the rationale that these approaches exert at least some of their therapeutic efficacy through inhibition of EMT. Initially, I envisage that CTC EMT profiling could be applied as an exploratory end point to test three hypotheses:

1. CTC EMT profiling prior to therapy, demonstrating high CTC vimentin expression, predicts subsequent response to therapy.

2. Change in CTC EMT profile on therapy, demonstrating a decrease in CTC vimentin expression, predicts subsequent response to therapy.

3. Change in CTC EMT profile on therapy, demonstrating a decrease in CTC vimentin expression, has utility as a pharmacodynamic biomarker to demonstrate proof of concept that the drug hitting target results in the desired biological effect.

3.4.9 Conclusion

To summarise, this chapter describes that development of an EMT CTC profiling assay which has been applied to SCLC and NSCLC patients. In an index NSCLC patient, from whom a NSCLC CDX tumour was generated, the CTCs had a predominantly mesenchymal (cytokeratin^{+}/vimentin^{+} or cytokeratin^{-}/vimentin^{+}) phenotype. Both the patient's tumour and the CDX model showed resistance to cytotoxic chemotherapy with cisplatin and pemetrexed. This CTC profiling assay has the potential to be applied as a biomarker alongside clinical trials of EMT inhibitors such as AXL kinase inhibitors, trials of which are underway in NSCLC.

4 EVALUATION OF VASCULOGENIC MIMICRY IN SMALL CELL LUNG CANCER USING PATIENT BIOPSIES, CIRCULATING TUMOUR CELLS AND CTC DERIVED EXPLANT MODELS

4.1 Introduction

The chemotherapy treatment for SCLC remains unchanged for 30 years.[6] Although SCLC is initially chemotherapy sensitive, disease relapse is inevitable and recurrent disease is usually chemotherapy resistant.[13] An improved understanding of SCLC biology *per se* and especially that underpinning disease recurrence and chemotherapy resistance is required to instruct development of novel therapeutic strategies, for example by overcoming mechanisms of drug resistance.

As described in detail in the General Introduction to this work (Section 1.9), vasculogenic mimicry (VM) describes the ability of tumour cells to adopt endothelial cell behaviours and form *de novo* vascular networks[186] in response to environmental stimuli such as hypoxia.[189-193]

VM has not previously been reported in SCLC, although it has been described in many other cancer types including NSCLC, in which setting it is associated with shorter patient survival.[197] However, I propose that the clinical effect of VM may be context dependent. The shorter patient survival frequently reported has been attributed to a ‘stem-like’ phenotype which was described in gene expression profiling of melanoma cells which are capable of VM.[199] It is important to acknowledge, as detailed in the General Introduction (Section 1.8.3)), that the cancer stem cell paradigm remains an

area of active debate in solid tumours such as lung cancer.[276] However, tumours harbouring a 'stem-like' gene expression profile have been associated with aggressive tumour cell behaviour.[277] Moreover, It is established that tumours need a blood supply to grow beyond 2 – 4mm diameter,[278] enabling delivery of oxygen and essential nutrients to the tumour. VM may therefore aid tumour growth providing the tumour vasculature without the requirement for angiogenesis to occur.

Conversely, tumour VM could improve tumour response to treatment with chemotherapy or radiotherapy. Through the production of a vascular network within the tumour, VM may permit an improved effect of chemotherapy due to a combination of reduced hypoxia, normalisation of tumour pH and improved drug penetration within the tumour, all of which are reported to enhance chemotherapy treatment effect.[25-30] This area is detailed in the General Introduction (Section 1.2). The potential for VM to have a clinical impact on SCLC may be amplified by the high response rates (up to 75% of patients having a radiological response to therapy) typically seen in the chemotherapy naive setting.[6]

In order to begin to address the functional impact of VM, if any, in SCLC, I sought to take multiple approaches. Firstly, SCLC patient biopsies were evaluated for evidence of VM, as tumour material obtained from patients remains the gold standard for evaluation of SCLC biology. This approach was complemented by the analysis of SCLC CTCs. If VM represents a novel route for tumour cells to access the circulation, I proposed that a population of CTCs exists within the circulation which expresses biomarkers of a VM

phenotype. As detailed in the General Introduction (Section 1.9.3), one such candidate is VE-cadherin, which is highly expressed in VM competent melanoma cells[199] and has been shown to have a functional role in VM via *in vitro* methods in melanoma,[202] oesophageal carcinoma,[213] glioblastoma[214] and osteosarcoma.[215]

Finally, as the CDX models arose from CTCs, interrogation of CDX models was used as a surrogate for SCLC patient tumour to evaluate for plasticity allowing VM after metastatic dissemination. If CDX models are shown to develop VM networks then these models may act as a pre-clinical model to study the therapeutic targeting of VM in SCLC.

Hypotheses

- Vasculogenic mimicry occurs in SCLC biopsies and/or in CDX models and correlates with aggressive disease.
- Tumour cells with VM phenotypes are present in the bloodstream.

Aims

- To evaluate the presence of VM in SCLC using patient biopsies and correlate with clinical outcomes.
- To utilise SCLC CDX models to determine whether secondary tumours arising from CTCs are able to produce VM networks.
- To evaluate the utility of SCLC CTCs as a biomarker of VM in SCLC using CTC VE-cadherin expression as a putative biomarker of VM.
- To address the functional role of VE-cadherin in VM in SCLC cell lines and SCLC xenografts.

- To explore drug delivery in tumours which express high or low levels of VE-cadherin *in vivo*.

4.2 Methods

As discussed with respect to the NSCLC CDX project in Chapter 3, the SCLC CDX project was also an integrated team project within the Clinical and Experimental Pharmacology (CEP) Lab. The author's role within the CDX team was in the identification of patients and patient recruitment, sample collection and CTC enrichment by RosetteSep. Sample processing was also performed by other members of the pre-clinical team, led by Dr Chris Morrow. The enriched CTC samples were passaged *in vivo.* All animal handling was carried out by the CEP pre-clinical team. Analysis of the patient biopsy and CDX tissue by IHC was performed by the author and Dr Francesca Trapani. Analysis of patient biopsy samples was performed by Dr Daisuke Nonaka as part of their clinical care. Clinical data collection, interpretation and analysis were performed by the author. The NCI-H446 VE-cadherin knock down cell line was generated by Dr Kathryn Simpson. All the ISET CTC assay development and analysis was performed by the author with support in CTC scoring from the CTC GCP analysts.

4.2.1 Patient recruitment and blood sampling

83 patients with histological or cytological confirmation of SCLC attending the University Hospital of South Manchester or the Christie NHS Foundation Trusts were recruited as part of our broader spectrum of SCLC research [European Union CHEMORES FP6 contract number LSHC-CT-2007-037665] according to ethically approved protocols (NHS North West 9 Research Ethics Committee).

Evidence of VM structures in patient biopsies was sought in a SCLC tissue microarray (TMA). Tissue from 41 limited stage SCLC patients was included in the TMA as previously reported.[279] No paired blood samples were available in this cohort for CTC analysis as these patients were recruited and treated in advance of the current study.

Blood was drawn from a further 38 patients with chemotherapy naïve SCLC (30 with extensive stage and 8 with limited stage disease) to enrich for circulating tumour cells (CTCs) by ISET microfiltration[280] as described in the General Methods (Section 2.8) for subsequent CTC profiling. Paired CellSearch counts were performed in these patients (Section 2.7). Bronchoscopic biopsies were obtained in 24 of the extensive stage patients in whom CTCs were analysed.

A separate cohort of 4 chemotherapy naïve extensive stage SCLC patients provided blood that led to the derivation of 4 SCLC CDX models[66] (patients 5 – 9 in Chapter 3). In these patients, blood was drawn prior to chemotherapy and CTCs were enumerated by CellSearch, and were enriched by RosetteSep (Section 2.5) to generate CTC derived explant (CDX) tumours sub-cutaneously in immune-compromised mice as previously described[66] (Section 2.6). A third blood sample was processed by ISET microfiltration for CTC enrichment and subsequent immunofluorescent analysis.

4.2.2 Immunohistochemistry and 'VM scoring' of patient biopsies and CDX samples

Formalin fixed and paraffin embedded sections from the TMA, CDX and xenograft tumours were stained on an automated stainer (i6000, BioGenex)

by IHC using antibodies against Cytokeratins (pan-cytokeratin antibody to cytokeratins 1–8, 10, 13–16 and 19, mouse AE1/AE3, M3515, 1:60, Dako), CD56 (mouse, 1B6, NCL-CD56-1B6, 1:100, Novocastra), synaptophysin (mouse, 27G12, NCL-L-SYNAP-299, 1:200, Novocastra), chromogranin A (mouse, LK2H10 + PHE5, MP-010-CM1, 1:600, Menapath), CD31 (Rabbit, polyclonal, CHG CD31-P1; 162.5 mg/ml, 1:600 (kindly gifted by N.R. Smith, AstraZeneca Pharmaceuticals) which reacts with mouse and human CD31) and Periodic Acid Schiff staining (PAS, comprising 0.5% periodic acid for 5 minutes (Sigma Aldrich 375810) and Schiff's reagent for 20 minutes (Sigma Aldrich S5133)).

Sections were prepared by de-waxing in xylene for 10 minutes x3 and rehydrating in alcohol. Antigen retrieval was performed in pH 6.0 citrate target retrieval solution (from 10x stock, DAKO S2369, in dH20) at 110 degrees Celsius for 5 minutes. Antibody incubations took place at room temperature for 60 minutes using antibody diluent (DAKO S0809). Sections were blocked with 3% endogenous peroxidase block (from hydrogen peroxide 10x stock (Sigma Aldrich 95321) and the avidin and biotin blocking kit (Vector Elite SP-2001) as per manufacturer's instructions. The biotinylated secondary antibody with chromogen was applied (vector elite avidin and biotinylated horseradish peroxidase macromolecular complex (ABC) kit (Rabbit IgG) (Vector PK-6101) and DAB + Substrate chromogen kit (DAKO K3468)) as per manufacturer's instructions.

Tumour vessels were classified as either endothelial vessels ($PAS^+/CD31^+$) or VM vessels ($PAS^+/CD31^-$). As the hypothesis had been generated that VM

vessels may have an effect of chemotherapy delivery, a 'VM vessel density' was calculated as the number of VM vessels per mm^2 of tumour area as vascular density has been shown to correlate with tumour perfusion.[281] To determine the density of VM vessels, the number of VM vessels was counted for the whole tissue section and the evaluable tumour area measured, reporting VM vessel density in VM vessels/mm^2. To determine the proportion of VM structures within the tumour vasculature, a VM score was calculated as the number of VM networks/total vascular structures ($PAS^+/CD31^+$ and $PAS^+/CD31^-$) per section, represented as a percentage as previously described.[282]

4.2.3 Immunofluorescence and 'VM scoring' of ISET filtered CTCs

ISET filtered CTCs were stained by IF using antibodies against CD45, cytokeratin, and VE-cadherin. Four individual filter 'spots' were excised for each patient (from 4 ml blood) and rehydrated for 1 min in PBST. The filters were placed in 0.2% Triton X-100 for 10min in a humidity chamber (used for all subsequent incubations at room temperature) to permeabilise deposited cells for antibody entry and washed for 1min in PBST. Filter spots were incubated with 10% goat serum block (Dako X0907) for 30min, then incubated in an cocktail (80µl) of two primary antibodies, unconjugated anti-CD45, (1:400 of 0.5mg/ml, Rabbit, Abcam AB10559) and unconjugated anti-VE-cadherin, (1:200 of 0.5mg/ml, Mouse, eBioscience 14-1449-82), for 1 hour. The filter spots were washed twice in PBST, then incubated with a cocktail (80µl) of two fluorescent secondary antibodies, goat anti-rabbit DY549 (1:500 of 1mg/ml, Thermo Scientific, 35558) and goat anti-mouse

AF647 (1:500 of 2mg/ml, Invitrogen, A-21235) for 1 hour. The filter spots were washed twice in PBST, then incubated with 80µl of anti-CK FITC (1:100 of 3mg/ml, Sigma F3418, clone C11 against CKs 4, 5, 6, 8, 10, 13 and 18), for 1 hour. The filter spots were washed twice in PBST, then incubated with 80µl DAPI (1:10,000 of 5mg/ml, Invitrogen D3571) for 5min. Filter spots were washed twice in PBST and twice in double distilled water before mounting and coverslipping (1.5 grade) on a glass slide with ProLong Gold anti-fade (Invitrogen P36934). Slides were left overnight at room temperature to dry before analysis. This assay distinguishes leucocytes (CD45 positive), circulating endothelial cells (VE-cadherin positive) and CTCs (CK positive). Filters were scanned on the Mirax automated slide scanner as described in the General Methods (Section 2.10). A VM score was generated for all patients, calculated as the number of VE-cadherin positive CTCs/total number of CTCs in 4 ml blood, represented as a percentage.

4.2.4 Cell lines and generation of shRNA targeted to VE-Cadherin

NCI-H446 (American Type Culture Collection) was authenticated (ampflstr, Applied Biosystems) and cultured in RPMI media (Life Technologies) and 10% foetal bovine serum (Biowest) at 37 degrees and 5% CO_2. H446 shRNA knock down of VE-cadherin was generated by Dr Kathryn Simpson within CEP. To perform VE-cadherin knockdown, viral particles containing five siRNAs targeted against VE-Cadherin cloned separately into the pLKO.1 lentiviral vector (Dharmacon, GE Lifesciences) and the pLKO.1 TRC Control vector (Addgene #10879) were generated by co-transfecting Lenti-X 293T (Clontech) cells with the respective shRNA or control plasmids and pCMV-

R8.91 and pMD2.G (kind gift from Dr Akira Orimo, Juntendo University, Tokyo, Japan) as previously described.[279] NCI-H446 cells were transfected with virus plus 6 µg/ml polybrene (Sigma) and selected with 1µg/ml puromycin (Sigma) for ~ 7 days and polyclonal mixes for each shRNA plus the control were generated and screened for knock-down of VE-Cadherin by western blot. Other cell lines were maintained as described in the General Methods (Section 2.1).

4.2.5 Western blotting

Cell lysates were analysed by western blotting as described in the general Methods Chapter. Antibodies against cytokeratins (1:500, Clone C11, mouse, Sigma, F3418), vimentin (1:500, clone V9 mouse, Santa-Cruz sc6260), CD45 (1:500, Polyclonal, rabbit, Abcam, ab10559), VE-cadherin (1:500, Clone 16B1, eBioscience, mouse, 14-1449), GAPDH (1:2500, polyclonal, rabbit, Abcam ab9485) and tubulin (1:2500, polyclonal, rabbit, Abcam, ab15246) were diluted in 1% milk in 0.1% PBS-T. Membranes were washed and incubated for 1 hour at 21 degrees Celsius with HRP linked secondary goat anti mouse or goat anti rabbit (Dako, CA USA) diluted 1:2500 in 1% milk in 0.1% PBS-T then washed and visualised with chemiluminescence (ECL+ system, Amersham).

4.2.6 Matrigel vasculogenic mimicry network assay

H446, H446 shRNA VE-cadherin and H1048 cells were seeded at $1x10^5$ cells per well in a 6-well plate on a monolayer of Matrigel (BD Biosciences) and maintained in RMPI media at 37 degrees Celsius and 5% carbon dioxide

according to a previously defined protocol.[186] Networks were imaged between 4 and 72 hours and at 7 to 14 days within 4 randomly selected fields of view per well by phase contrast microscopy at 5x and 10x magnification.

4.2.7 *In vivo* growth study H446 parental and VE-cadherin knock-down tumours

1 x 10^6 H446 parental or VE-Cadherin knock-down cells in 0.2 ml (1:1 media: Matrigel) were subcutaneously injected into the back/mid-dorsal region of 6-8 week old female NSG mice. Mice were housed and tumour size monitored until reaching 800 to 1000 mm^3 when animals were culled via a Schedule I method and formalin fixed and paraffin embedded for IHC analysis. All procedures were carried out in accordance with Home Office (UK) regulations and the UK Co-ordinating Committee on Cancer Research guidelines and by approved protocols (Home Office Project license no. 40-3306 and Cancer Research UK Manchester institute Animal Welfare and Ethical Review Advisory Board).

4.2.8 Platinum measurement in H446 parental and VE-cadherin knock-down tumour xenografts

1 x 10^6 H446 parental or VE-Cadherin knock-down cells in 0.2 ml (1:1 media: Matrigel) were subcutaneously injected into the flank of NSG mice. Animals were housed and tumours monitored until they reached ~250 mm^3 at which point animals were treated were treated with 7.5mg/kg intra-peritoneal cisplatin and the animals were culled at 1 hour post treatment by a schedule I method and the tumours harvested. Half the tumour was formalin fixed

paraffin embedded for IHC (CD31 and PAS staining) and half snap frozen for platinum measurement by inductively coupled plasma mass spectrometry (ICP-MS, Agilent 7500cx). For platinum measurement, whole tumours were weighed and dissolved in 1:1 Aqua Regia (3:1 mix of HCl and HNO_3) overnight at 70°C and the solution ionised and separated according to the mass charge ratio using a quadruple mass filter to detect and quantify platinum in each sample.

4.2.9 Measurement of tumour density using diagnostic computerised tomography

Diagnostic CT scan images were reviewed in PACS viewing software. Post-contrast axial images of the thorax were identified and the image showing the primary tumour with any confluent lymph nodes with the greatest area was selected for analysis. The tumour was outlined using the cursor and the tumour size and average tumour density was recorded in Hounsfield Units.

4.2.10 Statistical analysis

Statistical analysis was performed as outlined in the general statistical considerations in the General Methods section. Fisher's exact test was used to evaluate for association between the TMA VM score and prognostic factors (Hb <9 g/L, WBC >10x109/L, platelets <150x109/L, Na <135 mmol/L and LDH >550 IU/L). Univariate survival analysis was performed using Kaplan-Meier analysis, and difference between survival distributions was evaluated with the Log Rank test. A p-value of <0.05 was considered statistically significant throughout. Survival times were calculated as the time

between date of biopsy and date of death or last follow up. Patients alive at last follow up were censored.

To determine the TMA VM score with the greatest sensitivity and specificity of predicting patient survival, receiver operating characteristic (ROC) curves were analysed to calculate the area under the ROC curve and to determine the sensitivity and specificity for prediction of survival at 3 years (for the biopsy VM score in limited stage SCLC) and at 9 months (for the CTC VM score in extensive stage SCLC). As detailed in the General Methods (Section 2.11), these differing end points were purposefully selected as the most clinically relevant in each circumstance. In limited stage disease, with treatment with curative intent, long term (3 year) survival is considered the successful outcome following treatment. Current treatment in extensive stage disease is associated with few survivors at 3 years, however studies report a median survival of up to 9 months and this figure was therefore selected as an appropriate end-point.

The sensitivity and specificity of multiple thresholds around the median of each score were calculated to select the optimum cut-point. To evaluate for associations between clinical variables and VM score, correlation matrices were plotted, calculating a correlation co-efficient using Spearman's rank (if parametric) and Pearson's rank (if non-parametric distribution).

4.3 Results

4.3.1 Evaluation of vasculogenic mimicry (VM) in SCLC patient biopsies

In order to evaluate for the presence of vasculogenic mimicry in SCLC tumour samples, a SCLC tissue microarray (TMA) containing tissue from 41 patients with limited stage (LS) disease was stained with periodic acid Schiff (PAS) and anti-human CD31 (Figure 4.1). PAS positive laminin and collagen networks (pink) are shown surrounding malignant cells, identified by enlarged nuclei, mitotic figures and nuclear moulding (haematoxylin counter-stain, Figure 4.1A). $PAS^{+}/CD31^{+}$ endothelial vessels and $PAS^{+}/CD31^{-}$ vessels consistent with VM and referred to hereafter as VM vessels were clearly observed (Figure 4.1B). Endothelial and VM vessels were found in all patient samples. To determine the proportion of VM structures within the tumour vasculature, a VM score was calculated as the number of VM vessels/total number of vessels) x100 (as previously described[282]) and this ranged from 0-50% (mean 15.5%, median 12.1%).

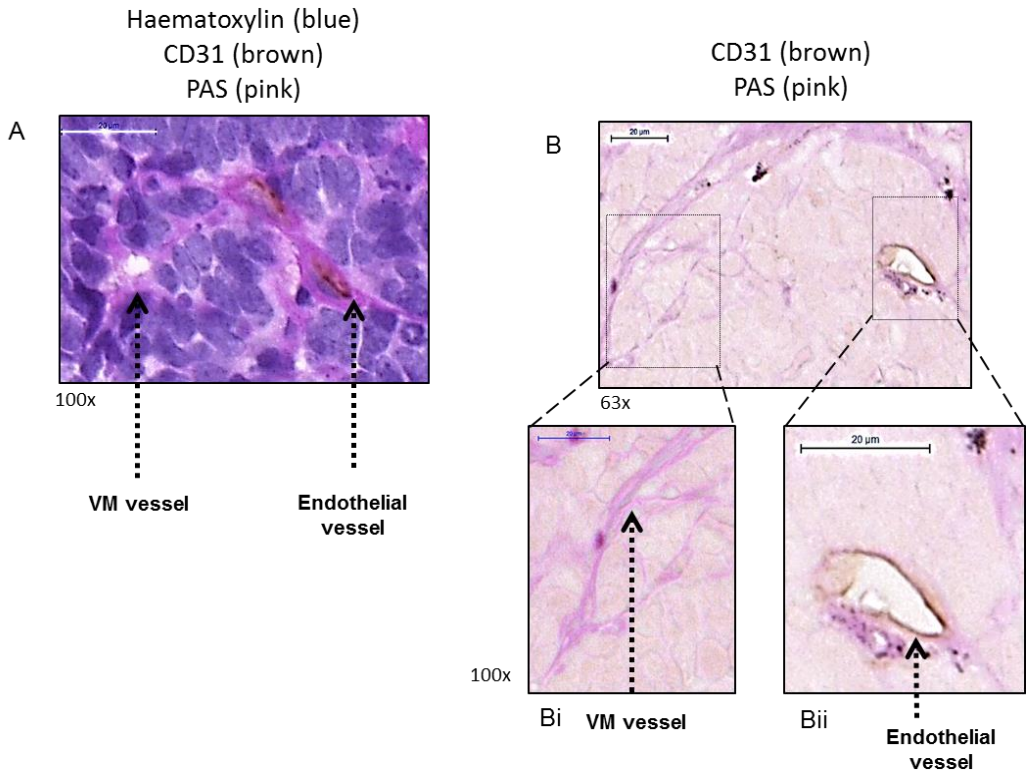

Figure 4.1 CD31/PAS staining of metastatic lymph node specimens in a micro-array generated from limited stage SCLC patients

1mm cores taken during lymph node resection were stained with CD31 (brown), Periodic acid Schiff (PAS) (pink) and with/without haematoxylin (purple). SCLC cells with malignant morphology were infiltrated by vascular channels which were $PAS^{+}/CD31^{+}$ (blood vessels) and $PAS^{+}/CD31^{-}$ (VM channels) (A, 100x magnification). PAS+ structures showed loops and whorls characteristic of VM and via light microscopy (B, 63x magnification). Bi VM structures identified by $PAS^{+}/CD31^{-}$, Bii; $PAS^{+}/CD31^{+}$ (blood vessels) (100x magnification).

4.3.2 Correlation between VM in patient biopsies and clinical characteristics

To explore any associations between VM score in patient biopsies and clinical characteristics, a correlation matrix was generated including baseline haematology and biochemistry data in addition to biopsy VM score (Figure 4.2). No further baseline clinical data were available for analysis. Only serum albumin correlated with biopsy VM score (R=-0.42, 95% CI -0.67 to -0.08, p=0.017). A reduced albumin is known to be associated with worse cancer survival[283] and albumin was also correlated with a other established prognostic factors in this clinical dataset: reduced haemoglobin, elevated leucocytes, neutrophils and lactate dehydrogenase.

Figure 4.2 (Over page). A correlation matrix to assess for associations between biopsy VM score and clinical characteristics. Baseline biochemistry and haematology data were included alongside biopsy VM score and patient age. Significant correlations were identified using Pearson's Rank (if parametric) and Spearman's Rank (if non-parametric) and are marked with a red asterix (*=p<0.05, **=p<0.01, ***=p<0.001).

Significant correlations	R value	95% CI	P value
VM score and albumin	-0.41	-0.67 to -0.08	0.0169
Albumin and haemoglobin	0.62	0.36 to 0.80	0.0001
Albumin and leucocytes	-0.40	-0.66 to -0.04	0.0247
Albumin and neutrophils	-0.36	-0.64 to -0.01	0.0452
Albumin and creatinine	-0.45	-0.70 to -0.09	0.0163
Albumin and LDH	-0.45	-0.72 to -0.06	0.0258
Leucocytes and LDH	0.54	0.17 to 0.78	0.0053
Leucocytes and haemoglobin	-0.38	-0.63 to -0.05	0.0245
Leucocytes and neutrophils	0.97	0.94 to 0.98	<0.0001
LDH and neutrophils	0.62	0.29 to 0.82	0.0010

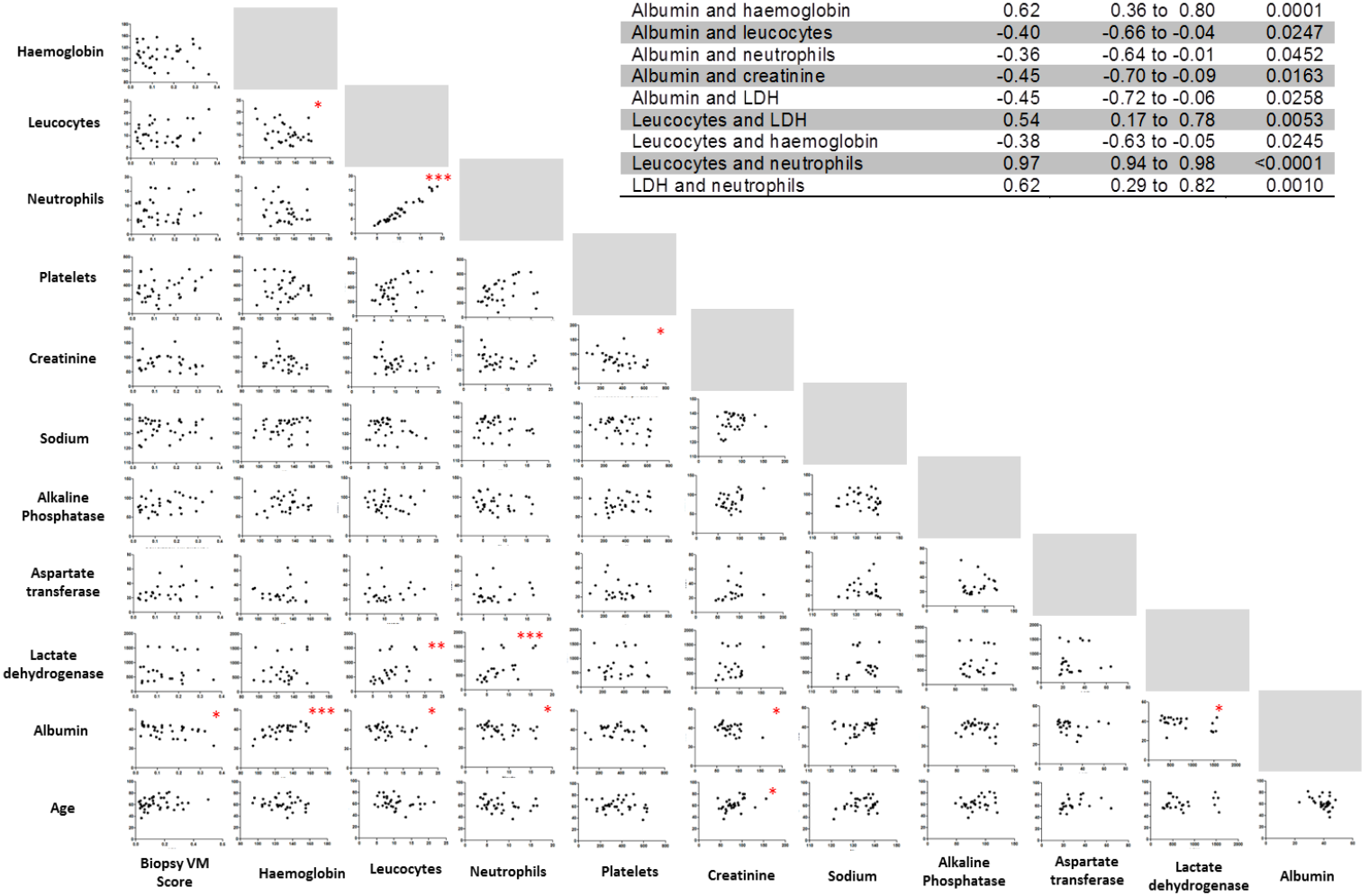

Figure 4.2 A correlation matrix to assess for associations between biopsy VM score and clinical characteristics

4.3.3 Correlation between VM in patient biopsies and patient survival

Clinical outcome data were analysed to determine any association between VM score and patient survival in this limited stage SCLC cohort. To determine a VM score cut-off with the highest sensitivity and specificity to predict patient survival at 3 years, a receiver operating characteristic (ROC) curve was plotted and the area under the ROC curve calculated for the prediction of 3 year survival. Three year survival was selected as the clinically meaningful end-point in this cohort of patients with limited stage disease where data from meta-analyses report the three year survival in the region of 15-20%[284]. This compares with <5% in extensive stage disease. If a biomarker can be validated which reliably separates the long term survivors in limited stage SCLC, this may have practical application to patient stratification for treatment.

The association between VM score and 3 year patient survival showed an area under the ROC curve of 0.78 (p=0.008, Figure 4.3A). The optimum cut-off for sensitivity and specificity to predict survival at 3 years was a VM score of 10% where a range of VM scores around the median value were tested (Figure 4.3B).

A

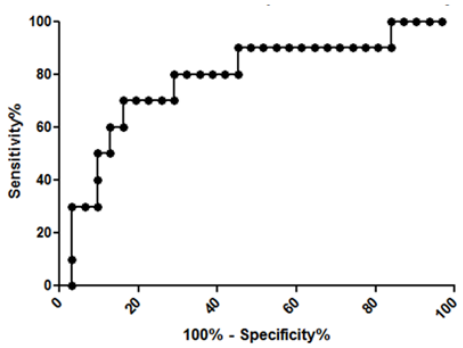

Area under the ROC curve	0.784
Standard Error	0.088
95% Confidence Interval	0.61 to 0.96
P value	0.0076

B

VM score (%)	Sensitivity (%)	95% CI	Specificity (%)	95% CI
5	50.0	18.7 to 81.3	90.3	74.3 to 97.8
10	80.0	44.4 to 97.5	70.9	52.0 to 85.8
15	90.0	55.5 to 99.8	54.9	36.0 to 72.7
20	90.0	55.5 to 95.8	54.8	36.0 to 72.7

Figure 4.3 Receiver operating characteristic (ROC) curve analysis for VM scores (A) and sensitivity and specificity values for a range of cut-off scores with respect to patient survival at three years (B)

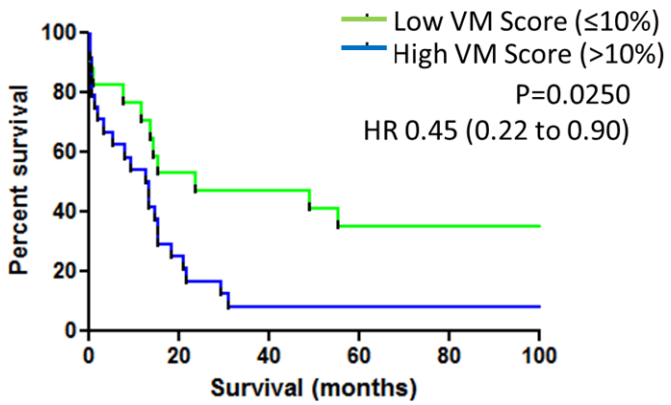

Figure 4.4 Univariate survival analysis by VM score in limited stage SCLC
Kaplan-Meier survival analysis for 41 patients dichotomised by VM score into high (n=24, blue) and low (n=17, green) VM using a threshold of 10% based upon ROC curve analysis.

Consistent with published data in other cancer types,[197] univariate survival analysis demonstrated that patients with an elevated VM score (≥10%) had significantly reduced 3 year survival (8.3 v 47%) and median survival (13.0 months v 23.8 months) (log rank p=0.025) compared to those patients whose tumours had a VM score <10% (Figure 4.4). In addition to VM score, univariate survival analysis was performed based upon haematology and biochemistry results at diagnosis. Alongside VM score, reduced sodium or albumin and elevated leukocyte count were associated with shorter patient survival (Table 4.1) which is consistent with previous reports on the prognostic value of these results in SCLC.[285]

Co-variate	n	Median OS (months)	95% CI	P value
Age				
<60	20	14.2	11.7 – 16.7	0.379
≥60	21	13.2	0.0 – 27.9	
Lactate dehydrogenase				
<550	10	15.4	12.8 – 17.9	0.399
≥550	15	11.7	0.0 – 26.1	
Sodium				
<132	12	7.8	0.0 – 19.1	0.034
≥132	23	15.4	4.6 – 26.1	
Albumin				
<35	8	0.8	0.0 – 1.6	0.019
≥35	24	14.8	12.8 – 16.8	
Haemoglobin				
<11	7	13.2	0.0 – 46.0	0.956
≥11	28	13.7	11.0 – 16.4	
Leucocytes				
<11	22	15.4	6.7 – 24.0	0.012
≥11	13	5.4	0.0 – 13.4	
Platelets				
<350	23	14.8	12.2 – 17.5	0.346
≥350	12	8.0	0.0 – 24.7	
Biopsy VM score				
≤10%	17	23.8	0.0 – 70.4	0.025
>10%	24	13.0	6.3 – 19.2	

Table 4.1 Univariate survival analysis of limited stage SCLC patients who underwent evaluation of VM score in tumour biopsy

To evaluate for potential confounding variables, baseline haematology and biochemistry values were compared between the limited stage SCLC patients who were classified as VM high (>10% n=24) or VM low (<10% n=17) (Table 4.2). No significant difference was seen in these variables between groups. There were too few cases to perform a multivariate analysis and a larger cohort study is planned to evaluate this further.

	All patients (n=41)	Biopsy VM Score, ≤10% (n=17)	Biopsy VM score, >10% (n=24)	
	Mean Units (SD)	Mean Units (SD)	Mean Units (SD)	P value
Haemoglobin (g/L)	128 (17)	127 (15.8)	128 (18.7)	0.95
Leukocytes (x10^9/L)	10.8 (4.3)	10.8 (3.6)	10.8 (4.8)	0.94
Neutrophils (x10^9/L)	8.2 (4.0)	8.3 (3.5)	8.1 (4.5)	0.90
Platelets (x10^9/L)	355 (152)	360 (144)	349 (159)	0.94
Creatinine (umol/L)	82 (24)	78 (20)	85 (27)	0.50
Sodium (mmol/L)	134 (5.7)	134 (6.5)	134 (5.1)	0.81
Lactate dehydrogenase (IU/L)	772 (439)	682 (358)	833 (477)	0.42
Aspartate aminotransferase (IU/L)	29 (11.7)	23 (4.1)	33 (13.2)	0.05
Alkaline phosphatase (IU/L)	84 (19.8)	78 (18.7)	88 (19.6)	0.19
Albumin (g/L)	39 (5.7)	41 (4.8)	37 (5.9)	0.06

Table 4.2 Clinical characteristics of the limited stage SCLC patients who underwent VM scoring within biopsy samples comparing the cases with high and low VM score

4.3.4 Characterisation of VM within the SCLC CDX models

Analysis of patient biopsies has provided the first evidence that VM occurs in limited stage SCLC and that it is prognostic by univariate analysis. The lack of available biopsy material has hampered the study of SCLC biology, and this is exemplified by findings described in section 4.3.3 above where there were too few cases to perform a multivariate analysis. However, the development of the SCLC CDX models[66] derived from SCLC CTCs has provided an alternate source of readily available SCLC derived tumour

material for study. Therefore, CDX samples were next examined as a model of SCLC metastasis. Four SCLC patients (Patients 6-9 Chapter 3, clinical details in Table 3.3) had a blood sample drawn for CTC enrichment with RosetteSep and implanted into NSG mice from which CDX models were generated. Figure 4.5 shows that expression of SCLC markers CD56, synaptophysin, cytokeratins (CK) and TTF1 by IHC in the patient biopsy mirrored that observed in CDX tumours arising from the same donors. CD31/PAS staining identified VM networks in which red blood cells can be clearly seen in all four CDX tumour models (Figure 4.6(i)). As the hypothesis had been generated that VM vessels may have an effect of chemotherapy delivery, a 'VM vessel density' was calculated as the number of VM vessels per mm^2 of tumour area as vascular density has been shown to correlate with tumour perfusion.[281] The VM vessel density ranged from 0-3 VM vessels/mm^2 (Figure 4.6(ii)).

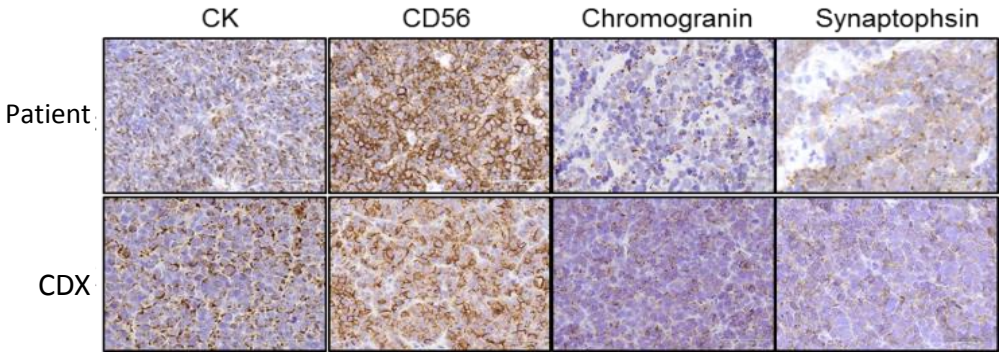

Figure 4.5 Comparison between IHC staining of patient tumour biopsies and SCLC CDX tumours for cytokeratins, CD56, chromogranin and synaptophysin
IHC staining for the SCLC markers CD56, synaptophysin, and cytokeratins (CK) for matched patient biopsy and CDX tumour from SCLC patient 6.

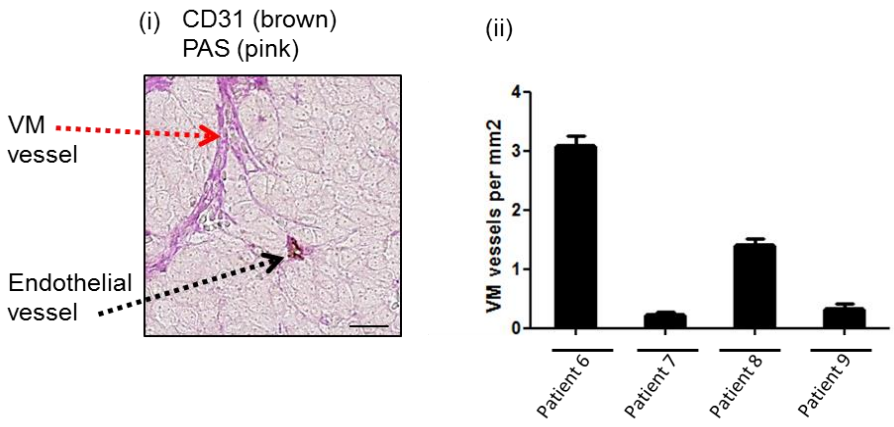

Figure 4.6 VM scoring of SCLC CDX tumours
Representative image of $PAS^+/CD31^+$ endothelial vessels and $PAS^+/CD31^-$ VM vessels in a SCLC CDX tumour **(i)** and the VM vessel density (number of VM vessels per mm^2) score from CDX tumours derived from CTCs enriched from SCLC patients 6 to 9 (ii, black bars [mean of two independent scores; SEM].

4.3.5 Evaluation of VE-cadherin expression by SCLC CTCs

Having demonstrated the presence of VM vessels in the SCLC CDX tumours, I then sought to determine whether CTCs expressing a putative biomarker of VM could be detected in SCLC patients. These CTCs are hypothesised to have entered the bloodstream from VM vessels. Using VE-cadherin expression as a putative VM biomarker[199,202,214] for the reasons described in the General Introduction (Section 1.9.3), I developed a method to determine the expression of VE-cadherin in SCLC CTCs captured by ISET microfiltration.

4.3.5.1 Multi-parameter immunofluorescent assay validation for VE-cadherin profiling of CTCs

In order to identify sub-populations of CTCs which co-express cytokeratins and VE-cadherin, the EMT assay described in chapter 3 was adapted

(described in materials and methods). Antibody specificity was verified with the new combination of antibodies with positive and negative control cell lines spiked into blood and filtered by ISET as performed for the EMT assay. Representative images from these validation experiments are shown in Figure 4.7 with the new VE-cadherin antibody tested against isotype control and no primary control (Figure 4.7A), then each antibody alone in turn (Figure 4.7B), each combination of two antibodies (Figure 4.7B) then all three antibodies combined (Figure 4.7D). The positive and negative control cell lines are the same as used in the previous results chapter for development of the EMT assay. The VM assay includes nuclear marker DAPI (white), cytokeratins (green), VE-cadherin (blue) and leukocyte exclusion through the expression of CD45 (red).

Figure 4.7 (over page) Fluorescent microscopy images of cell line controls (HUVEC, H526 or mixed populations) spiked into blood and filtered using ISET. Filters were stained for DAPI (white), CK (green), CD45 (red) and VE-cadherin (blue). Panel A: HUVEC (VE-cadherin positive cell line) alone (i) and HUVEC and PBMC (VE-cadherin negative control) (ii) with VE-cadherin primary antibody with the new secondary antibody (a), with isotype control (b) and no primary control (c). Panel B: single antibody controls using positive (i) and negative (ii) control cell lines. Panel C: each combination of two antibodies and panel D: the four colour assay on single cell lines and on a mixed cell line control. Scale bar 20 µm throughout.

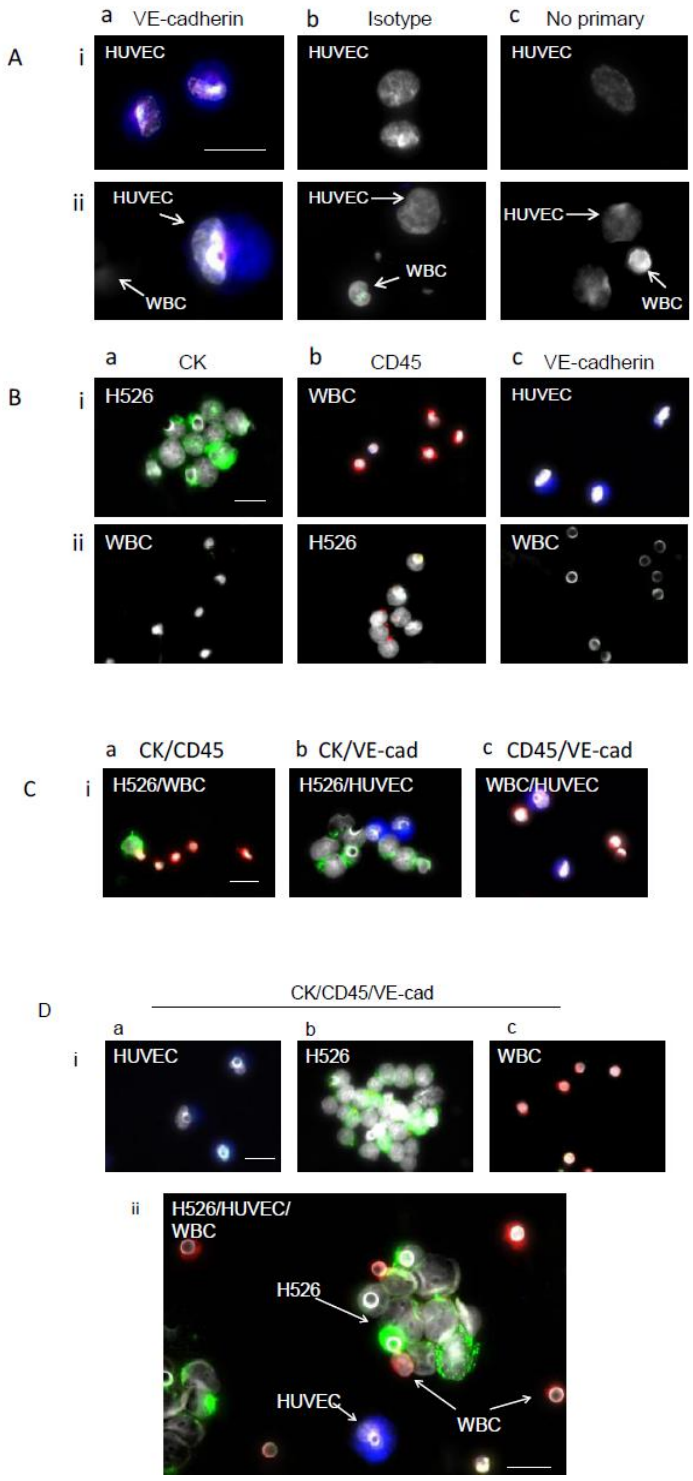

Figure 4.7 Assay validation for VE-cadherin profiling of SCLC CTCs

4.3.5.2 Pilot study to characterise a VE-cadherin profile of SCLC CTCs

In order to determine whether a sub-population of cytokeratin^{+}/VE-cadherin^{+} SCLC CTCs was present, this assay was then used in a pilot study to stain ISET filtered CTCs from the 4 extensive stage SCLC patients' samples who underwent CDX profiling for VM structures described above. Figure 4.8 shows that this assay was able to discriminate leukocytes (CK^{-}/VE-cadherin^{-}/CD45^{+}) from circulating endothelial cells (CK^{-}/VE-cadherin^{+}/CD45^{-}). In addition, CK^{+}/VE-cadherin^{+}/CD45^{-} cells were identified in all 4 patients studied representing CTCs with a putative VM phenotype. In order to compare CTC sub-populations between patients, a CTC profile was produced for each patient showing the prevalence of the cytokeratin^{+}/VE-cadherin^{+} (blue) and cytokeratin^{+}/VE-cadherin^{-} (green) sub-populations (Figure 4.9). The proportion of CTCs expressing VE-cadherin was calculated as a percentage ((VE-cadherin^{+} CTCs/total CTCs) x 100) and this percentage is from here onwards called the CTC VM score. In these first four patients, the mean CTC VM score was 15% (range 2 to 29%).

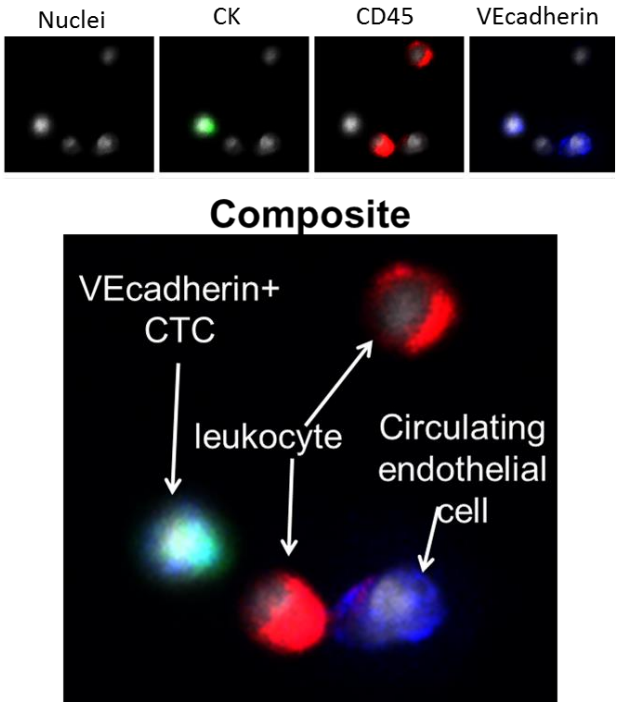

Figure 4.8 Immunofluorescent staining to detect SCLC CTCs which co-express cytokeratins and VE-cadherin
Cells are shown stained for cytokeratin (green), CD45 (red) and VE-cadherin (blue). DAPI stained nuclei are shown as white in all images. An example of a CTC expressing VE-cadherin is arrowed in the composite image. The other cells are leukocytes (staining for CD45, red) and a CEC (staining for VE-cadherin, blue). Imaged at x40 magnification. A gallery of CTCs from these patients are shown in Appendix 3.

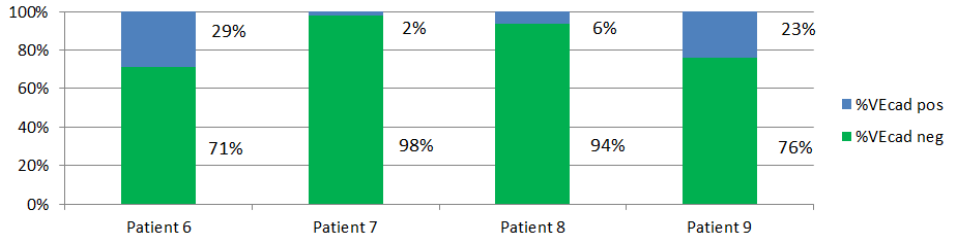

Figure 4.9 CTC VM profile in a pilot study of SCLC patients
Each bar represents the proportion of all CTCs which are CK^+/VE-cadherin$^+$ (blue) and CK^+/VE-cadherin$^-$ (green) for each patient.

4.3.5.3 Comparison between CTC VM score and CDX VM score

Examination of VM within the CDX tumours and CTC populations from the same patients may begin to provide evidence as to whether tumour cell VM is a property carried from the primary tumour by the CTCs or whether it is induced in the micro-environment within the metastasis, the latter approach being consistent with plasticity of the VM state. Therefore the results of the CDX VM profiling described above and the paired ISET filter CTC profiling were compared (Figure 4.10). Although the small numbers limit any statistical analysis, it is interesting to note that patient 6 had the highest VM score in the CDX and CTCs and patient 7 had the lowest VM score in the CDX and CTCs. This observation suggests that the correlation between CTC VE-cadherin expression and VM within the CDX tumours warrants further analysis in an expanded cohort. Analysis of CDX tumours and paired CTC samples is ongoing.

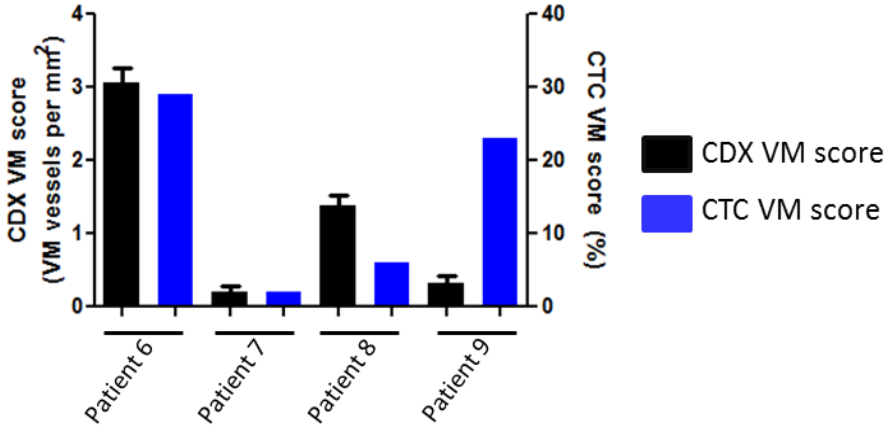

Figure 4.10 Comparison of VM score within paired CDX and CTCs from SCLC patients
CD31/PAS staining was performed on CDX sections to enumerate the number of VM vessels/mm^2 and ISET enriched CTCs from the same patients were stained for cytokeratin/VE-cadherin expression to produce CTC VM scores. All CDX samples were scored by two analysts (R.M, F.T.).

4.3.5.4 Analysis of CTC VE-cadherin expression in a larger cohort of SCLC patients

Having demonstrated that SCLC CTC sub-populations express VE-cadherin in this pilot analysis of blood samples from 4 patients, a larger cohort of 38 chemotherapy-naive SCLC patients (30 patients with extensive stage and 8 patients with limited stage) was recruited for CTC profiling to permit correlation with clinical findings. All patients had detectable CTCs by ISET (median 68/ml, mean 99/ml, range 10 to 403/ml) and this was greater than the number of CTCs detected by CellSearch in this cohort of patients (median 4/ml, mean 116/ml, range 0 to 2,775/ml, p=0.0001). 37/38 samples contained a sub-population of cytokeratin$^+$/VE-cadherin$^+$ ISET CTCs. The CTC VM score for these 38 patients, calculated as (the number of VE-cadherin positive CTCs/total number of CTCs) x 100, ranged from 0 – 100% (median 11%, mean 21%). Figure 4.11 shows the CTC VM profile for all 38 SCLC patients. Each bar represents the total CTC population for the patient

divided into cytokeratin^{+}/VE-cadherin^{-} population (green) and cytokeratin^{+}/VE-cadherin^{+} population (blue).

The stage of each patient is shown above each bar (L=limited stage and E=extensive stage) showing the 8 patients with limited stage disease were evenly distributed across the range of CTC VM scores. Earlier analysis within this chapter of VM vessels in SCLC tumour biopsies was performed in samples from patients with limited stage disease. In comparison, this study of CTC profiling was performed in SCLC patients who were mainly extensive stage. These proportions are consistent with the proportion of patients presenting with extensive stage disease to our institution. However, in order to reduce heterogeneity, extensive stage patients alone were included in the subsequent analysis of clinical characteristics.

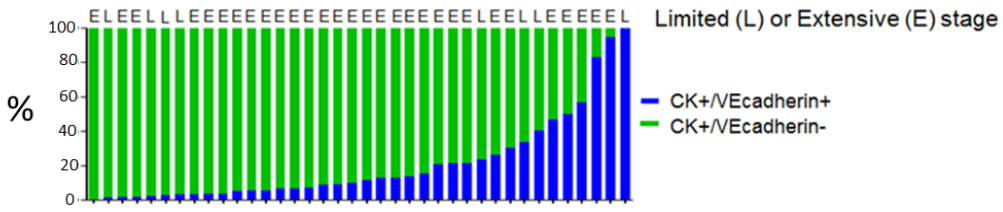

Figure 4.11 CTC VE-cadherin profiling in an expanded cohort of SCLC patients
CTC profiling was performed for 38 SCLC patients. The VE-cadherin expression of SCLC CTCs for each patient is shown as a bar (blue portion representing the population of VE-cadherin expressing CTCs within the total CTC population for each patient. When more than 200 CTCs were present on the filter a minimum of 200 CTCs were profiled.

4.3.5.5 Correlation between CTC VM score and clinical characteristics

To evaluate for any associations between clinical characteristics including CTC VM score, a correlation matrix was plotted including the data for the 30

patients with extensive stage disease (continuous variables shown in Figure 4.12 and categorical variables shown in Figure 4.13). In addition to patient age and baseline biochemistry and haematology results, CTC number was included as measured by ISET and CellSearch. Due to the proposed association between tumour hypoxia and VM, primary tumour characteristics (size and mean tumour density measured on the diagnostic computerised tomography (CT) scan images) were included. The only characteristics associated with CTC VM score were primary tumour density (R= 0.58, 95% CI 0.26 to 0.78, p=0.0011) and leukocyte count (R=-0.50, 95%CI -0.79 to -0.03, p=0.0355).

The correlation between tumour density on CT and CTC VM score must be interpreted with caution as the CT imaging was not included as part of the study protocol, rather it was performed as part of the diagnostic clinical assessment. Although the conduct of CT imaging itself is standardised for clinical diagnostic purposes, it was not performed at the same time as the blood sampling for CTC analysis. Therefore this finding although an interesting observation, would need confirmation in a prospective study. Acknowledging this limitation, assuming CT tumour density is a surrogate for tumour perfusion (necrotic tumours having reduced tumour density), and that CTC VE-cadherin expression is a surrogate for tumour VM, the observation that increased tumour density correlates with increased CTC VM score generates the hypothesis that an increase in tumour VM enables increased tumour perfusion. To test this hypothesis further, prospective evaluation of tumour perfusion using dynamic contrast enhanced magnetic resonance

imaging (DCE-MRI)[286,287] and its relationship to tumour VM are planned using xenograft models.

Figure 4.12 and 4.13 (over page). Correlation matrices to assess associations between CTC VM score and clinical characteristics. Plots show continuous co-variables (A) and categorical co-variables (B). Any correlations that reached statistical significance are marked (red asterix *p<0.05, **p<0.01).

Significant correlations	R value	95% CI	P value
VM score and tumour density	0.58	0.25 to 0.78	0.0011
VM score and leucocytes	-0.50	-0.79 to -0.03	0.0355
LDH and alkaline phosphatase	0.42	0.06 to 0.69	0.0206
LDH and CellSearch CTC count	0.40	-0.06 to 0.67	0.0275
Na and ISET CTC count	-0.37	-0.65 to -0.01	0.0422

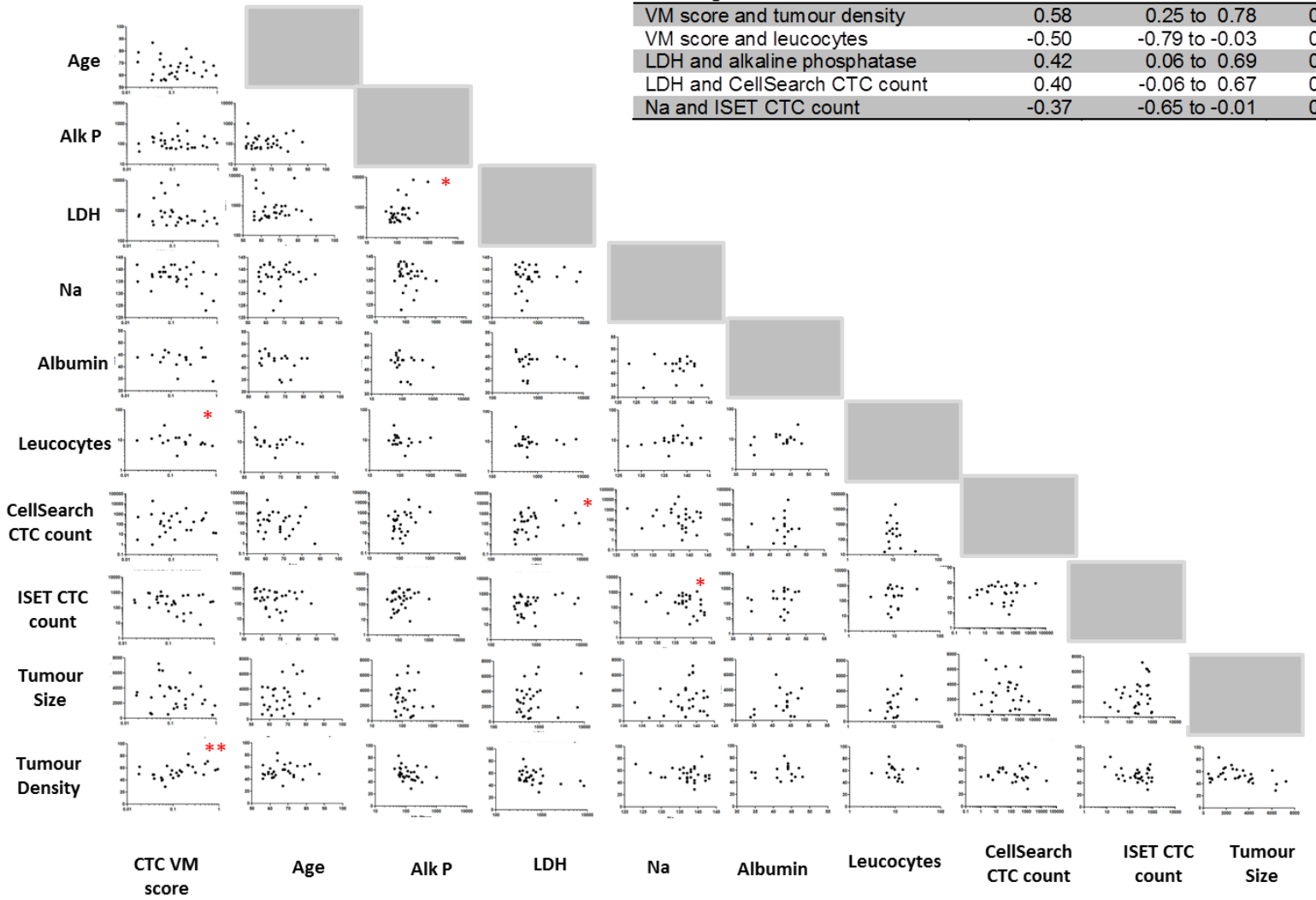

Figure 4.12 Correlation matrix to assess associations between CTC VM score and clinical characteristics (continuous co-variables)

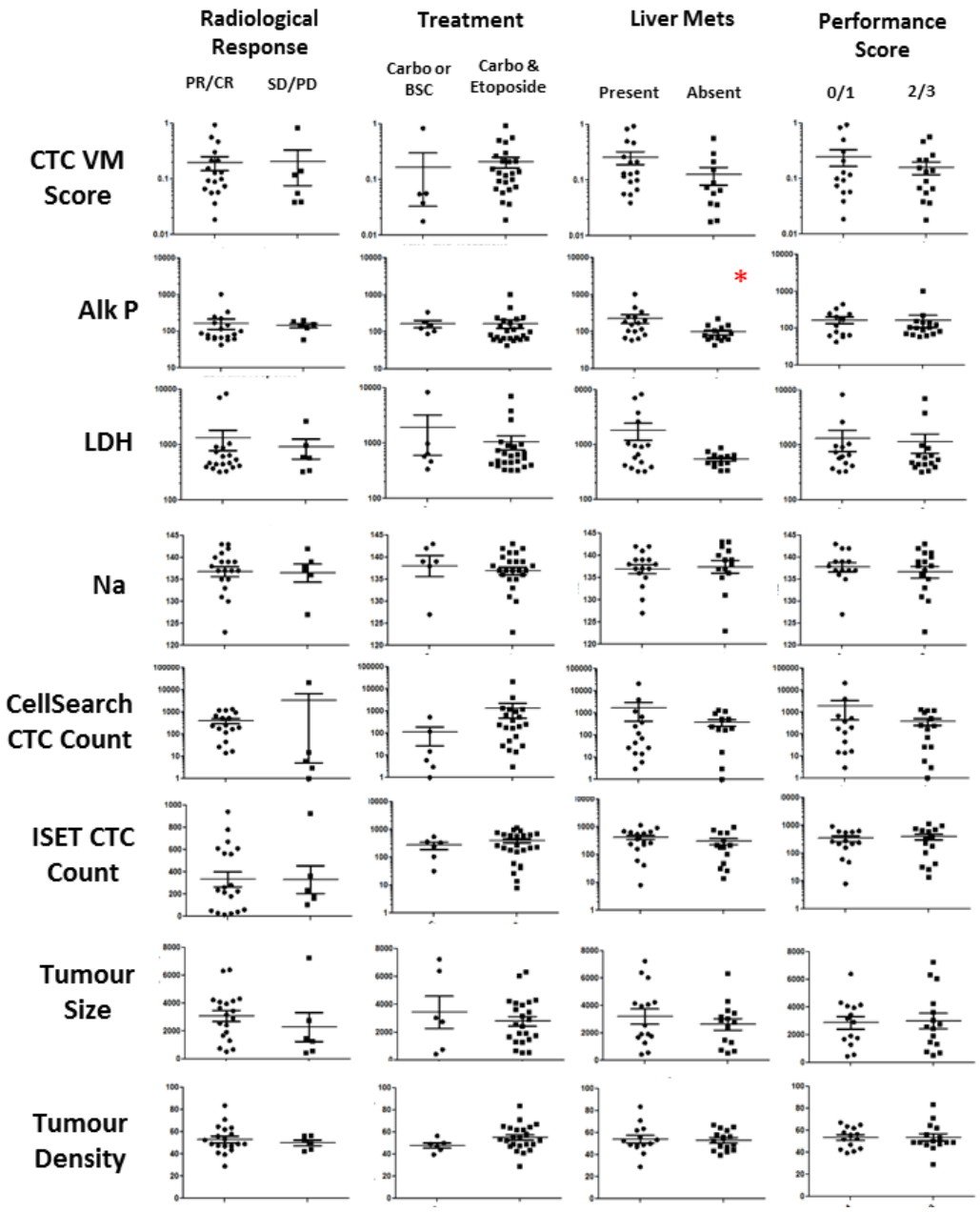

Figure 4.13 Correlation matrix to assess associations between CTC VM score and clinical characteristics (categorical co-variables)

4.3.5.6 Correlation between CTC VM score and patient survival

In order to determine a CTC VM score cut-off with the greatest sensitivity and specificity to predict patient survival at 9 months, a ROC curve was plotted and the area under the curve was calculated (Figure 4.14). Survival at nine months was selected in this population in contrast to survival at three years used in the analysis of biopsies in the cohort of patients with limited stage disease described in section 4.3.3 above as the patients who underwent CTC profiling had predominantly extensive stage disease in whom the median survival is in the region of 6 to 9 months, with very few survivors at 3 years. The sensitivity and specificity, using a range of cut-points around the median value for CTC VM score to predict survival at 9 months, is shown in Figure 4.13B, identifying an optimum cut-off of 8%.

Unexpectedly, univariate survival analysis of these patients demonstrated that although no significant difference in survival was seen when patients were analysed using total CTC count, patients with a CTC VM score below 8% had reduced survival (median 7.2 months v 19.9 months, p=0.073) compared to patients with a CTC VM score >8% (Figure 4.15 and Table 4.3).

If CTC VE-cadherin expression is subsequently confirmed as a biomarker for VM in SCLC, these data conflict with the paradigm that VM, through 'stem-like' plasticity and permitting metastatic dissemination, confers shorter patient survival. However, this observation may be consistent with the body of work describing chemotherapy resistance in association with increased distance from the vessels within a tumour as described in the General

Introduction (Section 1.2). In a population of patients with chemotherapy naive SCLC (which is initially a chemotherapy sensitive disease), the presence of VM vessels may improve patient survival either through improved delivery of chemotherapy to the tumour, reducing tumour hypoxia or normalising tumour pH, any of which may improve the response to chemotherapy. Experiments to begin to address these hypotheses are reported in section 4.3.10 below.

A

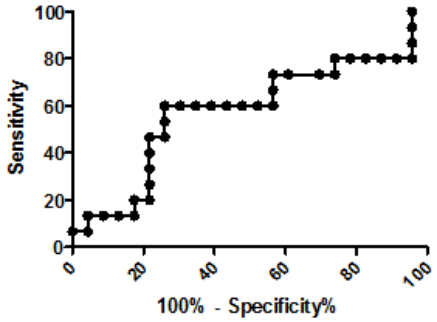

Area under the ROC curve	0.577
Standard Error	0.101
95% Confidence Interval	0.38 to 0.78
P value	0.4287

B

VM score (%)	Sensitivity (%)	95% CI	Specificity (%)	95% CI
4	26.7	7.8 to 55.1	78.3	74.3 to 97.8
8	**60.0**	**32.3 to 83.7**	**70.0**	**47.1 to 86.8**
12	60.0	32.3 to 83.7	52.2	30.1 to 73.2
18	73.3	44.9 to 92.2	43.5	23.2 to 65.5
22	73.3	44.9 to 92.2	30.4	13.2 to 52.9

Figure 4.14 Receiver operating characteristic (ROC) curve analysis for CTC VM scores (A) and sensitivity and specificity values for a range of cut-off scores with respect to patient survival at nine months (B)

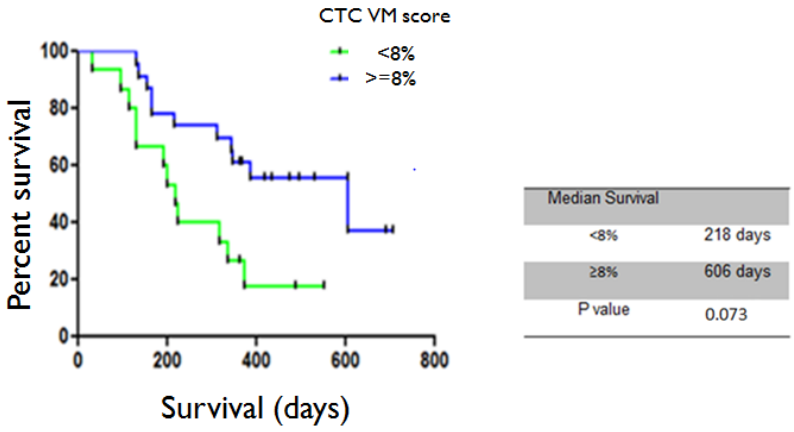

Figure 4.15 Kaplan-Meier survival analysis for overall survival for patients with SCLC by CTC VM score (n=30)
Low CTC VM score is shown in green, and high in blue.

Co-variate	n	Median OS (days)	95% CI	P-value
Gender				
Male	20	215	177-252	0.093
Female	10	372	313-431	
Age				
<67	15	387	316-459	0.040
≥67	15	201	124-278	
WHO Performance Score				
0-1	14	347	112-582	0.070
2-3	16	201	150-252	
Liver Metastasis				
Absent	14	218	3-433	0.275
Present	16	312	71-553	
CellSearch CTC Count / 7.5 ml				
<50	13	224	2-446	0.818
≥50	17	318	161-475	
ISET CTC Count / 4 ml				
<275	16	318	258-378	0.441
≥275	14	218	159-277	
CTC VM Score (%)				
<8	12	218	217-397	0.073
≥8	18	606	246-616	
Serum Lactate Dehydrogenase				
<550	14	372	124-620	0.346
≥550	16	224	40-408	
Serum Sodium				
<132	4	154	0-308	0.651
≥132	26	312	153-471	
Serum Alkaline Phosphatase				
<165	21	224	70-378	0.880
≥165	9	347	245-449	
Tumour Density (HU)				
<53	16	312	75-549	0.831
≥53	13	318	105-531	
Treatment				
Platinum Etoposide	24	347	266-428	<0.001
Carboplatin or BSC	6	115	66-164	
Number of cycles				
<4	9	166	149-183	<0.001
4	19	606	332-880	
Response to treatment				
CR/PR	19	372	286-458	0.284
SD/PD	5	166	104-228	

Table 4.3 Univariate survival analysis of extensive stage SCLC patients who underwent CTC VM profiling
Abbreviations: NR, not reached; BSC, best supportive care; PS, performance score; CR, complete response; PR, partial response; SD, stable disease; PD, progressive disease; HU, Hounsfield units

4.3.6 Relationship between CTC VE-cadherin expression and VM within primary tumour

To determine whether any correlation exists between CTC VE-cadherin expression and VM within the primary tumour, surplus diagnostic material was retrieved for CD31/PAS staining from patients who underwent CTC VE-cadherin profiling. From 38 patients included in this study, only 14 had sufficient tumour material for analysis and no correlation between CTC VE-cadherin expression and tumour VM were evident in this small cohort and this question remains to be addressed in a larger cohort of patients. No further analysis of the primary tumour took place in view of the small number of patients with matched CTC scores and the scarcity of this material. This further highlights the difficulties posed by lack of patient tumour material in the study of SCLC biology. As described earlier in this chapter, the patients who were included in the analysis of SCLC biopsies were recruited and treated many years previously and blood was not available for CTC analysis in this cohort. Further studies to evaluate the role of VE-cadherin in SCLC VM are reported below.

4.3.7 In vitro and in vivo evaluation of the functional role of VE-cadherin in VM in SCLC

Increased VE-cadherin expression has been shown to have a functional role in VM in melanoma,[202] oesophageal carcinoma,[213] osteosarcoma[215] and glioblastoma.[214] However, there are no previous data on VE-cadherin in SCLC VM. In order to determine its functional relevance, if any, in SCLC VM, a panel of SCLC cell lines was first screened by Western blotting for expression of VE-Cadherin (Figure 4.16). Of these, only 2 (H446 and H1694)

of 12 cells lines tested expressed detectable VE-cadherin and of these H446 had the strongest expression. This is consistent with Cancer Cell Line Encyclopaedia data[244] on gene expression profiling of these cell lines which report the highest VE-cadherin levels in H446 and H1694 cell lines.

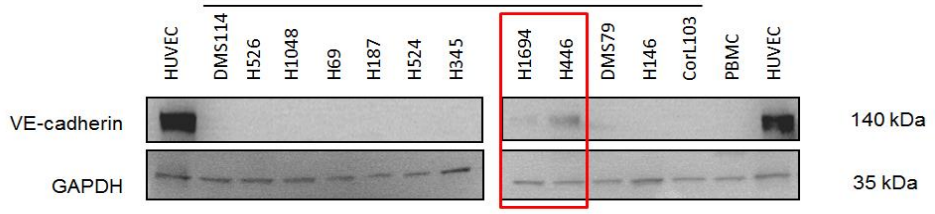

Figure 4.16 Western blotting for VE-cadherin and GAPDH in a panel of SCLC cell lines
SCLC cell lines are marked by the horizontal bar. Each blot has HUVEC as VE-cadherin positive control. Peripheral blood mononuclear (PBMCs) cells are shown negative for VE-cadherin.

In order to determine whether expression of VE-cadherin was able to promote the formation of VM networks *in vitro*, H446 cells containing VE-cadherin as well as H1048 cells (VE-cadherin negative) were grown in Matrigel. The C8161 aggressive melanoma cell line (kind gift of Prof. Mary Hendrix) which is known to form VM networks in these conditions[186] (Figure 4.17) was included as a positive control. When evaluated between 5 to 72 hours post seeding, H446 cells produced branching VM networks similar to those reported in seminal studies of VM using the C8161 melanoma cell line. In order to further elucidate the role of VE-Cadherin in the formation of these networks, H446 cells were stably transfected with VE-Cadherin shRNA (Figure 4.18) and when grown in Matrigel under the same conditions as described the H446 VE-cadherin knock-down cells were no longer able to

form networks (Figure 4.17). No effect was seen in the non-targeting control. VM networks were absent in cell lines e.g. H1048 which did not express VE-cadherin. Together, these data suggest that VE-Cadherin is required for VM network formation in SCLC.

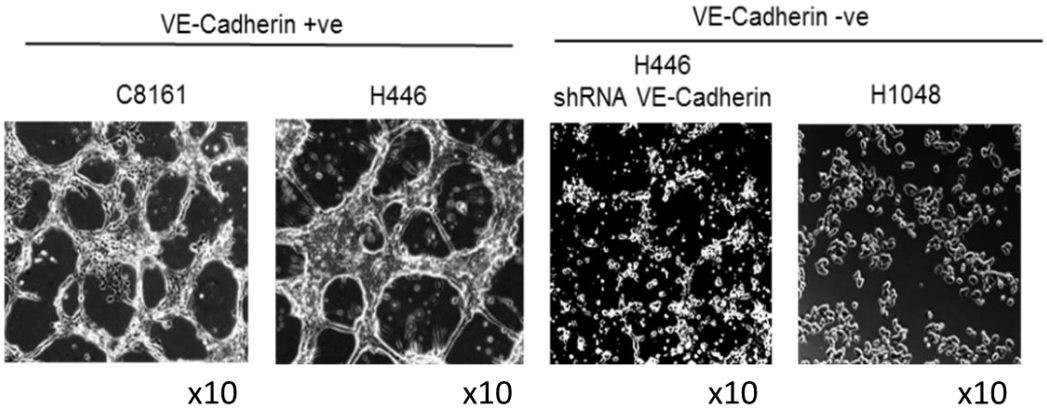

Figure 4.17 Growth of VE-cadherin positive and negative cell lines in Matrigel
VE-cadherin positive (H446 and C8161) and negative (H446 shRNA VE-cadherin and H1048) cell lines were cultured in Matrigel and imaged with phase contrast microscopy. Representative images of >3 experiments are shown.

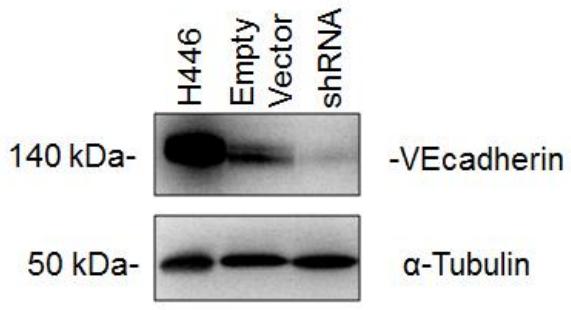

Figure 4.18 Western blotting for VE-cadherin in H446 parental cell line and following stable transfection with VE-cadherin shRNA and empty vector control

4.3.8 Evaluation of the effect of VE-cadherin knock-down on SCLC tumour growth *in vivo*

In order to determine whether knockdown of VE-cadherin affects tumour growth, H446 xenograft growth rates were measured following sub-cutaneous implantation of H446 parental and H446 VE-cadherin knock down (H446 KD) cell lines in NSG mice (Figure 4.19). Both H446 parental tumours (9/10) and H446 KD tumours (7/10) grew to the target tumour volume of 800 mm^3. The median time to target tumour volume was significantly increased in the H446 KD xenograft (median of 77 versus 44 days, p=0.0005, Figure 4.19C). However, once a palpable tumour was present, there was no difference in the doubling time between the H446 parental and H446 KD tumours (mean of 5.6 and 5.8 days respectively, p=0.84, Figure 4.19D). It is reported that a tumour cannot grow over 2-4 mm diameter without vascularisation[278], and this increased latency in the VE-cadherin knock down xenograft gives rise to the hypothesis that VE-cadherin knock-down reduces tumour vascularisation.

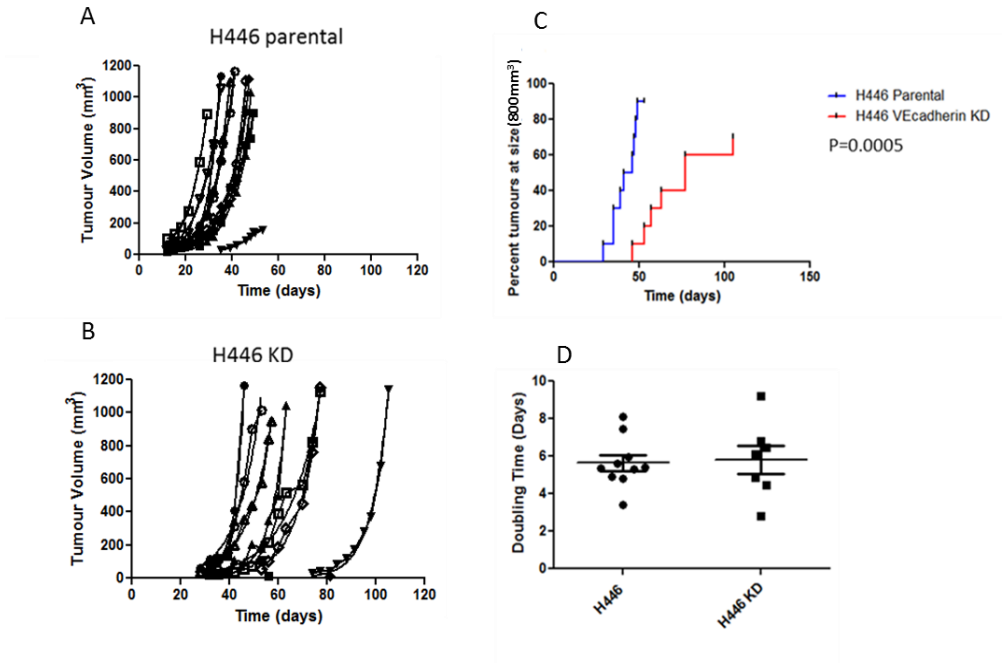

Figure 4.19 Sub-cutaneous tumour growth of H446 parental and H446 KD cell lines in NSG mice
Growth curves are shown for H446 parental (A) and VE-cadherin knock down cell lines (B). Comparison of the time (days) taken for each group to reach study end point (800mm^3) (C). Doubling time for the H446 parental and KD tumours (D).

4.3.9 Evaluation of the effect of VE-cadherin knock down on VM vessel formation in SCLC *in vivo*

In order to determine whether knock down of VE-cadherin had any effect on the presence of VM networks within tumours, tissue sections from the H446 and H446 KD xenografts (harvested at >800mm^3) were analysed following CD31/PAS staining. Because within this work it was hypothesised that VM vessels may contribute to chemotherapy delivery, the VM vessel density was calculated as the number of VM vessels per mm^2 as an indication of the extent of VM vessels contribution to tumour perfusion. VM networks were seen frequently in the H446 parental xenografts (representative image of H446 parental tissue section showing VM structure shown in Figure 4.20(i)) but rarely in the VE-cadherin knock down xenografts and this difference

reached statistical significance (Figure 4.20(ii), mean 2.24 and 0.07 VM vessels per mm^2 respectively, p=0.0228) consistent with a role of VE-cadherin in VM vessel formation. Next, a VM score was calculated as performed in the SCLC patient samples and there was a significant reduction in the VM score in H446 KD tumours compared to H446 parental tumours (8% v 17%, p=0.0016). These analyses confirm that following VE-cadherin knock down, VM vessels are rare within the xenograft tumour and that they make up a decreased proportion of all vessels within the tumour, therefore it may be expected that this will impact upon chemotherapy delivery to the tumour.

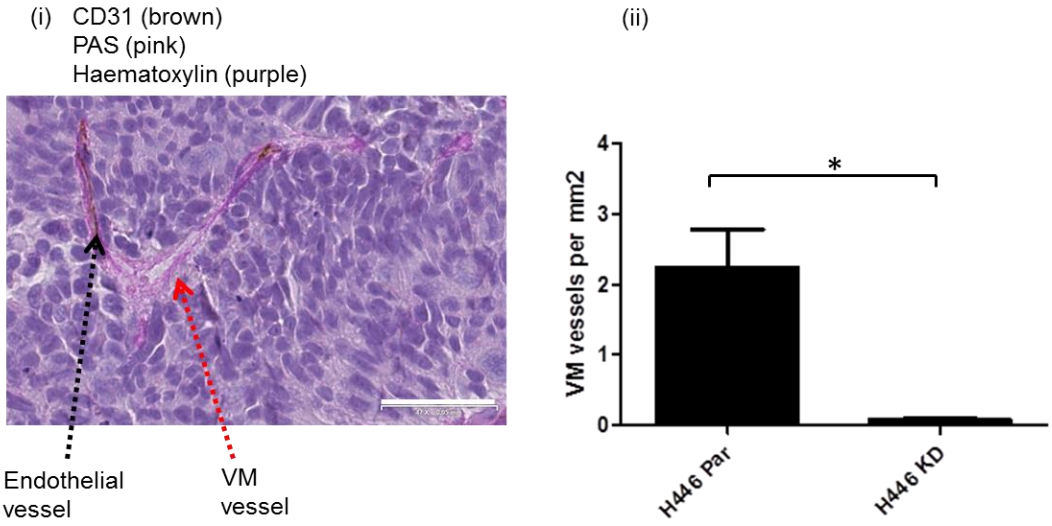

Figure 4.20 Measurement of VM vessels in H446 parental and H446 VE-cadherin knock down xenograft tumours

Representative image of VM vessels and endothelial vessel seen in H446 parental xenografts following CD31/PAS staining (i). Mean number of VM vessels per mm^2 in the H446 parental and VE-cadherin KD xenografts (ii, error bars: standard error of mean) p=0.0228, n=6 mice per group.

4.3.10 Pilot study of the role of VM in cisplatin delivery to tumours

As introduced in section 4.3.5.6 above, it was hypothesised that the functional consequence of VM within a SCLC tumour is that VM vessels increase drug delivery, reduce hypoxia and normalise pH, improving treatment response. This is one possible explanation for the correlation between improved survival and high CTC VM score in chemotherapy naïve extensive stage SCLC patients which is typically a chemotherapy sensitive disease. The opposite was seen in the limited stage biopsy specimens, where high biopsy VM score correlates with worse outcomes (Figure 4.4). In the setting of limited stage disease, it may be that the stem-like properties of VM cells, with associated propensity to seed distant metastasis, outweighs any benefit gained by improving chemotherapy delivery.

To begin to address the drug penetration hypothesis, a feasibility study was performed *in vivo* in order to measure total cisplatin levels in xenografts. We have previously quantified cisplatin in tumour cells *in vitro* using inductively coupled plasma mass spectrometry (ICP-MS).[288] When measured with a different platform (atomic absorption spectrometry), other groups have shown cisplatin levels within xenograft tumours between 1 to 2 ppm (at 1 hour post treatment with 7.5 mg/kg intra peritoneal dosing).[289] I therefore sought to use ICP-MS, which is able to quantify platinum levels as low as 1-5 ppb, to quantify cisplatin in H446 xenograft tumours (200-300 mm^3) (parental and VE-cadherin knock down) at one hour post treatment and compare cisplatin levels to those published using atomic absorption spectrometry. Tumours in this study were grown to 200 – 300 mm^3 then treated and

harvested at this size. This size was chosen for this study, as in other chemotherapy treatment studies in *in vivo* models this is the size to which tumours are grown before treatment, permitting evaluation of subsequent tumour growth or regression. Sections of the same tumours were retained permitting subsequent CD31/PAS staining to score VM vessels.

Although this study was not designed to detect a difference in platinum concentration between the parental and knock-down groups, Figure 4.21 shows that the ICP-MS approach was able to detect cisplatin levels in the tumours around 1ppm (mean in H446 parental and H446 KD tumours, 1048 and 883 ppb respectively, p=0.2105) showing the current approach is comparable to published data using atomic absorption spectrometry.[289] This approach will now need application in larger adequately powered studies to establish whether VM vessels play a significant role in chemotherapy delivery to tumours.

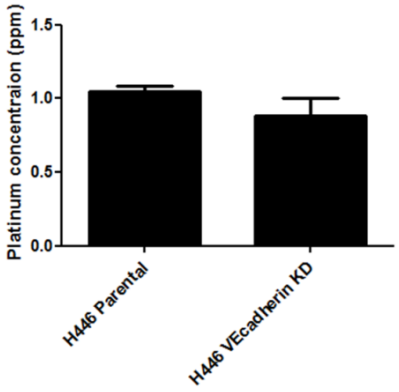

Figure 4.21 Cisplatin measurement in H446 parental and H446 KD xenografts at one hour following treatment with intra-peritoneal cisplatin
NSG mice bearing H446 parental and VE-cadherin KD xenografts were treated with 7.5mg/kg i.p. of cisplatin and tumours harvested after 1 hour for cisplatin measurement by inductively coupled plasma mass spectrometry. The platinum concentration is shown for parental and knock down tumours. n=3 per group, error bars represent SEM.

Next, tissue sections from the same tumours were analysed by CD31/PAS staining to determine if VM vessels were present. VM vessels were detected in both the H446 parental and knock down tumours following cisplatin treatment (Figure 4.22(i), black bars). This study was underpowered to identify a statistically significant difference in groups; however, there was a trend towards lower density of VM vessels than seen in the previous *in vivo* study (section 4.3.9, Figure 4.22(i) grey bars). This difference could be attributed to the fact that in the first study tumours were harvested at 800-1000 mm^3 and in this study tumours were much smaller at the point of harvest (200-300 mm^3) which was chosen as this is the optimal tumour volume for chemotherapy dosing.

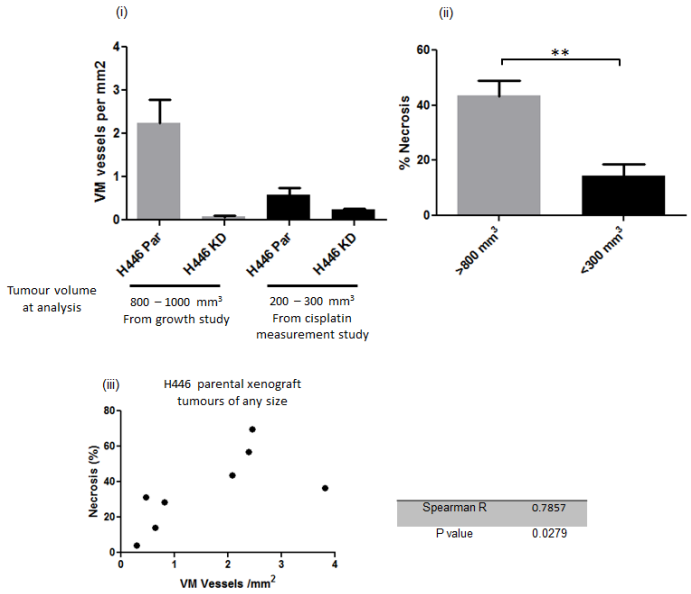

Figure 4.22 Comparison of tumour necrosis in xenografts collected at >800 mm^3 and 200mm^3
The number of VM vessels per mm^2 are shown comparing H446 parental and VE-cadherin knock down xenografts in tumours harvested at >800mm^3 (grey) (n=4 mice group) and at 200 to 300 mm^3 (black) (n=3 mice group), error bars represent SEM (i). No statistically significant difference was seen between VM vessel density within tumours at these different sizes. (ii) shows the amount of necrosis in tumours harvested at >800mm^3 (grey) and at 200 to 300 mm^3 (black); * indicates p<0.01. Correlation coefficient calculation for VM vessel density and necrosis in H446 parental xenografts of any size is shown (iii).

This observation that more VM vessels were seen in larger tumours suggested that the number of VM structures may be related to the tumour microenvironment, which may differ between tumours of different sizes. To further explore this hypothesis comparison of the proportion of necrosis of all tumours (parental and knock down) between these studies was carried out (Figure 4.22(ii)) and shows that there is significantly less necrosis in the smaller tumours compared to the larger ones (mean 43.4 v 14.5% per section, p=0.0039). There was a significant positive correlation between the number of VM vessels/mm^2 and the amount of tumour necrosis in H446 parental tumours (Figure 4.22(iii), R= 0.79, p=0.028). An explanation for this observation is that if tumour growth overwhelms its blood supply then this may result in increase in necrosis and in VM as a compensatory mechanism. These findings re-iterate that VM is likely to be context dependant and must be considered in the planning of future *in vivo* studies of VM. This pilot study has shown that cisplatin measurement within tumours can be performed. Although this study is limited by small numbers, these preliminary data suggest that the difference in VM structures seen in larger xenograft tumours may not be evident in small tumours at the start of chemotherapy studies. Although this should be considered when planning future *in vivo* studies, it must be borne in mind that in SCLC patients, tumours will many orders of magnitude larger in than in these xenograft models and as such may have a different tumour microenvironment.

4.4 Discussion

4.4.1 Summary and ongoing research

Since its discovery in 1999 in melanoma,[186] VM has been described in a number of human cancers where it is linked with poor patient outcomes.[197] In this Chapter, I have shown for the first time that VM occurs in SCLC patient biopsies and that in 41 limited stage SCLC tumour specimens, relatively high levels of VM were associated with worse overall survival (8 v 47% 3 year survival in the VM high v low group, p=0.025). This is consistent with previously published data on the association between high levels of VM within tumour biopsies and shorter patient survival.[197]

Using SCLC cell lines, (H446 which express VE-cadherin and an H446 VE-cadherin knock down cell line) I have also shown that VE-cadherin was required for VM-like network formation *in vitro* and enhanced both tumour growth and the number of VM vessels *in vivo*. These findings were consistent with other studies demonstrating a functional role for VE-cadherin in VM in melanoma,[202] oesophageal cancer,[213] osteosarcoma[215] and glioblastoma.[214]

Evaluation of SCLC CTCs identified sub-populations of CTCs co-expressing VE-cadherin and cytokeratins in 37/38 SCLC patients. In contrast to the clinical correlation in the limited stage patients, the presence of high levels of CTCs expressing VE-cadherin was associated with improved patient survival in this extensive stage cohort (30 extensive stage patients). The significance of these contrasting clinical correlations is discussed below (Section 4.4.2).

VM vessels were also seen in 4/4 CDX tumours demonstrating that this model could be used to test subsequent hypotheses. Follow on studies using CDX models are described below. Since completing my laboratory studies for this PhD thesis, the VM CDX project has continued within the lab (*manuscript under review: Vasculogenic mimicry in small cell lung cancer. Metcalf, Trapani, Simpson et al. Nature Communications 2016,* Appendix 4). These ongoing experiments, the findings of which are reported below, covered two themes:

1) To compare copy number alteration (CNA) profiles of areas of SCLC CDX tumour which were rich in VM vessels and areas in which VM vessels were absent to confirm the tumour origin of VM vessels and to evaluate for genetic divergence between VM high and low areas.

2) To compare CNA profiles of CTC populations which were cytokeratins^{+}/VE-cadherin^{+} and cytokeratins^{+}/VE-cadherin^{-} in order to confirm the malignant origin of these VE-cadherin^{+} CTCs and to evaluate whether these two populations contain a distinct genetic architecture.

4.4.1.1 VM vessels in SCLC CDX are comprised of genetically defined tumour cells

Having identified that SCLC tumour tissue contains vessels defined as VM by PAS^{+}/CD31^{-} staining, we next sought to prove that these VM structures were indeed composed of SCLC cells. My role in this research was in planning the experiments and subsequent data interpretation. Our lab previously reported the CNA profile of the chemotherapy sensitive SCLC CDX model CDX3L.[66] Subsequently, two replicate studies (CDX3L$^{\$}$ and CDX3L$^{\#}$) confirmed that VM vessels were present in this model with 8.7% of

all vessels in this SCLC CDX model having the VM phenotype. Regions were identified which were VM high (>75% of tumour area $PAS^{+}/CD31^{-}$) and VM low (≤ 20% $PAS^{+}/CD31^{-}$) and laser micro-dissected (Figure 4.23).

Consecutive FFPE sections were stained for VE-Cadherin and the SCLC neuroendocrine marker synaptophysin. VE-Cadherin expression in CDX tumours was calculated between 5-40% and co-localised with regions enriched for VM (defined by % area $PAS^{+}/CD31^{-}$) (Figure 4.23).

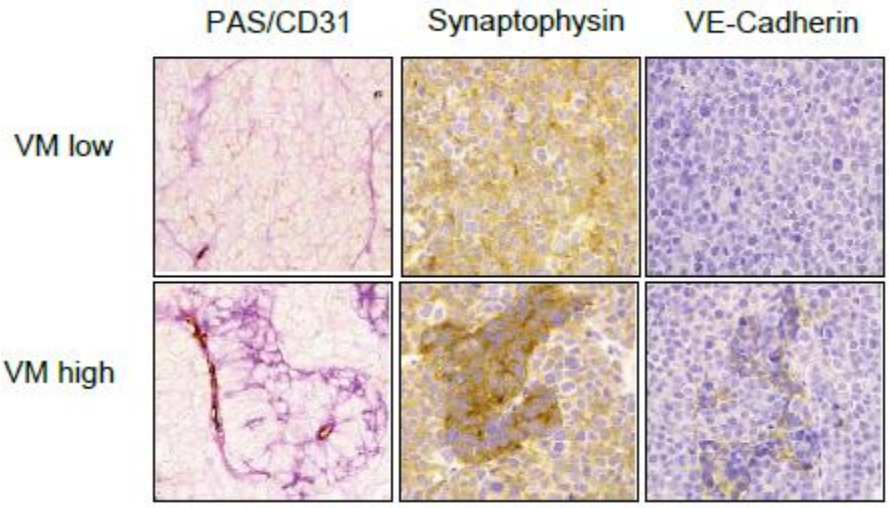

Figure 4.23 IHC staining for PAS/CD31, synaptophysin, and VE-cadherin with VM low/high LCM area from SCLC CDX3L tumour.

DNA was extracted from cells following laser capture microdissection and whole genome amplification (WGA) was performed. CNA profiles were compared between VM high, VM low and CDX3L bulk tumour which included VM high and low areas (Figure 4.24). CNA profiles aligned to show that VM high, VM low and CDX bulk tumour were genetically related. CNA patterns showed loss of chromosome 17p, characteristic of p53 deletion commonly

seen in SCLC and known to be harboured by this CDX,[66] further supporting the tumour origin of VM networks. Genomic comparison of CNA profiles between the VM low and VM high regions of CDX3L$^{\#}$ and CDX3L$^{\$}$ revealed the presence of distinct human molecular karyotypes with gain of 1q, 3p, 8p, 13q and loss of 2p, 10p, 15q in the VM high not observed in the VM low samples implying a selection of cells with a propensity to undergo VM had occurred. A germline DNA sample derived from white blood cells extracted from a parallel patient blood sample used to generate CDX3L was used as an internal control and showed no copy number changes.

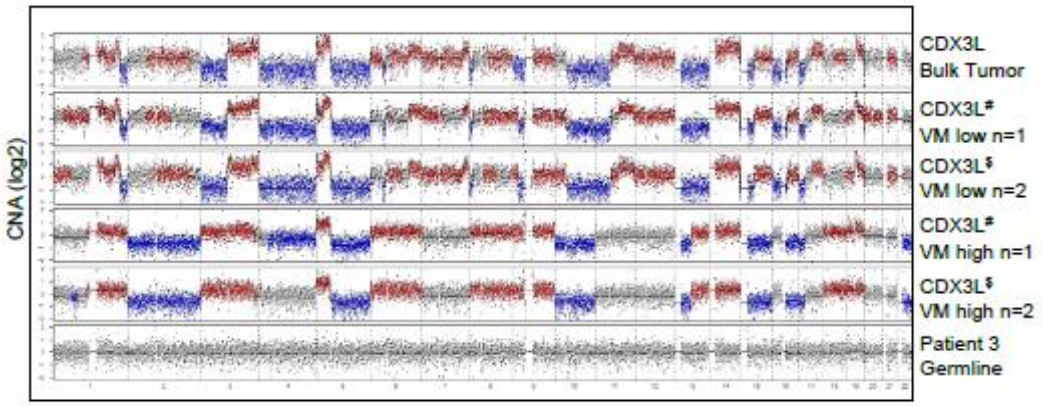

Figure 4.24 Copy number analysis (CNA) of VM vessels in CDX tissue, non-VM CDX tissue and the original CDX from which it was derived
Unsupervised hierarchical clustering of CNA analysis profiles from passage 1, bulk CDX3L tumour, LCM regions containing high or low VM from 2 mice bearing passaged CDX3L tumours (CDX3L$^{\#}$ and CDX3L$^{\$}$), and donor patient germline. The GC-normalized and mappability corrected read counts (log_2 scale) were segmented using HMM with red indicating copy number gains and blue indicating copy number losses.

Principal component analysis of CNA profiles showed that VM low tumour and CDX3L bulk tumour cells clustered most closely whilst the VM high region displayed more genetic diversity (Figure 4.25).

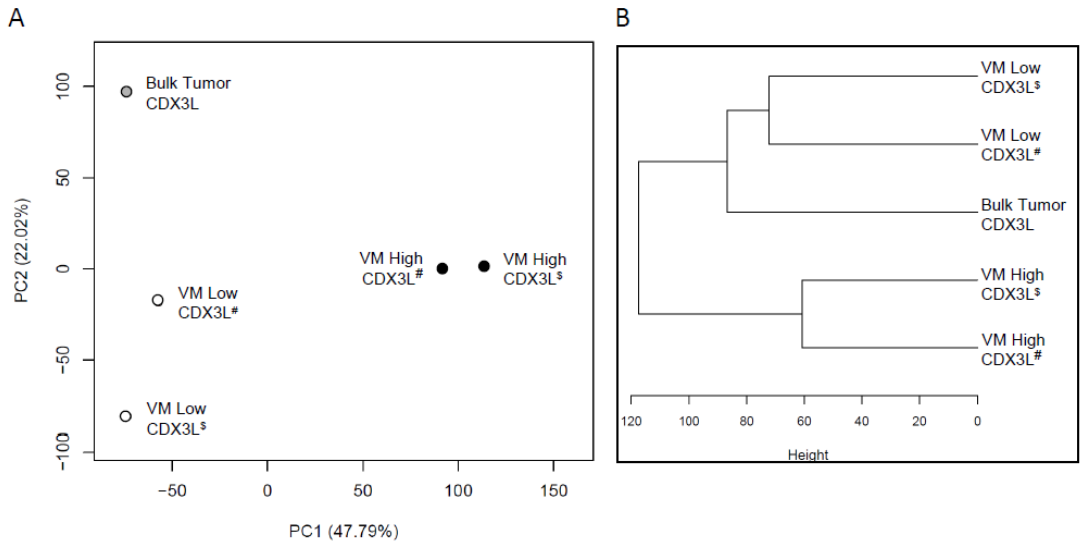

Figure 4.25 Principal component analysis (PCA) and dendrogram clustering of genome-wide CNA data. Shown in both PC1 **(A)** and clustering dendrogram **(B)** 'VM high' regions (black circles) from CDX3L$^{\$}$ and CDX3L$^{\#}$ tumours cluster closely together and away from the 'VM low' regions (open circles) and CDX3L bulk tumour (grey circle) from which CDX3L$ and CDX3L# were derived.

4.4.1.2 Copy Number Alteration analysis of single CTCs identified two genetically distinct populations based on VE-Cadherin expression

The second area of ongoing research sought to determine whether isolated, single CTCs co-expressing VE-Cadherin and cytokeratins had CNA profiles consistent with tumour origin. This was conducted in collaboration with Prof Peter Kuhn's CTC lab. My role in this was in establishing the collaboration and sharing the ISET CTC VM profiling method and data to establish an HD-CTC VM profiling assay, in planning the experiments and subsequent interpretation of the results. In this collaboration, two paired blood samples were collected from an extensive stage SCLC patient for CellSearch CTC enumeration and HD-CTC profiling.[290]

For this index SCLC patient, the first sample was found to contain 836 EpCAM^{+}/cytokeratin^{+} CTCs/7.5 ml by CellSearch. The parallel sample identified 4,552 cytokeratin^{+} CTCs/7.5 ml using the HD-CTC assay. The ~5 fold increase in CTCs detected in the HD-CTC sample is likely due to the EpCAM dependent enrichment process in CellSearch, which is not applied in the HD-CTC approach.

Cells captured by HD-CTC assay were stained using immunofluorescent antibodies for expression of cytokeratins (epithelial marker), CD45 (leukocyte marker), DAPI (nuclear marker) and VE-Cadherin (VM marker) (Figure 4.26). Using this approach it was possible to identify cytokeratins^{+}/VE-cadherin^{-} CTCs (Figure 4.26A(i) and (ii)), cytokeratins^{+}/VE-cadherin^{+} CTCs (Figure 4.26A(iii) and (iv)) and CD45^{+} leukocytes that provided patient germline DNA (non-tumour) (Figure 4.26A(v)). Genome-wide CNA analysis was performed on 24 isolated single cells. The genomic architecture of the CTCs (Figure 4.26B(i-iv)) displayed copy number gains and losses consistent with tumour origin, in contrast to germline DNA in which with no copy number changes were seen, indicative of somatic, non-tumour DNA (Figure 4.26B(v)). CNA of VE-Cadherin negative CTCs revealed a clonal population with copy number profiles containing high frequency SCLC hallmark gains and losses (Figure 4.26B(i) and (ii)). In contrast, VE-Cadherin positive CTCs expressed comparatively low cytokeratins and were of non-clonal composition and genetically distinct from the cytokeratins^{+}/VE-cadherin^{-} CTCs (Figure 4.26B(iii) and (iv)). This relative decrease in cytokeratin expression in VE-cadherin^{+} CTCs emphasizes the possibility that VM may be associated with complete loss of cytokeratin expression reflecting an epithelial to endothelial

transition,[168] or more broadly a 'stem-like de-differentiation' such as has been described in association with VM in melanoma.[199] The current study would therefore be complemented by future studies which identify CTCs which are cytokeratin^{-}/VE-cadherin^{+}.

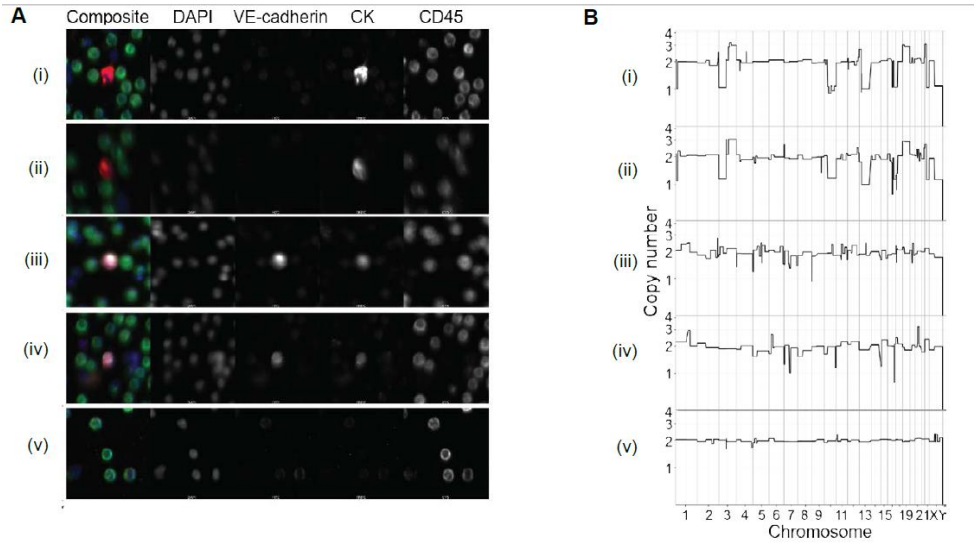

Figure 4.26 Single Cell CNA analysis of VE-Cadherin negative and VE-Cadherin positive CTCs from a SCLC patient indicating two genetically distinct sub-populations of cells.
A CTCs were identified using the HD-SCA assay whereby cells were stained for DAPI (white), VE-Cadherin (white), CKs (red), CD45 (green) and identified DAPI+/VE-Cadherin-/CK+/CD45- CTCs **(i)** and **(ii)** and DAPI+/VE-Cadherin+/CK+/CD45- CTCs **(iii)** and **(iv)**. A reference white blood cell (wbc) is included which is negative for all markers except CD45 **(v)**. B CNA analysis of cells from A shows the two populations of CTCs based on VE-Cadherin expression also have different genomic architecture, VE-Cadherin- CTCs are clonal **(i)** and **(ii)** whereas VE-Cadherin+ CTCs show non-clonal arrangements **(iii)** and **(iv)**. Representative images and profiles are shown.

4.4.2 Is the clinical effect of VM context dependent?

4.4.2.1 Chemotherapy naive limited stage SCLC

When determining the contribution of VM vessels to the total tumour vasculature, a high VM score (in which >10% of all vessels had the VM phenotype) as determined by ROC curve analysis was associated with an

adverse prognosis in limited stage SCLC patients. Eight of the ten patients who survived beyond 3 years were in the low VM category whilst survival of <3 years seen in 31/41 patients was associated with a high VM score. Although the entire population had a 5 year survival of 15% in this group of 41 limited stage patients which is in agreement with the expected survival rate for this group,[284] six of seventeen patients (35%) with a low VM score remained alive >8 years after diagnosis. This indicates that a low VM score may be a predictor of long term survival in this setting. This would have significant potential for clinical application as it may be a way of identifying patients likely to relapse following chemo-radiotherapy who could be identified for inclusion within clinical trials of novel adjuvant therapy.

4.4.2.2 Chemotherapy naive extensive stage SCLC

In contrast to the findings in limited stage SCLC biopsies, when determining the proportion of CTCs which express VE-cadherin (proposed as a surrogate for CTCs having a broader VM phenotype), a high VM score (in which >8% of all CTCs co-expressed cytokeratins and VE-cadherin) as determined by ROC curve analysis was associated with a better prognosis in extensive stage SCLC patients.

Exploratory analysis of the clinical data alongside the CTC data identified that there was a positive correlation between CTC VM score and tumour density measured on the diagnostic CT (R=0.58 95% CI 0.25 to 0.78, p=0.0011). Tumour density has been reported as a surrogate for tumour necrosis (necrotic areas of tumour have lower density on CT),[291] and from this it may be inferred that tumours with lower density have impaired

perfusion. However, confirmation of this observation is planned in a prospective study using DCE-MRI in SCLC xenografts. Additionally, there was a non-significant trend towards a low CTC VM score in patients who had no evidence of radiological response to chemotherapy (Fig 4.15). Both of these observations led to the generation of the hypothesis that in extensive stage SCLC, the presence of VM is associated with improved tumour perfusion and increased response to chemotherapy which may result in improved survival for these patients.

4.4.2.3 Hypothesis 1: the 'stem-like' quality of VM tumour cells dominates clinical impact in limited stage SCLC

The observation that patient survival <3 years was associated with a high VM score is consistent with the hypothesis that VM, potentially through tumour 'stemness' and plasticity,[292] leads to outgrowth of chemo-refractory or chemo-resistant sub-clones within the tumour which ultimately precedes treatment failure and worse clinical outcomes. As described in the General Introduction (Section 1.9), melanoma cell lines which are capable of forming VM networks express 'stem-like' gene expression profiles.[199] Although the cancer stem cell hypothesis remains an area of debate,[276] the expression of cancer stem cell markers in clinical samples has been associated with aggressive tumour behaviour.[277] Additionally, supporting the association between VM and treatment resistance in Merkel cell carcinoma, a neuroendocrine carcinoma of the skin, VM rich areas of Merkel cell carcinoma xenografts were demonstrated to be refractory to chemotherapy.[198]

In summary, I propose that in limited stage SCLC, where there is not yet distant metastatic spread, the 'stem-like' properties of VM cells may be the primary determinant of outcome by pre-disposing to metastatic spread and treatment resistance. The deleterious effect of this on patient survival outweighs any benefit conveyed by improved chemotherapy drug penetration into the tumour and tumour perfusion.

4.4.2.4 Hypothesis 2: the role of VM vessels in tumour perfusion and chemotherapy delivery dominates clinical impact in extensive stage SCLC

Based upon the observation that a high CTC VM score correlated with better patient survival, I hypothesise that this association is due to the role of VM in tumour perfusion. This effect would itself be expected to be multi-faceted. Firstly, VM may enable tumour growth through facilitating oxygen and nutrient delivery. However, conversely, VM may enable improved chemotherapy drug delivery and counteract hypoxia mediated therapy resistance (as detailed in the General Introduction Section 1.2), increasing the potential for cisplatin-induced tumour cell death. In extensive stage SCLC where metastatic spread has already occurred, the clinical benefit arising through enhanced response to chemotherapy may outweigh any pro-metastatic capability conferred by the VM cells due to metastatic disease being already established.

4.4.3 Future clinical applications of cytokeratin$^+$/VE-cadherin$^+$ CTCs as a biomarker of VM

Studies in SCLC xenografts (H446, VE-cadherin$^+$, which contains VM networks) confirmed that decreasing the levels of VM in tumours significant

slowed tumour growth kinetics (Figure 4.22). This finding suggests that targeting of VM may be a treatment strategy which effectively inhibits tumour growth in SCLC. Ultimately, the CTC profiling assay described in this chapter could be incorporated into early phase clinical trials of therapies targeting the tumour vasculature in patients with SCLC. Future research with the VM assay should address the following hypotheses:

1. CTC VM profiling prior to therapy, demonstrating high CTC VE-cadherin expression, predicts subsequent response to VM targeted therapy.

2. Change in CTC VM profile on therapy, demonstrating a decrease in CTC VE-cadherin expression, predicts subsequent clinical benefit from therapy.

3. Change in CTC VM profile on therapy, demonstrating a decrease in CTC VE-cadherin expression, has utility as a pharmacodynamic biomarker to demonstrate proof of concept that the drug hitting target results in the desired biological effect.

Approaches studied to date in order to target the tumour vasculature in patients in general, and potential approaches to target VM specifically, are discussed below.

4.4.3.1 Targeting angiogenesis as therapeutic strategy in lung cancer

Despite extensive clinical research into the use of anti-angiogenic therapy in solid tumours, there have only been modest improvements in patient survival

with the use of these agents. The most extensively studied anti-angiogenic agent in lung cancer is the vascular endothelial growth factor receptor monoclonal antibody bevacizumab. Although this has been studied in NSCLC in phase III trials showing improvement in and overall survival (10.3 to 12.3 months, HR 0.79, p=0.003) with the addition of bevacizumab to chemotherapy,[293] a meta-analysis of four prospective randomised studies evaluating the benefit of adding bevacizumab to standard platinum based doublet chemotherapy[294] identified only marginal improvement in overall survival (hazard ratio for death 0.90, 95% CI 0.81 – 0.99, p=0.03). These modest gains and the associated increased toxicity of anti-angiogenic therapy (significant bleeding occurring in 4.4% versus 0.7% of patients without bevacizumab)[293] has made lung cancer clinicians question whether the benefits of anti-angiogenic therapy outweigh the additional risk in NSCLC.[295]

There are fewer data on the benefits of anti-angiogenics in SCLC. However, SCLC has a higher microvessel density than NSCLC[296] and expresses VEGF receptors -2 and -3[297] which may predict that this approach may have greater therapeutic benefit in SCLC. Additionally, serum VEGF is elevated in SCLC patients.[298] A non-randomised phase II trial[299] demonstrated the feasibility of adding bevacizumab to chemotherapy in patients with SCLC and no previous treatment with acceptable toxicity. However there are no randomised data on bevacizumab in this setting. However, there is some signal of benefit from targeting angiogenesis following the data from CALGB-30504 study[300]. In this randomised phase II study, maintenance sunitinib (an

oral VEGF TKI) following induction chemotherapy in SCLC improved progression free survival from 2.1 to 3.7 months compared with placebo (HR 1.62 95% CI 1.02 – 2.6, one sided p=0.02). However, the clinical significance of this 6 week gain in progression free survival is questionable.

4.4.3.2 Lessons to learn from failures in targeting angiogenesis

Alternative mechanisms are proposed for the failure of VEGF targeted therapy to have significant clinical gains some or all of which may have a role in treatment resistance depending on the clinical context. Firstly, there are compensatory mechanisms which may be activated in response to anti-angiogenic therapy. Anti-angiogenics reduce tumour micro-vessel density causing increased hypoxic fraction causing elevated hypoxia inducible factor 1 alpha (HIF-1α) expression[301] as a compensatory mechanism in response to hypoxia[182] which regulates the transcription of genes controlling angiogenesis.

Additional mechanism of therapeutic failure include the up-regulation of other angiogenic factors such as platelet derived growth factor (PDGF) fibroblast growth factor type 2 (bFGF), or the physical response of pericytes covering the tumour endothelial cells preventing vascular collapse.[302] Finally, it has been suggested that endothelial progenitor cells may be recruited from within the bone marrow to support the tumour vasculature in response to anti-angiogenics.[303]

Alongside these compensatory mechanisms in response to anti-angiogenic therapy, targeting the tumour vasculature may promote the selection of hypoxia tolerant clones which may have increased invasive or metastatic

potential.[304] As discussed in the introduction to this work, it has also been suggested that cells may undergo an EMT or VM in response to hypoxia[192] both of which are reported to confer adverse tumour cell behaviours and promoting metastatic spread.[100,208]

In view of the potential complications of targeting the tumour vasculature, it is vital that we have a good understanding of the role of VM in SCLC tumour progression before this should be targeted as a therapeutic approach. Two existing vascular disrupting agents, thalidomide and fosbretabulin, may be utilised in this setting.

4.4.3.3 Directly Targeting VM with vascular disrupting agents

4.4.3.3.1 Thalidomide

Thalidomide is a synthetic derivative of glutamic acid. Although its mechanism of action is not well understood, it results in both immune modulation by inhibiting tumour necrosis factor alpha (TNF-α) in stimulated monocytes, and anti-angiogenesis through the inhibition of vascular endothelial growth factor (VEGF) and basic fibroblast growth factor (bFGF).[305] Thalidomide also has a role in modulating VM. In studies of melanoma tumour bearing C57 mice, treatment with thalidomide significantly reduced the tumour volume and the number of VM vessels compared with vehicle treatment.[306]

Two randomised studies have evaluated thalidomide use in SCLC patients.[307,308] In the phase III study by Lee *et al*.,[307] 724 patients with SCLC (limited and extensive stage) were randomised to receive carboplatin and

etoposide chemotherapy in addition to thalidomide or placebo. For extensive stage patients, thalidomide or placebo was continued as maintenance therapy following completion of chemotherapy until progression. No survival advantage was conferred by the addition of thalidomide to chemotherapy and in addition, thalidomide showed increased toxicity with thrombotic events consistent with previous reports with this agent.[309]

A randomised placebo-controlled phase II trial by Pujol *et al.*[308] evaluated maintenance therapy with thalidomide in 91 extensive stage SCLC patients following a four drug chemotherapy regimen with cisplatin, etoposide, cyclophosphamide and epirubicin. Although no survival advantage was seen in the whole study population, analysis of sub-groups within the study identified that for patients of good performance status (WHO PS 0-2) improved survival was seen in the thalidomide arm.

Acknowledging the chemotherapy treatment in this study differs from standard chemotherapy used for SCLC patients, these findings suggest that the use of vascular disrupting agents such as thalidomide may warrant further investigation. However, given the variability in the contribution of VM vessels to tumour vasculature seen in SCLC biopsies in the current study, biomarkers of angiogenesis and vasculogenic mimicry should be explored as a mode of predicting response to therapy in future studies.

4.4.3.3.2 Fosbretabulin (combrestatin A4 phosphate)

A second treatment which may target VM is fosbretabulin. Fosbretabulin is a stilbenoid phenol derivative and has been studied as a vascular disrupting agent. It binds to tubulin dimers, preventing microtubule polymerisation in

endothelial cells, selectively affecting immature endothelial cells (usually present preferentially in tumour vasculature rather than the normal vasculature) as these rely more on the tubulin to maintain the vessel shape as there are fewer pericytes and lack smooth muscle.[310,311] As tumour cells which undergo vasculogenic mimicry may also lack the pericytes and smooth muscle support, they may also be uniquely sensitive to this treatment approach. It also disrupts the engagement of VE-cadherin and reduces signalling in the VE-cadherin/β-catenin/Akt pathway which may reduce endothelial cell migration and capillary tube formation.[312] Through both of these mechanisms, fosbretabulin causes tumour blood vessel collapse and tumour necrosis.

A limitation to a drug which targets VE-cadherin signalling is that a predicted toxic effect of the drug would be damage to the normal endothelial cells. However, fosbretabulin has been studied in clinical trials and the only severe toxicities (CTC grade 3 and 4) reported were lymphopenia and pain related to the tumour.[313] An intriguing hypothesis is that the combination of fosbretabulin with an anti-angiogenic agent enables the tumour vasculature and VM vessels to both be targeted. The anti-angiogenic agent prevents compensatory endothelial vascularisation whilst fosbretabulin prevents VM vessel revascularisation.

This hypothesis that the combination of fosbretabulin with anti-angiogenic agents will improve efficacy is supported by new clinical data emerging from a study in recurrent ovarian cancer of combination therapy with fosbretabulin

and bevacizumab which has shown improved progression free survival compared with bevacizumab alone.[314]

In addition to using vascular disrupting agents, other approaches to targeting VE-cadherin signalling could be explored. Targeting VE-cadherin signalling via receptor tyrosine kinase activity is a potential therapeutic avenue. VE-cadherin is found in complexes with VEGF receptor, B catenin and PI3 kinase,[315,316] and engagement of VE-cadherin induces PI3 kinase which leads to the phosphorylation of AKT in melanoma cell lines.[212] Inhibition of PI3 kinase abrogates VM in melanoma cells *in vitro*.[212]

4.4.4 Conclusion

In summary, this chapter describes research which has identified a subpopulation of SCLC patient CTCs expressing the VM marker VE-Cadherin, has established for the first time that VM vessels are observed in SCLC biopsies, and has demonstrated that tumour VM networks are tumour derived and that VM is positively associated with poorer patient OS. Future research will interrogate the VM signaling pathway in SCLC and establish feasibility for therapeutic targeting where VM CTCs may serve as a minimally invasive predictive biomarker and a readily accessed disease monitoring approach.

5 EVALUATION OF DIGITAL TISSUE ANALYSIS SOFTWARE TO ANALYSE ISET FILTERED CTCs FROM PATIENTS WITH SMALL CELL LUNG CANCER

5.1 Introduction

The previous two results chapters have described immunofluorescent analysis of ISET filtered CTCs to characterise sub-populations of NSCLC and SCLC CTCs that express cytokeratins, vimentin or both; and to identify sub-populations of SCLC CTCs that co-express VE-cadherin and cytokeratins. However, these studies are limited in all cases by the number of patients which could be analysed within the time available to conduct this research. The most time consuming element for each sample was the analysis of the cells retained on the ISET filter once staining has taken place. This is because many thousand cells are typically retained on each filter which must be analysed in turn to identify cytokeratin^{+}/CD45^{-} CTCs prior to the sub-classification of each cell based upon its expression profile.

In carrying out the research, to analyse 4 ml of ISET filtered blood from a single patient following immunofluorescent staining took up to 16 hours of analysis time for an experienced operator. Early in the conduct of this research, I determined that the number of CTCs required to be classified (at a single time point for a single patient) in order to produce a representative CTC profile was 200 cells, as the relative size of CTC populations varied by less than 3% when this number of CTCs were classified (Fig 3.7, Section 3.3.4). This was successful at limiting the time required to analyse samples

with CTC counts significantly in excess of this figure. However, samples with lower CTC numbers would still take a long time to analyse as 4 ml of blood (4 ISET filter spots) would be analysed in total for these patients.

Although manual analysis remains the 'Gold Standard' for evaluating CTCs, if this could be automated or semi-automated akin to the automated digital microscopy included in CellSearch[55], this analysis could be applied to a larger number of clinical samples. This would enable the expansion of this research to a larger number of patients which would have two benefits. Firstly, it would enable the scaling up of the current research in order to increase the statistical power of the analysis. Second, it would permit the application of this processing to clinical trial samples. As one of the intentions of this work is to evaluate the utility of CTCs as a biomarker in lung cancer, it is important to enable the sample processing can be performed in a timely fashion on a larger scale within a clinical trial.

Furthermore, in view of the labour intensive requirements of manual analysis of ISET filters, analysis of larger numbers of patients, as reported in this work, requires multiple analysts to be involved. Our group has previously shown that there is significant inter-operator variability when either scoring CTCs using CellSearch[317] or classifying ISET CTCs following immunohistochemistry staining.[318] Although steps were taken within this research to mitigate inter-operator variability (through standardised training of all analysts on the classification of CTCs and second checking of all CTCs identified for review by a single, lead analyst) the requirement for multiple operators brings with it the potential for inter-operator error. Automation of

the CTC identification step, thereby removing analysts from this time consuming element of the analysis, may remove this potential for analytical variability. However, to date, there are no published data on semi-automated analysis of ISET filters.

Definiens Tissue Studio (Definiens AG, Munich, Germany) is a digital tissue analysis software package which processes multicolour fluorescent images and may be programmed to detect single cells, characterise them based upon their expression of proteins of interest, and determine expression profiles of markers of interest (eg vimentin or VE-cadherin) per cell.[319] This software package is typically used to analyse digital image files of tissue sections mounted on glass slides. The ISET filters are mounted on glass slides akin to tissue sections and the images captured using the Mirax automated slide scanner, and these image files are compatible with the Definiens Tissue Studio software.

Hypothesis

Definiens Tissue Studio can be utilised to perform semi-automated analysis of cells on an ISET filter and identify CTCs distinct from leucocytes and circulating endothelial cells.

Aims

- To utilise Definiens Tissue Studio to perform automated analysis to identify CTCs on ISET filters following multicolour immunofluorescent staining (for cytokeratins, CD45 and VE-cadherin).

- To compare the performance of manual and automated analyses in identification of CTCs.

5.2 Methods

5.2.1 Recruitment of patients and healthy volunteers and blood sampling

32 patients with histological or cytological confirmation of extensive stage small cell lung cancer, prior to any systemic anti-cancer therapy and 9 healthy volunteer subjects provided written informed consent as part of an ethically approved protocol. The SCLC patients were recruited as part of 'Chemores: molecular mechanisms underlying chemotherapy resistance, therapeutic escape, efficacy and toxicity', an EU funded collaboration of 17 European University organisations, which was approved by the NHS North West 9 Research Ethics Committee. Healthy volunteers were consented to a separate study: 'Plasma and serum collection from healthy volunteers for biomarker research and method validation purposes' which was approved by the University of Manchester Research Ethics Committee 1.

5.2.2 Sample processing by ISET

All blood samples collected in 10 ml EDTA tubes (Becton Dickinson, NJ, USA, 368589), were stored at 4 degrees Celsius and filtered by ISET (RareCells Diagnostics, Paris, France) within 4 hours of collection as described in the General Methods (Section 2.8).

5.2.3 Staining and image capture of ISET filters to identify CTCs, leukocytes and circulating endothelial cells

ISET filters were stained with the immunofluorescent assay described in Chapter 4 (Section 4.2.3) using fluorescent antibodies against cytokeratins, CD45 and VE-cadherin and nuclei stained using DAPI. After mounting the filters on a glass slides, slides were left overnight at room temperature to dry

before analysis. Slides were scanned with the Mirax automatic slide scanner and reviewed using the Panoramic viewing software (version 1.15.1.10 3DHistech, Budapest, Hungary as described in the General Methods Chapter) as detailed in the General Methods (Section 2.10). Using this software, pseudo-colouring was applied and kept consistent in the first assay showing DAPI as white, cytokeratins as green, CD45 as red and VE-cadherin as blue. This assay distinguishes leukocytes ($CD45^+$/$cytokeratins^-$), circulating endothelial cells (VE-$cadherin^+$/$cytokeratins^-$) and CTCs ($cytokeratins^+$/$CD45^-$).

5.2.4 Manual classification of cells (CTCs and leucocytes) on ISET filters

All ISET filters were scored manually by a trained CTC analyst. Analysts were blinded to the clinical details and to the result of the automated analysis. Analysts were trained to view the ISET filters using the 3DHistech panoramic viewing software (version 1.15.1.10) and enumerate the total number of CTCs ($DAPI^+$, CK^+, $CD45^-$ and) and classify these as VE-$cadherin^+$ or VE-$cadherin^-$. $CD45^+$/$cytokeratin^-$ leukocytes retained on the filter were used as the internal negative control for cytokeratins and VE-cadherin. Cells required a DAPI stained nucleus of 8 μm or greater (≥ the size of the filter pore), and at least 50% of the DAPI signal had to sit within the cell marker signal. The cell marker signal was required to be larger than the DAPI signal. Any objects which were inadequately focussed were not further classified. All CTCs were tagged using the viewing software for further review if required.

5.2.5 Automated classification of cells (CTCs and leucocytes) on ISET filters

The Mirax image files were imported into Definiens Tissue Studio (Definiens AG, Munich, Germany) software for automated analysis. This chapter describes the development of this method for automated analysis.

5.2.6 Statistical analyses

To compare the performance of manual and automated analyses in the identification of CTCs on ISET filters, CTC numbers identified per ml were plotted by each method and the correlation coefficient (Pearson's R value) was calculated. To evaluate for bias between methods, a Bland-Altman plot of the difference between CTC score with each method, plotted against the average CTC score was performed and paired t-test was used to compare the difference between means. To determine a prognostic cut-off for ISET CTC number by each method, receiver operating characteristic (ROC) curves were plotted and the area under the ROC curve calculated. The sensitivity and specificity of a range of CTC cut-offs in predicting survival at 12 months was tabulated. Kaplan-Meier survival curves were plotted dichotomizing patients using a CTC cut-off value selected based upon the results of ROC curve analysis, and a difference in survival curves between two groups calculated using the log rank test. P values of <0.05 were considered statistically significant.

5.3 Results

5.3.1 Manual analysis of ISET filtered CTCs

Blood samples from 32 chemotherapy naive extensive stage SCLC patients were collected into EDTA tubes and diluted in ISET buffer before being filtered through 8 µm pores under negative pressure. Filters were stained for CD45, cytokeratins and VE-cadherin.

5.3.1.1 Identification of cells retained on the filter

In order to identify cells on the ISET filter, the first step was to identify cell nuclei. Figure 5.1 shows representative images of nuclei captured on the ISET filters (stained with DAPI, white). Cells were classified as having intact nuclei if the DAPI signal was homogenous as shown in Figures 5.1 A and B. However, loss of central DAPI signal (as shown in Figure 5.1 C to G) was defined as 'pore artefact' whereby fragments of cells are thought to have been captured in the pores during the filtration process.

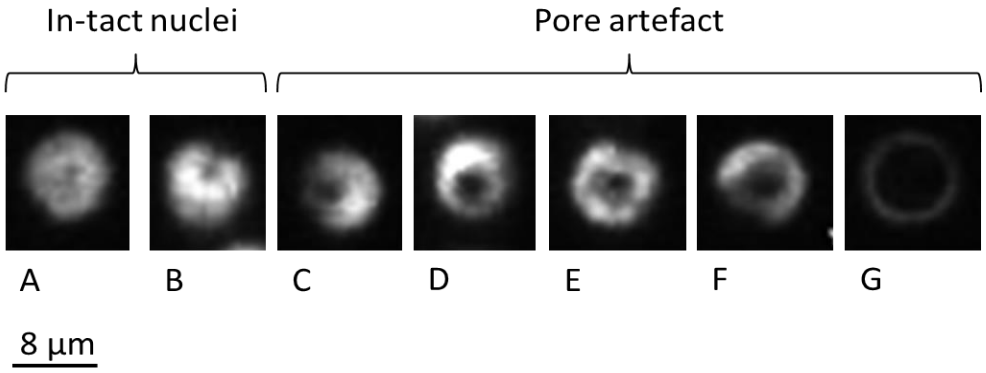

Figure 5.1 Characterisation of nuclei retained on ISET filters
Cell nuclei are shown stained with DAPI (white). Cells were classified as intact if they had homogenous DAPI signal (A-B). Cells with central loss of DAPI signal (C-G) were not classified further.

5.3.1.2 Manual identification of ISET filtered SCLC CTCs

Once nuclei were identified on the filter, each cell was classified based upon its expression of cytokeratins and CD45 as a CTC (cytokeratin^{+}/CD45^{-}) or a leukocyte (cytokeratin^{-}/CD45^{+}). A single operator identified all CTCs on each ISET filter. CTCs were then tagged using the analysis software (3DHistech Panoramic Viewer) for future analysis. The number of CTCs in 4 ml of blood was recorded for each patient. Figure 5.2 shows an example of two ISET filtered cells. The nuclei (stained with DAPI, white) are shown in Figure 5.2A with no evidence of filtration artefact. The expression of cytokeratins (green, Fig 5.2B) and CD45 (red, Fig 5.2C) is shown for each cell. The composite image is shown in Figure 5.2D showing the expression profile of a CTC (cytokeratin^{+}/CD45^{-}) and leukocyte (cytokeratin^{-}/CD45^{+}) (indicated with arrows). Figure 5.3 shows the number of CTCs identified per 1 ml of blood analysed for all patients. Each bar represents the total CTC number from an individual patient and the results are presented ranked from low to high CTC number. The number of CTCs ranged from 1 to 613 per ml (median 99, mean 138/ml).

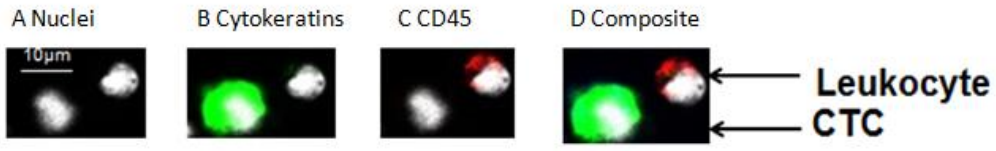

Figure 5.2 Representative image of a CTC and leukocyte from a SCLC patient following multicolour immunofluorescent staining
DAPI stained nuclei are shown in white in al images, cytokeratin staining in green (B) and CD45 staining in red (C). Cells were classified as CTCs if they had the expression profile cytokeratin^{+}/CD45^{-} and as leucocytes if cytokeratin^{-}/CD45^{+} (D).

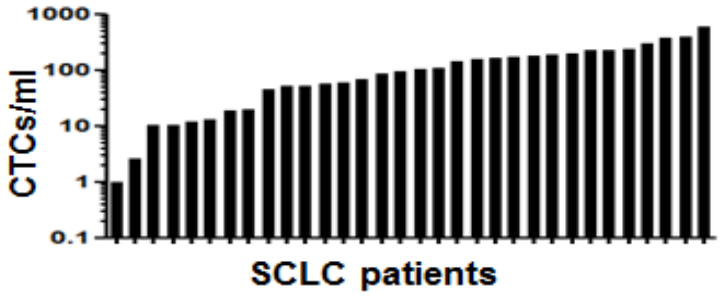

Figure 5.3 CTC count for each SCLC patient by manual analysis of ISET filters
Each bar represents the total CTC count per ml of blood analysed for each SCLC patient (n=32) by manual analysis of the ISET filters following immunofluorescent staining. Results are ranked by CTC number.

5.3.2 Automated analysis of ISET filtered CTCs

5.3.2.1 Automated identification of ISET filtered SCLC CTCs

In order perform automated analysis of ISET filtered CTCs following multicolour immunofluorescent staining, a rule set was developed using Definiens Tissue Studio software to process the digital image files of the ISET filters which had undergone manual analysis. The Definiens functions utilised in the rule-set are summarised in Table 5.1. Figure 5.4A shows the digital image file opened in Definiens Tissue Studio. The 6mm cellular area of the ISET filter is shown outlined in a white dashed circle. The program is trained to identify this cellular area as a region of interest for analysis (shown in orange in Figure 5.4B, the excluded area shown in blue). To identify cells within this area, four representative fields of view were selected from across the filter using the nuclear image layer (DAPI staining shown in white in

Figure 5.4C). This manual step is required during the development of the algorithm; however, there is no manual involvement at this stage once the algorithm has been defined. Using the rule-set outlined in Table 5.1, Definiens outlines cellular nuclei (shown outlined in blue in Figure 5.4D) and these were manually verified during the development of this rule-set. The cellular marker fluorescent layers were overlaid on the nuclei (Figure 5.4E shows the fluorescent image showing CD45 as red and cytokeratin as green (VE-cadherin not shown)) and the mean fluorescent intensity of each marker was measured and reported per cell.

Definiens Function	Instruction	Effect
Background separation	NA	Selects the scanned area
Composer initialisation	NA	Breaks down the image into segments
Composer training	Operator classifies segments of image that are the cellular area of the filter or other	Classify the cellular area on the ISET filter as the region of interest for analysis separate from the rest of the ISET filter
Composer reclassify region	Reclassifies misclassified areas based upon size <0.5 mm^2	Misclassified areas are re-classified as within the region of interest
Initialise cellular analysis	Select 10x magnification	Selects the magnification for image analysis
Nuclear threshold range	Set to 1.5	Selects positive nuclear staining
Typical nuclear size	Set to 60 μm^2	Set expected nuclear size
Nucleus morphology and filter	Exclude events with area <15 μm^2 and circularity measurement <6 (arbitrary scale where lower number equates to decreased circularity)	Exclude small specks of DAPI on the filter
Cell size selection	Typical cell size 260 μm^2	Set expected cell size equating to diameter of 18 µm to exclude large non-specific objects on the filter
Cell simulation	Fluorescent threshold set to 80	Detects and outlines cytoplasmic area around the nucleus
Exclusion 1: Relative area of nucleus	Nuclear to cytoplasmic ratio of >0.1	To exclude objects with incomplete nucleus
Exclusion 2: Circularity	Circularity of <6	To exclude streaks of cell fragments
Exclusion 3: Coefficient of variation (SD/mean) DAPI signal	CV >0.2	To exclude filtration artefact from incomplete DAPI signal in pores

Table 5.1 Definiens rule-set to identify cells on ISET filters

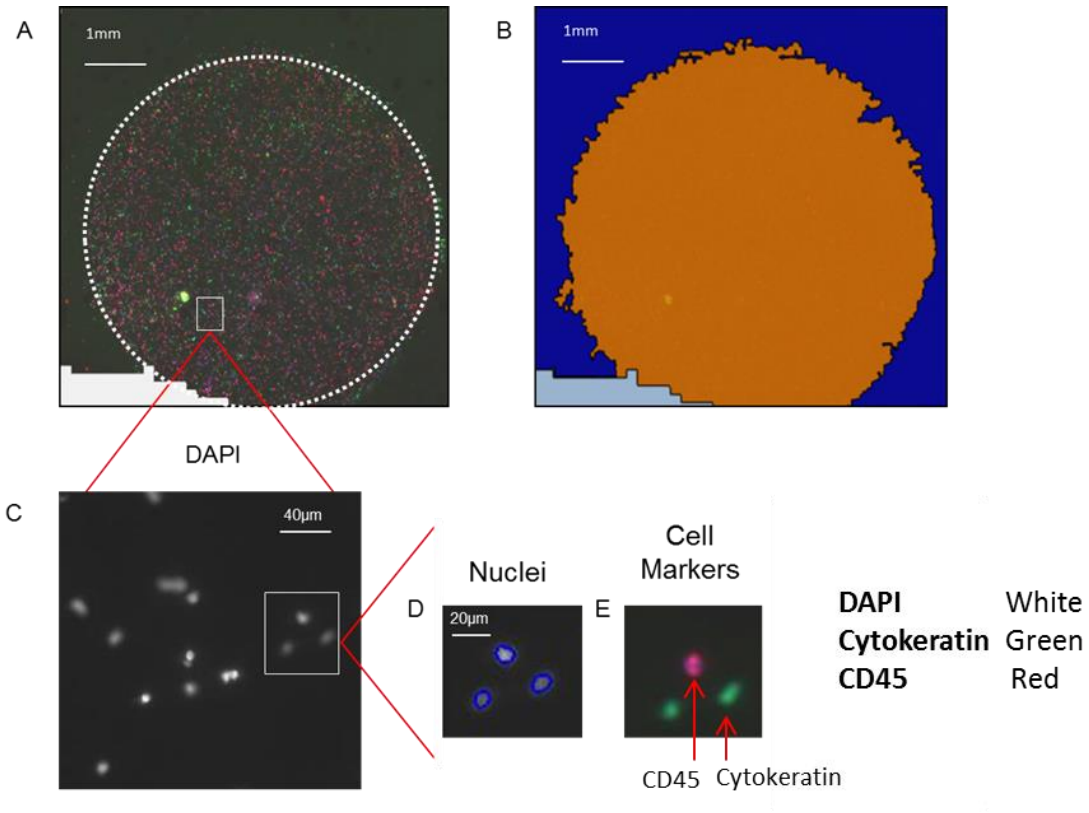

Figure 5.4 Definiens automated processing to detect and classify cells retained on the ISET filters
An overall image of an ISET spot imaged by the Mirax is shown in **A**. Definiens is programmed to identify the cellular area of the ISET spot as a region of interest (orange, **B**) within which cells are analysed. The nuclear layer of the fluorescent image (DAPI, white, **C**) is analysed and individual nuclei identified and outlined by Definiens (shown in blue, **D**). The fluorescent image is overlaid on the nuclei (**E**, showing cytokeratins as green and CD45 as red. VE-cadherin is not shown). The fluorescent intensity of each marker is measured and reported for each cell.

5.3.2.2 Verification of thresholds and cellular morphology of objects classified as cells using automated analysis

For cells to be classified as CTCs or leukocytes, thresholds were set for CD45 and cytokeratin expression defining the presence or absence of each marker. To do this, cells identified using the Definiens rule-set were reviewed using the Definiens Image Miner software, wherein the image file of the ISET filter was reduced to a gallery of cells for review. This step also permitted the cellular morphology to be verified manually. Definiens reports the mean

fluorescent intensity of each cellular marker (cytokeratins, CD45) and thresholds were verified above which cells were determined to be positive by selecting cells for evaluation from the gallery at a range of fluorescent intensities. Cells were then grouped by classification showing all CTCs per filter spot. Figure 5.5 shows 4 SCLC CTCs (cytokeratin^{+}/CD45^{-}) identified from this gallery. Each marker is shown separately as a white image (Figure 5.5A-D) and in the composite image (Figure 5.5E), cytokeratins are shown as green and DAPI as blue. As with the manual classification, this confirmed that cells identified by Definiens as CTCs had an intact DAPI signal (Figure 5.5A) within an area of cytokeratin signal (Figure 5.5C) and were negative for CD45 (leucocyte marker) (Figure 5.5B).

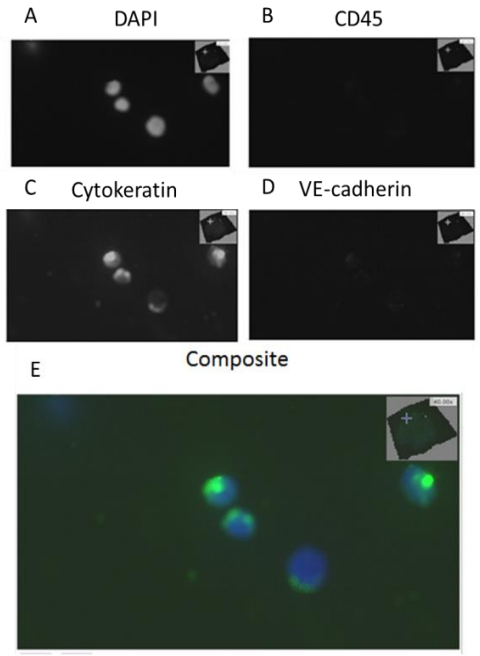

Figure 5.5 Manual verification of cellular morphology of cells identified as CTCs using Definiens analysis of Mirax image data
Four representative SCLC ISET filtered CK^{+}/CD45^{-}/VE-cadherin^{-} CTCs. Each of the markers is shown separately (**A** to **D** in grey scale) and the composite image (**E**) shows DAPI as blue, cytokeratin as green and CD45 as red (no CD45 positive cells shown).

5.3.2.3 CTC quantitation and evaluation of false positive rate for CTC identification using automated CTC analysis

To evaluate the false positive rate of automated analysis, the same algorithm was applied to ISET filtered blood samples from 9 healthy volunteers. Results are shown in Figure 5.6 (grey bars). Each bar represents the number of CTCs reported per ml of blood for each subject (grey bars, healthy volunteers; black bars, SCLC patients) and the results are ranked from low to high CTC number. 7/9 healthy volunteers had <10 CTCs/ml, 2 donors had <50 CTCs/ml. Manual verification of these samples confirmed that these cells were cytokeratin^{+}/CD45^{-} nucleated objects which fulfilled the criteria to be classified as CTCs. 18/32 SCLC patients had CTC counts higher than the false positive CTC count detected in healthy volunteers. These results suggest a false positive rate of up to 50 CTCs/ml must be considered when applying this automated algorithm to CTC enumeration in this patient group.

This false positive rate is unsurprising given the published results of other approaches to CTC enumeration using ISET. For example Hofman *et al*.[320] used ISET microfiltration and immunocytochemistry to analyse blood samples from 239 people without a prior or subsequent diagnosis of cancer (49 healthy volunteers, 152 patients with miscellaneous non-neoplastic disease and 38 cases with benign lung lesions). This study found that 11.1% of cases with benign pathology and 4% of healthy volunteers had 'circulating non haematological cells' detected. This study is considered in more detail in the following discussion (Section 5.4.4) alongside other studies pertaining to false positive CTC detection.

Enumeration of CTCs in 32 SCLC patients by automated analysis, identified CTCs in 27/32 SCLC patients. CTC number ranged from 0 – 2062/ml (median 88, mean 250/ml). Although the median is similar to that reported by manual analysis of the same patients (median 99, mean 138/ml range 0 – 613/ml), the range is much greater in the automated analysis. Although this could be explained by the false positive identification of CTCs, this may in fact be due to an underscoring of CTC counts at higher numbers by manual analysis. Operators, although blinded to the clinical details such as stage and response to therapy, may have been subconsciously moderating the CTC number, a widely recognised phenomenon of unconscious cognitive bias.[321] In this instance, if an operator is expecting to find ~100 CTCs per ml of blood based upon previous ISET filters analysed (approximating to the median in this dataset), in instances when there are in fact many fold more CTCs per ml, the analyst may unconsciously overlook CTCs that are present on the filter. It is difficult to accurately measure the degree to which such a bias may be occurring. However, the removal of that possibility is another potential benefit of an automated approach to CTC image processing as such bias clearly cannot occur in automated analysis following a pre-defined rule-set.

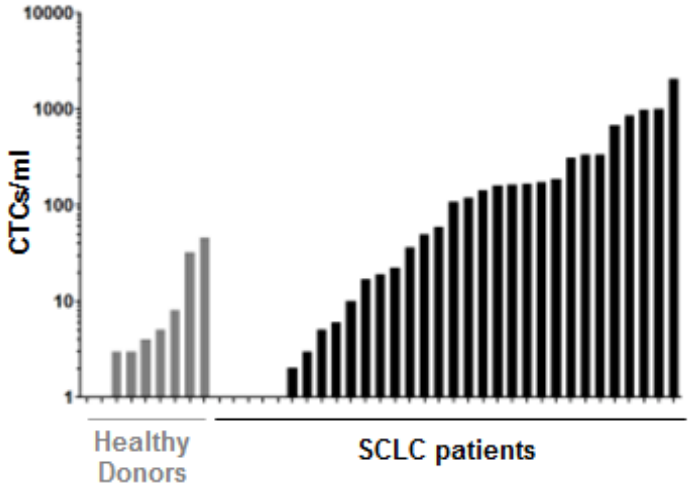

Figure 5.6 Automated CTC count for each SCLC patient (black) and for healthy volunteers (grey)
Each bar represents the CTC number per ml for an individual subject. Subjects are ranked by CTC number.

5.3.3 Comparison between manual and automated approaches to CTC detection

This study has shown how Definiens Tissue Studio can be programmed to identify CTCs on an ISET filter following immunofluorescent analysis with a low false positive rate relative to the CTC yield in SCLC patients. However, as the current gold standard for CTC classification is manual scoring. I subsequently sought to compare manual and automated CTC scores performed on the same samples.

5.3.3.1 Correlation between manual and automated analyses for CTC enumeration

Figure 5.7A shows the number of CTCs identified by manual and automated analyses performed on the same 32 samples, with a solid line connecting the score given for a single sample by each method. There was good agreement between methods for 27/32 samples, with <1 log-fold change. However, 5/32 patients had >2 log-fold change in CTC number between methods. The

digital image files were reviewed and these were found to have a reduced DAPI and CD45 fluorescent intensity, impacting upon the effect of the thresholds set on cellular classification.

CTC numbers identified per ml were plotted using the automated and manual methods (Figure 5.7B) and the correlation coefficient (Pearson's R value) was calculated. For all 32 patients, significant agreement was seen (r=0.43, p=0.001); however, following exclusion of the 5 patients with reduced fluorescent intensity, this agreement was further improved (r=0.74, p=<0.0001). Comparison of the linear regression line (black) and the 1 to 1 line (grey) shows that at lower CTC counts, the manual analysis gives higher CTC numbers and at higher counts the manual analysis gives lower CTC counts when compared with Definiens.

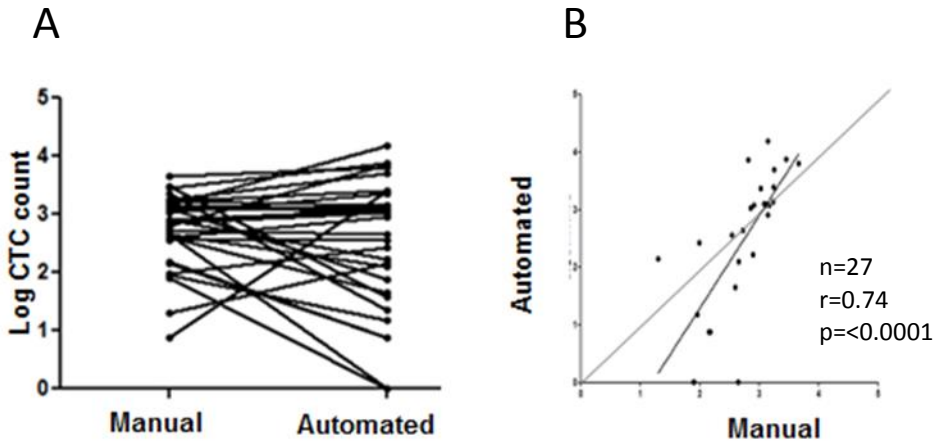

Figure 5.7 Comparison of manual and automated analysis of CTCs in SCLC patient samples
A shows manual and auotmated CTC numbers identified in SCLC patient samples, paired samples are connected by bars. **B** shows linear regression of manual against automated CTC count (black line is the linear; grey line is the 1:1 line). CTC data were logged prior to analysis.

In order to try to account for any variation in sample fluorescence, a second Definiens algorithm (subsequently referred to as 'Definiens 2' to distinguish from the first algorithm herein named 'Definiens 1') was generated with decreased thresholds for DAPI and CD45 (analysis with reduced CD45 and DAPI thresholds shown in Figure 5.8A) and applied to all 32 patients' samples. Although this was able to mitigate the effect of altered fluorescent intensity on individual filter samples, the Definiens 2 algorithm produced CTC numbers which were significantly lower from the manual identification ($p=<0.05$, Figure 5.8B), suggesting that it was not an overall improvement in identifying CTCs. However, both algorithms were taken forwards to formally evaluate for evidence of bias.

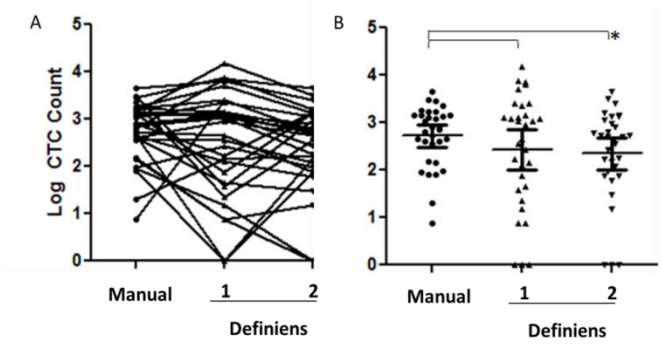

Figure 5.8 Comparison of individual CTC values between manual and the first and second Definiens algorithms

Line plot (A) in upper panel show individual CTC counts from manual analysis and first and second Definiens algorithms. Plot B shows the distribution of CTC counts by each approach. * represents a p value of less than 0.05 for a difference between the means for a two tailed paired t-test (the mean is plotted on each dataset and error bars represent the 95% confidence intervals).

5.3.3.2 Evaluation of bias between manual and automated approaches to SCLC CTC detection

To evaluate for bias between the Definiens 1 and manual methods, a Bland-Altman plot of the difference between CTC score with each method, plotted against the average CTC score was performed and paired t-test was used to compare the difference between means (Figure 5.9). Each point on the plot represents a single patient sample which has been scored by both methods. The *y* axis shows the difference in number of CTCs identified between the two methods (manual minus automated) with positive values showing that manual scores are greater than automated scores and negative values showing the inverse. The *x* axis shows the average score given with the two methods for each patient.

Figure 5.9A shows that at low CTC values, manual methods identify more CTCs than automated (using Definiens 1), and at high CTC values, manual method identifies fewer CTCs than automated. When the whole CTC dataset was plotted, no bias was seen between the methods (Figure 5.9B). However, when the data was split into tertiles by average CTC number (Figures 5.9C – E), there was no bias in the lower and mid tertile. In the upper tertile, the manual method identified significantly fewer CTCs than the automated method ($p=0.03$). This bias may however be a reflection of an advantage of automated over manual scoring. Although this has not been formally tested within this research, as suggested above, a possible explanation for this is that manual scorers introduce the bias by subconsciously moderating their scores at the extremes of the range of CTC counts, not counting all events seen when there are a large number of CTCs to be scored. The greatest

differences between methods were seen at the lowest CTC values (lower and mid tertiles, up to 3 log CTC values), and the smallest difference seen at higher CTC values (upper tertile, over 3 log CTC values).

In contrast, when Bland-Altman plots were generated for Definiens 2 minus the manual scoring (Figure 5.10), there was bias between these methods in the mid-tertile, with Definiens 2 identifying fewer CTCs than the manual method (p=0.001, Figure 5.10B). Accepting this bias which was identified at the upper range, the Definiens 1 algorithm provides the most reproducible assessment of manual CTC values at the upper end of the range, and this should be taken into consideration in future application of this approach to clinical samples.

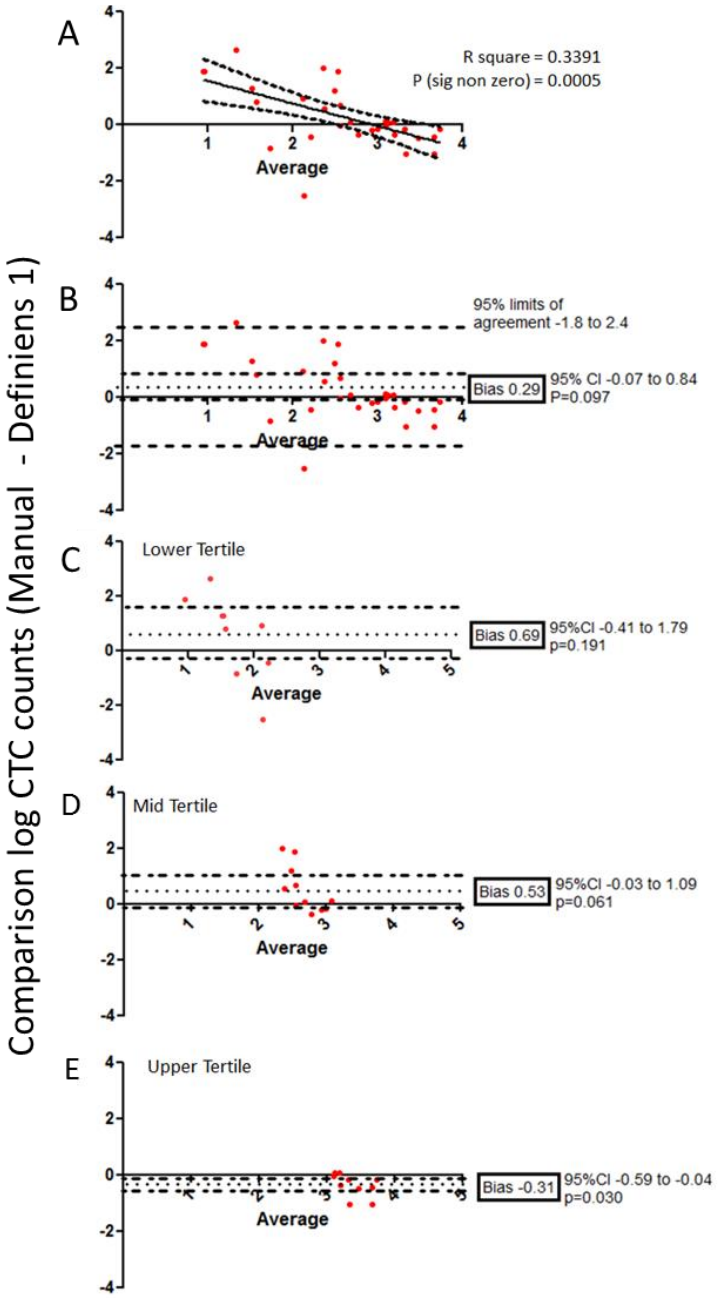

Figure 5.9 Bland-Altman comparison of manual CTC count and Definiens 1 algorithm to evaluate for bias between methods

Each point represents an average CTC score for an individual patient (average of the manual and Definiens 1 algorithm), plotted against the difference between the two scores (Definiens 1 subtracted from manual score). The whole dataset is plotted in A and B, then is split into tertiles in plots C-E. Plot A shows linear regression, Plots B to E show the evaluation for bias, with the bias and p value and 95% confidence intervals derived from a paired T test.

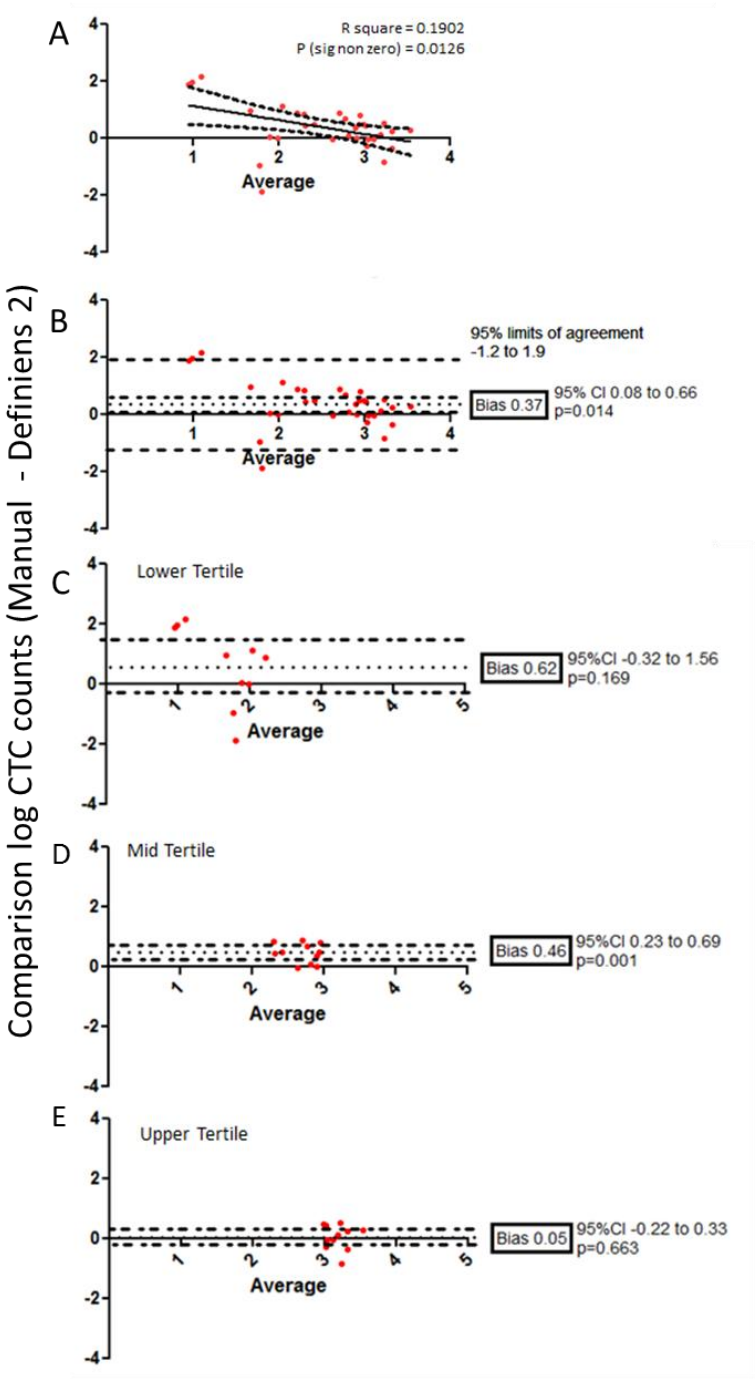

Figure 5.10 Bland-Altman comparison of manual CTC count and Definiens 2 algorithm to evaluate for bias between methods

Each point represents an average CTC score for an individual patient (average of the manual and Definiens 2 algorithm), plotted against the difference between the two scores (Definiens 2 subtracted from manual score). The whole dataset is plotted in A and B, then is split into tertiles in plots C-E. Plot A shows the linear regression, Plots B to E show the evaluation for bias, with the bias and p value and 95% confidence intervals derived from the T test.

5.3.3.3 Association between manual and automated SCLC CTC number and patient survival

To explore whether there was a similar biological significance of ISET CTCs evaluated by manual and automated (Definiens 1) approaches, univariate survival analysis was performed to assess for association between patient survival and CTC number by each approach. Patients were dichotomised into ≥150 CTCs/ml or <150 CTCs/ml and a Kaplan-Meier survival curve was plotted (Figure 5.11). Patients with fewer than 150 CTCs/ml had a trend towards improved overall survival compared with patients with ≥150 CTCs/ml with each method (manual scoring: median survival 6.7 v 11.4 months, log rank p=0.18; automated scoring median survival 7.2 v 16.2 months, log rank p=0.11). Although these differences did not reach statistical significance, this consistency in clinical outcomes when patients' CTCs are classified using either manual or Definiens approaches provides additional confidence in this approach to automated processing of clinical samples.

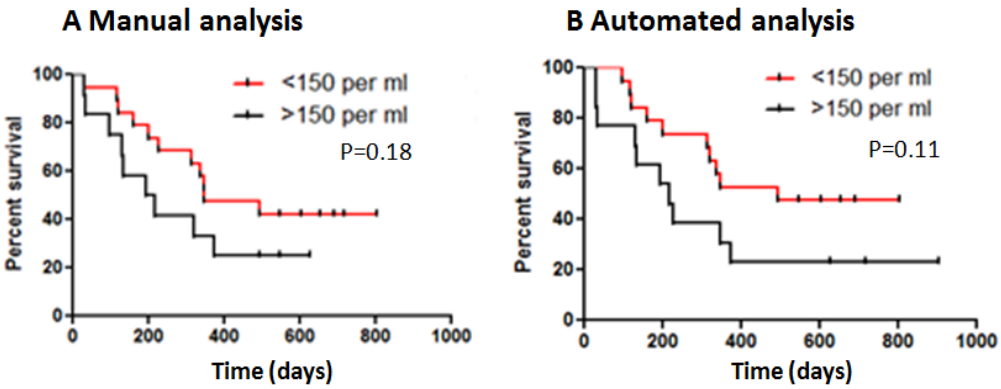

Figure 5.11 Kaplan-Meier survival analysis for overall survival for SCLC patients dichotomised by CTC number obtained through manual analysis (A) and automated analysis (B)
Patients with <150 per ml shown in red and ≥150 CTCs/ml shown in black.

5.4 Discussion

5.4.1 Summary of findings

In this Chapter, it has been demonstrated how the digital image analysis software Definiens Tissue Studio can be programmed to detect ISET enriched CTCs from SCLC patients following immunofluorescent analysis. When 4ml blood was examined from 32 extensive stage SCLC patients, manual analysis identified a median of 99 CTCs/ml (mean 138/ml, range 1 to 613/ml). Automated analysis of the same samples identified a median of 88 CTCs/ml (mean 250/ml, range 0 – 2062/ml).

Automated analysis enables the amount of time required to analyse these samples to be significantly reduced. The manual analysis took over 500 hours of analyst time. Although a significant amount of time has been invested in developing this Definiens algorithm, the application of the final algorithm to future clinical samples will enable multiple samples to be processed producing galleries of CTCs to be presented to the analyst for review. The evaluation of the gallery of cells within Definiens Image Miner rather than the manual search for cells on the filter followed by evaluation for their expression profile can now therefore be performed in much less time. This will enable the application of CTC profiling to larger numbers of patients and more timely profiling if this analysis were subsequently to be applied to clinical decision making.

5.4.2 Discrepancies between automated and manual analyses of ISET filters

Analyses of individual patient CTC numbers and image data identified discrepancies between automated and manual analyses in 5/32 patients attributed to variation in fluorescent intensity between staining batches. When there was a reduced fluorescent intensity on the ISET filters, this altered the effects of uniform thresholds which were set for cellular classification resulting in discrepancies between manual and automated CTC identification. Following exclusion of 5 samples for this reason, correlation co-efficient showed significant correlation between the automated and manual analyses ($r=0.74$, $p=<0.0001$). This discrepancy has implications for the approach to setting fluorescent thresholds for cell classification in future applications of this technology.

5.4.3 Future approaches to improve the automated detection of CTCs

One approach to improve the reliability of automated analysis would be to continue to use the fixed fluorescent thresholds as determined in this study, but to screen the mean fluorescent intensity for each fluorophore for all filters following staining to ensure it falls within pre-determined acceptable limits, excluding outliers from subsequent analyses.

An alternative approach would be to set unique thresholds for each staining batch. This would have the advantage of including all samples irrespective of any variation in fluorescent intensity. However, this would decrease the time saving associated with this approach and introduce once again operator variability.

The automated approach used in the Epic HD-CTC Assay[290] for enrichment free CTC identification using cytokeratin and CD45 fluorescent staining of blood smears is more refined. Fluorescent thresholds to determine the positivity of cytokeratin staining are set based upon the fluorescent signal being significantly above the surrounding cells. This takes advantage of the fact that CTCs are very rare and always surrounded by a large number of leukocytes using this enrichment free approach. Negativity for cytokeratins staining is defined by the fluorescent signal being below or at the same level as the surrounding cells. CD45 negativity is defined as signal being below visual detection, accepting that over 99% of cells in the sample are CD45 positive. An advantage of this approach is that not only does it account for any variation in fluorescence between staining batches, but it also accounts for any variation across a single sample.

5.4.4 Cytokeratin^{+}/CD45^{-} cells in healthy volunteer blood

Automated analysis identified cytokeratin^{+}/CD45^{-} cells in 7/9 healthy volunteer blood samples. Between 0 and 10 ‘CTCs’ /ml were seen in 7/9 healthy volunteers and less than 50/ml in the remaining 2 patients. As introduced above, the current study is not the first to identify cells classed as CTCs in patients without a diagnosis of cancer.

In a previous study using CellSearch (identifying cytokeratin 8, 18, 19 expressing cells) and EpiSpot assay (cytokeratin 19 positive cells) in 53 patients with benign colon disease[322] cytokeratin^{+}/CD45^{-} cells were seen in 11.3 and 18.9% of subjects respectively. These cells were attributed to being benign epithelial cells although no further profiling of these cells took place

within this study. The findings of this study would however suggest that normal epithelial cells can circulate in patients with no diagnosis of cancer.

In a study using ISET[320] microfiltration and immunocytochemistry following May-Grünwald-Giemsa staining, cells were classified by the presence of cytoplasmic irregularity of the nuclear membrane, nuclear size, anisonucleosis, high nuclear/cytoplasmic ratio, and the presence of tri-dimensional sheets. CTCs, defined as circulating non-haematological cells, were identified using these criteria and they were classified as CTCs if they had over three of these cytopathological features. This approach was applied to ISET filtered blood from 239 donors without malignant disease (49 healthy volunteers, 152 patients with miscellaneous non-neoplastic disease and 38 patients with benign lung lesions). 11.1% of cases with benign pathology and 4% of healthy volunteers had 'circulating non haematological cells' detected. However, the CNHCs in patients with benign pathology were limited to having a single adverse characteristic and were not therefore classified as CTCs. However, this report does confirm that using ISET, cells are present in the circulation which are not of haematological origin and these cells warrant further study. The genetic analysis performed on the cytokeratin^{+}/CD45^{-} cells identified using the EMT assay (Section 3.4.1) confirming tumour specific mutations in ISET filtered cytokeratin^{+}/CD45^{-} cells which are absent from germline DNA and present in the primary tumour is vital to our understanding of the significance of these cells. This genetic analysis confirms that at least a population of these cytokeratin^{+}/CD45^{-} cells (although is unable to confirm that all of these cells) is of tumour origin. A study involving the recruitment of

healthy volunteers to attempt to identify and profile cytokeratin^{+}/CD45^{-} cells looking for malignant features would be ethically difficult to perform due to the potential medical consequences following the identification a malignant cell. Rather, the emphasis must be on the positive confirmation that cells are malignant in patients with a known diagnosis of cancer to increase the degree of confidence in this approach.

In view of this current uncertainty generated by the presence of cytokeratin^{+}/CD45^{-} cells in healthy volunteer blood, future application of the current staining and processing protocol to clinical samples should interpret low CTC numbers (less than 50) with caution. This study has shown that it is possible to exclude low CTC counts and still have data to evaluate in SCLC, as CTCs are so abundant. However, this may not be the case for many other cancer types in which CTCs are less abundant and may prove to be a significant limitation in the applicability of this approach to other cancer types.

5.4.5 Bias between manual and automated approaches

This study has shown using Bland-Altman analyses that there is a statistical bias between the numbers of CTCs identified using manual and automated analyses of ISET filters. The manual analysis showed a non-statistically significant trend to give higher CTC counts at low CTC values and a significant bias giving lower CTC counts at higher CTC values. It is not possible to conclude whether the bias is a result of error in either approaches alone or a combination of both analyses. A consequence of this bias is the range of CTC values generated by automated analysis of the filters is greater than by manual analysis.

Although difficult to test this experimentally, it is possible that the automated score is more accurate than the manual score as human interpretation brings with it the possibility of unconscious cognitive bias.[321] For example, if an analyst is reviewing a large number of CTC samples and from experience expects to identify ~100 CTCs per ISET filter (approximating to the median value in this dataset), they may be more likely to try very hard to identify cells on a filter when there are not many present and to overlook cells on a filter when they are abundant. This is clearly a significant advantage of an automated or even semi-automated approach. A computer algorithm will make the same judgements based upon the same rule-set irrespective of the number of events which it has to evaluate.

Viewed in terms of sensitivity and specificity, the bias identified between manual and automated analyses may reflect an improved specificity of automated CTC scoring (lower false positive rate) at lower CTC values and increased sensitivity of automated CTC scoring (lower false negative rate) at higher CTC values.

5.4.6 Potential for automated analysis to remove inter-operator variability

The automated software provides a reproducible approach to identification and characterisation of CTCs on ISET filters. If the same image file is processed using Definiens Tissue Studio to obtain a gallery of CTCs on multiple occasions, the output will be identical on each occasion. However, we have previously shown that inter-operator variability can be considerable at low cell counts when analysing CellSearch CTC counts[317] and is also seen when characterising ISET enriched CTCs.[318] Consistent with our previous

findings that inter-operator variability is greatest at low CTC counts, the disagreement between automated and manual CTC scores is also greatest at low CTC numbers. By removing the requirement for multiple operators to analyse filters to identify CTCs, the introduction of a semi-automated CTC analysis would be a step towards improving the reproducibility of the assay which would improve its applicability for clinical use.

5.4.7 Future potential for quantitative analysis of CTC marker expression

Once CTCs are identified, the automated analysis is able to provide quantitative data on expression of additional markers of interest. This would provide a superior output to the binary CTC data (positive or negative for the marker of interest) generated so far within this study. A significant amount of data is lost when the level of expression of the marker of interest is not captured. For example, these data would permit the quantitation of the epithelial, mesenchymal or VM marker of expression with greater accuracy allowing a more precise definition of sub-populations of patients which may have better correlation to clinical characteristics.

However, as described above, a hurdle encountered in the optimisation this approach to analysis of the ISET filters was the finding that different staining batches have variable fluorescent intensity. This variation would have to be measured and corrected for or standardised before any quantitative expression data could be measured. However, it has not been possible within the confines of the time available to carry out this study to refine the quantitative expression data and this will be the subject of future work.

5.4.8 Conclusions and future applications of automated CTC analysis software

From the work performed so far, the Definiens Tissue Studio algorithm described in this chapter could now be applied to SCLC clinical samples in order to rapidly screen ISET filters for the presence of cytokeratin^{+}/CD45^{-} CTCs and to quantify them. Cells on ISET filters from patients containing no CTCs could quickly be reviewed and scored as zero whereas previously, the whole filter would have to be laboriously pored over to confirm the absence of any cells.

Definiens Image Miner then allows the CTCs to be reviewed for the expression of additional markers of interest. All samples with less than 50 CTCs by automated analysis should be reviewed manually in view of the false positive rates seen in healthy volunteers. As described above, further work is required to refine this approach to capture quantitative data on intensity of expression of markers of interest, however, this application would yield greater information than the binary classification of positive or negative for the marker of interest as is the output of the manual classification.

Application of this semi-automated approach to ISET filter analysis will allow increased numbers of clinical samples to be processed and facilitate the CTC profiling methods described within this thesis to undergo further validation. Moreover, if these approaches to CTC profiling are going to be applied to clinical samples as a biomarker alongside early trials of drugs targeting VM in SCLC, this analysis will enable an improved turnaround time from sample collection to readout.

6 GENERAL DISCUSSION

This thesis describes the evaluation of the clinical and biological utility of CTCs in lung cancer. Prior to the start of this research, publications by our lab identified CTCs in SCLC[57] and NSCLC[73] patients and demonstrated their prognostic utility in these cancer types when enumerated by CellSearch (which detects $EpCAM^+$/$cytokeratins^+$ CTCs). We also demonstrated that ISET microfiltration, which enriches for CTCs irrespective of their marker expression, detects significantly more CTCs compared with the number of $EpCAM^+$/$cytokeratins^+$ CTC detected by CellSearch in the same patients[59]. The research reported in this thesis sought to advance our understanding of lung cancer CTCs further. Specifically, I set out to develop CTC multicolour immunofluorescent assays to detect novel CTC sub-populations in lung cancer patients based upon the expression of markers of epithelial to mesenchymal transition (EMT, Chapter 3) and vasculogenic mimicry (VM, Chapter 4). For EMT profiling, the expression of the epithelial intermediate filament cytokeratins and its mesenchymal counterpart vimentin by CTCs was evaluated. For VM profiling, CTCs were evaluated for their expression of VE-cadherin, a protein which has a well described functional role in vasculogenic mimicry[202]. Finally, I sought to evaluate an approach to semi-automated analysis of ISET filtered CTCs (Chapter 5) to facilitate the application of this approach to larger numbers of clinical samples.

In this General Discussion, I summarise the findings of this thesis and identify the potential future applications of these findings to studies of tumour

biology and within clinical trials. Finally, I suggest next studies which I would recommend to enable this application.

6.1 Summary of findings

Chapter 3 describes the development of an immunofluorescent assay for the characterisation of lung cancer CTCs for markers of EMT (cytokeratins and vimentin) and its application to SCLC and NSCLC patients' blood samples. Specific findings were as follows:

1. Circulating endothelial cells (CECs, identified using CellSearch CEC assay detecting $CD146^{+}/CD105^{+}$ cells) are present in SCLC patients in numbers in excess of CTC number. This finding was subsequently confirmed in a larger cohort of SCLC patients.[227] The significance of this finding is that as endothelial cells are vimentin positive, this emphasised the need to include a marker of CECs in any EMT CTC profiling assay to confidently differentiate mesenchymal CTCs ($cytokeratins^{-}/vimentin^{+}$) from CECs which would have the same intermediate filament expression.
2. I developed an immunofluorescent assay for staining ISET filtered cells which could confidently distinguish CTCs of three sub-types (epithelial $cytokeratins^{+}/vimentin^{-}$, mesenchymal $cytokeratins^{-}/vimentin^{+}$, and mixed epithelial/mesenchymal $cytokeratins^{+}/vimentin^{+}$) from leukocytes and CECs based on the expression of CD45 by leukocytes and VE-cadherin by CECs. This is an advantage of the current study over the other studies reporting the expression of markers of EMT by CTCs, none of which have accounted for the

presence of CECs.[102-105,223] In pilot studies of small numbers SCLC and NSCLC patients, CTCs of each sub-population were detected in all patients studied.

3. In an index NSCLC patient, paired analysis of CTCs and a CTC derived explant (CDX) tumour which was generated from blood drawn at the same time point found that majority of CTCs were cytokeratins^{+}/vimentin^{+} and the CDX tumour had the same cytokeratins^{+}/vimentin^{+} co-expression.

The EMT CTC profiling data and the NSCLC CDX case study has been accepted for publication in Annals of Oncology (see Appendix 2).

Chapter 4 describes the development of an immunofluorescent assay for the characterisation of SCLC CTCs to identify CTC sub-populations which express VE-cadherin as a putative biomarker of VM and its application to SCLC patient blood samples. Alongside this, it describes the analyses of SCLC patient tumour samples to evaluate whether VM is present in SCLC (justifying the analysis of CTCs to this area of tumour biology in SCLC). Thirdly, this Chapter reports the evaluation of VE-cadherin in SCLC VM utilising SCLC cell lines and xenografts. Specific findings were as follows:

4. This research provides the first evidence that VM occurs in 41 limited stage SCLC patients and it is associated with shorter patient survival, consistent with the adverse prognosis reported in association with the presence of VM in other cancer types including NSCLC.[197]

5. Using CDX models from 4 extensive stage SCLC patients, I report that secondary tumours arising from CTCs were able to produce VM networks.
6. I developed an immunofluorescent assay for staining ISET filtered cells which could confidently identify sub-populations of CTCs with a putative VM phenotype (cytokeratins^{+}/VE-cadherin^{+}) and distinguish them from leukocytes and CECs. A sub-population of cytokeratins^{+}/VE-cadherin^{+} CTCs were detected in 37/38 SCLC patients (8 limited stage, 30 extensive stage). Intriguingly, the presence of a larger proportion of cytokeratins^{+}/VE-cadherin^{+} CTCs correlated with better patient survival generating the hypothesis that the clinical effects of VM are context dependent.
7. VE-cadherin is necessary for the formation of VM networks in Matrigel by SCLC cell lines and for the formation of PAS^{+}/CD31^{-} VM structures *in vivo* in SCLC xenografts.

The VM data in SCLC has been submitted to Nature Communications, manuscript under review (see Appendix 4).

Chapter 5 describes the evaluation of Definiens Tissue Studio digital image analysis software to perform semi-automated analysis of cells on ISET filters following immunofluorescent staining. Specific findings were as follows:

8. Definiens Tissue Studio can be programmed to process digital images of ISET filtered cells following immunofluorescent staining and distinguish CTCs from leukocytes and enumerate CTCs.
9. Evaluation of the output of digital analysis versus manual analysis of ISET filters identified bias at higher CTC numbers (digital analysis gave higher CTC values than manual analysis, p=0.030). However, the presence of higher CTC counts determined by digital analysis was associated with shorter patient survival.

The data on the evaluation of Definiens Tissue Studio to analyse ISET filters was presented at NCRI Cancer Conference, Liverpool, November 2014 *and was shortlisted for the BACR/Gordon Hamilton-Fairley Young Investigator award.*

6.2 Potential future applications of this research and next studies

6.2.1 EMT profiling

As described in the General Introduction (Section 1.8), EMT is an evolutionarily conserved developmental process during which cells of epithelial origin lose the apical-basal polarisation and cell-cell contacts in order to migrate as single cells through adjacent tissues. This is well described in embryology and wound healing and has more recently been ascribed to cancer cells in the process of metastasis.[123] This area of biology is of increased clinical significance in NSCLC as EMT has recently been proposed as a mechanism of acquired resistance to targeted therapy in NSCLC.[268] Moreover, inhibition of EMT for example using novel AXL inhibitors is currently the subject of early phase clinical trials in NSCLC

patients (NCT00697632, described in detail in Section 1.8). The development of the CTC profiling assay described in Chapter 3 now permits the identification and interrogation of epithelial, mesenchymal and mixed E/M CTCs in the circulation of lung cancer patients at multiple time points. The ultimate future application of this research would be to develop a CTC profiling assay which could be applied to clinical trials of EMT inhibitors to be used as either a predictive biomarker (e.g. patients who are EMT high being more likely to benefit from EMT inhibition) or as a proof of concept biomarker (e.g. showing that AXL inhibition results is the biological end point of decreasing the mesenchymal population of CTC). The next studies and future direction of research are suggested below in order to achieve this aim.

6.2.1.1 Recommended next studies

To test the hypothesis that EMT is associated with chemotherapy resistance in NSCLC the following clinical and pre-clinical studies are planned:

Clinical studies

- Serial ISET CTC samples will undergo CTC EMT profiling pre and post chemotherapy.
- Samples from patients showing chemotherapy sensitive disease which subsequently changes to become chemotherapy resistant will be analysed for the emergence of predominant mesenchymal CTC populations upon development of resistance.

Translational studies

- Further NSCLC patient blood samples will be collected and processed in order for additional NSCLC CDX models to be developed.
- Chemotherapy sensitive CDX models will be treated with chemotherapy in order to develop acquired chemotherapy resistance to develop paired sensitive and resistant CDX models.
- Gene expression profiling of paired sensitive and resistant CDX tumours will be compared for the development of an EMT gene expression signature consistent previously published EMT signatures.[106]

6.2.1.2 Recommended direction of future research

Reliable techniques for CTC gene expression profiling urgently need to be developed. This will permit a more comprehensive evaluation of the CTCs to determine the degree to which a genome wide set of cellular changes has occurred consistent with those described in EMT. Approaches other than ISET e.g. Parsortix[221] are being evaluated by our lab to enable CTC capture with minimal processing allow the subsequent evaluation of gene expression profiles. This technology will allow the following key hypotheses to be addressed:

1. CTCs with the expression profile cytokeratin^{+}/vimentin^{+} or cytokeratin^{-}/vimentin^{+} have genome wide changes compared with cytokeratin^{+}/vimentin^{-} (CTCs consistent with them having undergone a partial or complete EMT respectively).

2. There is overlap between gene expression profiles of CTCs with an EMT phenotype and vasculogenic mimicry and cancer stem cell gene expression profiles.

6.2.2 VE-cadherin profiling

As described in the General Introduction (Section 1.9), VM describes the ability of tumour cells to adopt endothelial cell behaviours and form *de novo* vascular networks[186] in response to environmental stimuli such as hypoxia.[189-193] The significance of this area of tumour biology is that VM may be a mechanism through which tumours develop resistance to chemotherapy and anti-angiogenic therapies.[188] Targeting VM is therefore a potential therapeutic approach (described in Section 4.4.3), for example though the use of vascular disrupting agents such as thalidomide and fosbretabulin. However, a better understanding of the biology of VM in SCLC is required to provide a robust scientific rationale to support the evaluation of these treatment approaches in SCLC. The development of the CTC profiling assay to identify CTCs co-expressing cytokeratins and VE-cadherin described in Chapter 4 now permits the identification of CTC sub-populations with a putative VM phenotype in the circulation of lung cancer patients at multiple time points. As with the CTC EMT profiling, the ultimate aim of this research would be for CTC VM profiling to be applied to clinical trials of VM targeting agents to be used as either a predictive biomarker (e.g. patients who are VM high being more likely to benefit from VM targeting intervention) or as a proof of concept biomarker (e.g. showing that fosbretabulin results is the biological end point of decreasing the VM population of CTCs). The recommended next

studies and future direction of research are outlined below in order to advance towards this aim.

6.2.2.1 Recommended next studies

Clinical studies

Although challenging to answer, a key question to be addressed is whether CTC VE-cadherin profiling provides a surrogate for VM within the tumour. Although recent development of endobronchial ultrasound guided fine needle aspiration has enabled more SCLC patients to undergo diagnostic tumour sampling, this approach only yields cytology and within this, the tissue architecture is not preserved preventing analysis for VM structures. Analysis of the SCLC patients in Chapter 4 identified that too few had adequate tissue remaining following diagnostic evaluation to perform analysis of VM networks. Additionally, a fair comparison of CTCs and primary tumour VM status will be hampered by the likely dynamic nature of VM within the tumour over time requiring tissue and blood samples to be collected at the same point in time. Although challenging, the following clinical study is recommended to test the hypothesis that cytokeratins^{+}/VE-cadherin^{+} CTCs are a surrogate for VM within the tumour.

- A cohort of treatment naive SCLC patients with disease which is readily accessible for surgical biopsy (e.g. cervical lymph node metastases) will be approached to undergo an additional surgical biopsy and have a paired CTC sample drawn immediately prior to the procedure.

- The tumour tissue will be analysed by IHC for the presence of VM and the CTCs profiled using the VM assay described in Chapter 4.

Translational studies

In order to understand the effects that targeting tumour VM may have in patients in different contexts, further pre-clinical studies should be considered to define the impact of VM on treatment delivery and patient response to treatment (described below). However, this may be limited by the likely impact of the micro-environment on VM within a tumour. If VM within a tumour is dynamic and alters as the tumour grows in size and outgrows its nascent blood supply, pre-clinical studies considering the tumour vascular are limited by the tumour size of *in vivo* studies having an upper limit of ~1000 mm^3. Clearly, almost no SCLC patients have tumours of this size at the point they are diagnosed and require treatment. As such, I recommend performing exploratory translational studies when agents which may have a role of targeting angiogenesis or VM are being studied within clinical trials. Specifically, to address the hypothesis that VM arises as an escape mechanism to anti-angiogenic therapies I propose the following:

- Tumour VM profiling and CTC VM profiling will be performed on patients receiving anti-angiogenic agents before and after treatment to evaluate for change in tumour VM and CTC VM populations.

This could be performed within early phase clinical trials where patients are undergoing additional pre- and post-treatment biopsies and blood sampling as part of the trial protocol.

Pre-clinical studies

Accepting the limitation described above, that pre-clinical studies may not recapitulate the clinical microenvironment, the following pre-clinical studies are suggested to further evaluate the biology of VM in SCLC.

To test the hypothesis that tumour VM correlates to tumour perfusion:

- Dynamic contrast enhanced MRI of H446 xenograft tumours followed by IHC analysis for vascular and VM structures will be performed to evaluate for the association between tumour perfusion and VM structures.
- SCLC xenografts will have VM modulated through knock-down of VE-cadherin in H446 xenograft, then tumour perfusion and VM structures compared in VM high and VM knock down tumours.

To test the hypothesis that tumour VM augments the delivery of chemotherapy to tumours:

- The measurement of cisplatin delivered to tumours (using inductively coupled plasma mass spectrometry) and its association with VM structures in VM high and VM low xenograft tumours will be repeated in an adequately powered study.

6.2.2.2 Recommended direction of future research

As with the direction of future research described for EMT CTC profiling above, the development of an approach to gene expression profiling of CTCs will significantly advance the understanding of the biology underlying sub-populations of CTCs classified based upon their co-expression of cytokeratins and VE-cadherin. This will allow the following hypotheses to be tested:

1. CTCs with the profile cytokeratins^{+}/VE-cadherin^{+} are a sub-population of CTCs with a 'VM signature' consistent with previously published gene expression profiles.[199]
2. There is overlap in gene expression signature of VM CTCs and EMT CTCs and tumour stem cell signatures.

6.3 Clinical development of immune checkpoint inhibitors in lung cancer

Since the completion of the research reported within this thesis in 2015, there have been paradigm changing advances in the management of NSCLC with immune checkpoint inhibition. Hanahan and Weinberg updated their seminal publication on the hallmarks of cancer in 2011[323] to include the avoidance of immune destruction as an emerging hallmark. The complexities of tumour-host immunological interactions are yet to be clearly defined, however, they may include the immune-suppressive effect of cancer cells through the secretion of suppressive factors such as TGFβ or the recruitment of regulatory T cells and myeloid derived suppressor cells which can decrease the tumour suppressing effect of lymphocytes[323].

Despite the limitations in our current understanding of the role of immune regulation in cancer, there have been significant clinical gains seen in NSCLC in two landmark clinical trials of immune checkpoint inhibition with nivolumab, which blocks the immune checkpoint programmed death 1 (PD1). In the first of these studies, 272 squamous NSCLC patients previously treated with platinum based chemotherapy were randomised to receive nivolumab or docetaxel. Nivolumab improved median survival from 6.0 to 9.2 months ($p<0.001$) and improved the one year survival rate from 24 to 42%.[324] This was followed by a second study in non-squamous NSCLC, 582 patients were randomised to receive nivolumab or placebo. Nivolumab increased median survival from 9.4 to 12.2 months ($P<0.001$) and 18 month survival rate from 23 to 39%.[325] From clinical experience in melanoma where immune checkpoint blockade has been investigated for a number of years, mature follow up data suggests that survival curves may plateau in patients responding to these agents consistent with long term disease control which is not seen with cytotoxic chemotherapy alone in NSCLC. As such, there is now a flurry of trials in lung cancer and across cancer types investigating how to optimally utilise these agents.

6.4 Potential application of liquid biopsies to clinical trials of immune checkpoint inhibitors

Although the clinical trials of immune checkpoint blockade have shown superiority over cytotoxic chemotherapy, the majority of patients do not have clinical benefit. The radiological response rate to nivolumab in the study by Brahmer *et al.* was 19%.[324] One strategy to improve the effectiveness of these treatments is to combine blockade of PD1 with other immune

checkpoints such as cytotoxic T lymphocyte associated protein 4 (CTLA4) or combined checkpoint blockade with cytotoxic chemotherapy or targeted therapy.[326] However, there is also an urgent need to develop better predictive biomarkers. Although there is no consensus on the optimal predictive biomarker for these agents, the current predictive biomarker within tumour which has received the greatest interest is the expression of the PD1-ligand (PDL1). CTCs may be used as a liquid biopsy in future studies of these agents, and their potential utility in this regard is demonstrated by studies reporting PDL1 expression on CTCs from breast cancer patients enriched by CellSearch.[327]

6.5 Recent developments in CTC enrichment platforms

Technologies for enrichment of CTCs from patients are reviewed in the General Introduction (Section 1.6.1 to 1.6.3) dividing technologies into marker dependant approaches, marker independent approaches and techniques which enrich viable CTCs. However, since the completion of this thesis, alternative CTC enrichment platforms continue to be developed. Methods with the greatest sensitivity for CTC detection will be marker independent and a notable recent improvement in marker free enrichment which has been developed and has potential advantages over ISET for subsequent CTC analysis is the Vortex microfluidic chip. This enriches CTCs based upon their large size using microfluidic vortices to trap larger cells.[328] This approach has the advantage over ISET in that the cells are not fixed during sample processing meaning they are viable for subsequent *in vitro* or *in vivo* studies. The cells are also spared the forces applied to the cells during the ISET filtration process which can result in damage to the CTCs

and could also change the gene expression profiles of CTCs prior to analysis, making the Vortex platform an attractive approach to capture of CTCs in future studies.

6.6 Recent developments in expression profiling of CTCs under clinical evaluation

In addition to the markers of EMT and VM included in this thesis and the analysis of CTC expression of known predictive biomarkers summarised in the General Introduction, and PDL1 expression by CTCs as described above, subsequent studies reporting alternative CTC profiling at the level of protein expression are continuing at break-neck pace demonstrating the widespread enthusiasm in both the scientific and the clinical community for CTCs as a liquid biopsy. These studies included: MRP1 expression by CTCs was shown to be associated with resistance to chemotherapy in patients with colorectal cancer;[329] PSMA expression on CTCs was identified as a potential predictive biomarker for PSMA directed therapy in patients with prostate cancer;[330] SOX10, TRF2, and CD10 expression by CTCs was evaluable in patients with metastatic melanoma, predominating in CTC clusters;[331] vimentin and Ki67 expression in prostate cancer CTCs was associated with shorter patient survival.[332] Of the studies of CTC profiling, the studies which will have the greatest clinical utility are those which are shown to predict response to therapy or have the potential to stratify the patient for molecularly targeted therapies as this maximises the potential of CTCs to impact on clinical decision making and therefore on improving patient outcomes.

6.7 Overall conclusion

In summary, the research reported in this thesis has contributed to the existing literature on tumour biology in lung cancer, describing how CTCs (analysing both CTCs and CTC derived explants) can be utilised alongside patient biopsy material to advance the understanding of the biology of vasculogenic mimicry and epithelial to mesenchymal transition in lung cancer. These advances have the potential to improve patient outcomes through their application to the development of novel therapeutic strategies to treat lung cancer, a disease in which patient outcomes have failed to improve for decades.

References

1 Parkin, D. M., Bray, F., Ferlay, J. & Pisani, P. Global cancer statistics, 2002. *CA Cancer J Clin* **55**, 74-108 (2005).

2 Youlden, D. R., Cramb, S. M. & Baade, P. D. The International Epidemiology of Lung Cancer: geographical distribution and secular trends. *J Thorac Oncol* **3**, 819-831 (2008).

3 Doll, R. & Hill, A. B. Smoking and carcinoma of the lung; preliminary report. *Br Med J* **2**, 739-748 (1950).

4 Wynder, E. L. & Graham, E. A. Tobacco smoking as a possible etiologic factor in bronchiogenic carcinoma; a study of 684 proved cases. *J Am Med Assoc* **143**, 329-336 (1950).

5 Sasco, A. J., Secretan, M. B. & Straif, K. Tobacco smoking and cancer: a brief review of recent epidemiological evidence. *Lung Cancer* **45 Suppl 2**, S3-9 (2004).

6 Amarasena, I. U., Walters, J. A., Wood-Baker, R. & Fong, K. Platinum versus non-platinum chemotherapy regimens for small cell lung cancer. *Cochrane Database Syst Rev*, CD006849 (2008).

7 Hanna, N. *et al.* Randomized phase III trial comparing irinotecan/cisplatin with etoposide/cisplatin in patients with previously untreated extensive-stage disease small-cell lung cancer. *J Clin Oncol* **24**, 2038-2043 (2006).

8 Niell, H. B. *et al.* Randomized phase III intergroup trial of etoposide and cisplatin with or without paclitaxel and granulocyte colony-stimulating factor in patients with extensive-stage small-cell lung cancer: Cancer and Leukemia Group B Trial 9732. *J Clin Oncol* **23**, 3752-3759 (2005).

9 Sundstrom, S. *et al.* Cisplatin and etoposide regimen is superior to cyclophosphamide, epirubicin, and vincristine regimen in small-cell lung cancer: results from a randomized phase III trial with 5 years' follow-up. *J Clin Oncol* **20**, 4665-4672 (2002).

10 Ardizzoni, A. *et al.* Topotecan, a new active drug in the second-line treatment of small-cell lung cancer: a phase II study in patients with refractory and sensitive disease. The European Organization for Research and Treatment of Cancer Early Clinical Studies Group and New Drug Development Office, and the Lung Cancer Cooperative Group. *J Clin Oncol* **15**, 2090-2096 (1997).

11 von Pawel, J. *et al.* Topotecan versus cyclophosphamide, doxorubicin, and vincristine for the treatment of recurrent small-cell lung cancer. *J Clin Oncol* **17**, 658-667 (1999).

12 O'Brien, M. E. *et al.* Phase III trial comparing supportive care alone with supportive care with oral topotecan in patients with relapsed small-cell lung cancer. *J Clin Oncol* **24**, 5441-5447 (2006).

13 Owonikoko, T. K. *et al.* A systematic analysis of efficacy of second-line chemotherapy in sensitive and refractory small-cell lung cancer. *J Thorac Oncol* **7**, 866-872 (2012).

14 Sederholm, C. *et al.* Phase III trial of gemcitabine plus carboplatin versus single-agent gemcitabine in the treatment of locally advanced or metastatic non-small-cell lung cancer: the Swedish Lung Cancer Study Group. *J Clin Oncol* **23**, 8380-8388 (2005).

15 D'Addario, G. *et al.* Platinum-based versus non-platinum-based chemotherapy in advanced non-small-cell lung cancer: a meta-analysis of the published literature. *J Clin Oncol* **23**, 2926-2936 (2005).

16 Shepherd, F. A. *et al.* Prospective randomized trial of docetaxel versus best supportive care in patients with non-small-cell lung cancer previously treated with platinum-based chemotherapy. *J Clin Oncol* **18**, 2095-2103 (2000).
17 Hanna, N. *et al.* Randomized phase III trial of pemetrexed versus docetaxel in patients with non-small-cell lung cancer previously treated with chemotherapy. *J Clin Oncol* **22**, 1589-1597 (2004).
18 Stewart, D. J. Mechanisms of resistance to cisplatin and carboplatin. *Crit Rev Oncol Hematol* **63**, 12-31 (2007).
19 Feuerhake, F., Sigg, W., Hofter, E. A., Dimpfl, T. & Welsch, U. Immunohistochemical analysis of Bcl-2 and Bax expression in relation to cell turnover and epithelial differentiation markers in the non-lactating human mammary gland epithelium. *Cell Tissue Res* **299**, 47-58 (2000).
20 Ben-Ezra, J. M., Kornstein, M. J., Grimes, M. M. & Krystal, G. Small cell carcinomas of the lung express the Bcl-2 protein. *Am J Pathol* **145**, 1036-1040 (1994).
21 Stefanaki, K. *et al.* Immunohistochemical detection of bcl2, p53, mdm2 and p21/waf1 proteins in small-cell lung carcinomas. *Anticancer Res* **18**, 1689-1695 (1998).
22 Park, D. *et al.* Novel small-molecule inhibitors of Bcl-XL to treat lung cancer. *Cancer Res* **73**, 5485-5496 (2013).
23 Gazzaniga, P. *et al.* Chemosensitivity profile assay of circulating cancer cells: prognostic and predictive value in epithelial tumors. *Int J Cancer* **126**, 2437-2447 (2010).
24 Postel-Vinay, S. *et al.* The potential of exploiting DNA-repair defects for optimizing lung cancer treatment. *Nat Rev Clin Oncol* **9**, 144-155 (2012).
25 Minchinton, A. I. & Tannock, I. F. Drug penetration in solid tumours. *Nat Rev Cancer* **6**, 583-592 (2006).
26 Tannock, I. F. The relation between cell proliferation and the vascular system in a transplanted mouse mammary tumour. *Br J Cancer* **22**, 258-273 (1968).
27 Raghunand, N., Gatenby, R. A. & Gillies, R. J. Microenvironmental and cellular consequences of altered blood flow in tumours. *Br J Radiol* **76 Spec No 1**, S11-22 (2003).
28 Tannock, I. F. & Rotin, D. Acid pH in tumors and its potential for therapeutic exploitation. *Cancer Res* **49**, 4373-4384 (1989).
29 Primeau, A. J., Rendon, A., Hedley, D., Lilge, L. & Tannock, I. F. The distribution of the anticancer drug Doxorubicin in relation to blood vessels in solid tumors. *Clin Cancer Res* **11**, 8782-8788 (2005).
30 Ma, J. & Waxman, D. J. Modulation of the antitumor activity of metronomic cyclophosphamide by the angiogenesis inhibitor axitinib. *Mol Cancer Ther* **7**, 79-89 (2008).
31 Lynch, T. J. *et al.* Activating mutations in the epidermal growth factor receptor underlying responsiveness of non-small-cell lung cancer to gefitinib. *N Engl J Med* **350**, 2129-2139 (2004).
32 Paez, J. G. *et al.* EGFR mutations in lung cancer: correlation with clinical response to gefitinib therapy. *Science* **304**, 1497-1500 (2004).
33 Kwak, E. L. *et al.* Anaplastic lymphoma kinase inhibition in non-small-cell lung cancer. *N Engl J Med* **363**, 1693-1703 (2010).
34 Mok, T. S. *et al.* Gefitinib or carboplatin-paclitaxel in pulmonary adenocarcinoma. *N Engl J Med* **361**, 947-957 (2009).
35 Maemondo, M. *et al.* Gefitinib or chemotherapy for non-small-cell lung cancer with mutated EGFR. *N Engl J Med* **362**, 2380-2388 (2010).

36 Zhou, C. *et al.* Erlotinib versus chemotherapy as first-line treatment for patients with advanced EGFR mutation-positive non-small-cell lung cancer (OPTIMAL, CTONG-0802): a multicentre, open-label, randomised, phase 3 study. *Lancet Oncol* **12**, 735-742 (2011).
37 Rosell, R. *et al.* Erlotinib versus standard chemotherapy as first-line treatment for European patients with advanced EGFR mutation-positive non-small-cell lung cancer (EURTAC): a multicentre, open-label, randomised phase 3 trial. *Lancet Oncol* **13**, 239-246 (2012).
38 Sequist, L. V. *et al.* Phase III study of afatinib or cisplatin plus pemetrexed in patients with metastatic lung adenocarcinoma with EGFR mutations. *J Clin Oncol* **31**, 3327-3334 (2013).
39 Sequist, L. V. *et al.* Implementing multiplexed genotyping of non-small-cell lung cancers into routine clinical practice. *Ann Oncol* **22**, 2616-2624 (2011).
40 Middleton, G. *et al.* The National Lung Matrix Trial: translating the biology of stratification in advanced non-small-cell lung cancer. *Ann Oncol* **26**, 2464-2469 (2015).
41 Cummings, J. *et al.* Validation of pharmacodynamic assays to evaluate the clinical efficacy of an antisense compound (AEG 35156) targeted to the X-linked inhibitor of apoptosis protein XIAP. *Br J Cancer* **92**, 532-538 (2005).
42 Booton, R., Blackhall, F. & Kerr, K. Individualised treatment in non-small cell lung cancer: precise tissue diagnosis for all? *Thorax* **66**, 273-275 (2011).
43 Ashworth, T. R. A case of cancer in which cells similar to those in the tumours were seen in the blood after death. *Aust Med J* **14**, 146-169 (1869).
44 Pantel, K., Brakenhoff, R. H. & Brandt, B. Detection, clinical relevance and specific biological properties of disseminating tumour cells. *Nat Rev Cancer* **8**, 329-340 (2008).
45 Pantel, K. *et al.* Frequency and prognostic significance of isolated tumour cells in bone marrow of patients with non-small-cell lung cancer without overt metastases. *Lancet* **347**, 649-653 (1996).
46 Nagrath, S. *et al.* Isolation of rare circulating tumour cells in cancer patients by microchip technology. *Nature* **450**, 1235-1239 (2007).
47 Stott, S. L. *et al.* Isolation of circulating tumor cells using a microvortex-generating herringbone-chip. *Proc Natl Acad Sci U S A* **107**, 18392-18397 (2010).
48 Galanzha, E. I. *et al.* In vivo magnetic enrichment and multiplex photoacoustic detection of circulating tumour cells. *Nat Nanotechnol* **4**, 855-860 (2009).
49 Vona, G. *et al.* Isolation by size of epithelial tumor cells : a new method for the immunomorphological and molecular characterization of circulatingtumor cells. *Am J Pathol* **156**, 57-63 (2000).
50 Talasaz, A. H. *et al.* Isolating highly enriched populations of circulating epithelial cells and other rare cells from blood using a magnetic sweeper device. *Proc Natl Acad Sci U S A* **106**, 3970-3975 (2009).
51 Lin, H. K. *et al.* Portable filter-based microdevice for detection and characterization of circulating tumor cells. *Clin Cancer Res* **16**, 5011-5018 (2010).
52 Wang, X. *et al.* Detection of circulating tumor cells in human peripheral blood using surface-enhanced Raman scattering nanoparticles. *Cancer Res* **71**, 1526-1532 (2011).
53 Desitter, I. *et al.* A new device for rapid isolation by size and characterization of rare circulating tumor cells. *Anticancer Res* **31**, 427-441 (2011).
54 Paterlini-Brechot, P. & Benali, N. L. Circulating tumor cells (CTC) detection: clinical impact and future directions. *Cancer Lett* **253**, 180-204 (2007).

55 Allard, W. J. *et al.* Tumor cells circulate in the peripheral blood of all major carcinomas but not in healthy subjects or patients with nonmalignant diseases. *Clin Cancer Res* **10**, 6897-6904 (2004).
56 Krebs, M. G. *et al.* Evaluation and prognostic significance of circulating tumor cells in patients with non-small-cell lung cancer. *J Clin Oncol* **29**, 1556-1563 (2011).
57 Hou, J. M. *et al.* Clinical significance and molecular characteristics of circulating tumor cells and circulating tumor microemboli in patients with small-cell lung cancer. *J Clin Oncol* **30**, 525-532 (2012).
58 Hofman, V. *et al.* Preoperative circulating tumor cell detection using the isolation by size of epithelial tumor cell method for patients with lung cancer is a new prognostic biomarker. *Clin Cancer Res* **17**, 827-835 (2011).
59 Krebs, M. G. *et al.* Analysis of circulating tumor cells in patients with non-small cell lung cancer using epithelial marker-dependent and -independent approaches. *J Thorac Oncol* **7**, 306-315 (2012).
60 Okumura, Y. *et al.* Circulating tumor cells in pulmonary venous blood of primary lung cancer patients. *Ann Thorac Surg* **87**, 1669-1675 (2009).
61 Wendel, M. *et al.* Fluid biopsy for circulating tumor cell identification in patients with early-and late-stage non-small cell lung cancer: a glimpse into lung cancer biology. *Phys Biol* **9**, 016005 (2012).
62 Peters, C. E., Woodside, S. M. & Eaves, A. C. Isolation of subsets of immune cells. *Methods Mol Biol* **302**, 95-116 (2005).
63 Peters, C. Microfluidic-based unbiased enrichment (negative selection) of circulating non-hematopoietic tumor cells directly from whole blood without centrifugation. *Cancer Res* **73**, 1451-1451 (2013).
64 Naume, B. *et al.* Detection of isolated tumor cells in peripheral blood and in BM: evaluation of a new enrichment method. *Cytotherapy* **6**, 244-252 (2004).
65 Baccelli, I. *et al.* Identification of a population of blood circulating tumor cells from breast cancer patients that initiates metastasis in a xenograft assay. *Nat Biotechnol* **31**, 539-544 (2013).
66 Hodgkinson, C. L. *et al.* Tumorigenicity and genetic profiling of circulating tumor cells in small-cell lung cancer. *Nat Med* **20**, 897-903 (2014).
67 Cristofanilli, M. *et al.* Circulating tumor cells, disease progression, and survival in metastatic breast cancer. *N Engl J Med* **351**, 781-791 (2004).
68 Hayes, D. F. *et al.* Circulating tumor cells at each follow-up time point during therapy of metastatic breast cancer patients predict progression-free and overall survival. *Clin Cancer Res* **12**, 4218-4224 (2006).
69 Sastre, J. *et al.* Circulating tumor cells in colorectal cancer: correlation with clinical and pathological variables. *Ann Oncol* **19**, 935-938 (2008).
70 Cohen, S. J. *et al.* Prognostic significance of circulating tumor cells in patients with metastatic colorectal cancer. *Ann Oncol* **20**, 1223-1229 (2009).
71 de Bono, J. S. *et al.* Circulating tumor cells predict survival benefit from treatment in metastatic castration-resistant prostate cancer. *Clin Cancer Res* **14**, 6302-6309 (2008).
72 Moreno, J. G. *et al.* Circulating tumor cells predict survival in patients with metastatic prostate cancer. *Urology* **65**, 713-718 (2005).
73 Krebs, M. G. *et al.* Evaluation and Prognostic Significance of Circulating Tumor Cells in Patients With Non-Small-Cell Lung Cancer. *J Clin Oncol* (2011).
74 Hirose, T. *et al.* Relationship of circulating tumor cells to the effectiveness of cytotoxic chemotherapy in patients with metastatic non-small-cell lung cancer. *Oncol Res* **20**, 131-137 (2012).

75 Isobe, K. *et al.* Clinical significance of circulating tumor cells and free DNA in non-small cell lung cancer. *Anticancer Res* **32**, 3339-3344 (2012).
76 Naito, T. *et al.* Prognostic Impact of Circulating Tumor Cells in Patients with Small Cell Lung Cancer. *J Thorac Oncol* **7**, 512-519 (2012).
77 Hiltermann, T. J. *et al.* Circulating tumor cells in small-cell lung cancer: a predictive and prognostic factor. *Ann Oncol* (2012).
78 Normanno, N. *et al.* Prognostic value of circulating tumor cells' reduction in patients with extensive small-cell lung cancer. *Lung Cancer* **85**, 314-319 (2014).
79 Wang, J., Wang, K., Xu, J., Huang, J. & Zhang, T. Prognostic significance of circulating tumor cells in non-small-cell lung cancer patients: a meta-analysis. *PLoS One* **8**, e78070 (2013).
80 Zhang, J., Wang, H. T. & Li, B. G. Prognostic significance of circulating tumor cells in small--cell lung cancer patients: a meta-analysis. *Asian Pac J Cancer Prev* **15**, 8429-8433 (2014).
81 Punnoose, E. A. *et al.* Evaluation of Circulating Tumor Cells and Circulating Tumor DNA in Non-Small Cell Lung Cancer: Association with Clinical Endpoints in a Phase II Clinical Trial of Pertuzumab and Erlotinib. *Clin Cancer Res* **18**, 2391-2401 (2012).
82 Hou, J. M. *et al.* Evaluation of circulating tumor cells and serological cell death biomarkers in small cell lung cancer patients undergoing chemotherapy. *Am J Pathol* **175**, 808-816 (2009).
83 Hiltermann, T. J. *et al.* Circulating tumor cells in small-cell lung cancer: a predictive and prognostic factor. *Ann Oncol* **23**, 2937-2942 (2012).
84 Smerage, J. B. *et al.* Circulating tumor cells and response to chemotherapy in metastatic breast cancer: SWOG S0500. *J Clin Oncol* **32**, 3483-3489 (2014).
85 Ilie, M. *et al.* ALK-gene rearrangement: a comparative analysis on circulating tumour cells and tumour tissue from patients with lung adenocarcinoma. *Ann Oncol* **23**, 2907-2913 (2012).
86 Maheswaran, S. *et al.* Detection of mutations in EGFR in circulating lung-cancer cells. *N Engl J Med* **359**, 366-377 (2008).
87 Punnoose, E. A. *et al.* Molecular biomarker analyses using circulating tumor cells. *PLoS One* **5**, e12517 (2010).
88 Klein, C. A. *et al.* Combined transcriptome and genome analysis of single micrometastatic cells. *Nat Biotechnol* **20**, 387-392 (2002).
89 Ulmer, A. *et al.* Immunomagnetic enrichment, genomic characterization, and prognostic impact of circulating melanoma cells. *Clin Cancer Res* **10**, 531-537 (2004).
90 Fabbri, F. *et al.* Detection and recovery of circulating colon cancer cells using a dielectrophoresis-based device: KRAS mutation status in pure CTCs. *Cancer Lett* (2013).
91 Gasch, C. *et al.* Heterogeneity of Epidermal Growth Factor Receptor Status and Mutations of KRAS/PIK3CA in Circulating Tumor Cells of Patients with Colorectal Cancer. *Clin Chem* **59**, 252-260 (2013).
92 Welty, C. J. *et al.* Single cell transcriptomic analysis of prostate cancer cells. *BMC Mol Biol* **14**, 6 (2013).
93 Cann, G. M. *et al.* mRNA-Seq of single prostate cancer circulating tumor cells reveals recapitulation of gene expression and pathways found in prostate cancer. *PLoS One* **7**, e49144 (2012).
94 Powell, A. A. *et al.* Single cell profiling of circulating tumor cells: transcriptional heterogeneity and diversity from breast cancer cell lines. *PLoS One* **7**, e33788 (2012).

95 Ramskold, D. *et al.* Full-length mRNA-Seq from single-cell levels of RNA and individual circulating tumor cells. *Nat Biotechnol* **30**, 777-782 (2012).
96 Deng, G. *et al.* Single cell mutational analysis of PIK3CA in circulating tumor cells and metastases in breast cancer reveals heterogeneity, discordance, and mutation persistence in cultured disseminated tumor cells from bone marrow. *BMC Cancer* **14**, 456 (2014).
97 Jamal-Hanjani, M. *et al.* Tracking genomic cancer evolution for precision medicine: the lung TRACERx study. *PLoS Biol* **12**, e1001906 (2014).
98 Edelman, G. M., Gallin, W. J., Delouvee, A., Cunningham, B. A. & Thiery, J. P. Early epochal maps of two different cell adhesion molecules. *Proc Natl Acad Sci U S A* **80**, 4384-4388 (1983).
99 Kim, K. K. *et al.* Alveolar epithelial cell mesenchymal transition develops in vivo during pulmonary fibrosis and is regulated by the extracellular matrix. *Proc Natl Acad Sci U S A* **103**, 13180-13185 (2006).
100 Thiery, J. P. Epithelial-mesenchymal transitions in tumour progression. *Nat Rev Cancer* **2**, 442-454 (2002).
101 Travis, W. D., World Health Organization., International Agency for Research on Cancer., International Association for the Study of Lung Cancer. & International Academy of Pathology. *Pathology and genetics of tumours of the lung, pleura, thymus and heart*. (IARC Press Oxford University Press (distributor), 2004).
102 Lecharpentier, A. *et al.* Detection of circulating tumour cells with a hybrid (epithelial/mesenchymal) phenotype in patients with metastatic non-small cell lung cancer. *Br J Cancer* (2011).
103 Balasubramanian, P. *et al.* Multiparameter analysis, including EMT markers, on negatively enriched blood samples from patients with squamous cell carcinoma of the head and neck. *PLoS One* **7**, e42048 (2012).
104 Armstrong, A. J. *et al.* Circulating tumor cells from patients with advanced prostate and breast cancer display both epithelial and mesenchymal markers. *Mol Cancer Res* **9**, 997-1007 (2011).
105 Kallergi, G. *et al.* Epithelial to mesenchymal transition markers expressed in circulating tumour cells of early and metastatic breast cancer patients. *Breast Cancer Res* **13**, R59 (2011).
106 Tan, T. Z. *et al.* Epithelial-mesenchymal transition spectrum quantification and its efficacy in deciphering survival and drug responses of cancer patients. *EMBO Mol Med* **6**, 1279-1293 (2014).
107 Kalluri, R. & Weinberg, R. A. The basics of epithelial-mesenchymal transition. *J Clin Invest* **119**, 1420-1428 (2009).
108 Bellovin, D. I. *et al.* Reciprocal regulation of RhoA and RhoC characterizes the EMT and identifies RhoC as a prognostic marker of colon carcinoma. *Oncogene* **25**, 6959-6967 (2006).
109 Gjerdrum, C. *et al.* Axl is an essential epithelial-to-mesenchymal transition-induced regulator of breast cancer metastasis and patient survival. *Proc Natl Acad Sci U S A* **107**, 1124-1129 (2010).
110 Otsuki, S. *et al.* Vimentin expression is associated with decreased survival in gastric cancer. *Oncol Rep* **25**, 1235-1242 (2011).
111 Lee, K. W. *et al.* Twist1 is an independent prognostic factor of esophageal squamous cell carcinoma and associated with its epithelial-mesenchymal transition. *Ann Surg Oncol* **19**, 326-335 (2012).

112 Soltermann, A. *et al.* Prognostic significance of epithelial-mesenchymal and mesenchymal-epithelial transition protein expression in non-small cell lung cancer. *Clin Cancer Res* **14**, 7430-7437 (2008).
113 Feng, J. *et al.* FoxQ1 overexpression influences poor prognosis in non-small cell lung cancer, associates with the phenomenon of EMT. *PLoS One* **7**, e39937 (2012).
114 Zhang, J. *et al.* MMP-7 is upregulated by COX-2 and promotes proliferation and invasion of lung adenocarcinoma cells. *Eur J Histochem* **58**, 2262 (2014).
115 Kim, S. H. *et al.* Correlation of epithelial-mesenchymal transition markers with clinicopathologic parameters in adenocarcinomas and squamous cell carcinoma of the lung. *Histol Histopathol* **27**, 581-591 (2012).
116 Subramanian, A. *et al.* Gene set enrichment analysis: a knowledge-based approach for interpreting genome-wide expression profiles. *Proc Natl Acad Sci U S A* **102**, 15545-15550 (2005).
117 Byers, L. A. *et al.* An epithelial-mesenchymal transition gene signature predicts resistance to EGFR and PI3K inhibitors and identifies Axl as a therapeutic target for overcoming EGFR inhibitor resistance. *Clin Cancer Res* **19**, 279-290 (2013).
118 Taube, J. H. *et al.* Core epithelial-to-mesenchymal transition interactome gene-expression signature is associated with claudin-low and metaplastic breast cancer subtypes. *Proc Natl Acad Sci U S A* **107**, 15449-15454 (2010).
119 Blick, T. *et al.* Epithelial mesenchymal transition traits in human breast cancer cell lines parallel the CD44(hi/)CD24 (lo/-) stem cell phenotype in human breast cancer. *J Mammary Gland Biol Neoplasia* **15**, 235-252 (2010).
120 Loboda, A. *et al.* EMT is the dominant program in human colon cancer. *BMC Med Genomics* **4**, 9 (2011).
121 Lee, J. M., Dedhar, S., Kalluri, R. & Thompson, E. W. The epithelial-mesenchymal transition: new insights in signaling, development, and disease. *J Cell Biol* **172**, 973-981 (2006).
122 Carretero, J. *et al.* Integrative genomic and proteomic analyses identify targets for Lkb1-deficient metastatic lung tumors. *Cancer Cell* **17**, 547-559 (2010).
123 Thiery, J. P., Acloque, H., Huang, R. Y. & Nieto, M. A. Epithelial-mesenchymal transitions in development and disease. *Cell* **139**, 871-890 (2009).
124 Cieply, B. *et al.* Suppression of the epithelial-mesenchymal transition by Grainyhead-like-2. *Cancer Res* **72**, 2440-2453 (2012).
125 Huang, R. Y., Chung, V. Y. & Thiery, J. P. Targeting pathways contributing to epithelial-mesenchymal transition (EMT) in epithelial ovarian cancer. *Curr Drug Targets* **13**, 1649-1653 (2012).
126 Zhang, J. *et al.* Overexpression of Rab25 contributes to metastasis of bladder cancer through induction of epithelial-mesenchymal transition and activation of Akt/GSK-3beta/Snail signaling. *Carcinogenesis* **34**, 2401-2408 (2013).
127 Moll, R., Franke, W. W., Schiller, D. L., Geiger, B. & Krepler, R. The catalog of human cytokeratins: patterns of expression in normal epithelia, tumors and cultured cells. *Cell* **31**, 11-24 (1982).
128 Steinert, P. M., Steven, A. C. & Roop, D. R. The molecular biology of intermediate filaments. *Cell* **42**, 411-420 (1985).
129 Yamashita, N. *et al.* Vimentin as a poor prognostic factor for triple-negative breast cancer. *J Cancer Res Clin Oncol* **139**, 739-746 (2013).
130 Liu, T. *et al.* Dysregulated expression of Slug, vimentin, and E-cadherin correlates with poor clinical outcome in patients with basal-like breast cancer. *J Surg Oncol* **107**, 188-194 (2013).

131 Dauphin, M. *et al.* Vimentin expression predicts the occurrence of metastases in non small cell lung carcinomas. *Lung Cancer* **81**, 117-122 (2013).
132 Singh, S. *et al.* Overexpression of vimentin: role in the invasive phenotype in an androgen-independent model of prostate cancer. *Cancer Res* **63**, 2306-2311 (2003).
133 Rodriguez, M. I. *et al.* PARP-1 regulates metastatic melanoma through modulation of vimentin-induced malignant transformation. *PLoS Genet* **9**, e1003531 (2013).
134 Hendrix, M. J. *et al.* Coexpression of vimentin and keratins by human melanoma tumor cells: correlation with invasive and metastatic potential. *J Natl Cancer Inst* **84**, 165-174 (1992).
135 Hendrix, M. J., Seftor, E. A., Seftor, R. E. & Trevor, K. T. Experimental co-expression of vimentin and keratin intermediate filaments in human breast cancer cells results in phenotypic interconversion and increased invasive behavior. *Am J Pathol* **150**, 483-495 (1997).
136 Havel, L. S., Kline, E. R., Salgueiro, A. M. & Marcus, A. I. Vimentin regulates lung cancer cell adhesion through a VAV2-Rac1 pathway to control focal adhesion kinase activity. *Oncogene* **34**, 1979-1990 (2015).
137 Abe, K. *et al.* Vav2 is an activator of Cdc42, Rac1, and RhoA. *J Biol Chem* **275**, 10141-10149 (2000).
138 Dahl, D., Rueger, D. C., Bignami, A., Weber, K. & Osborn, M. Vimentin, the 57 000 molecular weight protein of fibroblast filaments, is the major cytoskeletal component in immature glia. *Eur J Cell Biol* **24**, 191-196 (1981).
139 Tarin, D., Thompson, E. W. & Newgreen, D. F. The fallacy of epithelial mesenchymal transition in neoplasia. *Cancer Res* **65**, 5996-6000; discussion 6000-5991 (2005).
140 Thompson, E. W., Newgreen, D. F. & Tarin, D. Carcinoma invasion and metastasis: a role for epithelial-mesenchymal transition? *Cancer Res* **65**, 5991-5995; discussion 5995 (2005).
141 Yang, J. *et al.* Twist, a master regulator of morphogenesis, plays an essential role in tumor metastasis. *Cell* **117**, 927-939 (2004).
142 Brabletz, T. *et al.* Variable beta-catenin expression in colorectal cancers indicates tumor progression driven by the tumor environment. *Proc Natl Acad Sci U S A* **98**, 10356-10361 (2001).
143 Stark, K., Vainio, S., Vassileva, G. & McMahon, A. P. Epithelial transformation of metanephric mesenchyme in the developing kidney regulated by Wnt-4. *Nature* **372**, 679-683 (1994).
144 Tsuji, T. *et al.* Epithelial-mesenchymal transition induced by growth suppressor p12CDK2-AP1 promotes tumor cell local invasion but suppresses distant colony growth. *Cancer Res* **68**, 10377-10386 (2008).
145 Tsuji, T., Ibaragi, S. & Hu, G. F. Epithelial-mesenchymal transition and cell cooperativity in metastasis. *Cancer Res* **69**, 7135-7139 (2009).
146 Calbo, J. *et al.* A functional role for tumor cell heterogeneity in a mouse model of small cell lung cancer. *Cancer Cell* **19**, 244-256 (2011).
147 Valent, P. *et al.* Cancer stem cell definitions and terminology: the devil is in the details. *Nat Rev Cancer* **12**, 767-775 (2012).
148 Clarke, M. F. *et al.* Cancer stem cells--perspectives on current status and future directions: AACR Workshop on cancer stem cells. *Cancer Res* **66**, 9339-9344 (2006).
149 Gupta, P. B. *et al.* Identification of selective inhibitors of cancer stem cells by high-throughput screening. *Cell* **138**, 645-659 (2009).
150 Shackleton, M., Quintana, E., Fearon, E. R. & Morrison, S. J. Heterogeneity in cancer: cancer stem cells versus clonal evolution. *Cell* **138**, 822-829 (2009).

151 Prochazka, M., Gaskins, H. R., Shultz, L. D. & Leiter, E. H. The nonobese diabetic scid mouse: model for spontaneous thymomagenesis associated with immunodeficiency. *Proc Natl Acad Sci U S A* **89**, 3290-3294 (1992).
152 Al-Hajj, M., Wicha, M. S., Benito-Hernandez, A., Morrison, S. J. & Clarke, M. F. Prospective identification of tumorigenic breast cancer cells. *Proc Natl Acad Sci U S A* **100**, 3983-3988 (2003).
153 Singh, S. K. *et al.* Identification of a cancer stem cell in human brain tumors. *Cancer Res* **63**, 5821-5828 (2003).
154 O'Brien, C. A., Pollett, A., Gallinger, S. & Dick, J. E. A human colon cancer cell capable of initiating tumour growth in immunodeficient mice. *Nature* **445**, 106-110 (2007).
155 Fang, D. *et al.* A tumorigenic subpopulation with stem cell properties in melanomas. *Cancer Res* **65**, 9328-9337 (2005).
156 Schatton, T. *et al.* Identification of cells initiating human melanomas. *Nature* **451**, 345-349 (2008).
157 Bapat, S. A., Mali, A. M., Koppikar, C. B. & Kurrey, N. K. Stem and progenitor-like cells contribute to the aggressive behavior of human epithelial ovarian cancer. *Cancer Res* **65**, 3025-3029 (2005).
158 Alvero, A. B. *et al.* Molecular phenotyping of human ovarian cancer stem cells unravels the mechanisms for repair and chemoresistance. *Cell Cycle* **8**, 158-166 (2009).
159 Collins, A. T., Berry, P. A., Hyde, C., Stower, M. J. & Maitland, N. J. Prospective identification of tumorigenic prostate cancer stem cells. *Cancer Res* **65**, 10946-10951 (2005).
160 Hermann, P. C. *et al.* Distinct populations of cancer stem cells determine tumor growth and metastatic activity in human pancreatic cancer. *Cell Stem Cell* **1**, 313-323 (2007).
161 Reya, T., Morrison, S. J., Clarke, M. F. & Weissman, I. L. Stem cells, cancer, and cancer stem cells. *Nature* **414**, 105-111 (2001).
162 Yahata, T. *et al.* Functional human T lymphocyte development from cord blood CD34+ cells in nonobese diabetic/Shi-scid, IL-2 receptor gamma null mice. *J Immunol* **169**, 204-209 (2002).
163 Kanaji, N. *et al.* Higher susceptibility of NOD/LtSz-scid Il2rg (-/-) NSG mice to xenotransplanted lung cancer cell lines. *Cancer Manag Res* **6**, 431-436 (2014).
164 Notta, F., Doulatov, S. & Dick, J. E. Engraftment of human hematopoietic stem cells is more efficient in female NOD/SCID/IL-2Rgc-null recipients. *Blood* **115**, 3704-3707 (2010).
165 Quintana, E. *et al.* Efficient tumour formation by single human melanoma cells. *Nature* **456**, 593-598 (2008).
166 Dalerba, P. *et al.* Phenotypic characterization of human colorectal cancer stem cells. *Proc Natl Acad Sci U S A* **104**, 10158-10163 (2007).
167 Li, C. *et al.* Identification of pancreatic cancer stem cells. *Cancer Res* **67**, 1030-1037 (2007).
168 Ricci-Vitiani, L. *et al.* Identification and expansion of human colon-cancer-initiating cells. *Nature* **445**, 111-115 (2007).
169 Kelly, P. N., Dakic, A., Adams, J. M., Nutt, S. L. & Strasser, A. Tumor growth need not be driven by rare cancer stem cells. *Science* **317**, 337 (2007).
170 Ishizawa, K. *et al.* Tumor-initiating cells are rare in many human tumors. *Cell Stem Cell* **7**, 279-282 (2010).

171 Kreso, A. & Dick, J. E. Evolution of the cancer stem cell model. *Cell Stem Cell* **14**, 275-291 (2014).
172 Gerlinger, M. *et al.* Intratumor heterogeneity and branched evolution revealed by multiregion sequencing. *N Engl J Med* **366**, 883-892 (2012).
173 Nowell, P. C. The clonal evolution of tumor cell populations. *Science* **194**, 23-28 (1976).
174 Hanahan, D. & Weinberg, R. A. The hallmarks of cancer. *Cell* **100**, 57-70 (2000).
175 Mani, S. A. *et al.* The epithelial-mesenchymal transition generates cells with properties of stem cells. *Cell* **133**, 704-715 (2008).
176 Zavadil, J. & Bottinger, E. P. TGF-beta and epithelial-to-mesenchymal transitions. *Oncogene* **24**, 5764-5774 (2005).
177 Battula, V. L. *et al.* Epithelial-mesenchymal transition-derived cells exhibit multilineage differentiation potential similar to mesenchymal stem cells. *Stem Cells* **28**, 1435-1445 (2010).
178 Dontu, G. *et al.* In vitro propagation and transcriptional profiling of human mammary stem/progenitor cells. *Genes Dev* **17**, 1253-1270 (2003).
179 Kurrey, N. K. *et al.* Snail and slug mediate radioresistance and chemoresistance by antagonizing p53-mediated apoptosis and acquiring a stem-like phenotype in ovarian cancer cells. *Stem Cells* **27**, 2059-2068 (2009).
180 Bertolini, G. *et al.* Highly tumorigenic lung cancer CD133+ cells display stem-like features and are spared by cisplatin treatment. *Proc Natl Acad Sci U S A* **106**, 16281-16286 (2009).
181 Rothwell, D. G. *et al.* Evaluation and validation of a robust single cell RNA-amplification protocol through transcriptional profiling of enriched lung cancer initiating cells. *BMC Genomics* **15**, 1129 (2014).
182 Carmeliet, P. Mechanisms of angiogenesis and arteriogenesis. *Nat Med* **6**, 389-395 (2000).
183 Patan, S. Vasculogenesis and angiogenesis. *Cancer Treat Res* **117**, 3-32 (2004).
184 Folberg, R., Hendrix, M. J. & Maniotis, A. J. Vasculogenic mimicry and tumor angiogenesis. *Am J Pathol* **156**, 361-381 (2000).
185 Kirschmann, D. A., Seftor, E. A., Hardy, K. M., Seftor, R. E. & Hendrix, M. J. Molecular pathways: vasculogenic mimicry in tumor cells: diagnostic and therapeutic implications. *Clin Cancer Res* **18**, 2726-2732 (2012).
186 Maniotis, A. J. *et al.* Vascular channel formation by human melanoma cells in vivo and in vitro: vasculogenic mimicry. *Am J Pathol* **155**, 739-752 (1999).
187 Ruf, W. *et al.* Differential role of tissue factor pathway inhibitors 1 and 2 in melanoma vasculogenic mimicry. *Cancer Res* **63**, 5381-5389 (2003).
188 Carmeliet, P. & Jain, R. K. Molecular mechanisms and clinical applications of angiogenesis. *Nature* **473**, 298-307 (2011).
189 Hendrix, M. J. *et al.* Transendothelial function of human metastatic melanoma cells: role of the microenvironment in cell-fate determination. *Cancer Res* **62**, 665-668 (2002).
190 Chiao, M. T., Yang, Y. C., Cheng, W. Y., Shen, C. C. & Ko, J. L. CD133+ glioblastoma stem-like cells induce vascular mimicry in vivo. *Curr Neurovasc Res* **8**, 210-219 (2011).
191 Scully, S. *et al.* Transdifferentiation of glioblastoma stem-like cells into mural cells drives vasculogenic mimicry in glioblastomas. *J Neurosci* **32**, 12950-12960 (2012).
192 Soda, Y. *et al.* Transdifferentiation of glioblastoma cells into vascular endothelial cells. *Proc Natl Acad Sci U S A* **108**, 4274-4280 (2011).

193 Misra, R. M., Bajaj, M. S. & Kale, V. P. Vasculogenic mimicry of HT1080 tumour cells in vivo: critical role of HIF-1alpha-neuropilin-1 axis. *PLoS One* **7**, e50153 (2012).
194 Bertolini, F., Shaked, Y., Mancuso, P. & Kerbel, R. S. The multifaceted circulating endothelial cell in cancer: towards marker and target identification. *Nat Rev Cancer* **6**, 835-845 (2006).
195 Chang, Y. S. *et al.* Mosaic blood vessels in tumors: frequency of cancer cells in contact with flowing blood. *Proc Natl Acad Sci U S A* **97**, 14608-14613 (2000).
196 di Tomaso, E. *et al.* Mosaic tumor vessels: cellular basis and ultrastructure of focal regions lacking endothelial cell markers. *Cancer Res* **65**, 5740-5749 (2005).
197 Cao, Z. *et al.* Tumour vasculogenic mimicry is associated with poor prognosis of human cancer patients: a systemic review and meta-analysis. *Eur J Cancer* **49**, 3914-3923 (2013).
198 Lezcano, C. *et al.* Merkel cell carcinoma expresses vasculogenic mimicry: demonstration in patients and experimental manipulation in xenografts. *Lab Invest* (2014).
199 Bittner, M. *et al.* Molecular classification of cutaneous malignant melanoma by gene expression profiling. *Nature* **406**, 536-540 (2000).
200 Navarro, P., Ruco, L. & Dejana, E. Differential localization of VE- and N-cadherins in human endothelial cells: VE-cadherin competes with N-cadherin for junctional localization. *J Cell Biol* **140**, 1475-1484 (1998).
201 Giannotta, M., Trani, M. & Dejana, E. VE-cadherin and endothelial adherens junctions: active guardians of vascular integrity. *Dev Cell* **26**, 441-454 (2013).
202 Hendrix, M. J. *et al.* Expression and functional significance of VE-cadherin in aggressive human melanoma cells: role in vasculogenic mimicry. *Proc Natl Acad Sci U S A* **98**, 8018-8023 (2001).
203 Seftor, R. E. *et al.* Cooperative interactions of laminin 5 gamma2 chain, matrix metalloproteinase-2, and membrane type-1-matrix/metalloproteinase are required for mimicry of embryonic vasculogenesis by aggressive melanoma. *Cancer Res* **61**, 6322-6327 (2001).
204 Vartanian, A. *et al.* VEGFR1 and PKCalpha signaling control melanoma vasculogenic mimicry in a VEGFR2 kinase-independent manner. *Melanoma Res* **21**, 91-98 (2011).
205 Hardy, K. M. *et al.* Regulation of the embryonic morphogen Nodal by Notch4 facilitates manifestation of the aggressive melanoma phenotype. *Cancer Res* **70**, 10340-10350 (2010).
206 Topczewska, J. M. *et al.* Embryonic and tumorigenic pathways converge via Nodal signaling: role in melanoma aggressiveness. *Nat Med* **12**, 925-932 (2006).
207 Comito, G. *et al.* HIF-1alpha stabilization by mitochondrial ROS promotes Met-dependent invasive growth and vasculogenic mimicry in melanoma cells. *Free Radic Biol Med* **51**, 893-904 (2011).
208 Seftor, R. E. *et al.* Tumor cell vasculogenic mimicry: from controversy to therapeutic promise. *Am J Pathol* **181**, 1115-1125 (2012).
209 Hess, A. R. *et al.* Molecular regulation of tumor cell vasculogenic mimicry by tyrosine phosphorylation: role of epithelial cell kinase (Eck/EphA2). *Cancer Res* **61**, 3250-3255 (2001).
210 Hess, A. R. *et al.* VE-cadherin regulates EphA2 in aggressive melanoma cells through a novel signaling pathway: implications for vasculogenic mimicry. *Cancer Biol Ther* **5**, 228-233 (2006).
211 Hess, A. R. & Hendrix, M. J. Focal adhesion kinase signaling and the aggressive melanoma phenotype. *Cell Cycle* **5**, 478-480 (2006).

212 Hess, A. R., Seftor, E. A., Seftor, R. E. & Hendrix, M. J. Phosphoinositide 3-kinase regulates membrane Type 1-matrix metalloproteinase (MMP) and MMP-2 activity during melanoma cell vasculogenic mimicry. *Cancer Res* **63**, 4757-4762 (2003).
213 Tang, N. N. *et al.* HIF-1alpha induces VE-cadherin expression and modulates vasculogenic mimicry in esophageal carcinoma cells. *World J Gastroenterol* **20**, 17894-17904 (2014).
214 Mao, X. G. *et al.* CDH5 is specifically activated in glioblastoma stemlike cells and contributes to vasculogenic mimicry induced by hypoxia. *Neuro Oncol* **15**, 865-879 (2013).
215 Zhang, L. Z. *et al.* The role of VE-cadherin in osteosarcoma cells. *Pathol Oncol Res* **16**, 111-117 (2010).
216 Ricci-Vitiani, L. *et al.* Tumour vascularization via endothelial differentiation of glioblastoma stem-like cells. *Nature* **468**, 824-828 (2010).
217 Wang, R. *et al.* Glioblastoma stem-like cells give rise to tumour endothelium. *Nature* **468**, 829-833 (2010).
218 Vaupel, P. & Mayer, A. Hypoxia in cancer: significance and impact on clinical outcome. *Cancer Metastasis Rev* **26**, 225-239 (2007).
219 Cohen, S. J. *et al.* Relationship of circulating tumor cells to tumor response, progression-free survival, and overall survival in patients with metastatic colorectal cancer. *J Clin Oncol* **26**, 3213-3221 (2008).
220 Moreno, J. G. *et al.* Changes in circulating carcinoma cells in patients with metastatic prostate cancer correlate with disease status. *Urology* **58**, 386-392 (2001).
221 Chudziak, J. *et al.* Clinical evaluation of a novel microfluidic device for epitope-independent enrichment of circulating tumour cells in patients with small cell lung cancer. *Analyst* **141**, 669-678 (2016).
222 Hou, J. M. *et al.* Circulating tumor cells as a window on metastasis biology in lung cancer. *Am J Pathol* **178**, 989-996 (2011).
223 Yu, M. *et al.* Circulating Breast Tumor Cells Exhibit Dynamic Changes in Epithelial and Mesenchymal Composition. *Science* **339**, 580-584 (2013).
224 Muinelo-Romay, L. *et al.* Evaluation of Circulating Tumor Cells and Related Events as Prognostic Factors and Surrogate Biomarkers in Advanced NSCLC Patients Receiving First-Line Systemic Treatment. *Cancers (Basel)* **6**, 153-165 (2014).
225 Giometti, C. S., Willard, K. E. & Anderson, N. L. Cytoskeletal proteins from human skin fibroblasts, peripheral blood leukocytes, and a lymphoblastoid cell line compared by two-dimensional gel electrophoresis. *Clin Chem* **28**, 955-961 (1982).
226 Rowand, J. L. *et al.* Endothelial cells in peripheral blood of healthy subjects and patients with metastatic carcinomas. *Cytometry A* **71**, 105-113 (2007).
227 Ilie, M. *et al.* Clinical value of circulating endothelial cells and of soluble CD146 levels in patients undergoing surgery for non-small cell lung cancer. *Br J Cancer* **110**, 1236-1243 (2014).
228 Mancuso, P. *et al.* Resting and activated endothelial cells are increased in the peripheral blood of cancer patients. *Blood* **97**, 3658-3661 (2001).
229 Bidard, F. C. *et al.* Clinical value of circulating endothelial cells and circulating tumor cells in metastatic breast cancer patients treated first line with bevacizumab and chemotherapy. *Ann Oncol* **21**, 1765-1771 (2010).
230 Strijbos, M. H. *et al.* Circulating endothelial cells, circulating tumour cells, tissue factor, endothelin-1 and overall survival in prostate cancer patients treated with docetaxel. *Eur J Cancer* **46**, 2027-2035 (2010).

231 Ali, A. M. *et al.* Determining circulating endothelial cells using CellSearch system during preoperative systemic chemotherapy in breast cancer patients. *Eur J Cancer* **47**, 2265-2272 (2011).
232 Kuo, Y. H. *et al.* Dynamics of circulating endothelial cells and endothelial progenitor cells in breast cancer patients receiving cytotoxic chemotherapy. *BMC Cancer* **12**, 620 (2012).
233 Manzoni, M. *et al.* Circulating endothelial cells and their apoptotic fraction are mutually independent predictive biomarkers in Bevacizumab-based treatment for advanced colorectal cancer. *J Cancer Res Clin Oncol* **138**, 1187-1196 (2012).
234 Malka, D. *et al.* Clinical value of circulating endothelial cell levels in metastatic colorectal cancer patients treated with first-line chemotherapy and bevacizumab. *Ann Oncol* **23**, 919-927 (2012).
235 Chu, T. Q. *et al.* Can determination of circulating endothelial cells and serum caspase-cleaved CK18 predict for response and survival in patients with advanced non-small-cell lung cancer receiving endostatin and paclitaxel-carboplatin chemotherapy? a retrospective study. *J Thorac Oncol* **7**, 1781-1789 (2012).
236 Liu, Z. J. *et al.* Predictive value of circulating endothelial cells for efficacy of chemotherapy with Rh-endostatin in non-small cell lung cancer. *J Cancer Res Clin Oncol* **138**, 927-937 (2012).
237 Najjar, F., Alammar, M., Bachour, M. & Al-Massarani, G. Circulating endothelial cells as a biomarker in non-small cell lung cancer patients: correlation with clinical outcome. *Int J Biol Markers* **29**, e337-344 (2014).
238 Yuan, D. M. *et al.* Predictive and prognostic significance of circulating endothelial cells in advanced non-small cell lung cancer patients. *Tumour Biol* **36**, 9031-9037 (2015).
239 Sanchez Hernandez, A. *et al.* Quantification of circulating endothelial cells as a predictor of response to chemotherapy with platinum and pemetrexed in patients with advanced non-squamous non-small cell lung carcinoma. *Clin Transl Oncol* **17**, 281-288 (2015).
240 Liu, Y., Yuan, D., Ye, W., Lv, T. & Song, Y. Prognostic value of circulating endothelial cells in non-small cell lung cancer patients: a systematic review and meta-analysis. *Transl Lung Cancer Res* **4**, 610-618 (2015).
241 Lee, T. K., Esinhart, J. D., Blackburn, L. D. & Silverman, J. F. The size of small cell lung carcinoma cells. Ratio to lymphocytes and correlation with specimen size and crush artifact. *Anal Quant Cytol Histol* **14**, 32-34 (1992).
242 Travis, W. D. *et al.* International Association for the Study of Lung Cancer/American Thoracic Society/European Respiratory Society: international multidisciplinary classification of lung adenocarcinoma: executive summary. *Proc Am Thorac Soc* **8**, 381-385 (2011).
243 Charbonneau, H., Tonks, N. K., Walsh, K. A. & Fischer, E. H. The leukocyte common antigen (CD45): a putative receptor-linked protein tyrosine phosphatase. *Proc Natl Acad Sci U S A* **85**, 7182-7186 (1988).
244 Barretina, J. *et al.* The Cancer Cell Line Encyclopedia enables predictive modelling of anticancer drug sensitivity. *Nature* **483**, 603-607 (2012).
245 Goldstraw, P. *et al.* The IASLC Lung Cancer Staging Project: proposals for the revision of the TNM stage groupings in the forthcoming (seventh) edition of the TNM Classification of malignant tumours. *J Thorac Oncol* **2**, 706-714 (2007).
246 Hirsch, F. R. *et al.* Histopathologic classification of small cell lung cancer. Changing concepts and terminology. *Cancer* **62**, 973-977 (1988).

247 Adams, D. L. *et al.* The systematic study of circulating tumor cell isolation using lithographic microfilters. *RSC Adv* **9**, 4334-4342 (2014).
248 Wendel, M. *et al.* Fluid biopsy for circulating tumor cell identification in patients with early-and late-stage non-small cell lung cancer: a glimpse into lung cancer biology. *Phys Biol* **9**, 016005 (2012).
249 Ramaekers, F. C. *et al.* Coexpression of keratin- and vimentin-type intermediate filaments in human metastatic carcinoma cells. *Proc Natl Acad Sci U S A* **80**, 2618-2622 (1983).
250 Chu, Y. W., Seftor, E. A., Romer, L. H. & Hendrix, M. J. Experimental coexpression of vimentin and keratin intermediate filaments in human melanoma cells augments motility. *Am J Pathol* **148**, 63-69 (1996).
251 Zhu, Q. S. *et al.* Vimentin is a novel AKT1 target mediating motility and invasion. *Oncogene* **30**, 457-470 (2011).
252 Jordan, N. V., Johnson, G. L. & Abell, A. N. Tracking the intermediate stages of epithelial-mesenchymal transition in epithelial stem cells and cancer. *Cell Cycle* **10**, 2865-2873 (2011).
253 Abell, A. N. *et al.* Trophoblast stem cell maintenance by fibroblast growth factor 4 requires MEKK4 activation of Jun N-terminal kinase. *Mol Cell Biol* **29**, 2748-2761 (2009).
254 Abell, A. N. *et al.* MAP3K4/CBP-regulated H2B acetylation controls epithelial-mesenchymal transition in trophoblast stem cells. *Cell Stem Cell* **8**, 525-537 (2011).
255 Kong, D., Li, Y., Wang, Z. & Sarkar, F. H. Cancer Stem Cells and Epithelial-to-Mesenchymal Transition (EMT)-Phenotypic Cells: Are They Cousins or Twins? *Cancers (Basel)* **3**, 716-729 (2011).
256 Fischer, K. R. *et al.* Epithelial-to-mesenchymal transition is not required for lung metastasis but contributes to chemoresistance. *Nature* **527**, 472-476 (2015).
257 Zheng, X. *et al.* Epithelial-to-mesenchymal transition is dispensable for metastasis but induces chemoresistance in pancreatic cancer. *Nature* **527**, 525-530 (2015).
258 Kurokawa, M., Ise, N., Omi, K., Goishi, K. & Higashiyama, S. Cisplatin influences acquisition of resistance to molecular-targeted agents through epithelial-mesenchymal transition-like changes. *Cancer Sci* **104**, 904-911 (2013).
259 Yauch, R. L. *et al.* Epithelial versus mesenchymal phenotype determines in vitro sensitivity and predicts clinical activity of erlotinib in lung cancer patients. *Clin Cancer Res* **11**, 8686-8698 (2005).
260 Lim, S. *et al.* SNAI1-Mediated Epithelial-Mesenchymal Transition Confers Chemoresistance and Cellular Plasticity by Regulating Genes Involved in Cell Death and Stem Cell Maintenance. *PLoS One* **8**, e66558 (2013).
261 Rocken, M. Early tumor dissemination, but late metastasis: insights into tumor dormancy. *J Clin Invest* **120**, 1800-1803 (2010).
262 Pantel, K., Alix-Panabieres, C. & Riethdorf, S. Cancer micrometastases. *Nat Rev Clin Oncol* **6**, 339-351 (2009).
263 Shieh, Y. S. *et al.* Expression of axl in lung adenocarcinoma and correlation with tumor progression. *Neoplasia* **7**, 1058-1064 (2005).
264 Nagata, K. *et al.* Identification of the product of growth arrest-specific gene 6 as a common ligand for Axl, Sky, and Mer receptor tyrosine kinases. *J Biol Chem* **271**, 30022-30027 (1996).
265 Hong, C. C. *et al.* Receptor tyrosine kinase AXL is induced by chemotherapy drugs and overexpression of AXL confers drug resistance in acute myeloid leukemia. *Cancer Lett* **268**, 314-324 (2008).

266 Lee, W. P., Wen, Y., Varnum, B. & Hung, M. C. Akt is required for Axl-Gas6 signaling to protect cells from E1A-mediated apoptosis. *Oncogene* **21**, 329-336 (2002).
267 Keating, A. K. *et al.* Inhibition of Mer and Axl receptor tyrosine kinases in astrocytoma cells leads to increased apoptosis and improved chemosensitivity. *Mol Cancer Ther* **9**, 1298-1307 (2010).
268 Zhang, Z. *et al.* Activation of the AXL kinase causes resistance to EGFR-targeted therapy in lung cancer. *Nat Genet* **44**, 852-860 (2012).
269 Wilson, C. *et al.* AXL inhibition sensitizes mesenchymal cancer cells to antimitotic drugs. *Cancer Res* **74**, 5878-5890 (2014).
270 Burk, U. *et al.* A reciprocal repression between ZEB1 and members of the miR-200 family promotes EMT and invasion in cancer cells. *EMBO Rep* **9**, 582-589 (2008).
271 Singh, A. *et al.* A gene expression signature associated with "K-Ras addiction" reveals regulators of EMT and tumor cell survival. *Cancer Cell* **15**, 489-500 (2009).
272 Li, Y. *et al.* Up-regulation of miR-200 and let-7 by natural agents leads to the reversal of epithelial-to-mesenchymal transition in gemcitabine-resistant pancreatic cancer cells. *Cancer Res* **69**, 6704-6712 (2009).
273 Singh, A. & Settleman, J. EMT, cancer stem cells and drug resistance: an emerging axis of evil in the war on cancer. *Oncogene* **29**, 4741-4751 (2010).
274 Kota, J. *et al.* Therapeutic microRNA delivery suppresses tumorigenesis in a murine liver cancer model. *Cell* **137**, 1005-1017 (2009).
275 Liu, W. *et al.* Inhibition of TBK1 attenuates radiation-induced epithelial-mesenchymal transition of A549 human lung cancer cells via activation of GSK-3beta and repression of ZEB1. *Lab Invest* **94**, 362-370 (2014).
276 Jordan, C. T. Cancer stem cells: controversial or just misunderstood? *Cell Stem Cell* **4**, 203-205 (2009).
277 Ben-Porath, I. *et al.* An embryonic stem cell-like gene expression signature in poorly differentiated aggressive human tumors. *Nat Genet* **40**, 499-507 (2008).
278 Folkman, J. Proceedings: Tumor angiogenesis factor. *Cancer Res* **34**, 2109-2113 (1974).
279 Polanski, R. *et al.* Activity of the monocarboxylate transporter 1 inhibitor AZD3965 in small cell lung cancer. *Clin Cancer Res* **20**, 926-937 (2014).
280 Vona, G. *et al.* Impact of cytomorphological detection of circulating tumor cells in patients with liver cancer. *Hepatology* **39**, 792-797 (2004).
281 Tufto, I., Lyng, H. & Rofstad, E. K. Vascular density in human melanoma xenografts: relationship to angiogenesis, perfusion and necrosis. *Cancer Lett* **123**, 159-165 (1998).
282 El Hallani, S. *et al.* A new alternative mechanism in glioblastoma vascularization: tubular vasculogenic mimicry. *Brain* **133**, 973-982 (2010).
283 Gupta, D. & Lis, C. G. Pretreatment serum albumin as a predictor of cancer survival: a systematic review of the epidemiological literature. *Nutr J* **9**, 69 (2010).
284 Spiro, S. G. *et al.* Early compared with late radiotherapy in combined modality treatment for limited disease small-cell lung cancer: a London Lung Cancer Group multicenter randomized clinical trial and meta-analysis. *J Clin Oncol* **24**, 3823-3830 (2006).
285 Osterlind, K. & Andersen, P. K. Prognostic factors in small cell lung cancer: multivariate model based on 778 patients treated with chemotherapy with or without irradiation. *Cancer Res* **46**, 4189-4194 (1986).
286 Cuenod, C. A. & Balvay, D. Perfusion and vascular permeability: basic concepts and measurement in DCE-CT and DCE-MRI. *Diagn Interv Imaging* **94**, 1187-1204 (2013).

287 Bernstein, J. M. *et al.* Tumor plasma flow determined by dynamic contrast-enhanced MRI predicts response to induction chemotherapy in head and neck cancer. *Oral Oncol* **51**, 508-513 (2015).
288 Morrow, C. J. *et al.* Src family kinase inhibitor Saracatinib (AZD0530) impairs oxaliplatin uptake in colorectal cancer cells and blocks organic cation transporters. *Cancer Res* **70**, 5931-5941 (2010).
289 Johnsson, A. *et al.* Pharmacokinetics and tissue distribution of cisplatin in nude mice: platinum levels and cisplatin-DNA adducts. *Cancer Chemother Pharmacol* **37**, 23-31 (1995).
290 Marrinucci, D. *et al.* Fluid biopsy in patients with metastatic prostate, pancreatic and breast cancers. *Phys Biol* **9**, 016003 (2012).
291 King, A. D. *et al.* Necrosis in metastatic neck nodes: diagnostic accuracy of CT, MR imaging, and US. *Radiology* **230**, 720-726 (2004).
292 Hendrix, M. J., Seftor, E. A., Hess, A. R. & Seftor, R. E. Vasculogenic mimicry and tumour-cell plasticity: lessons from melanoma. *Nat Rev Cancer* **3**, 411-421 (2003).
293 Sandler, A. *et al.* Paclitaxel-carboplatin alone or with bevacizumab for non-small-cell lung cancer. *N Engl J Med* **355**, 2542-2550 (2006).
294 Soria, J. C. *et al.* Systematic review and meta-analysis of randomised, phase II/III trials adding bevacizumab to platinum-based chemotherapy as first-line treatment in patients with advanced non-small-cell lung cancer. *Ann Oncol* **24**, 20-30 (2013).
295 Vokes, E. E., Salgia, R. & Karrison, T. G. Evidence-based role of bevacizumab in non-small cell lung cancer. *Ann Oncol* **24**, 6-9 (2013).
296 Lucchi, M. *et al.* Small cell lung carcinoma (SCLC): the angiogenic phenomenon. *Eur J Cardiothorac Surg* **21**, 1105-1110 (2002).
297 Tanno, S., Ohsaki, Y., Nakanishi, K., Toyoshima, E. & Kikuchi, K. Human small cell lung cancer cells express functional VEGF receptors, VEGFR-2 and VEGFR-3. *Lung Cancer* **46**, 11-19 (2004).
298 Tas, F. *et al.* Serum vascular endothelial growth factor (VEGF) and interleukin-8 (IL-8) levels in small cell lung cancer. *Cancer Invest* **24**, 492-496 (2006).
299 Ready, N. E. *et al.* Cisplatin, irinotecan, and bevacizumab for untreated extensive-stage small-cell lung cancer: CALGB 30306, a phase II study. *J Clin Oncol* **29**, 4436-4441 (2011).
300 Ready, N. E. *et al.* Chemotherapy With or Without Maintenance Sunitinib for Untreated Extensive-Stage Small-Cell Lung Cancer: A Randomized, Double-Blind, Placebo-Controlled Phase II Study-CALGB 30504 (Alliance). *J Clin Oncol* **33**, 1660-1665 (2015).
301 Franco, M. *et al.* Targeted anti-vascular endothelial growth factor receptor-2 therapy leads to short-term and long-term impairment of vascular function and increase in tumor hypoxia. *Cancer Res* **66**, 3639-3648 (2006).
302 Bergers, G. & Hanahan, D. Modes of resistance to anti-angiogenic therapy. *Nat Rev Cancer* **8**, 592-603 (2008).
303 Resch, T., Pircher, A., Kahler, C. M., Pratschke, J. & Hilbe, W. Endothelial progenitor cells: current issues on characterization and challenging clinical applications. *Stem Cell Rev* **8**, 926-939 (2012).
304 Moserle, L. & Casanovas, O. Anti-angiogenesis and metastasis: a tumour and stromal cell alliance. *J Intern Med* **273**, 128-137 (2013).
305 Li, X. *et al.* Thalidomide down-regulates the expression of VEGF and bFGF in cisplatin-resistant human lung carcinoma cells. *Anticancer Res* **23**, 2481-2487 (2003).

306 Zhang, S. *et al.* Thalidomide influences growth and vasculogenic mimicry channel formation in melanoma. *J Exp Clin Cancer Res* **27**, 60 (2008).
307 Lee, S. M. *et al.* Anti-angiogenic therapy using thalidomide combined with chemotherapy in small cell lung cancer: a randomized, double-blind, placebo-controlled trial. *J Natl Cancer Inst* **101**, 1049-1057 (2009).
308 Pujol, J. L. *et al.* Phase III double-blind, placebo-controlled study of thalidomide in extensive-disease small-cell lung cancer after response to chemotherapy: an intergroup study FNCLCC cleo04 IFCT 00-01. *J Clin Oncol* **25**, 3945-3951 (2007).
309 Mehta, P. Thalidomide and thrombosis. *Clin Adv Hematol Oncol* **1**, 464-465 (2003).
310 Lin, C. M., Ho, H. H., Pettit, G. R. & Hamel, E. Antimitotic natural products combretastatin A-4 and combretastatin A-2: studies on the mechanism of their inhibition of the binding of colchicine to tubulin. *Biochemistry* **28**, 6984-6991 (1989).
311 Iyer, S. *et al.* Induction of apoptosis in proliferating human endothelial cells by the tumor-specific antiangiogenesis agent combretastatin A-4. *Cancer Res* **58**, 4510-4514 (1998).
312 Vincent, L. *et al.* Combretastatin A4 phosphate induces rapid regression of tumor neovessels and growth through interference with vascular endothelial-cadherin signaling. *J Clin Invest* **115**, 2992-3006 (2005).
313 Mooney, C. J. *et al.* A phase II trial of fosbretabulin in advanced anaplastic thyroid carcinoma and correlation of baseline serum-soluble intracellular adhesion molecule-1 with outcome. *Thyroid* **19**, 233-240 (2009).
314 Monk, B. J. Randomized phase 2 evaluation of bevacizumab versus bevacizumab/fosbretabulin in recurrent ovarian, tubal or peritoneal carcinoma: a gynecologic oncology group study. *Society of Gynecologic Oncology's Annual Meeting on Women's Cancer*, Seminal Abstract 4 (2015).
315 Carmeliet, P. *et al.* Targeted deficiency or cytosolic truncation of the VE-cadherin gene in mice impairs VEGF-mediated endothelial survival and angiogenesis. *Cell* **98**, 147-157 (1999).
316 Gerber, H. P. *et al.* Vascular endothelial growth factor regulates endothelial cell survival through the phosphatidylinositol 3'-kinase/Akt signal transduction pathway. Requirement for Flk-1/KDR activation. *J Biol Chem* **273**, 30336-30343 (1998).
317 Cummings, J. *et al.* Method validation of circulating tumour cell enumeration at low cell counts. *BMC Cancer* **13**, 415 (2013).
318 Cummings, J. *et al.* Optimisation of an immunohistochemistry method for the determination of androgen receptor expression levels in circulating tumour cells. *BMC Cancer* **14**, 226 (2014).
319 Baatz, M., Zimmermann, J. & Blackmore, C. G. Automated analysis and detailed quantification of biomedical images using Definiens Cognition Network Technology. *Comb Chem High Throughput Screen* **12**, 908-916 (2009).
320 Hofman, V. J. *et al.* Cytopathologic detection of circulating tumor cells using the isolation by size of epithelial tumor cell method: promises and pitfalls. *Am J Clin Pathol* **135**, 146-156 (2011).
321 Nuzzo, R. How scientists fool themselves - and how they can stop. *Nature* **526**, 182-185 (2015).
322 Pantel, K. *et al.* Circulating epithelial cells in patients with benign colon diseases. *Clin Chem* **58**, 936-940 (2012).
323 Hanahan, D. & Weinberg, R. A. Hallmarks of cancer: the next generation. *Cell* **144**, 646-674 (2011).

324 Brahmer, J. *et al.* Nivolumab versus Docetaxel in Advanced Squamous-Cell Non-Small-Cell Lung Cancer. *N Engl J Med* **373**, 123-135 (2015).
325 Borghaei, H. *et al.* Nivolumab versus Docetaxel in Advanced Nonsquamous Non-Small-Cell Lung Cancer. *N Engl J Med* **373**, 1627-1639 (2015).
326 Melero, I. *et al.* Evolving synergistic combinations of targeted immunotherapies to combat cancer. *Nat Rev Cancer* **15**, 457-472 (2015).
327 Mazel, M. *et al.* Frequent expression of PD-L1 on circulating breast cancer cells. *Mol Oncol* **9**, 1773-1782 (2015).
328 Che, J. *et al.* Classification of large circulating tumor cells isolated with ultra-high throughput microfluidic Vortex technology. *Oncotarget* (2016).
329 Abdallah, E. A. *et al.* MRP1 expression in CTCs confers resistance to irinotecan-based chemotherapy in metastatic colorectal cancer. *Int J Cancer* (2016).
330 Gorges, T. M. *et al.* Heterogeneous PSMA expression on circulating tumor cells - a potential basis for stratification and monitoring of PSMA-directed therapies in prostate cancer. *Oncotarget* (2016).
331 Long, E. *et al.* High expression of TRF2, SOX10, and CD10 in circulating tumor microemboli detected in metastatic melanoma patients. A potential impact for the assessment of disease aggressiveness. *Cancer Med* (2016).
332 Lindsay, C. R. *et al.* Vimentin and Ki67 expression in circulating tumour cells derived from castrate-resistant prostate cancer. *BMC Cancer* **16**, 168 (2016).

Appendix 1 Gallery of NSCLC CTCs identified following immunofluorescent staining of ISET filters with the EMT assay

Each row shows a grey scale image of a single CTC stained for nuclei, cytokeratins, CD45 and/or VE-cadherin and vimentin and a composite image showing nuclei (white), cytokeratins (green), CD45/VE-cadherin (red) and vimentin (blue).

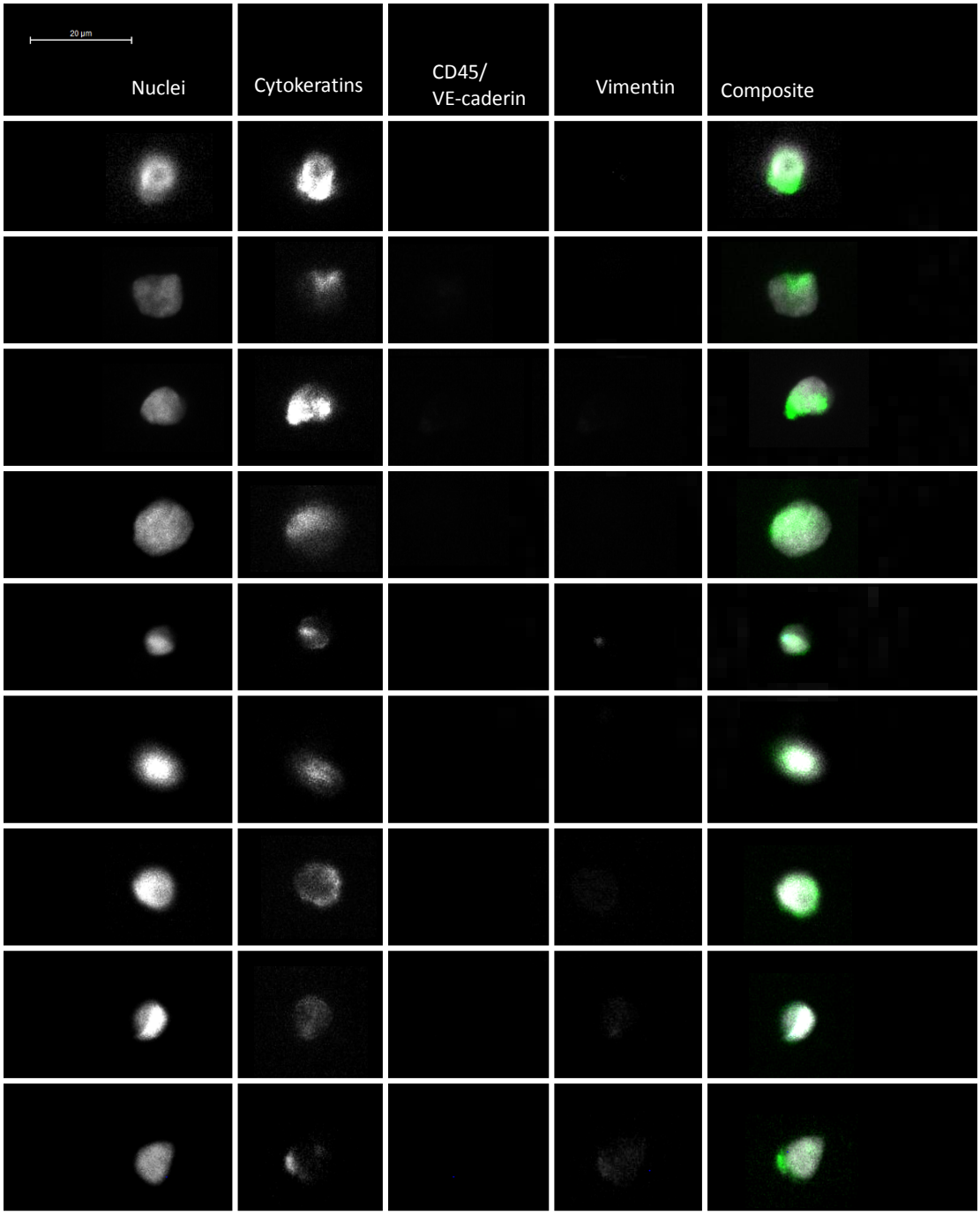

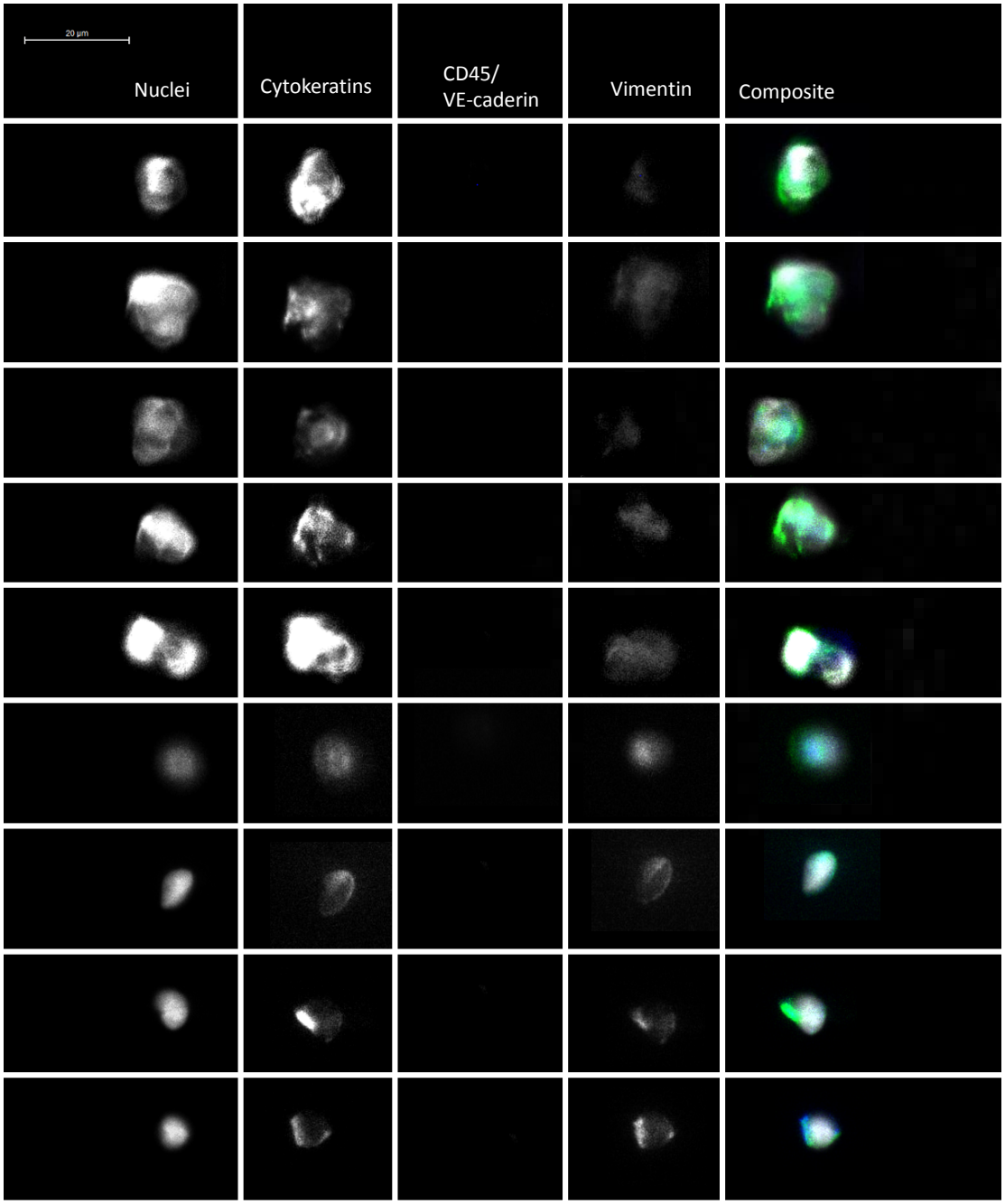
20 µm
Nuclei
Cytokeratins
CD45/
VE-caderin
Vimentin
Composite

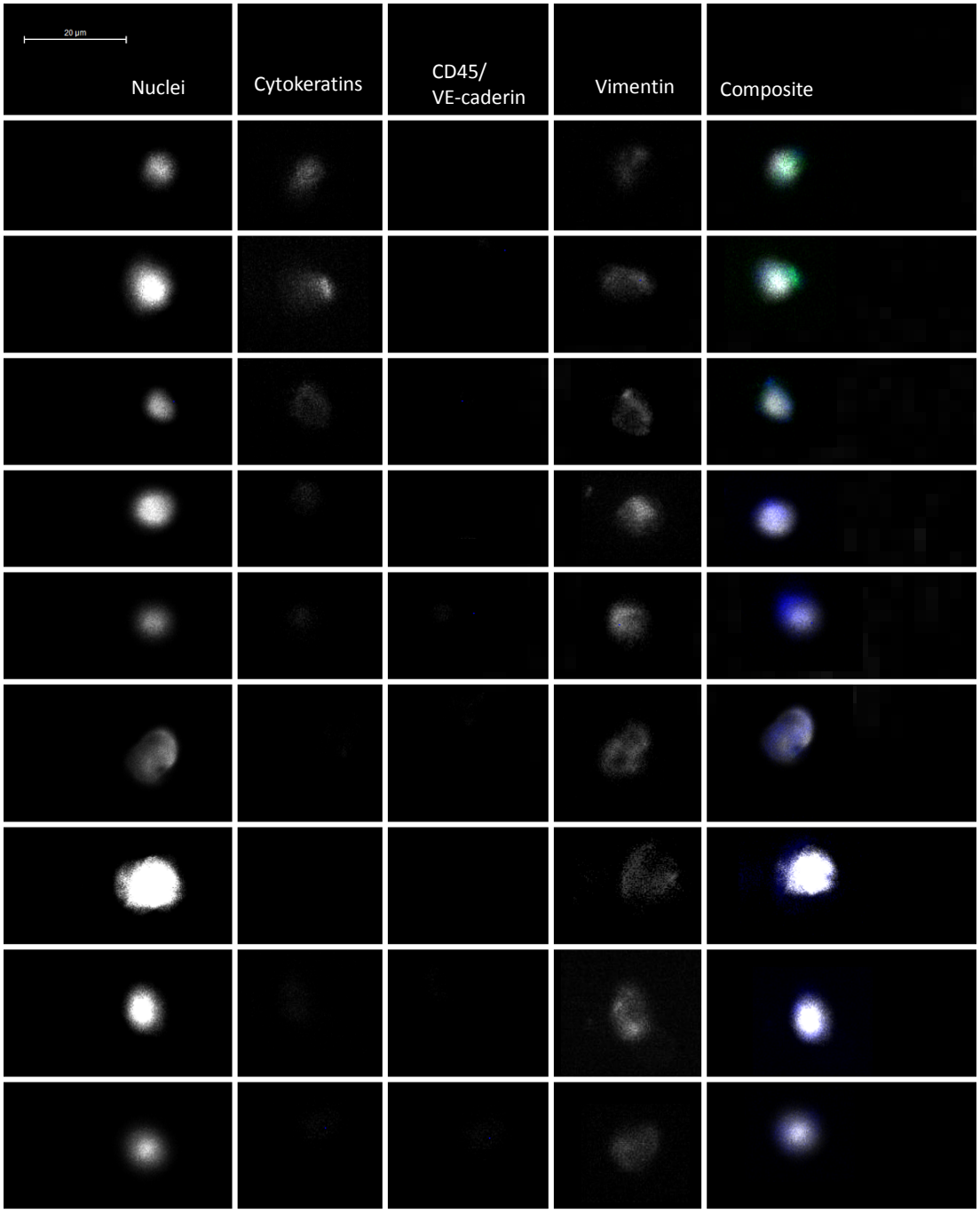

Raw image data enclosed as USB drive.

Appendix 2 Abstract of manuscript submitted to Annals of Oncology (in press): Tumourigenic non-small cell lung cancer mesenchymal circulating tumour cells - a clinical case study

Christopher J. Morrow[†], Francesca Trapani[†], Robert L. Metcalf[†], Giulia Bertolini, Cassandra L. Hodgkinson, Garima Khandelwal, Paul Kelly, Melanie Galvin, Louise Carter, Kathryn L. Simpson, Stuart Williamson, Christopher Wirth, Nicole Simms, Lynsey Priest, Kristopher Frese, Dominic G. Rothwell, Daisuke Nonaka, Crispin J Miller, Ged Brady, Fiona H. Blackhall, Caroline Dive.

[†]these authors made equal contribution

Background Over the past decade numerous reports describe the generation and increasing utility of non-small cell lung cancer (NSCLC) patient-derived xenografts (PDX) from tissue biopsies. While PDX have proven useful for genetic profiling and preclinical drug testing, the requirement of a tissue biopsy limits the available patient population, particularly those with advanced oligometastatic disease. Conversely, 'liquid biopsies' such as circulating tumour cells (CTCs) are minimally invasive and easier to obtain. Here we present a clinical case study of NSCLC patient with advanced metastatic disease, a never smoker whose primary tumour was EGFR and ALK wild type. We demonstrate for the first time, tumorigenicity of their CTCs to generate a patient CTC Derived eXplant (CDX). **Materials and methods** CTCs were enriched at diagnosis and again two months later during disease progression from 10ml blood from a 48 year old NSCLC patient and implanted into immunocompromised mice. Resultant tumours were morphologically, immunohistochemically, and genetically compared to the donor patient's diagnostic specimen. Mice were treated with cisplatin and pemetrexed to assess preclinical efficacy of the chemotherapy regimen given to the donor patient. **Results** The NSCLC CDX expressed lung lineage markers TTF1 and CK7 and was unresponsive to cisplatin and pemetrexed. Examination of blood samples matched to that used for CDX generation revealed absence of CTCs using the CellSearch EpCAM dependent platform, whereas size based CTC enrichment revealed abundant heterogeneous CTCs of which ~80% were mesenchymal marker vimentin positive. Molecular analysis of the CDX, mesenchymal and epithelial CTCs revealed a common somatic mutation confirming tumour origin and showed CDX RNA and protein profiles consistent with the predominantly mesenchymal phenotype. **Conclusions** This study shows that absence of NSCLC CTCs detected by CellSearch (EpCAM+) does not preclude CDX generation highlighting epithelial to mesenchymal transition and the functional importance of mesenchymal CTCs in dissemination of this disease.

Appendix 3 Gallery of SCLC CTCs identified following immunofluorescent staining of ISET filters with the VM assay

Each row shows a grey scale image of a single CTC stained for nuclei, cytokeratins, CD45, VE-cadherin and a composite image showing nuclei (white), cytokeratins (green), CD45 (red) and VE-cadherin (blue).

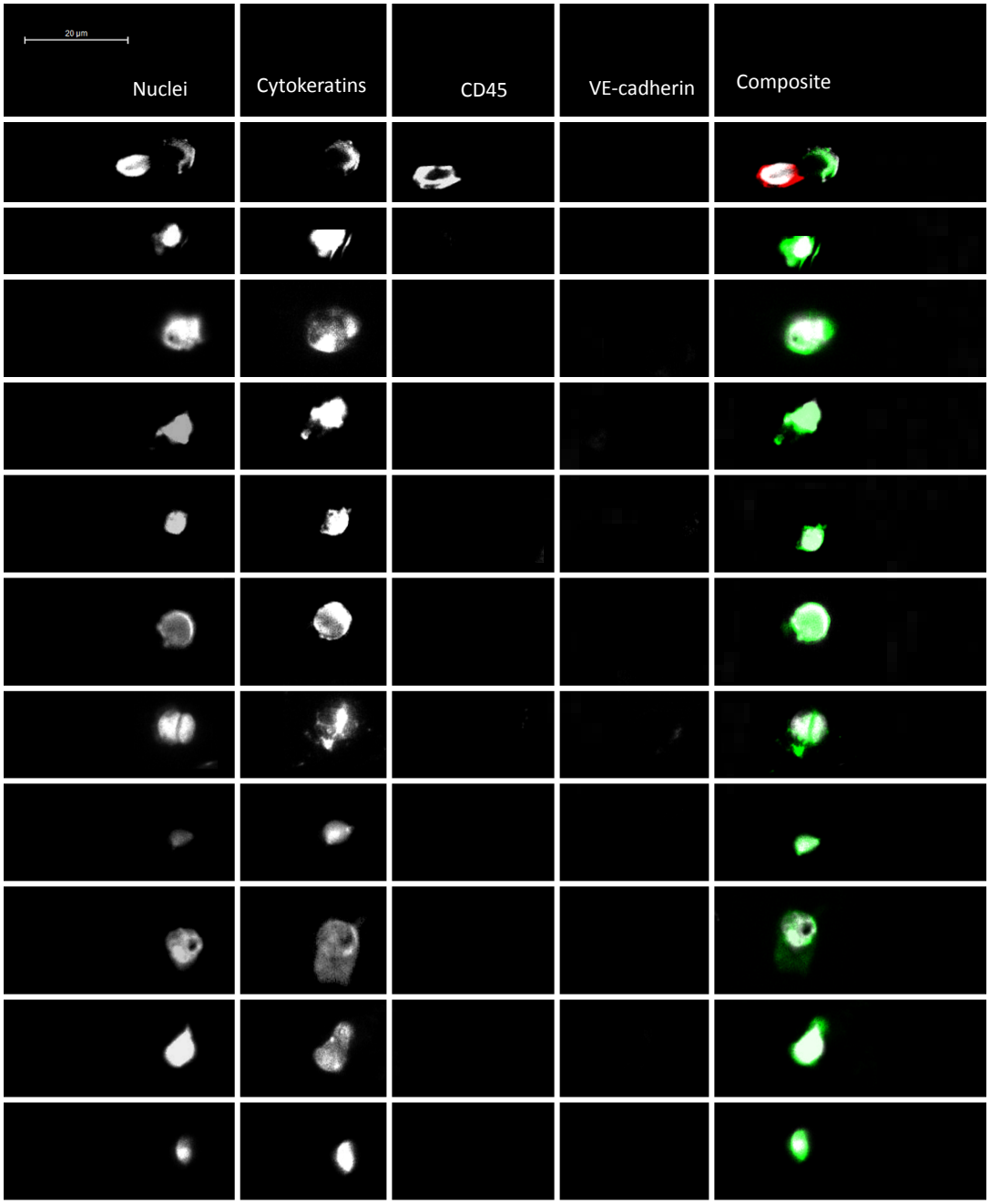

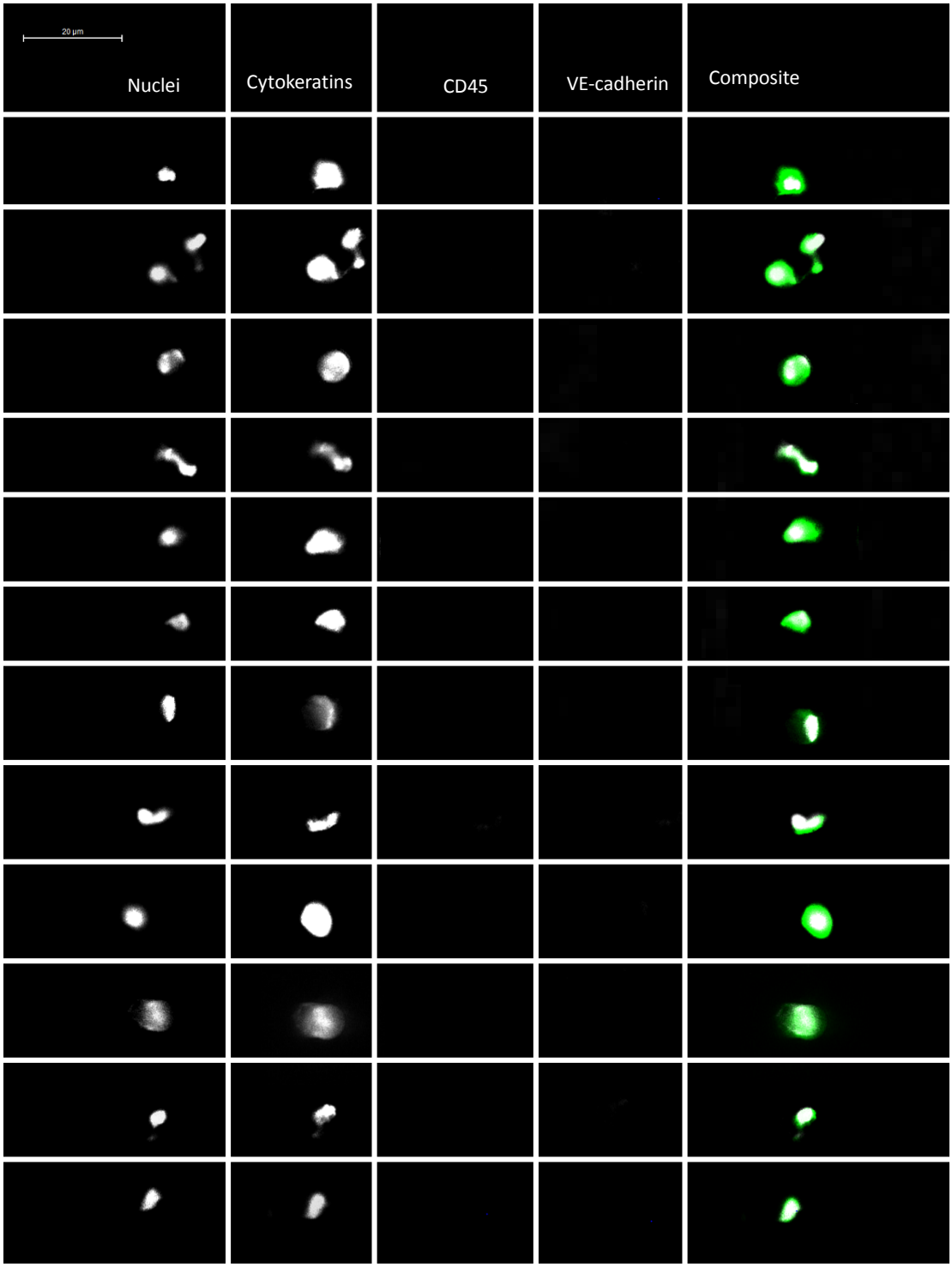
20 µm
Nuclei
Cytokeratins
CD45
VE-cadherin
Composite

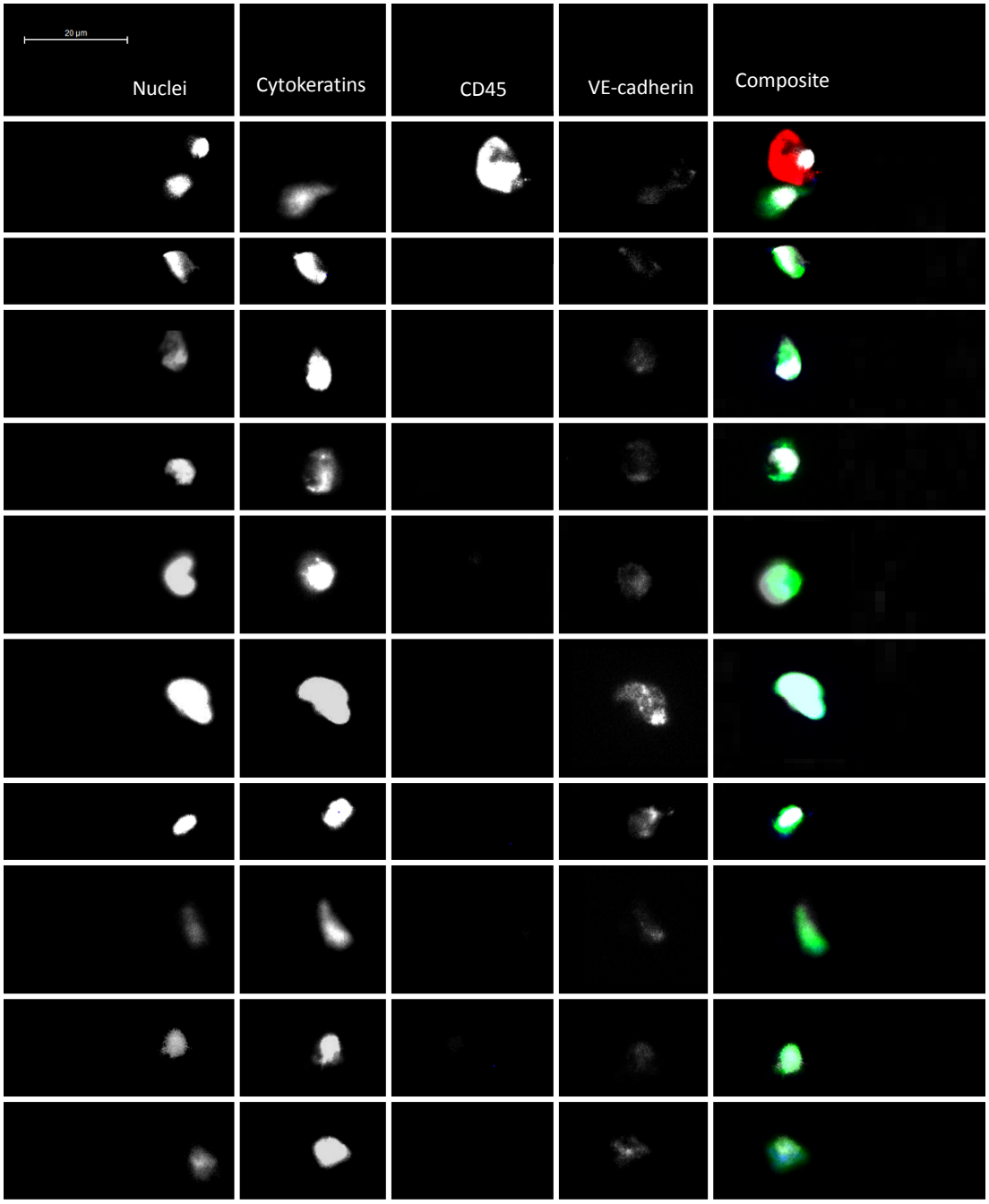

Raw image data enclosed as USB drive.

Appendix 4 Abstract of manuscript submitted to Nature Communications (in review): Vasculogenic mimicry in small cell lung cancer

Robert L Metcalf[†], Francesca Trapani[†], Kathryn L Simpson[†], Stuart Williamson, HuiSun Leong, Benjamin Abbott, Jenny Antonello, Cassandra L Hodgkinson, Radoslaw Polanski, Alberto Fusi, Diasuke Nonaka, Lynsey Priest, Fredrikka Carlsson, Anders Carlsson, Mary J.C Hendrix, Richard E.B Seftor, Elisabeth A Seftor, Dominic G Rothwell, Andrew Hughes, Peter Kuhn, James Hicks, Crispin Miller, Ged Brady, Fiona H Blackhall, and Dive C

[†]these authors made equal contribution

SCLC is characterised by prevalent circulating tumour cells (CTCs) and early metastasis. We show that SCLC patients (37/38) had CTC sub-populations co-expressing Vascular Endothelial-Cadherin (VE-Cadherin) and cytokeratins consistent with vasculogenic mimicry (VM), a phenotypic switch whereby tumour cells form 'endothelial like' vessels. In a tissue microarray of 41 tumour specimens, relatively high levels of VM associated with worse overall survival in limited stage patients (median 13.0 vs. 23.8 months, 8 vs. 47% 3 year survival for high vs. low VM vessel score, p=0.025). VM vessels, seen in 9/10 Circulating Tumour Cell (CTC) patient Derived explants (CDX) had copy number alteration profiles that confirmed tumour origin. Isolated VE-Cadherin+/Cytokeratin+ CTCs displayed distinct clonal architecture to VE-Cadherin-/Cytokeratin+ CTCs. VE-Cadherin was required for VM-like network formation in Matrigel and enhanced both tumour growth and cisplatin delivery in SCLC xenografts. These data suggest that the role of VM in SCLC warrants further investigation.